Silica Immobilized Pincer-Metal Complexes

Catalysis, Recycling, and Retrospect on Active Species

Silica-geïmmobiliseerde Tang-Metaalcomplexen

Katalyse, Hergebruik en Heroverweging van de Actieve Katalysator

(met een samenvatting in het Nederlands)

Proefschrift

ter verkrijging van de graad van doctor aan de Universiteit Utrecht
op gezag van de rector magnificus, prof.dr. W.H. Gispen,
ingevolge het besluit van het college voor promoties
in het openbaar te verdedigen
op woensdag 14 maart 2007 des ochtends te 10.30 uur

door

Nilesh Chandrakant Mehendale

geboren op 1 augustus 1975 te Baramati, India

Promotoren: Prof.dr. G. van Koten
Prof.dr. R. J. M. Klein Gebbink

This investigation was financially supported by the Dutch Technology Foundation STW and Utrecht University.

Silica Immobilized Pincer-Metal Complexes

Catalysis, Recycling, and Retrospect on Active Species

To my parents and grand parents

प्रिय आजी, अण्णा, आई व पप्पांस...

Mehendale, Nilesh Chandrakant

Silica Immobilized Pincer-Metal Complexes
Catalysis, Recycling and Retrospect on Active Species

Utrecht, Utrecht University, Faculty of Science
Thesis Utrecht University – with ref. – with summary in Dutch

ISBN: 978-90-393-4484-2

The work described in this thesis was carried out at the Organic Chemistry and Catalysis Group, Faculty of Science, Utrecht University, The Netherlands.

Cover painting:Vijay Gavhankar

Table of Contents

Chapter 1

Silica Supported Organometallic Complexes

Abstract

This chapter reviews silica immobilized organometallic, homogeneous catalysts. It focuses on the synthetic procedures to attach the currently available catalysts onto a silica support. These procedures involve either surface modification or metal complex modification in order to connect both *via* a covalent interaction. Comparison with their homogeneous counterparts in catalysis reveals an increased activity in some of the cases. Comparison amongst various supports (plain silica *vs.* structured silica) shows an advantage of using structured, mesoporous silicas. A variety of synthetic transformations can be brought about by using these catalysts with a high activity and selectivity. In addition, these catalysts can be recycled due to their heterogeneous nature.

1.1. Introduction

1.1.1. Catalysis

Catalysis is a widely occurring process in Nature. Enzymes catalyze numerous biological transformations and involve complex and large molecular weight structures that have evolved in Nature over millions of years to carry out particular reactions very selectively.

Man-made catalysts are traditionally either relatively simple, soluble molecules of lower masses or insoluble inorganic solids. Historically important examples are the production of H_2SO_4 using V_2O_5 and the production of ammonia using iron-based catalysts. Research on the mode of operation and the synthesis of catalysts, including an improved understanding of thermodynamics due to the pioneering works of Ostwald and Van't Hoff, paved the way for a rational approach in developing more sophisticated and superior catalysts.[1]

The basic principle of all catalysts is that they lower the energy barrier between reactants and products by offering an alternative reaction path. A catalyst decreases the activation energy of a reaction ($\Delta G^{\neq}$ is lowered), thereby increasing the rate of the reaction, but has no effect on the chemical equilibrium of the reaction (ΔG remains the same). The action of a catalyst can be very specific, which under ideal conditions, results in selective formation of the desired product and avoids side reactions. Further advantages of the use of catalytic reagents are reduced time and energy requirements, which results in an overall process with increased environmental sustainability. A catalyst can be poisoned when another compound binds to it irreversibly or chemically alters it. This effectively destroys the usefulness of the catalyst, as it cannot anymore participate in the reaction that it was designed to catalyze.

There are mainly three types of catalysis processes: biocatalysis, homogeneous catalysis, and heterogeneous catalysis. Table 1 highlights major advantages of both homogeneous and heterogeneous catalytic processes (biocatalysis is out of the scope of this thesis and is not described further).

Table 1 Advantages of homogeneous and heterogeneous catalytic processes.

Homogeneous	Heterogeneous
▪ High and controllable chemo-, regio-, and enantio-selectivity	▪ Easy separation of the catalyst from the product
▪ High activity in terms of TON and TOF	▪ Excellent reuse of the catalyst (high total TON)
▪ Excellent accessibility of catalytic sites, no mass transfer limitations, no pressure drop	▪ Continuous operation frequently applied
▪ Use of complex ligand systems to modify the catalyst	▪ Resistance to drastic operational conditions
▪ Excellent catalyst description, mechanistic understanding	▪ Choice of a large variety of supports, *e.g.* silica, alumina, zeolites, carbon *etc.*

Many homogeneous catalysts contain a metal ion that is surrounded by a ligand system which stabilizes it in a certain oxidation state and offers coordination sites for substrates and reagents. By ingenious designing of ligands, more active and selective catalysts can be obtained. Transition metal catalysts are the largest class of homogeneous metal catalysts available to the synthetic chemist.

In heterogeneous processes, the catalytic sites are part of an insoluble inorganic solid or are distributed on the surface of an insoluble support like silica, alumina or carbon. One of the limiting factors of the catalytic activity of heterogeneous catalysts is the number of active sites, *i.e.* the surface area of the bulk material or of the supported species. Without surrounding organic ligands, it can be difficult to achieve high product selectivity; moreover, achieving enantioselectivity is generally not possible. On the other hand the big advantage of this kind of process is the easy separation of the catalyst from the reaction mixture. This allows easy purification of the product and facile reuse of the catalytic material. Hence, most of the industrial catalysts are heterogeneous in nature. In spite of this, there are a lot of important industrial processes based on homogeneous catalysis.[2] It is estimated that 85% of all chemical processes are run catalytically, with a ratio of applications of heterogeneous to homogeneous catalysis of approximately 75:25.[3] In general, the advantages of the two systems are complementary to each other. A hybrid system which combines the advantages of the two could constitute an 'ideal' catalytic system.

1.1.2. Recycling of homogeneous catalysts

In case of a homogeneous catalyst, the cost of the metal and the (chiral) ligand system is of significant importance. Also, the products that are made by homogeneous catalytic processes often need to be absolutely free from metal and ligand impurities, particularly in the case of products with pharmaceutical applications. These issues put severe constraints on the practical use of homogeneous catalysts. To overcome the problem of separation with these catalysts, a third generation of catalysts called supported metal complex catalysts have been designed.[4] This approach tries to combine properties of both homogeneous and heterogeneous catalysis, sometimes providing synergically beneficial effects.[5] For a useful application of these supported catalysts, they need to be very stable and yet active. Moreover, their activity should be comparable to their homogeneous counterparts and they should be equally or even more selective.

There are various methods to support a homogeneous catalyst.[6] One of the most common ways is to immobilize them on an insoluble supporting agent to arrive at so-called heterogenized homogeneous catalyst. The supports that are used in this approach include inorganic materials such as silica and alumina or organic polymers.[7-9] Both types of supports have their strengths and their weaknesses. Advantages of organic polymers are their large variety and the high loading capacities of functional groups. Disadvantages are the often high price and their restricted solvent compatibility, since they usually have to be used in a solvent in which they swell. In contrast, inorganic supports such as silica gels are relatively cheap and can be used in most organic solvents. On the other hand, loading

capacities on inorganic supports tends to be lower than for organic polymers. Supported catalysts based on both types of supports can be separated from reaction media by means of simple filtration techniques. Next to this 'insoluble supporting' strategy, several 'soluble supporting' strategies have been developed. Catalysts can, *e.g.* be anchored to soluble macromolecules like dendrimers[10] and separated by nanofiltration.[11] Another supporting technique is to modify homogeneous catalysts in order to solubilize them in a particular medium for the use in so-called biphasic catalysis. In this case, the supporting agent is a solvent. Media that have been used for this approach include water, ionic liquids, fluorous solvents and supercritical CO_2.[12]

As described by Choplin *et al.*, there are two major classes of heterogenized homogeneous catalysts: supported homogeneous catalysts and heterogeneous molecular catalysts.[9] In supported homogeneous catalysts, the structure of the supported catalyst is nearly identical to that of the precursor homogeneous catalyst. The coordination sphere of the metal is preserved as much as possible during the immobilization. This can be achieved in different ways. A homogeneous catalyst can be anchored to a support *via* bonds between the solid and one (or more) ligand(s) at a position remote from the atom coordinated to the metal center (eq. 1, Ligand L' is a ligand L functionalized so as to allow for a reaction with the support of interest).

$$ML_n \longrightarrow \text{support}-L'ML_{n-1} \qquad L' \sim L \qquad (1)$$

It can also be encapsulated or encaged in the voids of a porous, inorganic or organic, solid (eq. 2).

$$ML_n \longrightarrow \text{[support } ML_n \text{]} \qquad (2)$$

Alternatively, it can be immobilized in a film of solvent (non-volatile or hydrophilic) deposited on a solid like in supported liquid phase catalysts (SLPC), where reactants and products are either in the gas phase or are in a second solvent non-miscible with the first one (eq. 3).

$$\frac{R + P \,/\, solv._2}{ML_n / \, solv._1} \qquad (3)$$

In heterogeneous molecular catalysts, the metal is anchored *via* a direct bond between the metal center and a surface atom (eq. 4).

$$ML_n \longrightarrow \text{support}-ML_{n-i} \qquad (4)$$

This procedure induces important changes to the ligand environment around the metal center, which now includes a ''solid'' ligand. This kind of catalyst is either made through the reaction of a molecular homogeneous catalyst or of a catalyst precursor complex or salt with the supporting

material. In the former case, the hybrid material requires no further treatment before its application as a catalyst, whereas in the latter case, additional (synthetic) steps are required to arrive at the actual catalyst.

Most successful homogeneous catalytic systems have been supported on a variety of silica supports. A literature search on supported catalysts results in a vast number of examples. It is clear from these examples that almost every type of catalyst involving transition metal complexes has been immobilized. For a complete account, we refer to several of the excellent reviews on this subject.[5,8,13]

1.2. Silica supported homogeneous catalysts

This chapter summarizes the approaches undertaken to functionalize homogeneous catalysts in such a way that they can be immobilized on a silica surface. We mainly focus on the organic modification of the silica surface and/or the homogeneous catalyst in order to make a bridge between the two. The use of such hybrid systems in catalysis will also be discussed. Later we will highlight some examples of cyclometalated complexes immobilized on silica and their application in catalysis.

The ligand system surrounding the metal highly influences the overall activity and selectivity of the catalyst. In order to maintain the homogeneous catalyst characteristics, it is desirable to retain the metal surrounding as is present in the case of its homogeneous counterpart upon immobilization on the silica surface. A homogeneous complex can be immobilized by two approaches, ligand immobilization and complex immobilization.

1.2.1. Ligand immobilization

In ligand immobilization, first the ligand system is immobilized onto the surface followed by complex formation by reacting the heterogeneous ligand with the metal source. During such immobilization onto silica, the metal precursor may also interact with surface silanol groups, which can lead to an overall loss of catalytic activity and in the formation of alternative catalytic sites. The advantage of this immobilization method is the introduction of the metal in the end, which is economical in terms of metal use. This process is also suitable for complexes that are unstable under the conditions of immobilization. This approach is highlighted by the following examples.

Seebach *et al.* have immobilized the TADDOL ligand onto silica *via* a stepwise synthesis on the silica support (Scheme 1).[14] After treatment of the supported ligand with $TiCl_2(O\textit{i}Pr)_2$, the resulting heterogenized Ti-TADDOLates were used in enantioselective nucleophilic additions to aldehydes and in a 1,3-dipolar cycloaddition (Scheme 2). The enantioselectivities (up to 95% for the nucleophilic additions and 80% for the cycloaddition) and conversions similar to the homogeneous catalyst were obtained. The catalyst activity and the selectivity decreased over the first few runs but it could be fully restored by a HCl/H_2O/acetone hydrolysis step with subsequent Ti-reloading. This behavior was attributed to the accumulation of byproducts on the support and not to catalyst leaching or decomposition. Silica was recycled over 11 runs and it was found that, each time the amount of

catalyst could be decreased (from 0.5 equivalent to 0.1 equivalent) without affecting the conversion or *ee* values. This is an example where the ligand is recycled and the metal had to be replenished each time.

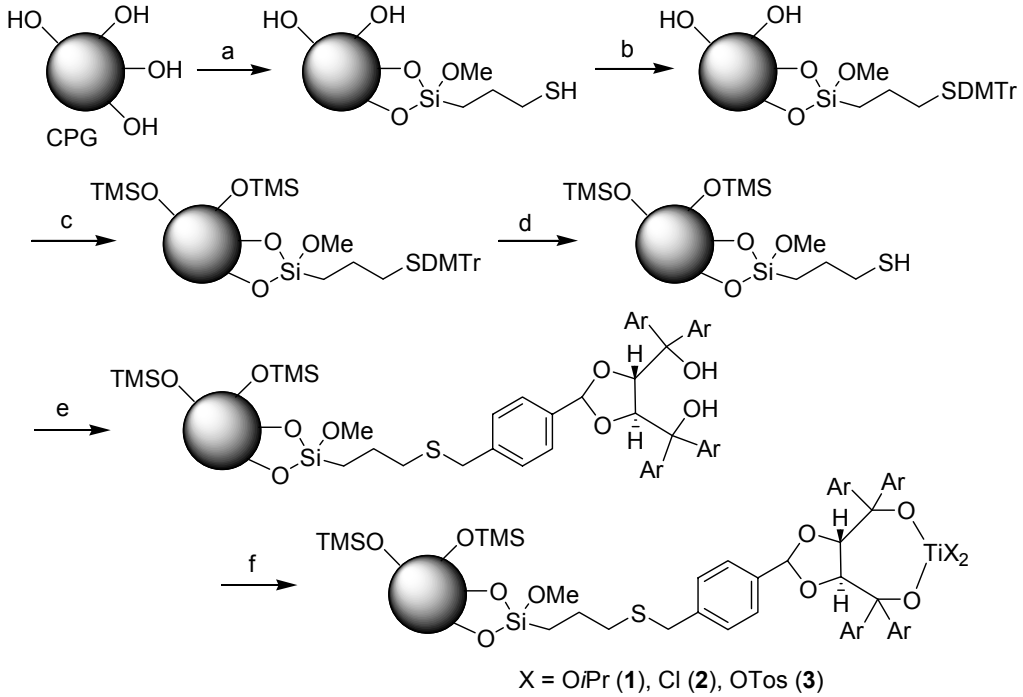

Scheme 1 Preparation of the immobilized Ti-TADDOLates **1-3** starting from commercially available CPG. a) $(MeO)_3Si(CH_2)_3SH$, imidazole, DMF, 100 °C, 20 h; b) DMTrCl, Et_3N, 4 h, r.t.; c) TMSIm, neat, 60 °C, 1 h; d) 1% TFA in CH_2Cl_2, Et_3SiH; e) benzyl bromide derivative of TADDOL, $EtNiPr_2$, toluene, 70 °C, 12 h. a) $TiX_2(OiPr)_2$, toluene, azeotropic removal of the *i*PrOH formed.

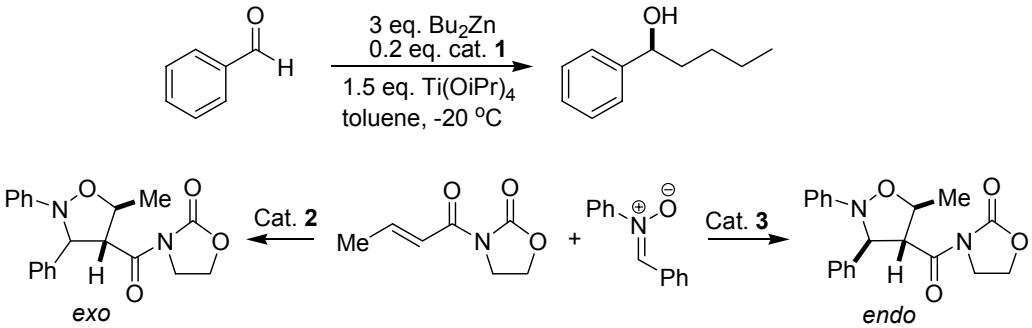

Scheme 2 Enantioselective nucleophilic addition to aldehydes and 1,3-dipolar cycloaddition.

The selective oxidation of alcohols to aldehydes was carried out by heterogenized phosphinite-Ru catalysts developed in the group of Marchand-Brynaert (Scheme 3).[15] The spacer arm required for the construction of the monodentate catalyst was prepared by reacting (4-aminophenyl)ethyl alcohol with 3-isocyanato-1-(triethoxysilyl)propane. The resulting compound was grafted on silica by heating in THF. The modified silica with the monodentate precursor was further treated with chlorodiphenylphosphine and triethylamine in refluxing dichloroethane and immediately transformed into Ru-catalyst by reaction with $[RuCl_2(DMSO)_4]$. For synthesis of the tridentate catalyst, 3-isocyanato-1-(triethoxysilyl)propane was first grafted on silica in refluxing THF and the

resulting material was coupled to a triol precursor of the tripodal ligand to get the modified silica containing triol-precursor. This silica was deprotonated by treatment with lithium hexamethyldisilazane (LiHMDS) in THF at −70 °C and then treated with chlorodiphenylphosphine in the presence of DMAP and refluxed for 1 day. The resulting silica was further reacted with $[RuCl_2(DMSO)_4]$ in refluxing dichloromethane to furnish the tridentate catalyst.

The heterogenized monodentate catalyst was three times more active than the soluble phosphinite-Ru complex, while the heterogenized tridentate catalyst showed almost the same activity. All catalysts showed good selectivity for aldehyde formation (up to 100%). The heterogenized monodentate catalysts could not be efficiently recycled; on the other hand, the heterogenized tridentate catalyst worked for four cycles. Note that for the deprotonation of OH groups, a strong base LiHMDS was utilized during the synthesis of tridentate catalyst. It is possible that the reaction had taken place also with surface SiOH groups during the process. This possibility has not been considered by the authors.

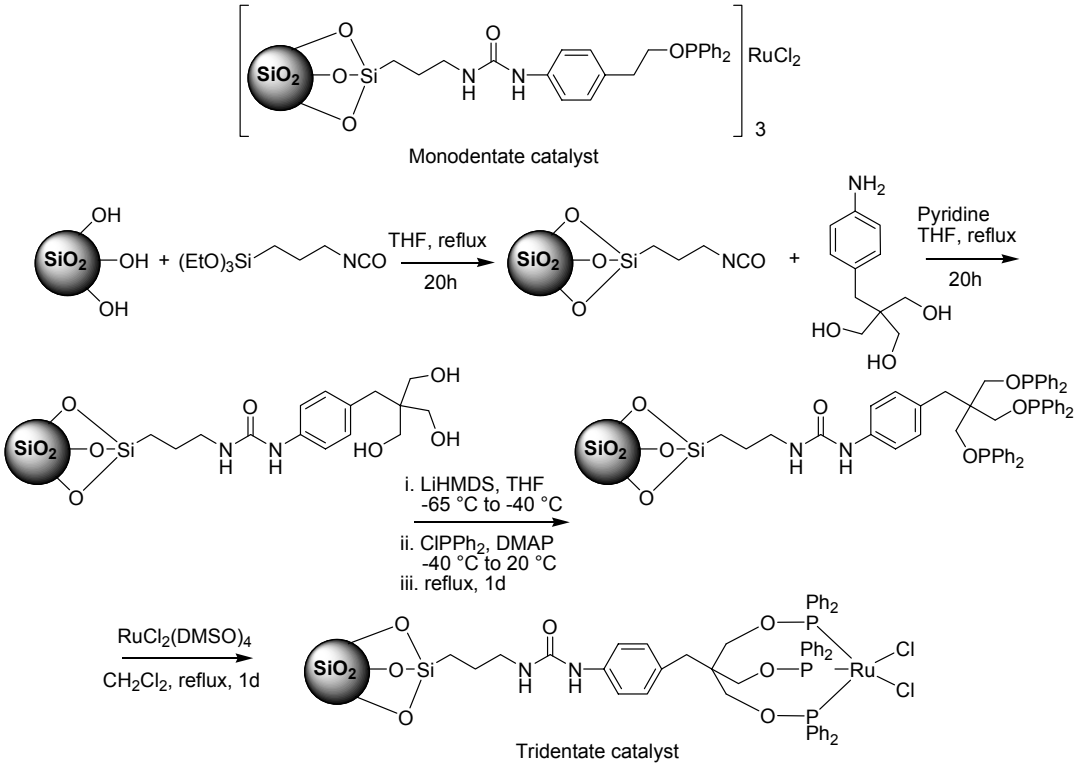

Scheme 3 Immobilization of monodentate and tridentate phosphinite-Ru(II) catalyst.

Li *et al.* have immobilized a chiral tartaric acid derivative onto mesoporous MCM-41 material and to silica.[16] Chiral catalysts were synthesized by reacting these silicas directly with titanium tetraisopropoxide (Scheme 4). These were tested in the enantioselective epoxidation of allylic alcohols and showed a similar activity (TON = 10-14) and selectivity (*ee* = 85%) to that of the homogeneous catalyst. It was concluded that, for the chiral hybrids, the environment surrounding the immobilized species is analogous to that of the homogeneous chiral complexes.

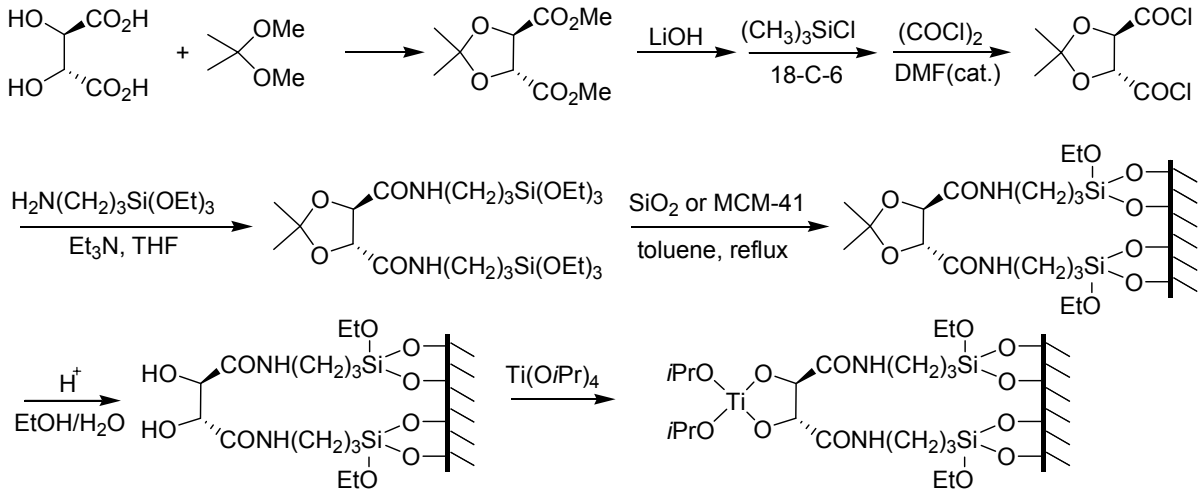

Scheme 4 The synthesis of epoxidation catalyst on the surface of silica.

An unsymmetrical manganese(III) salen complex was anchored onto the surface of MCM-41 by Zhao *et al.* as shown in the Scheme 5.[17] The authors tested the immobilized catalyst under various conditions of temperature, time, molar ratio of isobutyraldehyde (reductant) to alkene, and solvent amount. It showed a relatively high activity and epoxide selectivity in the aerobic epoxidation of cyclohexene, styrene, 1,2-dihydronaphthalene, and α-methylstyrene. The immobilized catalyst can be reused six times. However, the conversion of cyclohexene decreased from more than 99% in the first run to 73.7% in the sixth, while 64.8% of manganese leaching was observed after the sixth run.

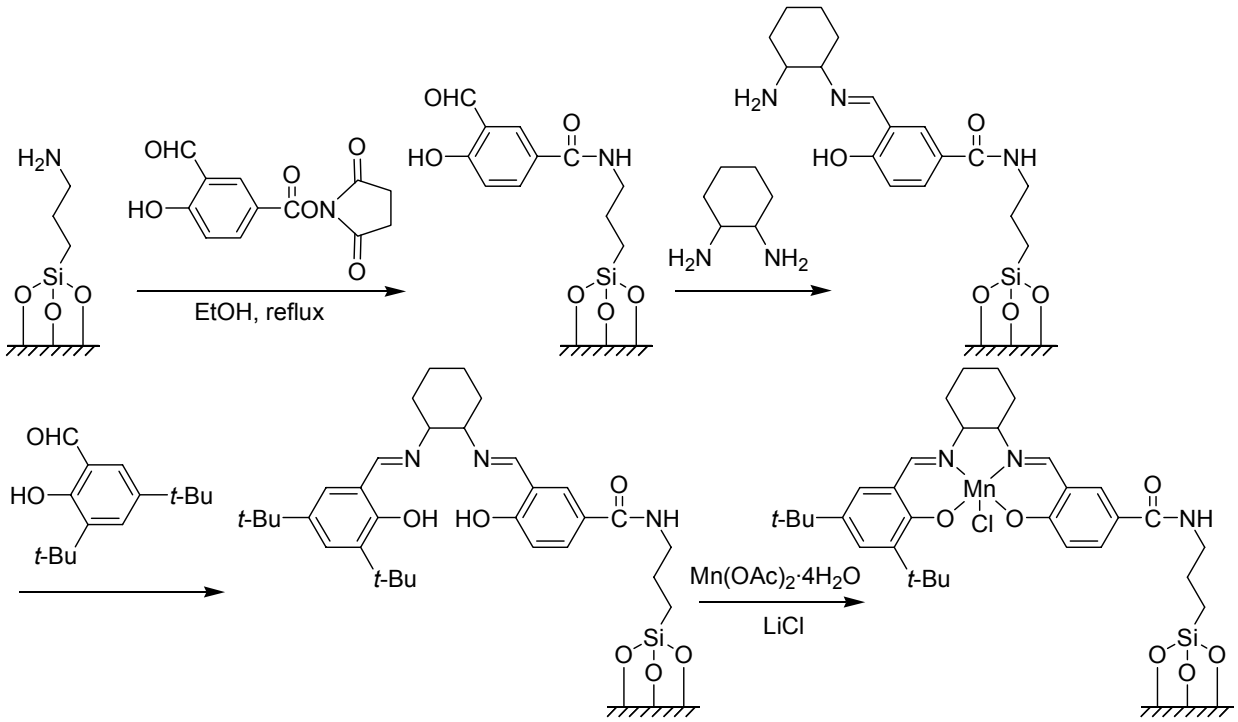

Scheme 5 Synthesis of Mn-salen complex anchored onto MCM-41.

Chiral bisoxazolines were covalently immobilized onto siliceous mesocellular foams (MCF) by Ying *et al.* MCF were partially surface-modified with trimethylsilyl (TMS) groups prior to the immobilization of chiral *t*-butylbisoxazolines (Scheme 6).[18] The resulting MCF-supported

bisoxazoline-Cu(I) catalyst showed superior enantioselectivity (up to 95% *ee*) in asymmetric cyclopropanation, compared to the catalyst supported on MCF with TMS postcapping (capping after immobilization of BOX ligand, up to 90% *ee*) and without TMS capping (up to 82% *ee*). It is proposed that this increased selectivity is due to a diminished interaction between the nitrogen donor atoms of the BOX ligand and surface silanol groups due to precapping. This heterogenized catalyst exhibited excellent recyclability (up to 12 runs) without the loss of any *ee*. Also the *ee* values improved after immobilization as compared to the homogeneous counterpart. These results illustrated that TMS precapping and postcapping of the silica support are both to be considered towards optimizing the enantioselectivity and reactivity of heterogenized catalysts.

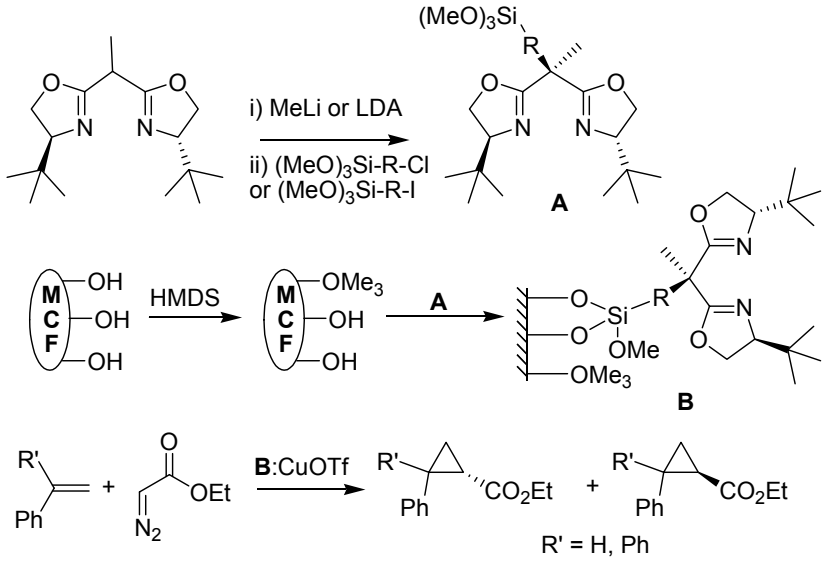

Scheme 6 Chiral bisoxazolines covalently immobilized onto siliceous mesocellular foams.

Constrained Geometry catalysts (CGC) were immobilized on silica and utilized for ethylene polymerization by Jones *et al.*[19] Type A has isolated amine sites whereas type B and C have more densely packed amine sites. This resulted in isolated single sites in A (CGC), whereas, in B and C there are multiple sites as shown (Scheme 7).

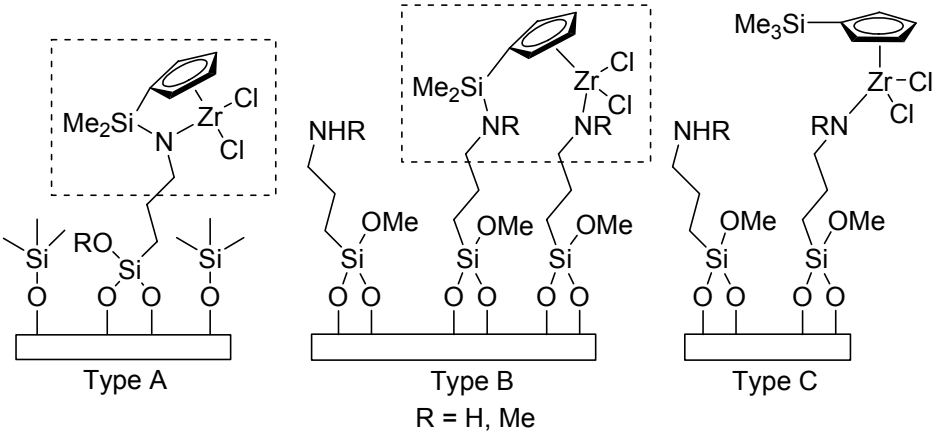

Scheme 7 Single site (CGC) and multiple site Zr-catalysts immobilized on silica.

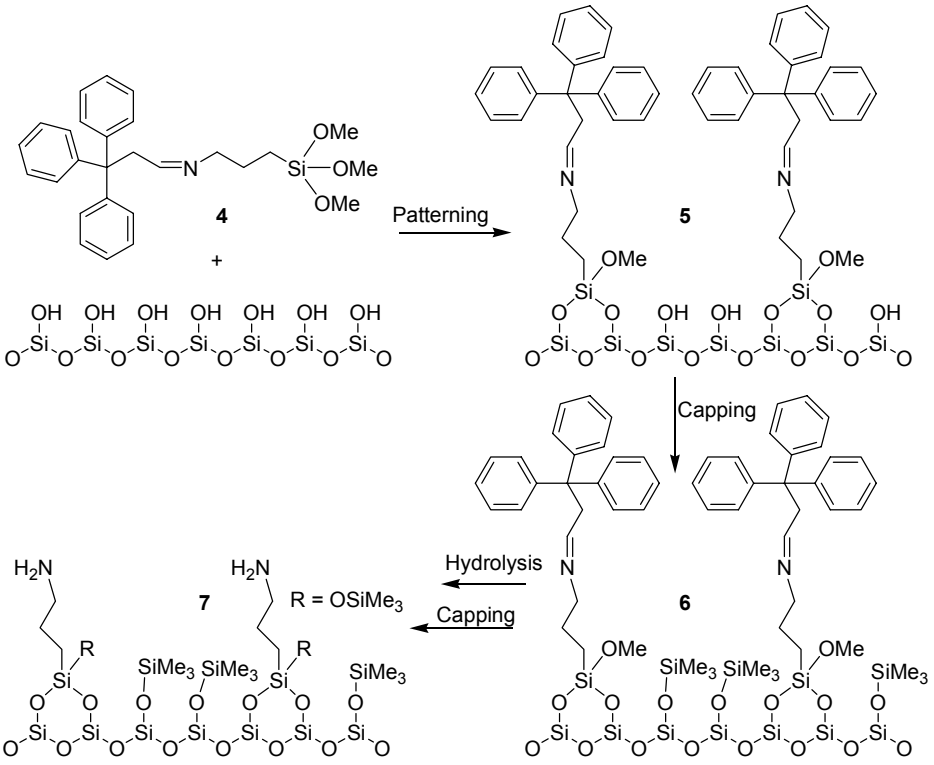

Scheme 8 Synthesis of isolated amine sites on silica.

When these silicas were tested in ethylene polymerization, a higher activity was observed for the catalyst of type A (3086 kg of PE (mol of Zr h)$^{-1}$). Leaching experiments showed no leaching even when the catalyst was treated with $AlMe_3$ or $Al(^iPr)_3$; but after treatment with MAO, leaching was observed. The single-site catalysts are synthesized as shown in the Scheme 8. A patterning molecule (**4**) was designed and synthesized that allows for the effective spacing of aminosilane groups on a silica surface. The large trityl groups on the patterning agent prevent incorporation of the silane on the surface at sites immediately adjacent to each other (**5**). After this functionalization, any additional, unreacted silanols on the surface are covered *via* treatment with hexamethyldisilazane yielding material **6**. The imine bond is then selectively hydrolyzed to remove the trityl groups from the functionalized surface, leaving aminopropyl species on material. A final capping step is used to cover any additional silanol groups that might be produced in the hydrolysis step, giving material **7**. This was further used to prepare catalyst of type A in Scheme 7. Ti-CGC were also supported on these silicas and used in ethylene polymerization.[20] These catalysts also showed higher activity (28.7 kg of PE (mol of Ti h)$^{-1}$) than non-controlled immobilized catalysts.

Sugi *et al.* immobilized pyridine and isoquinoline-carboimine ligands on silica and their Pd(II), Ru(III) and Pt(IV) complexes were prepared and characterized (Scheme 9).[21] Pd(II) based catalysts were tested in Heck and Suzuki reactions. In case of the Heck reaction between 4-bromoacetophenone and methyl acrylate, silica catalysts could be recycled up to 7 cycles without significant loss of activity. However, in case of less reactive aryl bromides, quaternary ammonium salts had to be added in order to increase the activity, which caused significant leaching of Pd.

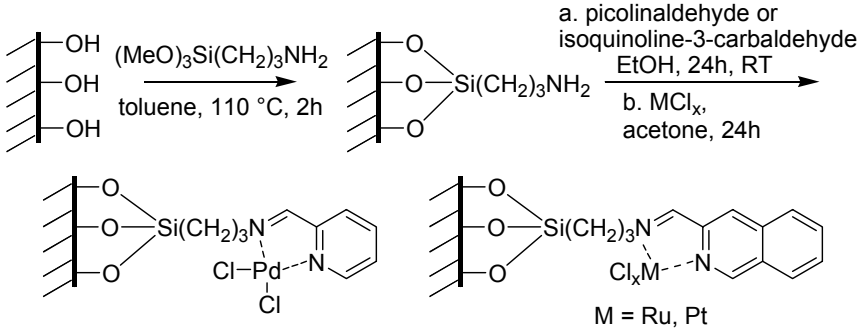

Scheme 9 Silica immobilized carboimine complexes.

For Suzuki reactions, a good activity was observed even for the hindered substrates such as 9-bromoanthracene and 9,10-dibromoanthracene; however, no recycling experiments were carried out. Also Ru and Pt complexes were active in Heck-type reactions with the Pt complexes being less active than the Ru complexes. Leaching of metal was found in both these cases.

Corma *et al.* prepared supported chiral palladium and nickel complexes with Schiff bases as ligands (Scheme 10).[22] Supports used were ordered mesoporous silica (MCM-41), delaminated ITQ-2 and ITQ-6 zeolites, and amorphous silica. Hydrogenation of various alkenes and imines was studied with the heterogenized catalysts. The high accessibility introduced by the structure of the supports allows the preparation of highly efficient immobilized catalysts with TOF's of 1,000,000 h^{-1} for alkene hydrogenation and 600,000 h^{-1} for imine hydrogenation, which were higher than for their homogeneous counterparts. A moderate acidity in the support increased the catalytic activity considerably. The robustness of these catalysts was highlighted when they were recycled over 8 runs without loss of any activity. No deactivation of the catalysts was observed after repeated recycling.

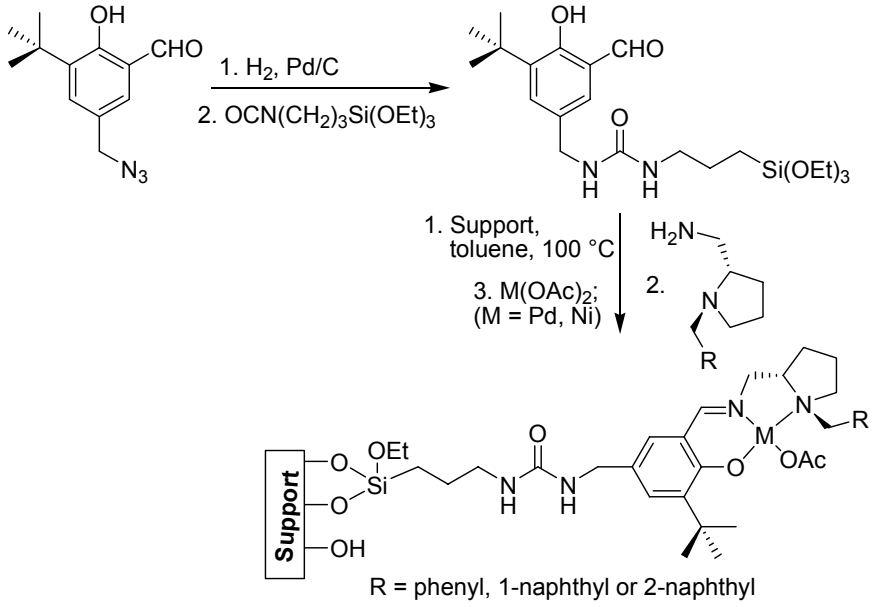

Scheme 10 Immobilization of Schiff base Pd and Ni complexes.

Functionalized Biphemp and MeO-Biphep biaryl diphosphine ligands were covalently attached to silica gel by Pugin *et al*. (Scheme 11).[23] The catalytic performance of the immobilized ligands was

tested in the asymmetric hydrogenation of methyl acetamidocinnamate with Rh and of methyl phenylglyoxylate with Ru and compared with that of the homogeneous analogues.

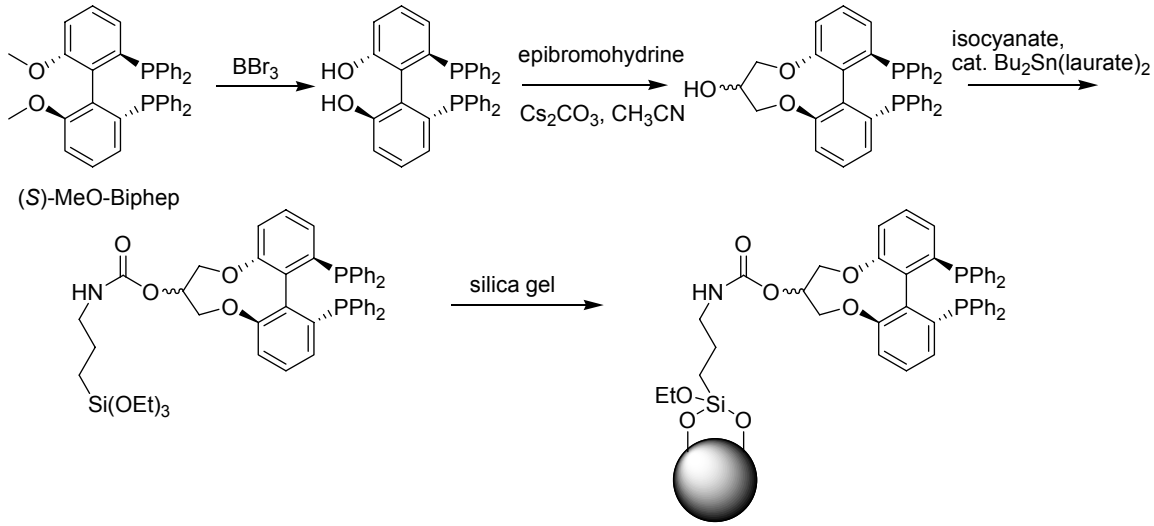

Scheme 11 Immobilization of a MeO-biphep ligand on silica.

In case of the Rh-catalyzed hydrogenation, an increase of *ee* from 29% for the unfunctionalized ligand, to 40% for the functionalized ligand and 45% for the immobilized ligand was observed. TOF's of about 200 h^{-1} were observed for the immobilized catalyst which are comparable to the homogeneous counterpart. Recycling experiments showed a significant drop in the activity, whereas the *ee* was maintained constant. In case of the Ru-catalyzed hydrogenation, functionalization and immobilization did not significantly affect the catalytic properties as compared to the homogeneous counterpart. By adding methanesulfonic acid and LiBr, the best *ee*'s of 90% were obtained for this system with the immobilized MeO-Biphep ligand, which is comparable with those of the homogeneous catalyst. These catalysts could be recycled up to 10 catalytic runs, which showed their robustness as compared to the Rh catalysts.

Tu *et al.* prepared chiral Ru-TsDPEN [*N*-(*p*-toluenesulfonyl)-1,2-diphenylethylene diamine]-derived catalysts which were successfully immobilized onto amorphous silica gel and mesoporous silicas of MCM-41 and SBA-15 (Scheme 12).[24] The catalyst immobilized on silica gel demonstrated remarkably high catalytic activities and excellent enantioselectivities (up to >99% *ee*) for the heterogeneous asymmetric transfer hydrogenation of various ketones. These results were comparable to the results from the homogeneous counterparts. Furthermore, the heterogenized catalyst (on silica gel) could be readily recovered and reused in multiple consecutive catalytic runs (up to 10 uses) with an unaltered enantioselectivity. Surprisingly, the same catalyst immobilized on mesoporous materials (MCM-41 and SBA-15) demonstrated a very poor recyclability although the first run gave similar results as for the silica gel-immobilized catalyst. This could be due to a larger pore size of the silica gel (9.0 nm compared to 1.9 and 6.2 nm for MCM-41 and SBA-15, respectively), which allows better accessibility for the substrate and also because in case of silica gel a higher catalyst

loading was achieved (0.15 as compared to 0.14 and 0.10 mmol/g for MCM-41 and SBA-15, respectively). Another observation was that protection of surface silanol groups with hexamethyldisiloxane (HMDSO) after ligand immobilization rendered the silica gel catalyst with a very poor recycling ability. This could be due to the same reasons (0.12 mmol/g loading and 8.7 nm pore size) as explained above.

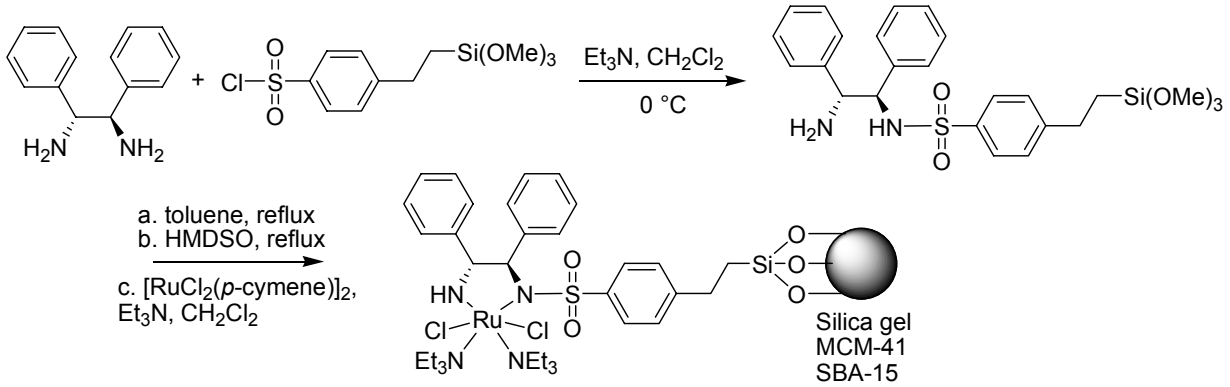

Scheme 12 Immobilization of chiral TsDPEN ligand on silica.

1.2.2. Complex immobilization

In complex immobilization, an intact transition metal complex (catalyst) is grafted onto a support. To this end, one of its ligands is modified in such a way that it provides a tethering group to be utilized for immobilization. If such modification is away from the metal center, the process of immobilization will not influence the metal surrounding and hence the properties of the catalyst. Provided that the complex is stable enough to survive the immobilization process, and the ligands are strong enough not to undergo exchange processes with the surface silanol groups, there will be no other metal to surface interaction. This will lead to a single catalytic species on the surface. Some examples to highlight this approach are presented below.

Herrmann *et al.* synthesized 2,6-bis[1-((2,6-diisopropylphenyl)imino)ethyl]pyridine iron(II) complexes functionalized with varying alkandiyl spacer groups.[25] These were immobilized on a modified silica surface *via* hydrosilation (Scheme 13). These precatalysts were employed in ethene polymerization with MMAO (modified methylaluminoxane) as cocatalyst. All heterogenized precatalysts showed a good polymerization activity in the range of 10^3-10^4 kg of PE/(mol Fe)·h·bar). Analogous to the homogeneous precatalysts, the compound with the shortest alkandiyl moiety, the allyl-functionalized compound **8**, exhibited the lowest activity, whereas the activity increased with increasing length of the alkandiyl chain. The activities decreased at higher temperatures for all heterogenized precatalysts, reaching a minimum activity of only 500 kg of PE/(mol Fe)·h·bar) at 80 °C. However, in comparison to the homogeneous precatalysts, which provided no activity after 45 min. at temperatures higher than 20 °C, the activity of the heterogeneous precatalysts were higher at elevated temperatures. The highest molecular weights were obtained with precatalyst **8**, which has the shortest alkandiyl moiety. An increase of chain length of the alkandiyl moiety decreased the

molecular weight of the produced polymers slightly, so that the lowest molecular weights were obtained by using the heterogeneous precatalyst **10**. For all three supported catalysts no reactor fouling was observed during the whole polymerization process at all polymerization conditions, in contrast to the case for the homogeneous precatalysts.

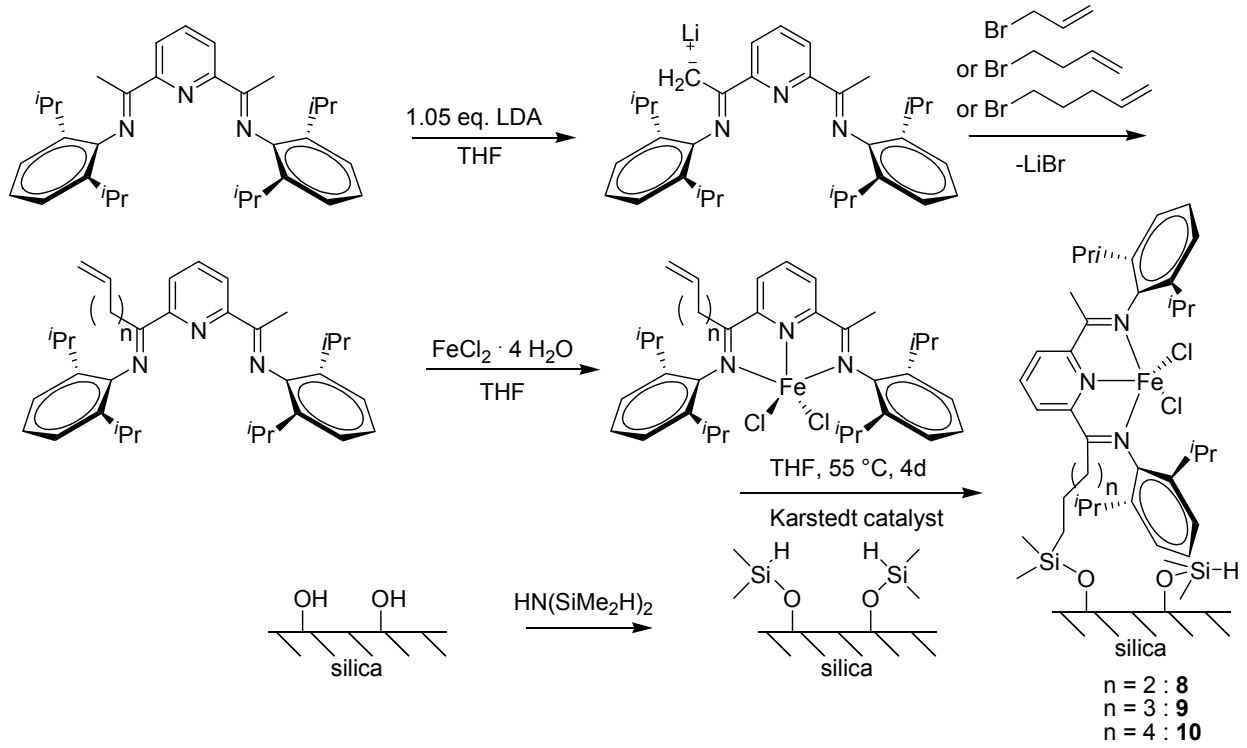

Scheme 13 Preparation of the alkenyl functionalized [bis(imino)pyridyl]iron(II) complexes and their immobilization on a modified silica surface.

Lindner *et al.* have immobilized a modified Vaska's complex in a sol-gel process.[26] A urea linker was formed between a siloxy group and a phosphine by reacting triethoxy(3-isocyanatopropyl)silane with 4-(diphenylphosphino)phenylamine (Scheme 14).

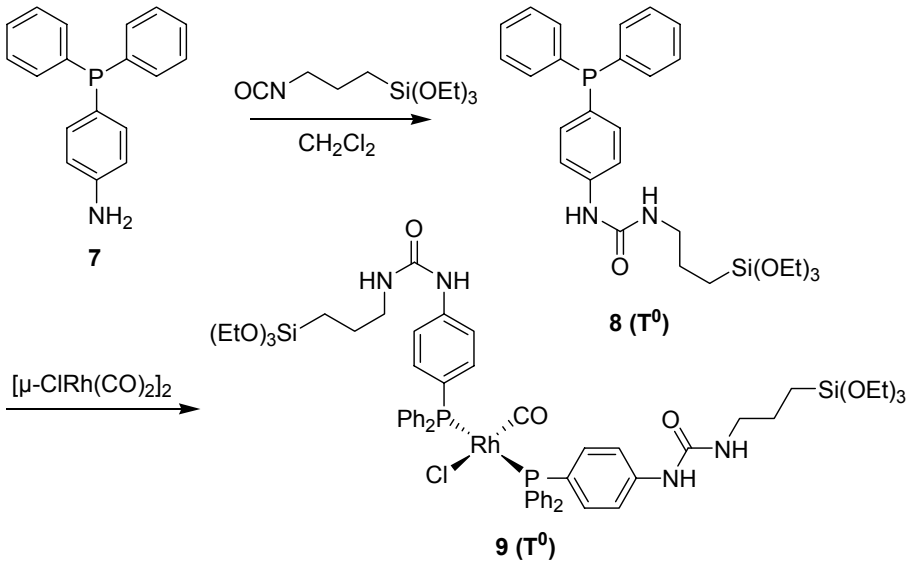

Scheme 14 Synthesis of siloxy-functionalized Vaska's complex.

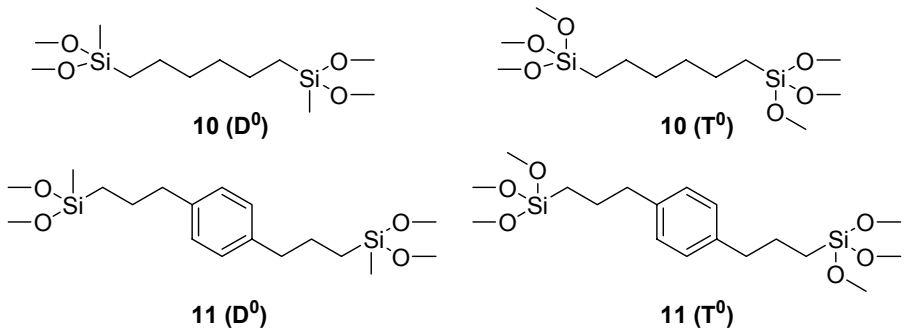

Scheme 15 Various co-condensation agents used in sol-gel processes; **T** = T-type of silicon atom (three oxygen substituents), **D** = D-type of silicon atom (two oxygen substituents).

A modified Vaska's complex was formed upon rection of $[\mu\text{-ClRh(CO)}_2]_2$ with this ligand in which two phosphines were bonded to Rh in *trans*-position (see **9**). This bis-siloxy functionalized complex was used in sol-gel processes with various co-condensation agents carried out in THF with water and TBAF as a condensation catalyst (Scheme 15). The resulting silica-based polymers were utilized in the hydroformylation of 1-hexene. A comparison between these materials under catalytic conditions showed that a higher cross-linkage polymer provided by T-silyl bifunctionalized copolycondensates, was more active in catalysis (xerogel from **9(T^0)**:**10(T^0)** = 1:20 gave TON of 13000 and TOF of 800 h^{-1}) under a pressure of 60 bar. The D-silyl bifunctionalized siloxanes showed a lower activity under these medium pressure conditions. Properties like the swelling capability and the mobility of the different parts of the polymer became less important for catalytic activity of the reactive centers. The accessibility of the reactive centers and thus the catalytic activity increased with the more rigid polymer backbone of T-silyl bifunctionalized co-condensation agents under the described conditions. Furthermore, no metal leaching was observed during the catalysis.

Hermann *et al.* have immobilized organometallic molybdenum complexes on structured silica using both the complex immobilization and the ligand immobilization approach (Scheme 16).[27] η^5-$CpMo(CO)_3R$ complexes with a triethoxysilane coupling group were synthesized and immobilized on the surface of mesoporous silicas. The linker was connected to the complex through either the cyclopentadiene ring or directly to the metal. Additionally, the ligand itself was first immobilized and the modified silica was subsequently reacted with $Na[CpMo(CO)_3]$ as a metal precursor. These silicas were utilized in the epoxidation of cyclooctene using *t*-butyl hydroperoxide as oxidizing agent. Complex-functionalized silicas were found to be more active (TOF's up to 10000, probably due to higher Mo loading), while both materials showed 100% epoxide selectivity. Recycling up to 3 runs was reported with some loss of activity (50%) during subsequent runs, although no catalyst leaching was observed.

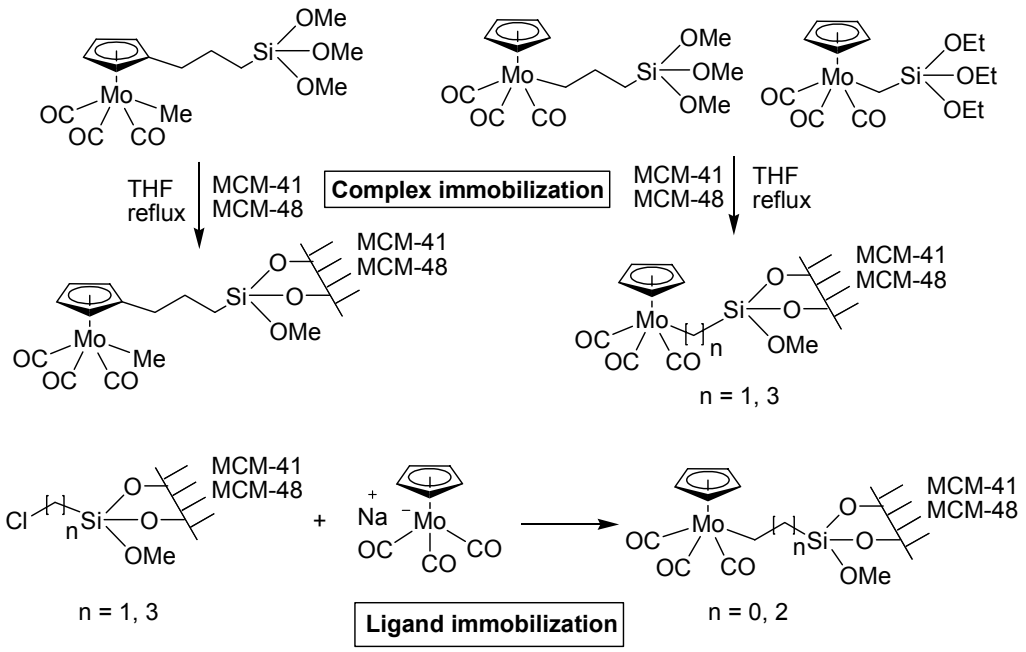

Scheme 16 Immobilization of η^5-CpMo(CO)$_3$R complexes using various approaches.

A chiral vanadyl salen complex containing two siloxy side chains was synthesized by Corma *et al.* and a chiral mesostructured organosilica (ChiMO) was prepared from this complex by using the sol-gel method (Scheme 17).[28]

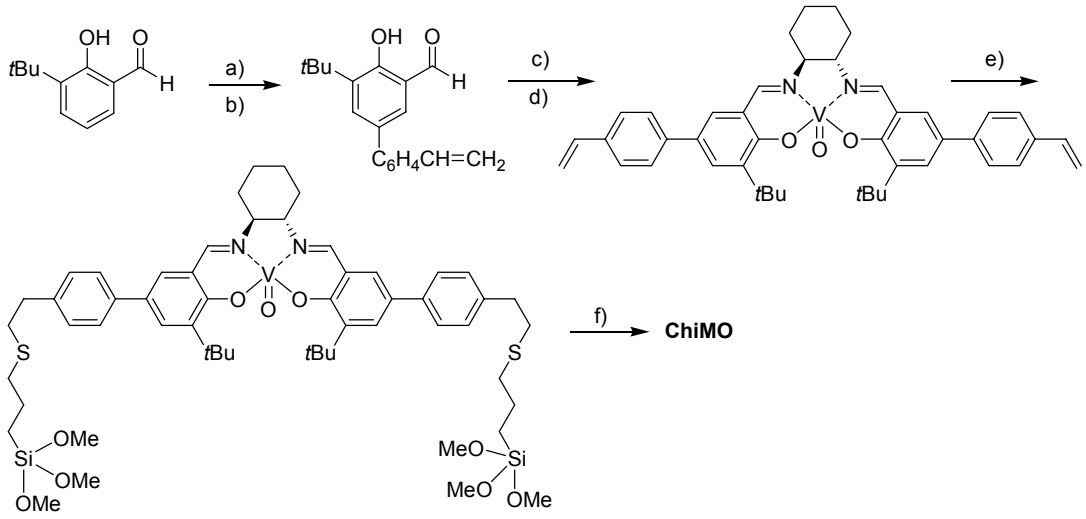

Scheme 17 a) Br_2, CH_2Cl_2, 0 °C, 1 h; b) 4-vinylphenylboronic acid, [$Pd(PPh_3)_4$], 2M Na_2CO_3, THF, 70 °C, 3h; c) (1*R*,2*R*)-diaminocyclohexane, EtOH, reflux, 1h; d) VOacac, MeOH, r.t., overnight; e) 3-mercaptopropyltrimethoxysilane, AIBN, $CHCl_3$ (degassed), 70 °C, 20h; f) TEOS, CTABr, NH_3, H_2O, EtOH, 90 °C, 4d.

TEOS and V-complex were used as a silicon source in various proportions (85:15 and 95:5) and cetyltrimethylammonium bromide (CTABr) was used as a surface-directing agent. The resulting solid had a typical pattern of hexagonal MCM-41-like ordering. From ^{29}Si NMR, it was observed that the complex was covalently immobilized to the inorganic framework through Si atoms of both side chains. A measurement of the optical activity of the solid showed that the material was chiral (–2.54°/g). This material was used in the cyanosilylation of benzaldehyde with TMSCN. A high TON

(320) and a poor enantiomeric excess of 30% was observed (lower than V-salen grafted covalently on MCM-41, 63% *ee*). The catalyst was stable and no leaching was observed according to chemical vanadium analysis.

Metathesis is a very versatile tool in organic synthesis. A lot of interesting compounds particularly relevant to pharmaceutical chemistry can be synthesized by this class of reaction. For this purpose, contamination of products with metal ions and/or ligands needs to be low. Moreover, modern metathesis catalysts significantly add to the total costs of a product. For these reasons, regeneration and/or reuse of the metathesis catalyst are highly desirable.

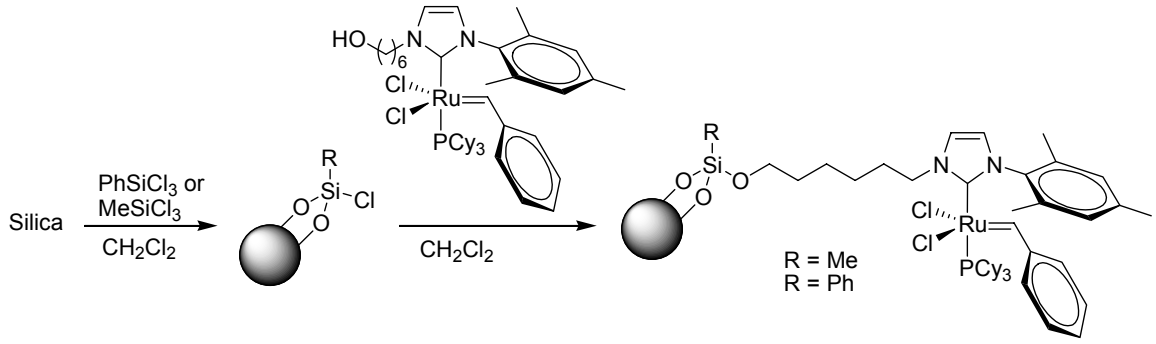

Scheme 18 Immobilization of a second-generation Ru-based metathesis catalyst on silica.

Fürstner *et al.* immobilized "second-generation" ruthenium benzylidene metathesis catalysts (Scheme 18) bearing hydroxyalkyl chains on their N-heterocyclic carbene ligands.[29] They were tested on prototype RCM reactions and although they were found to be less active than the homogeneous catalysts, comparable yields were obtained. These materials could be reused up to three times. A colorless product indicated complete removal of ruthenium species.

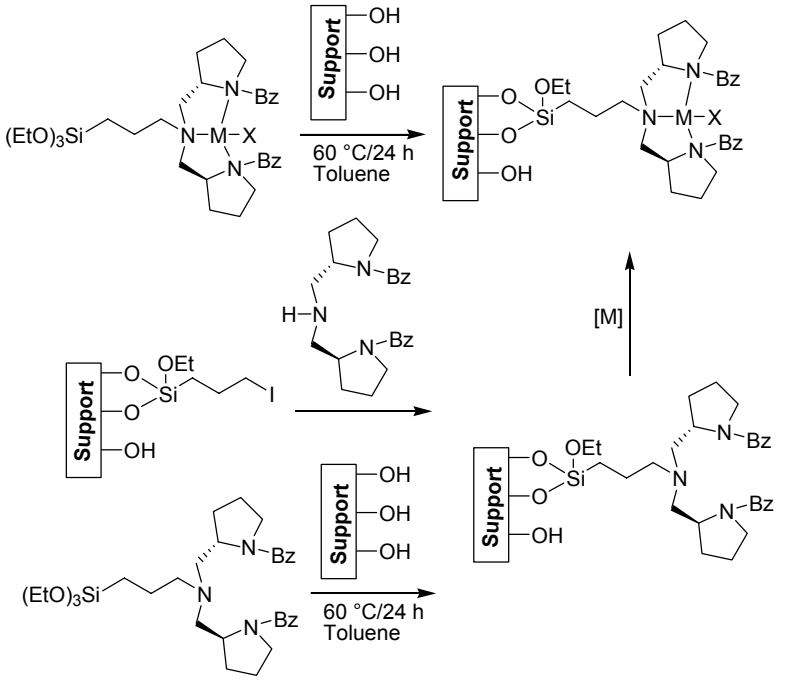

Scheme 19 Heterogenization of triaza complex by covalent bond; **Support**: Silica, MCM-41, ITQ-2, ITQ-6; **[M]**: $[RhCl(cod)]_2$, $[IrCl(cod)]_2$, $[PdCl_2(cod)]$.

Palladium complexes with chiral triaza ligands were immobilized on mesostructured silicates and delaminated zeolites (silica, MCM-41, ITQ-2 and ITQ-6) by Sánchez *et al.* using three different strategies (Scheme 19).[30] The heterogenized complexes were used for the hydrogenation of 2-naphthylidene succinate. The activity of the catalysts on plain silica was found to be similar to that observed under homogeneous conditions. On the other hand, the catalytic activity and selectivity were higher in case of MCM-41 and delaminated zeolites. This has been ascribed to the high surface area of the supports and, as a consequence, a higher accessibility to the reactants. The strength of a stable covalent bond between support and supported complex allowed the recovery and recycling of the supported catalysts for a number of cycles. Atomic absorption analysis of the reaction solutions showed that there was no metal leaching into the solutions. A comparative catalytic study with the respective Rh(I) and Ir(I) complexes for olefin hydrogenation reactions was also given.

Lin *et al.* synthesized siloxy-functionalized Ru-complexes based on 4,4'-substituted BINAP's (Scheme 20).[31] These were immobilized on SBA-15 and the modified mesoporous silica was used for the hydrogenation of β-alkyl β-ketoesters with up to 98.6% *ee* which is comparable to the homogeneous counterpart. In case of β-aryl β-ketoesters the modified silica gave *ee*'s up to 95.2%, which is somewhat lower than the homogeneous counterpart, but much higher than for $[RuCl_2(BINAP)(DMF)_2]$. Silica could be recycled up to 5 times, but in the fourth cycle conversion and *ee* started to drop. This was not due to leaching of Ru and no metal was found to be present in the supernatant. The authors suggested that this drop could be due to the air-sensitivity of the catalytically active Ru-hydride species.

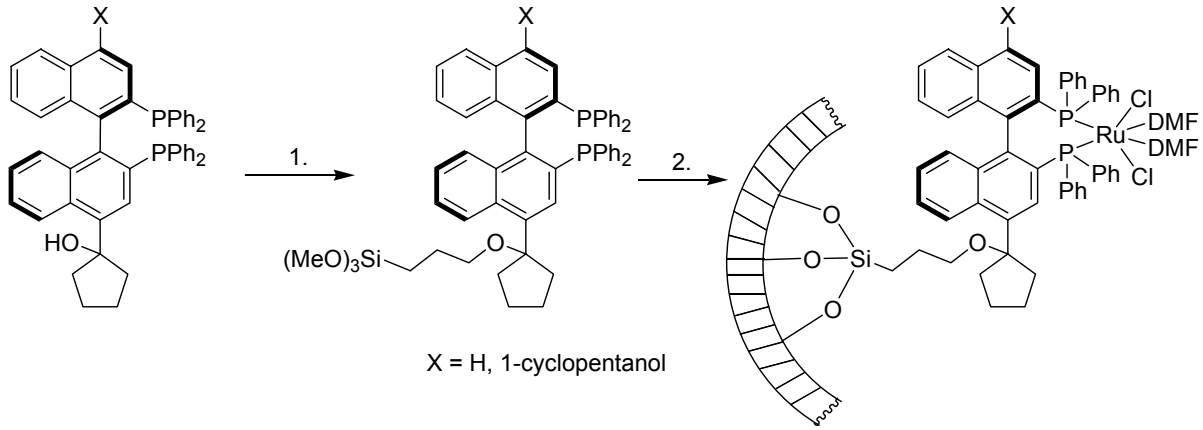

Scheme 20 Immobilization of a Ru-BINAP complex on SBA-15; 1. a) *n*BuLi; b) 3-iodopropyltrimethoxysilane; 2. a) $[RuCl_2(p\text{-cymene})]_2$; DMF, 100 °C; b) SBA-15, toluene, reflux.

1.2.3. Immobilized cyclometalated complexes and their application in catalysis

Corma *et al.* synthesized a preformed oxime–carbapalladacycle complex (**PdL**) which was covalently anchored onto mercaptopropyl modified silica (Scheme 21).[32] This silica was tested in the Suzuki reaction of *p*-chloroacetophenone and phenylboronic acid in water. It was found to be highly active (>99% yield) and no leaching occurred. The catalyst was reused eight times without decrease in activity. Comparison experiments showed that, interestingly, TBAB which is a crucial cocatalyst

for the homogeneous catalysis, was in fact found to be of negative influence for the heterogenized catalyst (62% yield). Also pure water was found to be a much better solvent than a water-dioxane mixture (55% yield).

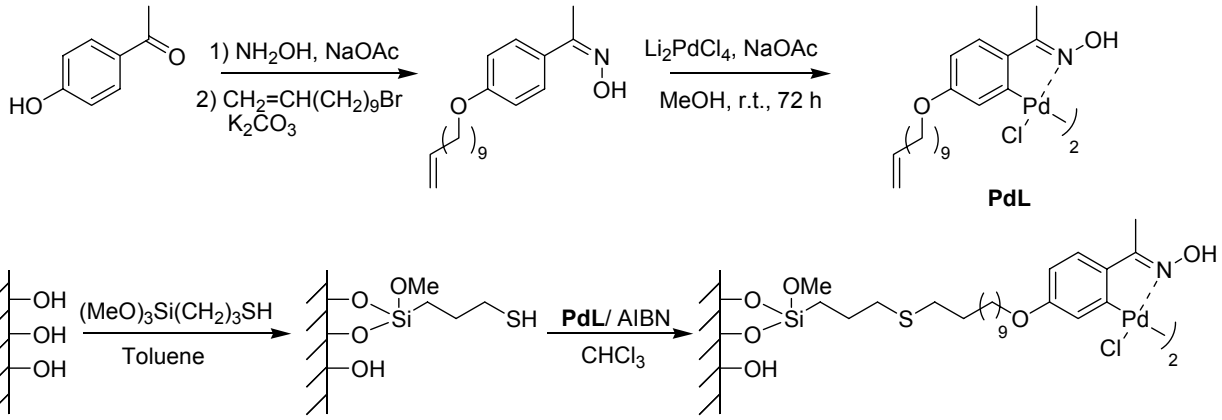

Scheme 21 Anchoring procedure of the oxime carbapalladacycle onto the mercaptopropyl modified high surface silica.

G-0, **G-1** and **G-2** type polyaminoamido (PAMAM) dendrimers were immobilized on silica by Alper *et al.*[33] These dendrimers were then functionalized with PCP-pincer palladium complexes and tested in intramolecular cyclocarbonylation reactions of 2-allylphenol to form lactones (Scheme 22).

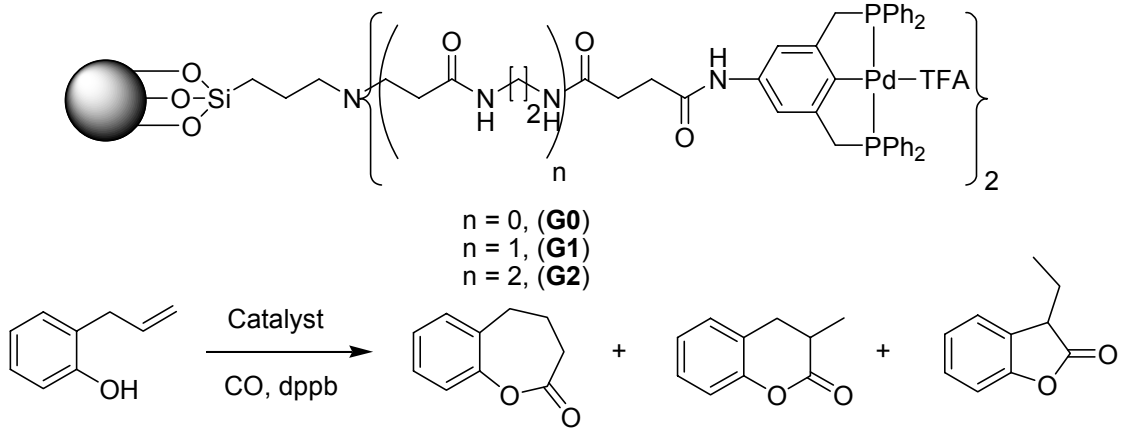

Scheme 22 Silica immobilized generation zero to two (**G0**-**G2**) dendrimers with PCP-pincer complex.

Selectivity could be modified by controlling the CO/H_2 partial pressure (total pressure 600 psi). However, under most of the conditions, the catalysts could be recycled for only 2 runs. **G-2** dendrimer on silica was found to be more active than the rest. Only when the CO/H_2 ratio was 5, silica immobilized **G-0** dendrimer could be recycled up to 5 runs. Catalysis takes place only at 120 °C and above and in presence of external diphosphine (dppb). Exchange of ligands between the PCP complexes and dppb is a key to catalytic activity, but also could lead to leaching and deactivation of the catalyst.

Weck *et al.* immobilized SCS-pincer palladium complexes on silica (Scheme 23).[34] These were utilized in the Heck reaction between iodobenzene and *n*-butyl acrylate. Although silica could be recycled up to three times, catalytic activity was found in the filtrate, indicating leaching of the

catalyst. Moreover, from kinetic experiments and from poisoning studies, it was indicated that the pincer complex is a precursor in this reaction and acts as a source of Pd(0). This species is leached out in the solution by rupture of Pd–C pincer bond. From all the experiments performed, it was evident that there was no catalysis from intact Pd(II) complexes and moreover, it rules out a Pd(II)-Pd(IV) mechanism.

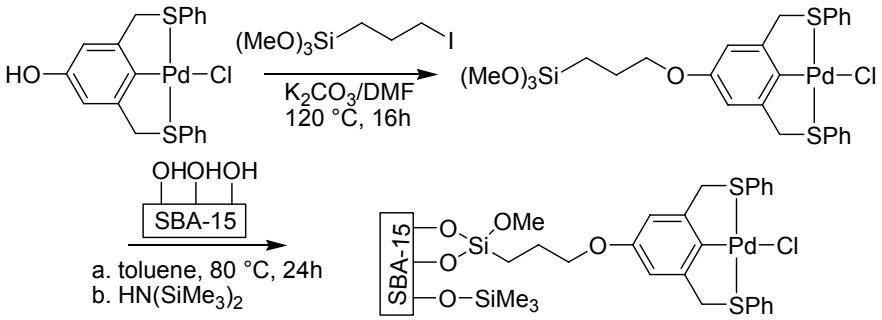

Scheme 23 Silica immobilized SCS-pincer palladium complex.

Swager *et al.* synthesized bimetallic SCS-pincer palladium complexes in which two SCS-pincer palladium units are linked by a chiral spacer in an effort to produce stereo-induction.[35] Two surface-immobilized silicas (**Si1** and **Si2**) were synthesized as shown in Scheme 24.

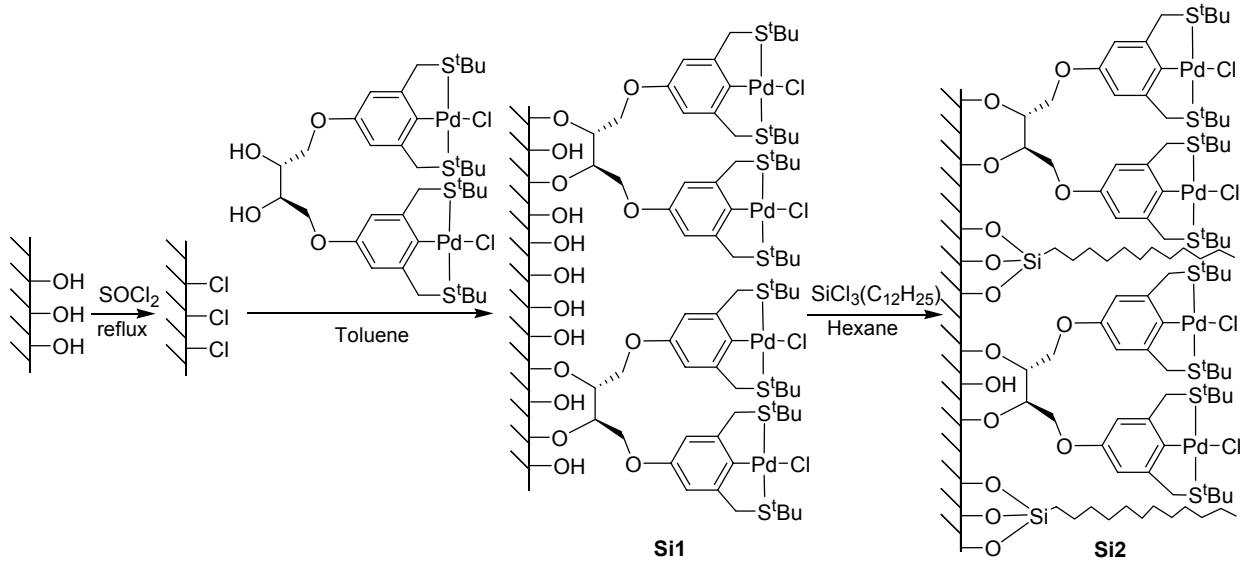

Scheme 24 Immobilization of a chiral SCS-pincer palladium complex onto silica.

Si1 was prepared by treatment of the activated silica gel with the binuclear pincer-palladium complex containing a vicinal diol when a portion of the surface chloride groups are replaced with the binuclear palladium complex. In the second step of the procedure to produce **Si2**, the silica gel **Si1** is treated with dodecyltrichlorosilane to cap all of the remaining free Si–OH surface hydroxyl groups. The homogeneous as well as immobilized catalysts were tested in aldol reactions of methyl isocyanoacetate with aldehydes (isobutyraldehyde and benzaldehyde) and ethyl methyl ketone. The supported catalysts gave similar activity and selectivity as that of the solution species, although the

enantioselectivity observed by the immobilized catalysts was very low (< 2-3%). Recycling and leaching behavior of the immobilized catalysts was not reported.

1.3. Conclusions and Outlook

Better catalyst recycling has a direct positive impact on the economy of catalytic processes that are carried out in a batchwise fashion. As environmental regulations become gradually more and more stringent, catalytic processes in general and catalyst recycling in particular will gain importance. Research in this area will be focused among others on the following issues.

Although many catalysts exist for a variety of industrial processes, there is always a scope for improvement in terms of higher activity and selectivity, higher turn-over numbers, catalyst separation and recycling. As newer generations of catalysts are developed by novel ligand design to achieve higher activity, selectivity and TON's, the obvious next step would be to immobilize these catalysts to facilitate product purification and subsequent catalyst reuse. This immobilization has to be accomplished without loss of any of the original properties of the catalyst. Ideally, as some of the examples above demonstrate, a higher activity and selectivity could emerge from the heterogenization process because of favorable interplay between unique properties of the surface and the anchored catalyst. Particularly, when structured mesoporous silicas or zeolites are used, the high surface area of these materials allows an improved interaction of catalyst and substrate to the effect that mass-transfer effects are reduced. Moreover, as the catalyst is molecularly dispersed it is less likely to undergo self-degradation.

Existing approaches of catalysts recycling have several challenges to overcome before they become viable for application in an industrial context, which comprises specifically the occurrence of metal leaching and ligand degradation during long-term use. The development of more robust catalyst is desirable to overcome these problems. One way of achieving this is by employing catalysts with a strong M–C bond which will ensure less leaching.

Finally, a precise knowledge of the pathways by which a catalyst acts and the conditions that cause catalyst decomposition is required. Gathering this knowledge for heterogenized catalysts is still difficult. However, new and powerful spectroscopic techniques are presently developed which will allow eventually to learn more about the intimate details of these processes.[36]

1.4. Aim and Scope of this Thesis

ECE-pincer metal complexes (ECE = $[C_6H_3(CH_2E)_2\text{-}2,6]^-$, E = NMe_2, PPh_2 and SPh) are a versatile class of compounds which among others are interesting catalysts to achieve a variety of synthetically useful C–C and C–X bond formation reactions. In this thesis, we have made use of their robust nature to immobilize them on various types of silica supports. In order to test the performance of

these immobilized pincer-metal complexes, they were utilized in catalysis and recycling experiments.

Chapter 1 describes the various approaches depicted in the literature for the immobilization of homogeneous catalysts on silicas. The reason for continued interest to heterogenize homogeneous catalysts is their much easier recovery from product solutions as well as the possibilities to reuse the catalytic material in subsequent reactions.

Chapter 2 describes the synthesis of siloxane-functionalized pincer complexes. NCN-pincer palladium and platinum as well as PCP- and SCS-pincer palladium complexes with a *para*-hydroxy functionality were synthesized. The resulting molecules show interesting H-bonding properties which lead to molecular chains in the solid state. These ECE-pincer metal complexes were tethered *via* the *para*-OH group to triethoxysilyl groups to facilitate immobilization on silica surfaces. The structure of an NCN-pincer platinum analog in the solid state was determined by single crystal X-ray diffraction analysis.

Chapter 3 deals with immobilization of siloxane-functionalized NCN-pincer palladium and platinum complexes on a silica surface. Various commercial silicas differing in pore diameter and particle size were utilized. Different protocols of silica immobilization (grafting and sol-gel) were used and the materials were tested as catalysts in aldol reaction (1) between benzaldehyde and methyl isocyanoacetate.

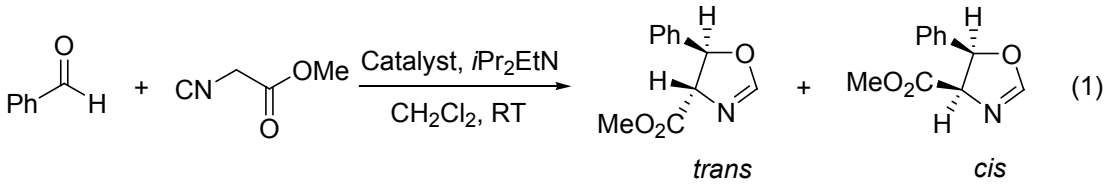

In *Chapter 4*, SCS- and PCP-pincer palladium complexes with a siloxane tether were immobilized on the structured silicas MCM-41 and SBA-15. The influence of complex grafting on the silica was studied in detail using various techniques such as N_2-adsorption, XRD and TEM. [PdCl(PCP)] immobilized on SBA-15 showed a persistent activity in aldol reaction (1) upon recycling.

In *Chapter 5*, the insertion reaction of isocyanides in the Pd–C bond of ECE-pincer palladium complexes has been studied. These reactions take place rapidly for the NCN- and SCS-pincer complexes and form metallo-imidoyl complexes at room temperature.

Chapter 6 depicts the activity of the imidoyl insertion complexes derived from NCN- and SCS-pincer palladium complexes in aldol reaction (1). The fact that these insertion complexes are formed very rapidly from pincer palladium complexes in presence of isocyanides and catalyze aldol reaction (1) indicates that the actual catalytic species in the pincer-based aldol reaction are these imidoyl complexes, which are formed at the onset of the catalytic process.

In *Chapter 7*, a new unsymmetrically substituted PCS-pincer palladium complex with one phosphine and one thiol donor, *ortho*-substituted to the central Pd–C bond, was synthesized. A study of the

effect of the different S–Pd and P–Pd coordination strength on the isocyanide insertion process was carried out. The resulting PCS-imidoyl complexes showed an enhanced activity in aldol reaction (1) as compared to both symmetric SCS- and PCP-pincer palladium complexes.

Finally in *Chapter 8*, the role of silver salts as catalysts in aldol reaction (1) has been studied. The formation of Ag-isocyanide complexes from Ag-salts and methyl isocyanoacetate was investigated. It appeared that these complexes are active catalysts themselves. This result questions the utilization of Ag-salts to generate cationic palladium complexes that are commonly used both as homogeneous and as heterogeneous catalysts in aldol reaction (1) in the literature.

1.5. References

1. R. A. van Santen, P. W. N. M. van Leeuwen, J. A. Moulijn, B. A. Averill, *Catalysis: An Integrated Approach*, Second ed., Elsevier, Amsterdam, **1999**.
2. H.-U. Blaser, A. Indolese, A. Schnyder, *Curr. Sci.* **2000**, *78*, 1336-1344.
3. B. Cornils, W. A. Herrmann, *J. Catal.* **2003**, *216*, 23-31.
4. F. R. Hartley, *Supported Metal Complexes*, Kluwer Academic, Dordrecht, **1985**.
5. C. E. Song, D. H. Kim, D. S. Choi, *Eur. J. Inorg. Chem.* **2006**, 2927-2935.
6. D. J. Cole-Hamilton, *Science* **2003**, *299*, 1702-1706.
7. D. E. Bergbreiter, *Chem. Rev.* **2002**, *102*, 3345-3384; T. J. Dickerson, N. N. Reed, J. K. D., *Chem. Rev.* **2002**, *102*, 3325-3344; Y. R. de Miguel, E. Brulé, R. G. Margue, *J. Chem. Soc., Perkin Trans. 1* **2001**, *23*, 3085-3094; Y. R. de Miguel, *J. Chem. Soc., Perkin Trans. 1* **2000**, *24*, 4213-4221; J. Y. Ying, C. P. Mehnert, M. S. Wong, *Angew. Chem., Int. Ed.* **1999**, *38*, 56-77; D. Brunel, N. Bellocq, P. Sutra, A. Cauvel, M. Laspéras, P. Moreau, F. Di Renzo, G. Anne, F. François, *Coord. Chem. Rev.* **1998**, *178-180*, 1085-1108; J. H. Clark, D. J. Macquarrie, *Chem. Commun.* **1998**, 853-860.
8. C. E. Song, S. Lee, *Chem. Rev.* **2002**, *102*, 3495-3524.
9. A. Choplin, F. Quignard, *Coord. Chem. Rev.* **1998**, *178-180*, 1679-1702.
10. R. van de Coevering, M. Kuil, R. J. M. Klein Gebbink, G. van Koten, *Chem. Commun.* **2002**, 1636-1637; G. Rodriguez, M. Lutz, A. L. Spek, G. van Koten, *Chem. Eur. J.* **2002**, *8*, 45-57; R. Kreiter, A. W. Kleij, R. J. M. Klein Gebbink, G. van Koten, *Top. Curr. Chem.* **2001**, *217*, 163-199; C. Schlenk, A. W. Kleij, H. Frey, G. van Koten, *Angew. Chem., Int. Ed.* **2000**, *39*, 3445-3447.
11. G. P. M. van Klink, H. P. Dijkstra, G. van Koten, *C. R. Chim.* **2003**, *6*, 1079-1085; H. P. Dijkstra, N. Ronde, G. P. M. van Klink, D. Vogt, G. van Koten, *Adv. Synth. Catal.* **2003**, *345*, 364-369; H. P. Dijkstra, G. P. M. van Klink, G. van Koten, *Acc. Chem. Res.* **2002**, *35*, 798-810; H. P. Dijkstra, M. D. Meijer, J. Patel, R. Kreiter, G. P. M. van Klink, M. Lutz, A. L. Spek, A. J. Canty, G. van Koten, *Organometallics* **2001**, *20*, 3159-3168; U. Kragl, T. Dwars, *Trends Biotechnol.* **2001**, *19*, 442-449.
12. R. Sheldon, *Chem. Commun.* **2001**, 2399-2407; W. Leitner, *C. R. Chimie* **2000**, *3*, 595-600.
13. J. M. Thomas, R. Raja, D. W. Lewis, *Angew. Chem., Int. Ed.* **2005**, *44*, 6456-6482; N. End, K.-U. Schoening, *Top. Curr. Chem.* **2004**, *242*, 241-271; J. M. Thomas, R. Raja, *J. Organomet. Chem.* **2004**, *689*, 4110-4124; F. Quignard, A. Choplin, *Compr. Coord. Chem. II* **2004**, *9*, 445-470; P. McMorn, G. J. Hutchings, *Chem. Soc. Rev.* **2004**, *33*, 108-122; L.-X. Dai, *Angew. Chem., Int. Ed.* **2004**, *43*, 5726-5729; J. M. Basset, J. P. Candy, C. Coperet, F. Lefebvre, E. A. Quadrelli, *Nanotech. Catal.* **2004**, *2*, 447-466; S. L. Scott, E. W. Deguns, *Nanostructured Catal.* **2003**, 1-14; D. E. De Vos, M. Dams, B. F. Sels, P. A. Jacobs, *Chem. Rev.* **2002**, *102*, 3615-3640; D. E. De Vos, I. F. J. Vankelecom, P. A. Jacobs, *Chiral Catalyst Immobilization and Recycling*, Wiley-VCH, Weinheim, Germany, **2000**.
14. A. Heckel, D. Seebach, *Chem. Eur. J.* **2002**, *8*, 559-572.
15. E. Dulière, M. Devillers, J. Marchand-Brynaert, *Organometallics* **2003**, *22*, 804-811.
16. S. Xiang, Y. Zhang, Q. Xin, C. Li, *Angew. Chem., Int. Ed.* **2002**, *41*, 821-824.
17. Y. R. Zhang, J. Q. Zhao, L. Q. He, D. M. Zhao, S. M. Zhang, *Microporous Mesoporous Mater.* **2006**, *94*, 159-165.
18. S. S. Lee, S. Hadinoto, J. Y. Ying, *Adv. Synth. Catal.* **2006**, *348*, 1248-1254; S. S. Lee, J. Y. Ying, *J. Mol. Catal. A* **2006**, *256*, 219-224.
19. K. Yu, M. W. McKittrick, C. W. Jones, *Organometallics* **2004**, *23*, 4089-4096.
20. M. W. McKittrick, C. W. Jones, *J. Am. Chem. Soc.* **2004**, *126*, 3052-3053; M. W. McKittrick, C. W. Jones, *J. Catal.* **2004**, *227*, 186-201.

21. J. Horniakova, T. Raja, Y. Kubota, Y. Sugi, *J. Mol. Catal. A* **2004**, *217*, 73-80; J. Horniakova, H. Nakamura, R. Kawase, K. Komura, Y. Kubota, Y. Sugi, *J. Mol. Catal. A* **2005**, *233*, 49-54.
22. C. González-Arellano, A. Corma, M. Iglesias, F. Sánchez, *Adv. Synth. Catal.* **2004**, *346*, 1316-1328.
23. I. Steiner, R. Aufdenblatten, A. Togni, H.-U. Blaser, B. Pugin, *Tetrahedron: Asymmetry* **2004**, *15*, 2307-2311.
24. P. N. Liu, P. M. Gu, F. Wang, Y. Q. Tu, *Org. Lett.* **2004**, *6*, 169-172.
25. F. A. R. Kaul, G. T. Puchta, H. Schneider, F. Bielert, D. Mihalios, W. A. Herrmann, *Organometallics* **2002**, *21*, 74-82.
26. E. Lindner, T. Salesch, S. Brugger, F. Hoehn, P. Wegner, H. A. Mayer, *J. Organomet. Chem.* **2002**, *641*, 165-172.
27. A. Sakthivel, J. Zhao, M. Hanzlik, A. S. T. Chiang, W. A. Herrmann, F. E. Kuehn, *Adv. Synth. Catal.* **2005**, *347*, 473-483.
28. C. Baleizão, B. Gigante, D. Das, M. Alvaro, H. Garcia, A. Corma, *Chem. Commun.* **2003**, 1860-1861.
29. S. Prühs, C. W. Lehmann, A. Fürstner, *Organometallics* **2004**, *23*, 280-287.
30. C. González-Arellano, A. Corma, M. Iglesias, F. Sánchez, *Catal. Today* **2005**, *107-08*, 362-370.
31. B. Kesanli, W. B. Lin, *Chem. Commun.* **2004**, 2284-2285.
32. C. Baleizão, A. Corma, H. Garcia, A. Leyva, *Chem. Commun.* **2003**, 606-607.
33. R. Chanthateyanonth, H. Alper, *Adv. Synth. Catal.* **2004**, *346*, 1375-1384.
34. K. Yu, W. Sommer, M. Weck, C. W. Jones, *J. Catal.* **2004**, *226*, 101-110.
35. R. Gimenez, T. M. Swager, *J. Mol. Catal. A* **2001**, *166*, 265-273.
36. B. M. Weckhuysen, P. Van Der Voort, G. Catana, *Spectroscopy of transition metal ions on surfaces*, Leuven University Press, Belgium, **2000**.

Chapter 2

Self-Assembly and Polymerization of *Para*-OH Functionalized ECE-Metalated Pincer Complexes

Abstract

Various *para*-OH functionalized ECE-pincer metal complexes [MX(ECE-OH)L_n] (ECE-OH = $[C_6H_2(CH_2E)_2$-2,6-OH-4$]^-$, E = NMe_2, PPh_2 and SPh) were synthesized. The X-ray crystal structures of neutral [PdCl(SCS-OH)], [PdCl(NCN-OH)], and cationic [Pd(PCP-OH)(MeCN)](BF_4) are reported. The neutral halide complexes exhibit self-assembly to form polymeric chains *via* H-bonding involving the *para*-OH group as donors and the halide ligand on the metal as acceptors. Moreover, the halide ligand can be replaced by a monomeric aryloxy-O ligand leading to the formation of a covalently bonded dimer. The crystal structure of such a dimer derived from [PdI(NCN-OH)] is reported.

Furthermore, these pincer-metal complexes were tethered through a carbamate linker to a siloxane functionality with the aim to be immobilized on a silica support. The crystal structure of a siloxane-functionalized [PtI(NCN-Z)] complex exemplifies how other H-bonding interactions not involving the metal-halide groupings can lead to polymeric networks as well.

2.1. Introduction

ECE-pincer metal complexes [MX(ECE-Z)L_n] (ECE-Z = [$C_6H_2(CH_2E)_2$-2,6-Z-4]$^-$, E = NMe_2, PPh_2 and SPh) with a *para*-functionality (Z) on the aromatic ring of the pincer anion are well known.[1-9] Electronic properties of the metal center can be tuned by inductive and mesomeric effects of this substituent.[10] Ample evidence has been gathered to show that *via* the nature of the Z-substituent, also catalytic properties of the pincer complex can be affected.[2,11,12] Furthermore, Z can be used to attach tethering groups which are suited to immobilize pincer-metal complexes to various supports, like polymers,[3,13-15] silica,[16] dendrimers,[17,18] and bucky-balls,[19] or peptides,[6,20] and enzymes.[21]

The Z-substituent can be introduced on the monoanionic ECE-ligand manifold prior to the binding of the metal, *i.e.* first the organic ligand is synthesized followed by a lithiation, *trans*-metalation, or oxidative addition reaction to attach the metal to the pincer ligand system. In many cases it could be demonstrated, however, that due to the stability of the pincer-metal grouping, it is possible to perform the *para*-functionalization directly on the ECE-pincer metal complex itself.[5,22] In the present study, we have taken advantage of the excellent stability and reactivity properties of ECE-pincer metal complexes and show that a *para*-OH substituent (Z = OH) on these complexes can be utilized for various purposes; *e.g.* for the formation of NCN-pincer metal polymers *via* non-covalent H-bonding as well as for the synthesis of siloxane-functionalized compounds which can be immobilized on silica.

Self-assembly of functionalized pincer-metal complexes controlled by H-bonding through a H-donor (Z-substituent) and a H-acceptor site (M–X) both in the solid state and in solution has led to the finding of interesting polymers[23] and supramolecular structures.[4,8,24-27] For example, NCN-pincer Pt-complexes [PtCl(NCN-Z)] with Z = OH or C≡C–H form one-dimensional polymeric chains *via* intermolecular hydrogen bonds of the O–H···Cl[8] or C≡C–H···Cl[4,27] type, respectively, in the solid state. These materials revealed reversible binding of SO_2 in the solid-state with retention of the polymeric structure.[25,28] Here, we have extended this concept to ECE-pincer Pd-complexes which are also known to be excellent catalysts for C–C and C–X bond formation reactions.[5,11,15,18,20,29] Interestingly, these ECE-pincer Pd-complexes likewise form polymeric structures *via* non-covalent H-bonding (**A**, Figure 1). Moreover, we demonstrate how the zwitterionic species formed by HX elimination self-assemble to oligomeric structures via covalent M–O bonding (**B**, Figure 1).[30]

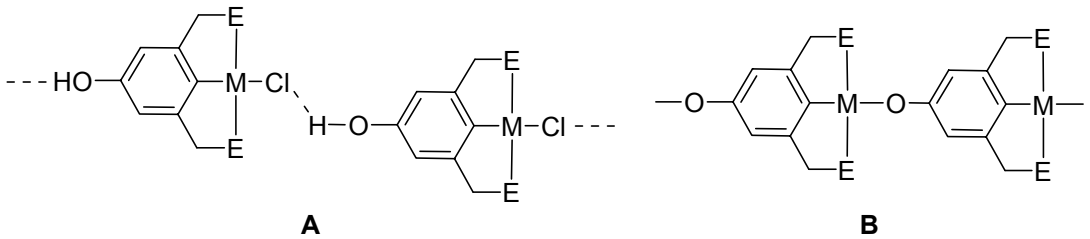

A **B**

Figure 1 Self-assembled polymers (**A**) *via* non-covalent H-bonding. Oligomers (**B**) *via* covalent M–O bonding.

2.2. Results and Discussion

2.2.1. Synthesis of (ECE-OH)-pincer Pt- and Pd-complexes

Synthesis of the (ECE-OH)-pincer arene ligands **3**-**5** was initiated from *t*-butyldimethylsilyl-protected 3,5-bis(hydroxymethyl)phenol precursor **1** as shown in Scheme 1.

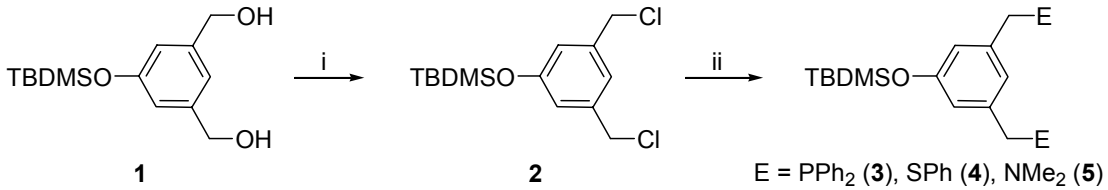

Scheme 1 Synthesis of (ECE-OH)-pincer arene ligands; i. $MeSO_2Cl$, NEt_3, CH_2Cl_2, RT, 16 h; ii. a. $LiPPh_2$, THF; b. NaSPh, THF; or c. $HNMe_2$, NEt_3, THF.

This compound was synthesized from 5-hydroxy-isophthalic acid by a reported procedure in three steps.[9,14,31] Precursor **1** was converted to the bis-chloride **2** by a reaction with methane sulfonyl chloride followed by a simple treatment with suitable reagents ($LiPPh_2$, NaSPh, or Me_2NH) to afford the respective ECE-pincer arene ligand (E = PPh_2 **3**, SPh **4**, NMe_2 **5**). For the synthesis of (SCS-OH)- and (PCP-OH)-pincer Pd-complexes **6** and **7**, a direct bis-(*ortho*)-palladation route was used involving regioselective C–H activation using $[Pd(MeCN)_4](BF_4)_2$ as the palladating reagent (Scheme 2).[9]

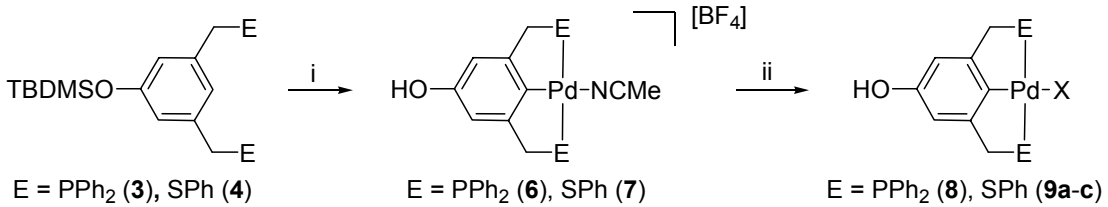

Scheme 2 PCP- and SCS-pincer Pd-complexes by a direct bis-(*ortho*)-palladation route; i. $[Pd(MeCN)_4](BF_4)_2$, MeCN; ii. NaX, CH_2Cl_2/H_2O (**8**, **9a**: X = Cl; **9b**: X = Br; **9c**: X = I).

In this reaction HBF_4 is generated as a co-product which, in a subsequent reaction, leads to complete deprotection of the 4-$OSiMe_2t$Bu group. This avoids the deprotection step which otherwise would be necessary as is the case for the NCN-pincer complex. Further treatment of cationic (ECE-OH)-pincer Pd-complexes **6** and **7** with halide salts yielded the corresponding neutral ECE-pincer Pd-halide complexes **8** (X = Cl) and **9** (X = Cl (**9a**), Br (**9b**) and I (**9c**)).

The direct palladation route is not regioselective in the case of NCN-pincer ligands as both *ortho-ortho* and *ortho-para* palladation takes place.[32] Here, the use of an *ortho-ortho* directing group such as a trimethylsilyl one allows regioselective bis-(*ortho*)-palladation (Scheme 3).[33] In this reaction, the tBuMe$_2$Si protection is not affected by the cyclopalladation reaction and has to be removed subsequently. The corresponding platinum complex **14a** was prepared by a published procedure (Scheme 3).[26,31]

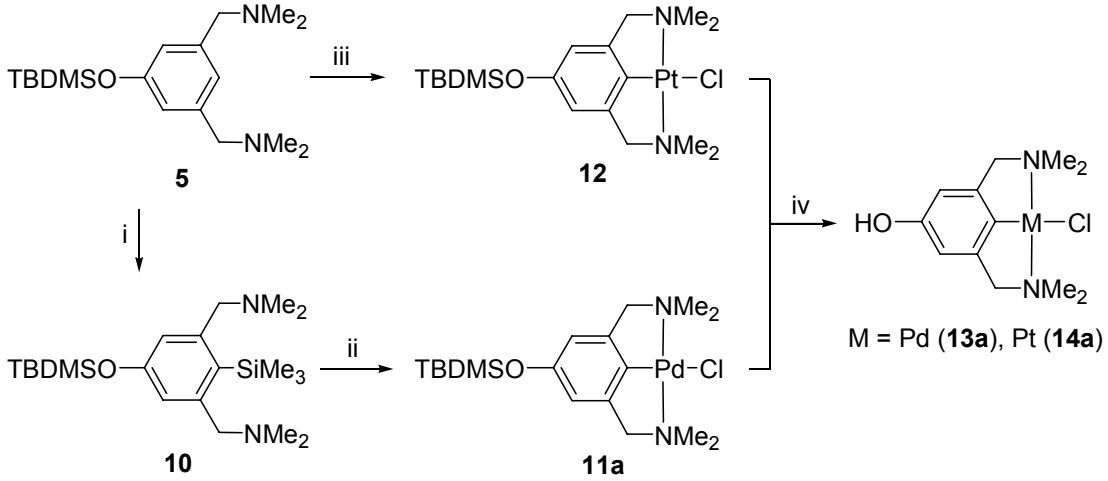

Scheme 3 NCN-pincer Pd and Pt-complexes by the transmetalation route; i. a. *n*BuLi, –78 °C, hexane, b. Me_3SiCl, 0 °C,THF; ii. a. $Pd(OAc)_2$, MeOH, b. LiCl, MeOH; iii. a. *n*BuLi, –78 °C, hexane, b. $[PtCl_2(Me_2S)_2]$, ether; iv. a. nBu_4NF, THF, b. 0.2 M HCl.

*2.2.2. Structures of [Pd(PCP-OH)(MeCN)]BF_4 (**6**), [PdCl(SCS-OH)] (**9a**), and [PdCl(NCN-OH)] (**13a**)*

The cationic complex [Pd(PCP-OH)(MeCN)]BF_4 (**6**) was crystallized from its solution in acetonitrile. In the crystal structure there are two independent monomeric cations with the NCMe ligand coordinated *trans* to C_{ipso} (Figure 2).

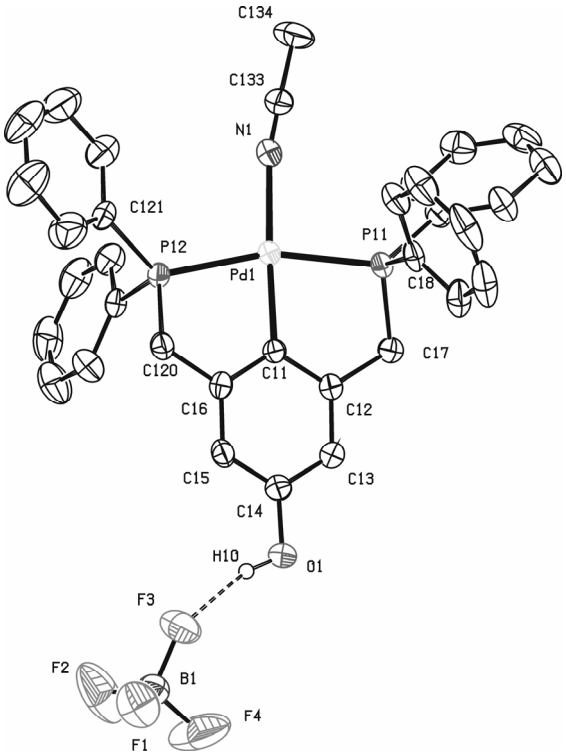

Figure 2 Displacement ellipsoid plot of one of the two independent molecules of cationic PCP-pincer Pd(II)-complex **6** in the crystal, drawn at the 50% probability level. H-atoms are omitted for clarity.

Like other pincer-metal complexes, the cation comprises a distorted square planar Pd center with an approximate C_2 symmetry axis along C_{ipso}–Pd–NCMe. The puckering of the five-membered chelate

rings is in opposite direction with large torsion angles of –33.3(2)° for Pd(1)–P(11)–C(17)–C(12) and –38.1(2)° for Pd(1)–P(12)–C(120)–C(16). The 4-OH group acts as a hydrogen bond donor and the BF_4 anions act as acceptors. Each 4-OH group is hydrogen bonded to exactly one fluorine acceptor resulting in discrete monomeric species. Selected bond lengths are reported in Table 1.

[PdCl(SCS-OH)] (**9a**) was found to be less soluble in most organic solvents except in DMSO, from which single crystals suitable for X-ray diffraction could be obtained. The molecular structure shows the common structural features for SCS-pincer Pd-complexes, such as a four-coordinate Pd center with square planar geometry and an approximate C_2 symmetry axis along C_{ipso}–Pd–Cl (Figure 3a).

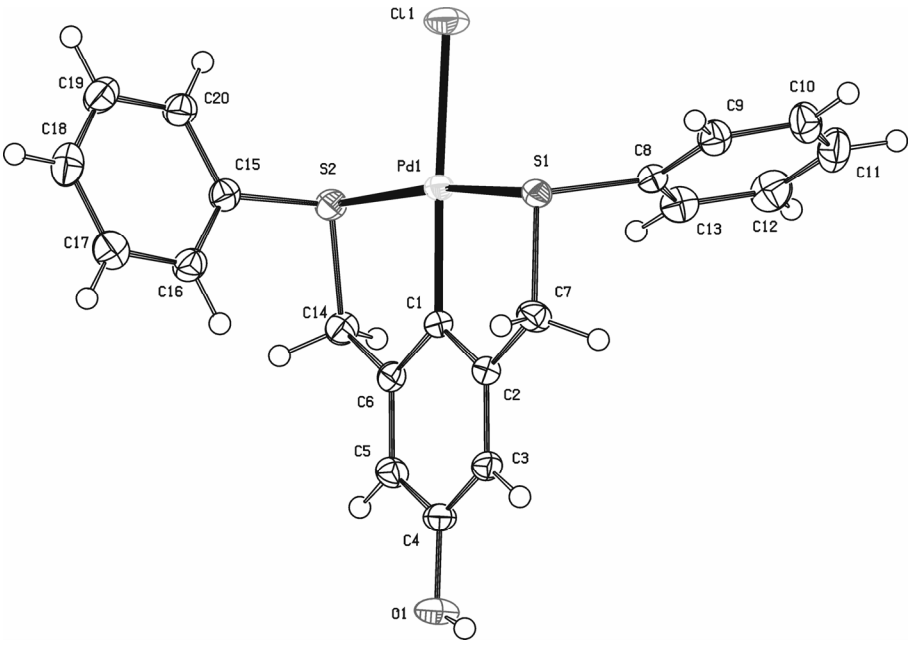

Figure 3a Displacement ellipsoid plot of [PdCl(SCS-OH)] (**9a**) in the crystal, drawn at the 50% probability level.

The five-membered palladacycles are puckered in opposite directions with torsion angles Pd(1)–S(1)–C(7)–C(2) and Pd(1)–S(2)–C(14)–C(6) of 10.25(15) and 15.95(15)°, respectively. The phenyl ring on S(2) is orientated almost parallel to the C_2 axis, whereas that on S(1) is perpendicular to it. The crystal structure reveals some more unique features. The molecular units form non-covalently bonded polymers in the direction of the crystallographic *a,b*-diagonal involving intermolecular H-bonding between the OH group as a H-donor and the chloride ligand as a H-acceptor (Figure 3b). The O–H bond length is 0.79(3) Å and the Cl···H distance is 2.31(3) Å, while the O–H···Cl angle amounts to 178(3)°. Amongst the complexes **9a**, **13a**, and **14a**, it is observed that **9a** has the shortest Cl···H distance and the largest O–H···Cl angle, indicating the strongest H-bonding interaction. Selected bond lengths and angles are reported in Table 1. In the crystal, two parallel chains run in the same direction, while due to the centrosymmetric space group there are also two parallel chains running in opposite direction cancelling the directionality as a whole (not shown).

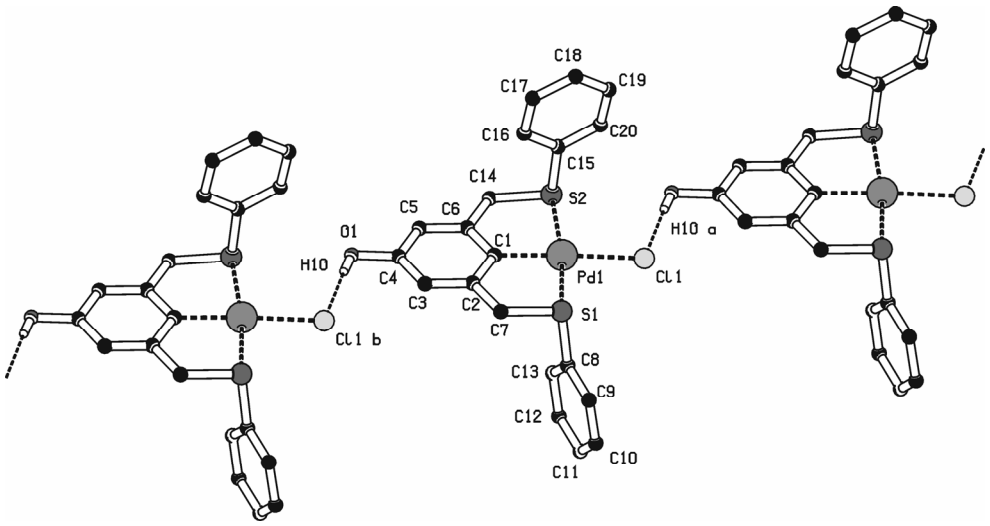

Figure 3b Hydrogen bonding interactions forming a one-dimensional chain in the crystal structure of [PdCl(SCS-OH)] (9a). Projection along the crystallographic *c* axis. C–H hydrogen atoms are omitted for clarity. Symmetry operations i: x+0.5, y+0.5, z; ii: x-0.5, y-0.5, z.

Finally, single crystals of complex [PdCl(NCN-OH)] (**13a**) suitable for X-ray crystallography were obtained by slow evaporation of its methanol solution. Interestingly, **13a** is isostructural with the corresponding platinum complex [PtCl(NCN-OH)] (**14a**).[8] A molecular plot of **13a** is given in Figure 4. Torsion angles Pd(1)–N(1)–C(7)–C(2) and Pd(1)–N(2)–C(10)–C(6) of –28.5(2) and –29.5(2)°, respectively, are found with puckering of the five-membered palladacycles in opposite directions. Crystal packing and the hydrogen bonding interactions, which form a one-dimensional chain, have already been described for the isostructural platinum complex.[8]

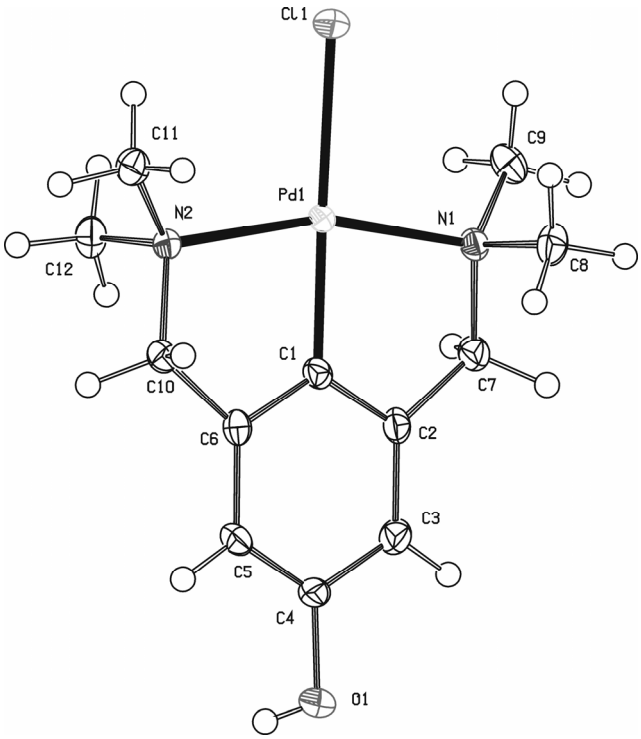

Figure 4 Displacement ellipsoid plot of [PdCl(NCN-OH)] (**13a**) in the crystal, drawn at the 50% probability level.

Table 1 Selected bond lengths (Å) and angles (°) of **6**, **9a**, **13a** and **14a**.

	[Pd(PCP-OH)(NCMe)](BF$_4$) (**6**)[a]	[PdCl(SCS-OH)] (**9a**)	PdCl(NCN-OH) (**13a**)	PtCl(NCN-OH) (**14a**)[8]
M–Cl	2.082(3) (Pd-N)	2.4095(5)	2.4420(6)	2.433(2)
M–C	2.021(3)	1.9831(18)	1.928(2)	1.915(9)
M–E	2.2994(8), 2.3098(7)	2.2861(5), 2.3140(5)	2.114(2), 2.111(2)	2.083(8), 2.094(8)
O–H	0.86	0.79(3)	0.72(3)	0.84(14)
Cl···H	-	2.31(3)	2.42(3)	2.32(13)
O–Cl	-	3.1040(18)	3.119(2)	3.127(8)
O–C	1.378(4)	1.368(2)	1.375(3)	1.389(12)
O–H–Cl	-	178(3)	165(4)	162(15)
M–Cl–H	-	106.5(7)	119.0(7)	115(4)

a. Only one of two independent molecules is considered.

2.2.3. IR studies

The O–H vibration of various neutral [PdX(SCS-OH)] (**9**) type complexes with different halides reveals that the O–H stretching frequency increases from X = Cl to Br to I (3213, 3269, 3305 cm^{-1}, respectively) in the solid-state, indicating a weakening of the H-bonding interaction going from Cl to Br to I (Table 2). In the series [PdCl(ECE-OH)] (E = N (**13a**), P (**8**) and S (**9a**)), the OH stretching frequencies of the NCN- (3252 cm^{-1}) and PCP- (3254 cm^{-1}) pincer complexes are similar, whereas, the SCS-pincer complex has a lower value (3213 cm^{-1}). This corroborates the findings from X-ray crystallography, in that the H-bonding interaction between [PdCl(SCS-OH)] complexes is stronger than for the other two complexes. This trend is also reflected in the solubility of these complexes in common organic solvents like dichloromethane. Apparently, complexes with stronger H-bonding form more stable aggregates and, therefore, are more difficult to dissolve. SCS-pincer complex **9a** (X=Cl) has the lowest solubility, which improves when the halide is changed to Br (**9b**) or I (**9c**). Similarly, PCP- and NCN-pincer complexes have a better solubility than the SCS-pincer ones.

Table 2 O–H stretching vibration of [MX(ECE-OH)L$_n$] pincer metal complexes in the solid state.

Compound	O–H vibration (cm^{-1})
[Pd(PCP-OH)(NCMe)](BF$_4$) (**6**)	3431
[Pd(SCS-OH)(NCMe)](BF$_4$) (**7**)	3436
[PdCl(PCP-OH)] (**8**)	3254
[PdCl(SCS-OH)] (**9a**)	3213
[PdBr(SCS-OH)] (**9b**)	3269
[PdI(SCS-OH)] (**9c**)	3305
PdCl(NCN-OH) (**13a**)	3252
PtCl(NCN-OH) (**14a**)	3280
PtI(NCN-OH) (**14b**)	3335

A similar trend for the O–H vibration is observed for the [PtX(NCN-OH)] complexes (X = Cl (**14a**) and I (**14b**)). The OH stretching frequency in the solid-state increases from Cl to I indicating weaker H-bonding in **14b**, which also has the higher solubility in organic solvents compared to **14a**.

The cationic PCP- and SCS-pincer Pd-complexes **6** and **7** have similar O–H stretching frequencies at 3431 and 3436 cm^{-1}, respectively. For the [Pd(PCP-OH)(NCMe)] cation $[\mathbf{6}]^+$, H-bonding exists with the BF_4 anion as established in the solid-state (Figure 2). Most likely, complex **7** shows a similar H-bonding with the anion. Both complexes can be seen either as a cationic complex to which the BF_4 anion is bonded *via* H-bonding (Structure **C**, Figure 5) or as a zwitterionic complex having an anionic O-grouping H-bonded to $H(BF_4)$, while the cationic site is blocked by coordination of a neutral acetonitrile ligand (Structure **D**). This prevents polymeric chain formation in these complexes and thereby increases their solubility. The higher O–H stretching frequencies of both cationic complexes **6** and **7** (3431 and 3436 cm^{-1}, respectively) compared to those of neutral complexes **8** and **9**, indicate a weak H-bonding in both **6** and **7** and consequently point to the structural moiety **C** in Figure 5.

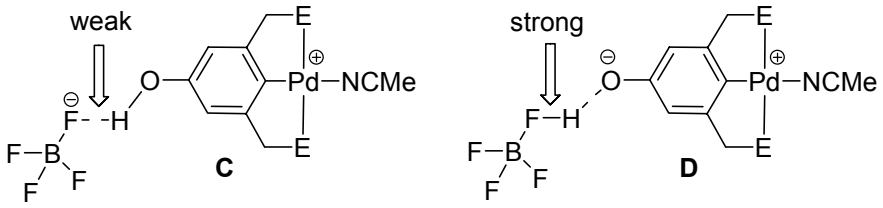

Figure 5 Two possible binding motifs of ECE-OH-pincer palladium cationic complexes.

*2.2.4. Synthesis of dimer **15***

In general, deprotection of the TBDMS-group from the *para*-OTBDMS grouping in NCN-pincer Pd-complex **11** involves treatment of the pincer metal complex with tetrabutylammonium fluoride (TBAF) in THF, followed by an acidic work-up.[14,31] The yields for these reactions are moderate (about 50%). In the case of the NCN-pincer palladium complex **11b** more detailed information about the possible reason for this observation was obtained. Deprotection of [PdI(NCN-OSi*t*BuMe$_2$)] (**11b**) was carried out by reaction with a 1 M solution of TBAF in THF. A subsequent non-acidic work-up was used to avoid halide scrambling (Scheme 4).

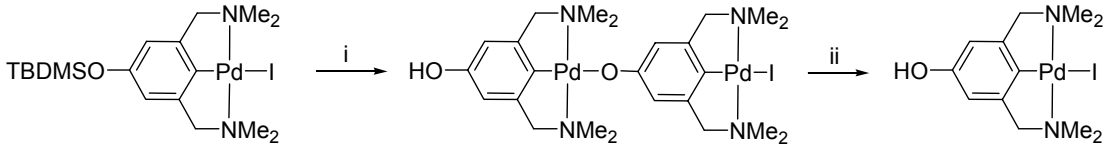

Scheme 4 Deprotection of **11b** and formation of dinuclear **15**; i. *n*Bu$_4$NF, THF. Reaction of **15** with NH_4I (ii) affording mononuclear [PdI(NCN-OH)] **13b**.

The yellow product obtained after work-up was found to be less soluble than the silyl-protected analog in solvents like methanol and dichloromethane. The ^{1}H NMR spectrum of a solution of the yellow product in $(CD_3)_2SO$ showed only one set of broad peaks. However, the ^{1}H NMR spectrum of a CD_2Cl_2 solution revealed two distinct sets of signals for the N-methyl, benzyl and aromatic hydrogens, indicating the presence of two non-equivalent pincer moieties. On the basis of ^{1}H and ^{13}C

NMR data and elemental analysis, the product was formulated as dimer **15** (see Scheme 4). Further structural analysis confirmed the dimeric nature of **15** in the solid state.

*2.2.5. X-ray crystal structure of **15***

Crystals of **15**·MeOH suitable for X-ray structure determination were obtained from a saturated solution in methanol. The molecular picture shows a unique structure consisting of a Pd-cation $[Pd(NCN\text{-}OH)]^+$ bonded *via* a Pd–O bond to a phenolate-anion $[PdI(NCN\text{-}O)]^-$ (Figure 6). Moreover, in a distinct manner one molecule of methanol per dimeric unit is bonded to the two kinds of O-atoms present, *i.e.* to the phenoxy-O and the phenol-O, respectively. Selected bond lengths and bond angles are reported in Table 3.

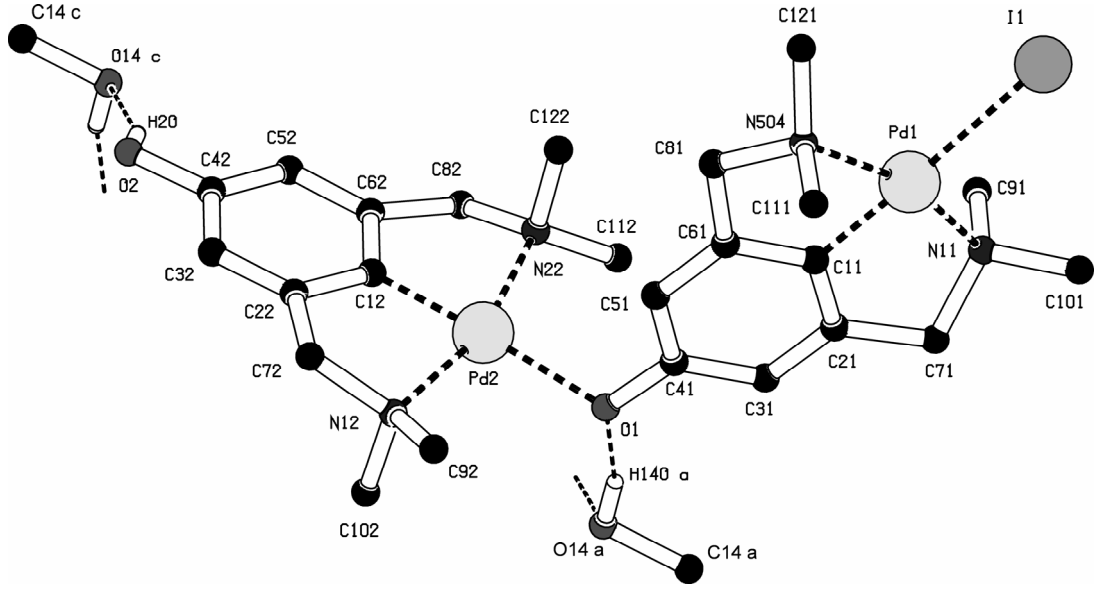

Figure 6 Molecular geometry of dimer **15**·MeOH; hydrogens, except those involved in H-bonding, are omitted for clarity.

Table 3 Selected bond lengths (Å) and angles (°) of dinuclear complex **15**·MeOH.

Pd(1)–I(1)	2.7373(4)
Pd(2)–O(1)	2.159(3)
Pd(1)–C(11)	1.930(4)
Pd(2)–C(12)	1.914(4)
O(1)–C(41)	1.338(4)
O(2)–C(42)	1.381(5)
Pd(2)–O(1)–C(41)	117.1(3)

The Pd(2)–O(1)–C(41) angle is 117.1(3)° while the O(1)–C(41) bond length (1.338(4) Å) of the $[PdI(NCN\text{-}O)]^-$ phenolate anion is shorter than the O(2)–C(42) (1.381(5) Å) bond in the $[Pd(NCN\text{-}OH)]^+$ cation. In fact, for all monomeric [MX(ECE-OH)] *para*-OH pincer complexes reported so far, the O–C bond length falls in the range of 1.36 to 1.38 Å (Table 1), which is considerably longer than O–C bond length (1.338(4) Å) in the phenolate anion itself. These results are comparable to the results from the crystal structure of the parent [Pd(OPh)NCN] complex published earlier, which contains a phenoxy anion as the fourth ligand.[34] It is interesting to note that in the NCN-palladium

dimer **15** one molecule of methanol is H-bonded to the phenoxy-O anion while the phenol-OH of the same dimer is also involved in H-bonding with another methanol molecule. Each methanol molecule is involved in two H-bonds. It acts as a H-bond donor to the phenoxy-O anion of one dimer and as a H-bond acceptor to the phenol grouping of another dimer, thereby forming a network structure. In aryloxypalladium and platinum chemistry, these binding motifs are a common feature, *e.g.* they have been found in [Pt(Me)(OPh)(bpy)]·HOPh,[35] [Pd(OCH(CF_3)$_2$)(OPh)(bpy)]·HOPh,[36] [Pt(OPh)(NCN)] ·HOPh, and [Pt(catecholate)(NCN)],[34] respectively.

Reaction of dimer **15** (yellow) with ammonium iodide resulted in the formation of monomeric [PdI(NCN-OH)] (**13b**; colorless, Scheme 4), which was confirmed by ^{1}H NMR spectroscopic and elemental analytic data, as well as by comparison of these data with those of an authentic sample. Thus, dimer formation is a reversible process and can be achieved by treatment of the dimer with NH_4I which provides HI to form monomer **13b**. In fact, by increasing the pH of a solution of **13b** in MeOH, HX can be removed from [MX(NCN-OH)] to form the dimer **15**, whereas, by decreasing the pH, this dimer can be transformed back into its monomeric form. Dimerization is also a first step in the process of organometallic polymer formation *via* a direct metal-oxygen bond (**B**, Figure 1). Thus it is possible to form polymeric chains by removal of the phenolic proton from [PdX(NCN-OH)] by a base, with the resulting phenoxide then replacing the halide from palladium of the next molecule to form a Pd–O bond. This process is currently under investigation as it may give rise to the formation of unique organometallic polymers in which the organo-metal phenoxide is the repetitive unit.

*2.2.6. Synthesis of siloxane-functionalized ECE-pincer complexes (**16-19**)*

The current interest in the catalytic activity of ECE-pincer Pd-complexes in C–C and C–X cross-coupling reactions[5,11,15,18,20,29] combined with the possibility to recycle these complexes *via* the *para*-OH functionality make the present complexes highly interesting. Immobilization of these complexes on silica has a two-fold advantage; separation of the catalyst from the product can be achieved as well as recycling. One of the major problems in heterogenizing homogeneous catalysts on inorganic supports like silica is the determination of the exact catalyst structure on the support; *i.e.* whether the molecular structure has been retained after immobilization and whether the catalytic centre is still accessible. In this respect, we decided to use the *para*-OH grouping of the present complexes for the synthesis of modified pincer-metal complexes tethered with a *para*-siloxane group suitable for immobilization.

The triethoxysilane tethered complexes **16-19** were prepared by refluxing the respective (ECE-OH)-pincer metal complexes with triethoxysilylpropyl isocyanate in the presence of a combination of two Lewis bases; 0.05 equivalent of 4-(dimethylamino)pyridine (DMAP) and 1.1 equivalent of NEt_3. The siloxane-functionalized complexes were isolated in about 90% yield (Scheme 5). Prior to the reaction of [PdCl(SCS-OH)] **9a** with triethoxysilylpropyl isocyanate, the chloride was exchanged to bromide (**9b**) in order to first increase the solubility of the SCS-pincer palladium complex. It

appeared that this approach facilitated a faster and more complete conversion to **19**. For the same reason, the chloride of [PtCl(NCN-OH)] **14a** was first exchanged to iodide (**14b**). Complexes **16-19** all comprise a trialkoxysilane and an organometallic fragment covalently connected through a propylcarbamate linker. Again, the absence of H-bond forming *para*-OH groups and the presence of a non-polar tail including a silyl grouping increased the solubility of these complexes considerably. They are even soluble in non-polar solvents such as benzene or toluene, which allowed grafting of these complexes on silica in these solvents.[37]

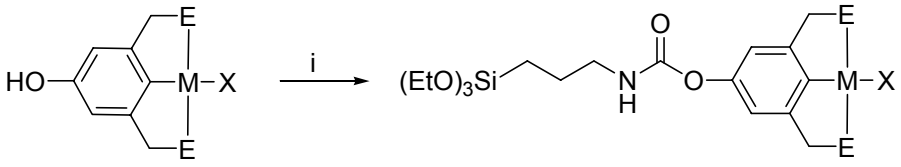

M = Pd: **16**, E = NMe_2, X = Cl; **18**, E = PPh_2, X = Cl;
19, E = SPh, X = Br
M = Pt: **17**, E = NMe_2, X = I

Scheme 5 Pincer metal-complexes functionalized with a triethoxysilane grouping suitable for coupling to silica; i. 1.1 eq. $(EtO)_3Si(CH_2)_3NCO$, 1.1 eq. NEt_3, 0.05 eq. DMAP, CH_2Cl_2, reflux.

*2.2.7. X-ray crystal structure of **17***

The molecular structure of the NCN-pincer Pt-complex **17** in the solid-state was determined by single crystal X-ray crystallography (Figure 7).

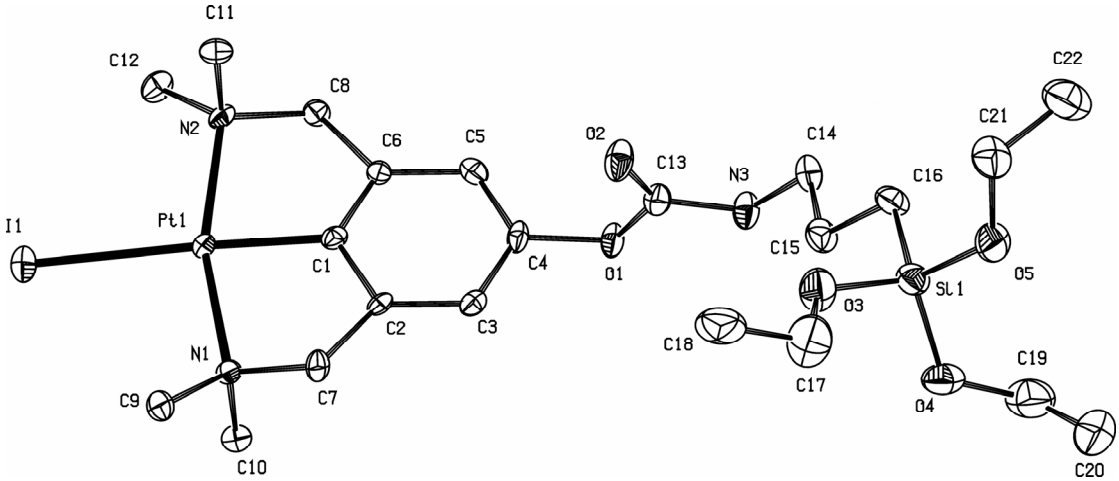

Figure 7 Displacement ellipsoid plot of the NCN-pincer Pt-complex **17**, drawn at the 50% probability level. Hydrogen atoms have been omitted for clarity.

The platinum atom has a square planar coordination environment. The phenyl grouping of the NCN-pincer ligand makes a dihedral angle of 14.95(16)° with respect to the platinum coordination plane. The two five-membered Pt–C–C–C–N chelate rings are puckered in such a way, that a local C_2 symmetry is generated. The torsion angles Pt(1)–N(1)–C(7)–C(2) and Pt(1)–N(2)–C(8)–C(6) are –33.9(4)° and –32.4(4)°, respectively. The carbamate group (*i.e.* the NC(=O)O plane) is positioned almost perpendicularly to the phenyl ring with a dihedral angle of 84.9(2)°. The C_3-alkyl chain with

the triethoxysilyl end group is in an extended conformation. Selected bond lengths and angles are reported in Table 4.

Table 4 Selected bond lengths (Å) and angles (°) for **17**.

Bond lengths		Bond angles	
Pt1–C1	1.940(4)	C1–Pt1–N1	81.47(17)
Pt1–N1	2.104(4)	C1–Pt1–N2	80.91(16)
Pt1–N2	2.094(4)	N2–Pt1–N1	162.36(14)
Pt1–I1	2.7013(4)	C1–Pt1–I1	175.96(13)
O1–C13	1.365(6)	N2–Pt1–I1	99.98(10)
O2–C13	1.214(6)	N1–Pt1–I1	97.65(10)
N3–C13	1.331(6)	C4–O1–C13	115.8(3)
		O1–C13–N3	110.5(4)
		C13–N3–C14	121.1(4)

An interesting structural feature is the way the carbamate groupings are intermolecularly connected by non-covalent H-bonding. In contrast with previous structures (as in *e.g.* **14a**) this is not involving the Pt–Cl grouping, but occurs through the hydrogen of the NH-grouping of one molecule with the C=O grouping of a neighboring molecule [H(3)···O(2)^{i} 2.21 Å, N(3)···O(2)^{i} 2.955(5) Å, N(3)–H(3)···O(2)^{i} 143°, symmetry operation i: x, 0.5–y, z–0.5]. By this non-covalent hydrogen bonding, an infinite chain is formed in the direction of the crystallographic c-axis (Figure 8).

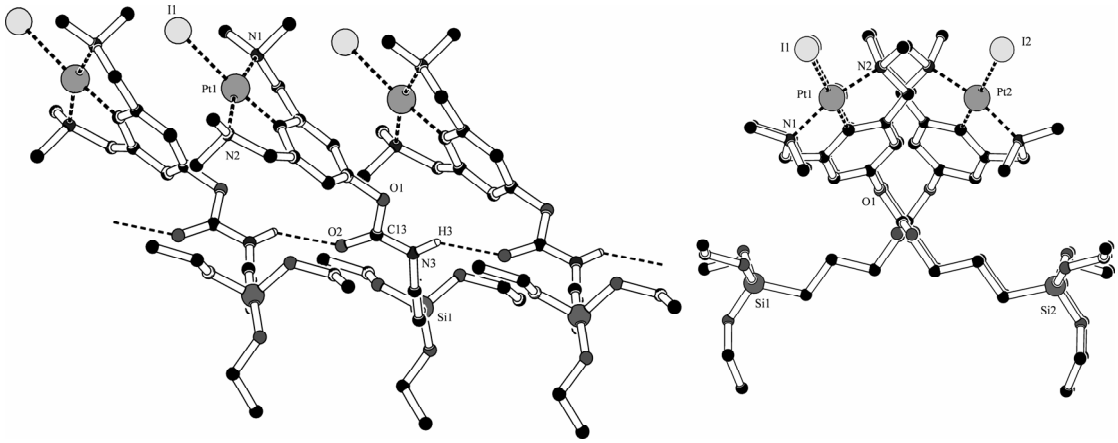

Figure 8 H-bonding in the NCN-pincer Pt-complex **17**; lateral view (left) and axial view (right) showing the regular arrangement of siloxy-groups. (Hydrogen atoms, except those involved in H-bonding, have been omitted for clarity).

As a result, all NCN-pincer platinum units are arranged at one site with the $Si(OEt)_3$ groups residing on the opposite site, which creates a kind of model mimicking possible surface arrangements of the NCN-pincer platinum groupings upon immobilization of **17** on a silica surface (see axial view in Figure 8).

2.3. Conclusions

The possibility to induce selective H-bonding between organometallic complexes is of prime interest in the field of crystal engineering.[38] It can be used to direct formation of aggregates with special

shapes (rings, chains, polymers etc.) and distinct stereochemistries. These materials could have various interesting applications such as conducting polymers, as LED's, or as materials with NLO properties.

The [MX(ECE-OH)] complexes are bifunctional molecules, which have unique H-bonding properties *via* a combination of the *para*-OH and M-halide entities present in one building block. Ample evidence has been collected now that in the protonated form, they afford self-assembled, non-covalent polymeric chains.[25,28] Moreover, *via* selective deprotonation followed by halide-phenoxy anion exchange, dimeric structures are accessible. This deprotonation approach with ultimate HX elimination and removal provides a possibility to form oligomers or even polymers through mutual intermolecular M–O bond formation. Consequently, these complexes can be interesting building blocks to form novel organometallic polymers.

In addition, the excellent stability of these [MX(ECE-OH)] complexes under severe reaction conditions (*e.g.* highly acidic and electrophilic or highly basic and nucleophilic conditions) allows their direct *para*-functionalization with siloxane substituted tethers providing [MX(ECE-Z)] complexes which are potential candidates for the synthesis of recyclable, immobilized homogeneous catalysts.[3,13,15,16] At the same time this approach also allows for the introduction of other H-bonding moieties, not including the M–Cl grouping, like, *e.g.*, carbamates. This approach could be of interest in the field of self-assembling and self-organizing polymers.[23]

2.4. Experimental Section

2.4.1. General Comments

Synthetic procedures were conducted under a dry nitrogen atmosphere using standard Schlenk techniques. Solvents were dried over appropriate materials and distilled prior to use. Moreover, for the synthesis of PCP-pincer ligands and complexes, solvents were degassed prior to use. Reagents were obtained from commercial sources and were used without further purification. Siloxane materials were stored under nitrogen atmosphere. ^{1}H (200.1 and 300.1 MHz), $^{13}C\{^{1}H\}$ (50.3 and 75.5 MHz) and $^{31}P\{^{1}H\}$ (81 MHz) NMR spectra were recorded at room temperature on either Varian Mercury 200 or Varian Inova 300 spectrometers. FT-IR spectra were recorded using a Mattson Instruments Galaxy Series FTIR 5000 spectrometer. Microanalyses were obtained from H. Kolbe Mikroanalytisches Laboratorium, Mülheim an der Ruhr, Germany.

Compounds **1-4** were synthesized following literature procedures.[7,9,39] 3,5-Bis[(dimethylamino)methyl]-4-(trimethylsilyl)phenyl *tert*-butyldimethylsilyl ether (**10**)[9,14,31] and (2,6-bis[(dimethylamino)methyl]-4-(hydroxy)phenyl)platinum(II) iodide (**14b**)[8,26] were prepared as described previously.

2.4.2. Procedures

*2.4.2.1. Synthesis of [Pd{$C_6H_2(CH_2PPh_2)_2$-2,6-(OH)-4}(MeCN)]BF_4 (**6**)*

[$PdCl_2(MeCN)_2$] (0.33 g, 1.26 mmol) was dissolved in refluxing acetonitrile (30 mL). $AgBF_4$ (0.49 g, 2.52 mmol) dissolved in acetonitrile (10 mL) was added to this solution, upon which immediate precipitation of AgCl occurred. The reaction mixture was stirred for another hour. The precipitate formed was allowed to settle, after which the supernatant was decanted into a solution of **3** (0.76 g, 1.26 mmol) in warm acetonitrile (30 mL). The resulting orange mixture was stirred at 50 °C for 16 h to yield a yellowish coloured turbid mixture. The mixture was allowed to settle and the supernatant was filtered off, all volatiles were evaporated, and the resulting light yellow solid was redissolved in a dichloromethane/acetonitrile mixture (10 mL/3 mL) and this solution was filtered again. After evaporation of all volatiles, the product was washed with diethyl ether and dried *in vacuo*. A light yellow powder **6** (0.85 g, 1.17 mmol) was obtained in 94% yield. ^{1}H NMR (300.1 MHz, CD_3CN, 25 °C): δ = 1.96 (s, 3H, C*H*$_3$CN); 3.99 (vt, $^2J_{H,P}$ = 4.7 Hz, 4H, C*H*$_2$P); 6.67 (s, 2H, Ar*H*); 7.5-7.6 (m, 12H, Ph*H*); 7.7-7.75 (m, 8H, Ph*H*). ^{13}C NMR (75.5 MHz, CD_3CN, 25 °C): δ = 41.12 (vt, $^1J_{C,P}$ = 15.3 Hz, *C*H$_2$P); 112.63 (vt, $^3J_{C,P}$ = 12 Hz, *m*-C Ar), 130.31 (vt, $^3J_{C,P}$ = 4.9 Hz, *m*-C Ph), 131.39 (vt, $^1J_{C,P}$ = 23.1 Hz *ipso*-C Ph), 132.64 (*p*-C Ph), 133.76 (vt, $^2J_{C,P}$ = 7.1 Hz, *o*-C Ph), 144.86 (*ipso*-C Ar), 149.83 (vt, $^2J_{C,P}$ = 10.3 Hz, *o*-C Ar), 157.71 (*p*-C Ar). ^{31}P NMR (81 MHz, CD_3CN, 25 °C): δ = 41.9. IR (ATR): $\tilde{\nu}$ (cm^{-1}) = 3430, 3059, 2943, 2893, 2323, 2293, 1591, 1568, 1484, 1455, 1435, 1305, 1069, 742. Anal. Calcd. for $C_{34}H_{30}BF_4NOP_2Pd$ (723.78): C, 56.42; H, 4.18; N, 1.94; P, 8.56. Found: C, 56.48; H, 4.33; N, 1.94; P, 8.52.

*2.4.2.2. Synthesis of [Pd{$C_6H_2(CH_2SPh)_2$-2,6-(OH)-4}(MeCN)]BF_4 (**7**)*

A similar procedure was followed as for the synthesis of **6**. Using **4** (1.1 g, 2.43 mmol), **7** was obtained as an orange coloured powder in 84% yield. ^{1}H NMR (300.1 MHz, CD_3CN, 25 °C): δ = 4.63 (bs, 4H, C*H*$_2$S); 6.56 (s, 2H, Ar*H*); 7.46-7.54 (m, 6H, Ph*H*); 7.80-7.84 (m, 4H, Ph*H*). ^{13}C NMR (75.5 MHz, CD_3CN, 25 °C): δ = 50.72 (*C*H$_2$S); 111.45 (*m*-C Ar), 131.09 (*o*-C Ph), 131.75 (*p*-C Ph), 132.02 (*ipso*-C Ph), 132.57 (*m*-C Ph), 146.84 (*ipso*-C Ar), 152.34 (*o*-C Ar), 156.40 (*p*-C Ar). IR (ATR): $\tilde{\nu}$ (cm^{-1}) = 3437, 3059, 2937, 2288, 1593, 1576, 1473, 1441, 1431, 1312, 1053, 743. Anal. Calcd. for $C_{22}H_{20}BF_4NOPdS_2$ (571.76): C, 46.21; H, 3.53; N, 2.45; S, 11.22. Found: C, 46.12; H, 3.64, N, 2.38; S, 11.27.

*2.4.2.3. Synthesis of [PdCl{$C_6H_2(CH_2PPh_2)_2$-2,6-(OH)-4}] (**8**)*

To an orange solution of **6** (0.2 g, 0.276 mmol) in acetonitrile (3 mL), a solution of NaCl (0.24 g, 4.1 mmol) in demineralised water (5 mL) was added. A turbid orange coloured mixture was obtained, stirred for another 16 h at ambient temperature, and then concentrated to dryness. The resulting residue was dissolved in dichloromethane and washed with excess water, dried over $MgSO_4$, filtered and volatiles evaporated *in vacuo*. A yellow coloured **8** was obtained in quantitative yield. ^{1}H NMR (300 MHz, CD_3CN + $(CD_3)_2SO$, 25 °C): δ = 3.96 (vt, $^2J_{H,P}$ = 4.8 Hz, 4H, C*H*$_2$P); 6.62 (s, 2H, Ar*H*); 7.43-7.47 (m, 12H, Ph*H*); 7.84-7.90 (m, 8H, Ph*H*); 8.86 (s, 1H, O*H*). ^{13}C NMR (75.5 MHz, CD_3CN + $(CD_3)_2SO$, 25

°C): δ = 42.22 (vt, $^{1}J_{C,P}$ = 15 Hz, *C*H_2P); 111.93 (vt, $^{3}J_{C,P}$ = 11.9 Hz, *m*-C Ar), 129.67 (vt, $^{3}J_{C,P}$ = 4.9 Hz, *m*-C Ph), 131.68 (*p*-C Ph), 133.34 (vt, $^{1}J_{C,P}$ = 21 Hz *ipso*-C Ph), 133.76 (vt, $^{2}J_{C,P}$ = 7 Hz, *o*-C Ph), 148.64 (*ipso*-C Ar), 149.45 (vt, $^{2}J_{C,P}$ = 11 Hz, *o*-C Ar), 157.28 (*p*-C Ar). ^{31}P NMR (81 MHz, CD_3CN + $(CD_3)_2SO$, 25 °C): δ = 39.04. IR (ATR): $\widetilde{\nu}$ (cm^{-1}) = 3254, 3051, 1590, 1564, 1482, 1434, 1417, 1304, 742, 692. Anal. Calcd. for $C_{32}H_{27}ClOP_2Pd$ (631.38): C, 60.87; H, 4.31; P, 9.81. Found: C, 60.73; H, 4.38; P, 9.76.

*2.4.2.4. Synthesis of [PdX{$C_6H_2(CH_2SPh)_2$-2,6-(OH)-4}] (**9**)*

A solution of **7** (0.5 g, 0.875 mmol) in acetonitrile (20 mL) was treated with a solution of NaX (0.5 g, 8.7 mmol) in distilled water (5 mL), which resulted in the formation of a turbid orange coloured mixture. After stirring at ambient temperature for 2 h, the reaction mixture was concentrated to remove volatiles. The residue obtained was washed with excess water leaving an orange coloured product which was dried *in vacuo*. **9** was obtained in almost quantitative yield. ^{1}H NMR (300 MHz, $(CD_3)_2SO$, 25 °C): δ = 4.67 (s, 4H, CH_2S); 6.48 (s, 2H, Ar*H*); 7.43-7.48 (m, 6H, Ph*H*); 7.82-7.85 (m, 4H, Ph*H*); 9.25 (s, 1H, O*H*). ^{13}C NMR (75.5 MHz, $(CD_3)_2SO$, 25 °C): δ = 49.80 (*C*H_2S); 109.68 (*m*-C Ar), 129.39 (*p*-C Ph), 129.54 (*o*-C Ph), 130.69 (*m*-C Ph), 132.41 (*ipso*-C Ph), 149.69 (*ipso*-C Ar), 150.25 (*o*-C Ar), 154.82 (*p*-C Ar). IR (ATR): $\widetilde{\nu}$ (cm^{-1}) = 3213, 3043, 2906, 1591, 1574, 1471, 1439, 1421, 1314, 741. Anal. Calcd. for $C_{20}H_{17}BrOPdS_2$ (**9b**, 523.8): C, 45.86; H, 3.27; S, 12.24. Found: C, 45.95; H, 3.19; S, 12.24.

*2.4.2.5. Synthesis of [PdCl{$C_6H_2(CH_2NMe_2)_2$-2,6-(t-$BuMe_2SiO$)-4}] (**11a**)*

$Pd(OAc)_2$ (0.569 g, 2.54 mmol) was added to a solution of **10** (1 g, 2.54 mmol) in methanol (25 mL). The resulting red-brown coloured, clear solution was stirred at room temperature for 2 h after which an excess of LiCl (0.5 g, 10 mmol) was added and stirring was continued for 1 h. After evaporation of volatiles, the resulting green coloured solid was dissolved in dichloromethane. The solution was filtered over a packed celite column. The filtrate was concentrated and a solid was precipitated by addition of pentane. Centrifugation followed by drying of the precipitate in vacuum led to the isolation of **11a** as a colourless solid in 89% yield. ^{1}H NMR (300 MHz, $CDCl_3$, 25 °C): δ 0.16 (s, 6H, $SiMe_2$); 0.96 (s, 9H, Si*t*Bu); 2.92 (s, 12H, NCH_3); 3.92 (s, 4H, CH_2N); 6.30 (s, 2H, Ar*H*). ^{13}C NMR (50 MHz, $CDCl_3$, 25 °C): δ –4.19 (Si*C*H_3); 18.33 (Si*C*$(CH_3)_3$); 25.88 (SiC(*C*$H_3)_3$); 53.33 (N*C*H_3); 74.86 (*C*H_2N); 111.97, 145.56, 147.51, 153.53 (Ar*C*). Anal. Calcd. for $C_{18}H_{33}ClN_2OPdSi$ (463.43): C, 46.65; H, 7.18; N, 6.04. Found: C, 46.78; H, 7.04; N, 5.93.

*2.4.2.6. Synthesis of [PdCl{$C_6H_2(CH_2NMe_2)_2$-2,6-(OH)-4}] (**13a**)*

A solution of **11a** (1 g, 2.16 mmol) in THF (25 mL) was treated with a solution of tetrabutylammonium fluoride in THF (1M, 2.5 mL, 2.5 mmol), which formed a clear red-brown coloured solution. After stirring for 2 h at ambient temperature, the reaction mixture was concentrated to a quarter of its volume and then treated with 0.2 M HCl (12.5 mL), which caused turbidity. Stirring was continued for 1 h. The precipitate was then filtered and washed with water (25 mL) and diethyl ether (25 mL) and dried *in vacuo*. White solid **13a** was obtained in 50% yield. ^{1}H NMR (300 MHz, CD_3OD, 25 °C): δ 2.84 (s, 12H, NCH_3); 3.96 (s, 4H, CH_2N); 6.32 (s, 2H, Ar*H*). ^{13}C NMR (75.5 MHz, CD_3OD, 25 °C): δ 53.19 (N*C*H_3);

75.35 (*C*H_2N); 108.27, 145.06, 146.98, 156.72 (Ar*C*). Anal. Calcd. for $C_{12}H_{19}ClN_2OPd$ (349.16): C, 41.28; H, 5.48; N, 8.02. Found: C, 41.28; H, 5.59; N, 7.95.

*2.4.2.7. Preparation of [Pd{$OC_6H_2(CH_2NMe_2)_2$-3,5-(PdI)-4}{$C_6H_2(CH_2NMe_2)_2$-2,6-(OH)-4}] (**15**)*

[PdI{$C_6H_2(CH_2NMe_2)_2$-2,6-(*t*-$BuMe_2SiO$)-4}] (**11b**, 0.9 mmol) was dissolved in THF (20 mL). Tetrabutylammonium fluoride (1 mmol, 1 mL of 1 M solution in THF) was added to this solution. The solution turned turbid and then became clear. The resulting reaction mixture was stirred for 1 h. It became turbid again during this time. THF was evaporated and the product was washed with water, acetone and ether, and dried *in vacuo*. Compound **15** was obtained as a yellow coloured powder.

^{1}H NMR (300 MHz, CD_2Cl_2, 25 °C): δ = 2.70, 2.96 (s, 24H, NC*H*$_3$); 3.84, 3.88 (s, 8H, NC*H*$_2$); 6.55, 6.61 (Ar*H*, 4H). ^{1}H NMR (300 MHz, $(CD_3)_2SO$, 25 °C): δ = 2.75 (s, 24H, NC*H*$_3$); 3.83 (s, 8H, NC*H*$_2$); 6.10 (Ar*H*, 4H). ^{13}C NMR (75.5 MHz, $(CD_3)_2SO$, 25 °C): δ = 52.52 (N*C*H$_3$); 73.84 (N*C*H$_2$); 107.16, 144.94, 145.94, 154.44 (Ar*C*). Anal. Calcd. for $C_{24}H_{37}IN_4O_2Pd_2$ (753.32): C, 38.26; H, 4.95; I, 16.85; N, 7.44. Found: C, 38.18; H 5.06; I 16.72; N 7.38.

*2.4.2.8. Preparation of [PdI{$C_6H_2(CH_2NMe_2)_2$-2,6-(OH)-4}] (**13b**)*

Compound **15** (100 mg, 0.133 mmol) was treated with ammonium iodide (21 mg, 0.146 mmol) in methanol (10 mL). A white precipitate formed which was allowed to settle down. The supernatant yellowish solution was separated and residue was washed with methanol (2 × 5 mL). The combined washings and supernatant were subjected to vacuum. Compound **13b** was obtained as a white powder in 80% yield.

^{1}H NMR (300 MHz, CD_2Cl_2, 25 °C): 2.97 (s, 12H, NC*H*$_3$); 3.94 (s, 4H, NC*H*$_2$); 6.32 (Ar*H*, 2H). Anal. Calcd. for $C_{12}H_{19}IN_2OPd$ (440.62): C, 32.71; H, 4.35; I 28.80; N, 6.36. Found: C, 32.62; H 4.28; I 28.74; N 6.27.

*2.4.2.9. Synthesis of [PdCl{$C_6H_2(CH_2NMe_2)_2$-2,6-($(EtO)_3Si(CH_2)_3NHC(O)O$)-4}] (**16**)*

Triethoxysilylpropyl isocyanate (0.54 g, 2.2 mmol) was added to a solution of **13a** (0.7 g, 2 mmol), triethylamine (0.22 g, 2.2 mmol), and 4-(dimethylamino)pyridine (27 mg, 0.1 mmol) in dry dichloromethane (15 mL). The resulting reaction mixture was refluxed for 16 h after which a clear yellowish coloured solution had formed. After allowing the reaction mixture to attain room temperature, all volatiles were removed *in vacuo*. The residue was washed with pentane (2 × 15 mL). The product was extracted from the residue by treating it with benzene (3 × 15 mL). The combined extracts were filtered to remove insoluble impurities and the solvent was evaporated *in vacuo* to obtain **16** as a yellowish solid in more than 90% yield. ^{1}H NMR (300 MHz, C_6D_6, 25 °C): δ 0.68 (t, $^3J_{H,H}$ = 8.4 Hz, 2H, SiC*H*$_2$); 1.16 (t, $^3J_{H,H}$ = 6.9 Hz, 9H, OCH_2CH_3); 1.81 (quin, $^3J_{H,H}$ = 7.6 Hz, 2H, C*H*$_2$); 2.63 (s, 12H, NC*H*$_3$); 3.28 (quart, $^3J_{H,H}$ = 6.6 Hz, 2H, NHC*H*$_2$); 3.30 (s, 4H, C*H*$_2$N); 3.77 (quart, $^3J_{H,H}$ = 6.9 Hz, 6H, OC*H*$_2$); 6.11 (t, $^3J_{H,H}$ = 6.0 Hz, 1H, N*H*); 6.62 (s, 2H, Ar*H*). ^{13}C NMR (50 MHz, C_6D_6, 25 °C): δ 8.67 (Si*C*H$_2$); 19.02 (OCH_2CH_3); 24.31 (*C*H$_2$); 44.51 (NH*C*H$_2$); 53.22 (N*C*H$_3$); 58.96 (O*C*H$_2$); 74.90 (*C*H$_2$N); 114.36 (*m*-C Ar), 146.13 (*ipso*-C Ar), 150.01 (*o*-C Ar), 153.61 (*p*-C Ar); 155.60 (*C*=O). ^{29}Si NMR (59.6 MHz, C_6D_6, 25 °C, TMS as reference): δ –45.7. IR (ATR): $\tilde{\nu}$ (cm^{-1}) = 731 (N–H wag); 956 (sym Si–O–C

stretching); 1100-1074 (asym. Si–O–C stretching, doublet); 1228 (C–N stretching); 1440 (N–H bending); 1520 (CHN group); 1730 (C=O stretching); 2887, 2926, 2975 (C–H stretching); 3313 (N–H stretching, associated). Anal. Calcd. for $C_{22}H_{40}ClN_3O_5PdSi$ (596.53): C, 44.30; H, 6.76; N, 7.04; Si, 4.71. Found: C, 44.46; H, 6.81; N, 7.11; Si, 4.75.

*2.4.2.10. Synthesis of [PtI{$C_6H_2(CH_2NMe_2)_2$-2,6-$((EtO)_3Si(CH_2)_3NHC(O)O)$-4}] (**17**)*

For the synthesis of this complex, a similar procedure was followed as described above for **16**. Using 0.75 g (1.42 mmol) of **14b**, compound **17** was isolated in 90% yield. ^{1}H NMR (200 MHz, C_6D_6, 25 °C): δ 0.67 (t, $^3J_{H,H}$ = 8.8 Hz, 2H, SiCH_2); 1.17 (t, $^3J_{H,H}$ = 7.0 Hz, 9H, OCH_2CH_3); 1.79 (quin, $^3J_{H,H}$ = 7.6 Hz, 2H, CH_2); 2.75 (t, $^3J_{H,Pt}$ = 16.0 Hz, 12H, NCH_3); 3.28 (quart, $^3J_{H,H}$ = 6.6 Hz, 2H, NHCH_2); 3.36 (t, $^3J_{H,Pt}$ = 21.2 Hz, 4H, CH_2N); 3.78 (quart, $^3J_{H,H}$ = 7.0 Hz, 6H, OCH_2); 5.87 (t, $^3J_{H,H}$ = 6.2 Hz, 1H, N*H*); 6.69 (s, 2H, Ar*H*). ^{13}C NMR (50 MHz, C_6D_6, 25 °C): δ 8.63 (Si*C*H_2); 19.01 (OCH_2CH_3); 24.29 (*C*H_2); 44.47 (NH*C*H_2); 54.48 (N*C*H_3); 58.95 (O*C*H_2); 77.83 (*C*H_2N); 114.04 (*m*-C Ar), 143.29 (*ipso*-C Ar), 144.47 (*o*-C Ar), 149.04 (*p*-C Ar), 155.60 (*C*=O). IR (ATR): $\tilde{\nu}$ (cm^{-1}) = 765 (N–H wag); 945 (sym Si–O–C stretching); 1100-1073 (asym. Si–O–C stretching, doublet); 1232 (C–N stretching); 1441 (N–H bending); 1522 (CHN group); 1712 (C=O stretching); 2888, 2924, 2973 (C–H stretching); 3284, 3340 (N–H stretching, associated).

*2.4.2.11. Synthesis of [PdCl{$C_6H_2(CH_2PPh_2)_2$-2,6-$((EtO)_3Si(CH_2)_3NHCOO)$-4}] (**18**)*

For the synthesis of this complex, a similar procedure was followed as described above for **16**. Using 0.2 g (0.317 mmol) of **8**, compound **18** was isolated in quantitative yield. ^{1}H NMR (300 MHz, C_6D_6, 25 °C): δ = 0.65 (t, $^3J_{H,H}$ = 7.95 Hz, 2H, SiCH_2); 1.17 (t, $^3J_{H,H}$ = 7.14 Hz, 9H, OCH_2CH_3); 1.73 (quin, $^3J_{H,H}$ = 7.68 Hz, 2H, CH_2); 3.21 (quart, $^3J_{H,H}$ = 6.33 Hz, 2H, NHCH_2); 3.47 (vt, $^2J_{H,P}$ = 4.5 Hz, 4H, PCH_2); 3.78 (quart, $^3J_{H,H}$ = 6.1 Hz, 6H, OCH_2); 5.47 (t, $^3J_{H,H}$ = 5.8 Hz, 1H, N*H*); 7.06 (s, 2H, Ar*H*); 6.9-7.0 (m, 12H, Ph*H*); 7.9-8.0 (m, 8H, Ph*H*). ^{13}C NMR (75.5 MHz, C_6D_6, 25 °C): δ = 8.17 (Si*C*H_2); 18.55 (OCH_2CH_3); 23.76 (*C*H_2); 42.51 (vt, $^1J_{C,P}$ = 14.7 Hz, *C*H_2P); 43.95 (NH*C*H_2); 58.56 (O*C*H_2); 116.92 (vt, $^3J_{C,P}$ = 12.0 Hz, *m*-C Ar), 128.84 (vt, $^3J_{C,P}$ = 5.5 Hz, *m*-C Ph), 130.48 (*p*-C Ph), 132.90 (vt, $^1J_{C,P}$ = 21.8 Hz, *ipso*-C Ph), 133.34 (vt, $^2J_{C,P}$ = 7.1 Hz, *o*-C Ph), 149.27 (vt, $^2J_{C,P}$ = 11.4 Hz, *ipso*-C Ar), 150.56 (*o*-C Ar), 154.78 (*p*-C Ar); 157.0 (*C*=O). ^{31}P NMR (81 MHz, C_6D_6, 25 °C): δ = 33.4. IR (ATR): $\tilde{\nu}$ (cm^{-1}) = 740 (N–H wag); 955 (sym Si–O–C stretching); 1100-1071 (asym. Si–O–C stretching, doublet); 1227 (C–N stretching); 1435 (N–H bending); 1513 (CHN group); 1734 (C=O stretching); 2886, 2926, 2973, 3052 (C–H stretching); 3314 (N–H stretching, associated). Anal. Calcd. for $C_{42}H_{48}ClNO_5P_2PdSi$ (878.74): C, 57.41; H, 5.51; N, 1.59; P, 7.05. Found: C, 57.54; H, 5.46; N, 1.53; P, 7.02.

*2.4.2.12. Synthesis of [PdBr{$C_6H_2(CH_2SPh)_2$-2,6-$((EtO)_3Si(CH_2)_3NHCOO)$-4}] (**19**)*

For the synthesis of this complex, a similar procedure was followed as described above for **16**. Using 0.2 g (0.38 mmol) of **9b**, compound **19** was isolated in quantitative yield. ^{1}H NMR (300 MHz, $CDCl_3$, 25 °C): δ = 0.63 (t, $^3J_{H,H}$ = 8.1 Hz, 2H, SiCH_2); 1.20 (t, $^3J_{H,H}$ = 6.9 Hz, 9H, OCH_2CH_3); 1.65 (quin, $^3J_{H,H}$ = 6.9, 7.8 Hz, 2H, CH_2); 3.19 (quart, $^3J_{H,H}$ = 6.3 Hz, 2H, NHCH_2); 3.80 (quart, $^3J_{H,H}$ = 6.9 Hz, 6H, OCH_2); 4.51 (s, 4H, SCH_2); 5.52 (t, $^3J_{H,H}$ = 5.5 Hz, 1H, N*H*); 6.74 (s, 2H, Ar*H*); 7.31-7.33 (m, 6H, Ph*H*); 7.76-

7.79 (m, 4H, Ph*H*). ^{13}C NMR (75.5 MHz, $CDCl_3$, 25 °C): δ = 7.72 (Si*C*H$_2$); 18.31 (OCH$_2$*C*H$_3$); 23.06 (*C*H$_2$); 40.96 (NH*C*H$_2$); 51.53 (S*C*H$_2$); 58.50 (O*C*H$_2$); 115.75 (*m*-C Ar), 129.68 (*o*-C Ph), 129.88 (*p*-C Ph), 131.44 (*m*-C PhS), 132.19 (*ipso*-C Ph), 148.75 (*ipso*-C Ar), 150 (*o*-C Ar), 154.54 (*p*-C Ar); 156.91 (*C*=O). ^{29}Si NMR (59.6 MHz, $CDCl_3$, 25 °C): δ = –45.85. IR (ATR): $\tilde{\nu}$ (cm^{-1}) = 742 (N–H wag); 953 (sym Si–O–C stretching); 1100-1074 (asym. Si–O–C stretching, doublet); 1221 (C–N stretching); 1441 (N–H bending); 1519 (CHN group); 1731 (C=O stretching); 2885, 2926, 2973 (C–H stretching); 3302 (N–H stretching, associated). Anal. Calcd. for $C_{30}H_{38}BrNO_5PdS_2Si$ (771.17): C, 46.72; H, 4.97; N, 1.82; S, 8.32. Found: C, 46.11; H, 4.71; N, 1.94; S, 8.43.

2.4.3. X-ray crystal structure determinations.

X-ray intensities were measured on a Nonius KappaCCD diffractometer with rotating anode and graphite monochromator (λ = 0.71073 Å) at a temperature of 150 K up to a resolution of $(\sin\theta/\lambda)_{max}$ = 0.65 Å^{-1}. The structures were solved with automated Patterson Methods (DIRDIF-99[40] for **6**, **9a**, **15**, and **17**). The starting coordinates for **13a** were taken from the isostructural Pt compound. Refinement was performed with SHELXL-97[41] against F^2 of all reflections. Thereby non-hydrogen atoms were refined freely with anisotropic displacement parameters. Geometry calculations and checking for higher symmetry were performed with the PLATON[42] program.

In **9a** and **13a**, all hydrogen atoms were located in the Difference Fourier map. The OH hydrogen atom was refined freely with isotropic displacement parameters. All other hydrogen atoms were refined with a riding model.

In **6** and **17**, all hydrogen atoms were introduced in calculated positions and refined with a riding model. The crystal structure of **6** was refined as a pseudo-orthorhombic twin with a twofold rotation about the reciprocal c* axis as twin operation. The twin fraction refined to 0.4315(5).

In **15**, the OH hydrogen atoms were located in the Difference Fourier map and kept fixed in their located positions. All other hydrogen atoms were introduced in calculated positions and refined with a riding model. One methanol was refined with full occupancy, the second methanol with a partial occupancy of 2/3.

Further crystallographic details are given in Table 5.

Table 5 Experimental details for the X-ray crystal structure determinations

	6	**9a**	**13a**	**15**	**17**
formula	$[C_{34}H_{30}NOP_2Pd](BF_4)$	$C_{20}H_{17}ClOPdS_2$	$C_{12}H_{19}ClN_2OPd$	$C_{24}H_{37}IN_4O_2Pd_2 \cdot 1.66\ CH_3OH$	$C_{22}H_{40}IN_3O_5PtSi$
fw	723.74	479.31	349.14	806.63	776.65
crystal colour	yellow	yellow	yellow	yellow	colourless
crystal size [mm^3]	0.30x0.18x0.15	0.21x0.15x0.09	0.54x0.03x0.03	0.45x0.09x0.03	0.33x0.21x0.03
crystal system	monoclinic	monoclinic	orthorhombic	triclinic	monoclinic
space group	$P2_1/c$ (no. 14)	C2/c (no. 15)	$Pna2_1$ (no. 33)	$P\overline{1}$ (no. 2)	$P2_1/c$ (no. 14)
a [Å]	9.9213(1)	16.4462(1)	24.0793(4)	8.8967(2)	15.7949(3)
b [Å]	23.9549(2)	11.2934(1)	10.2284(2)	12.0046(2)	17.8749(4)
c [Å]	26.5616(3)	19.7447(2)	5.4805(1)	15.9649(4)	10.3566(2)
α [°]	90	90	90	74.7907(10)	90
β [°]	90.0730(4)	100.5980(4)	90	81.4599(11)	104.918(2)
γ [°]	90	90	90	68.9075(19)	90
V [$Å^3$]	6312.72(11)	3604.70(5)	1349.81(4)	1532.34(6)	2825.45(10)
Z	8	8	4	2	4
D_x [g/cm^3]	1.523	1.766	1.718	1.748	1.826
μ [mm^{-1}]	0.742	1.415	1.559	2.215	6.136
abs. corr. method	multiscan	multiscan	multiscan	multiscan	analytical
abs. corr. range	0.84-0.89	0.83-0.88	0.89-0.98	0.89-0.94	0.24-0.83
refl. (meas./unique)	90213 / 14433	37575 / 4119	18532 / 3018	23177 / 6915	39447 / 9750
param./restraints	796 / 0	230 / 0	162 / 1	343 / 1	299 / 150
R1/wR2 [$I>2\sigma(I)$]	0.0327 / 0.0692	0.0215 / 0.0543	0.0195 / 0.0382	0.0364 / 0.0842	0.0322 / 0.0646
R1/wR2 [all refl.]	0.0445 / 0.0736	0.0264 / 0.0568	0.0256 / 0.0396	0.0541 / 0.0912	0.0440 / 0.0683
S	1.028	1.029	1.051	1.048	1.153
Flack x parameter	-	-	–0.01(2)	-	-
$\rho_{min/max}$ [$e/Å^3$]	–0.66 / 0.64	–0.61 / 0.49	–0.34 / 0.75	–1.10 / 2.72	–1.34 / 1.24

2.5. References

1. D. E. Bergbreiter, J. D. Frels, J. Rawson, J. Li, J. H. Reibenspies, *Inorg. Chim. Acta* **2006**, *359*, 1912-1922; A. V. Chuchuryukin, H. P. Dijkstra, B. M. J. M. Suijkerbuijk, R. J. M. Klein Gebbink, G. P. M. van Klink, A. M. Mills, A. L. Spek, G. van Koten, *Angew. Chem., Int. Ed.* **2003**, *42*, 228-230; H. P. Dijkstra, M. D. Meijer, J. Patel, R. Kreiter, G. P. M. van Klink, M. Lutz, A. L. Spek, A. J. Canty, G. van Koten, *Organometallics* **2001**, *20*, 3159-3168; P. Dani, B. Richter, G. P. M. van Klink, G. van Koten, *Eur. J. Inorg. Chem.* **2001**, 125-131; S. Back, R. A. Gossage, H. Lang, G. van Koten, *Eur. J. Inorg. Chem.* **2000**, 1457-1464.
2. H. P. Dijkstra, M. Q. Slagt, A. McDonald, C. A. Kruithof, R. Kreiter, A. M. Mills, M. Lutz, A. L. Spek, W. Klopper, G. P. M. van Klink, G. van Koten, *Eur. J. Inorg. Chem.* **2003**, 830-838.
3. D. E. Bergbreiter, P. L. Osburn, J. D. Frels, *J. Am. Chem. Soc.* **2001**, *123*, 11105-11106.
4. S. Back, M. Albrecht, A. L. Spek, G. Rheinwald, H. Lang, G. van Koten, *Organometallics* **2001**, *20*, 1024-1027.
5. M. Albrecht, G. van Koten, *Angew. Chem., Int. Ed.* **2001**, *40*, 3750-3781.
6. M. Albrecht, G. Rodriguez, J. Schoenmaker, G. van Koten, *Org. Lett.* **2000**, *2*, 3461-3464.
7. W. T. S. Huck, B. Snellink-Ruël, F. C. J. M. van Veggel, D. N. Reinhoudt, *Organometallics* **1997**, *16*, 4287-4291.
8. P. J. Davies, N. Veldman, D. M. Grove, A. L. Spek, B. T. G. Lutz, G. van Koten, *Angew. Chem., Int. Ed.* **1996**, *35*, 1959-1961.

9. W. T. S. Huck, F. C. J. M. van Veggel, B. L. Kropman, D. H. A. Blank, E. G. Keim, M. M. A. Smithers, D. N. Reinhoudt, *J. Am. Chem. Soc.* **1995**, *117*, 8293-8294.
10. M. Q. Slagt, G. Rodriguez, M. M. P. Grutters, R. J. M. Klein Gebbink, W. Klopper, L. W. Jenneskens, M. Lutz, A. L. Spek, G. van Koten, *Chem. Eur. J.* **2004**, *10*, 1331-1344.
11. R. A. Gossage, L. A. van de Kuil, G. van Koten, *Acc. Chem. Res.* **1998**, *31*, 423-431.
12. I. Goettker-Schnetmann, P. S. White, M. Brookhart, *Organometallics* **2004**, *23*, 1766-1776.
13. D. E. Bergbreiter, S. Furyk, *Green Chem.* **2004**, *6*, 280-285.
14. M. Q. Slagt, J. T. B. H. Jastrzebski, R. J. M. Klein Gebbink, H. J. van Ramesdonk, J. W. Verhoeven, D. D. Ellis, A. L. Spek, G. van Koten, *Eur. J. Org. Chem.* **2003**, 1692-1703.
15. D. E. Bergbreiter, P. L. Osburn, Y.-S. Liu, *J. Am. Chem. Soc.* **1999**, *121*, 9531-9538.
16. N. C. Mehendale, C. Bezemer, C. A. van Walree, R. J. M. Klein Gebbink, G. van Koten, *J. Mol. Catal. A* **2006**, *257*, 167-175; R. Gimenez, T. M. Swager, *J. Mol. Catal. A* **2001**, *166*, 265-273; R. Chanthateyanonth, H. Alper, *J. Mol. Catal. A* **2003**, *201*, 23-31; R. Chanthateyanonth, H. Alper, *Adv. Synth. Catal.* **2004**, *346*, 1375-1384.
17. H. P. Dijkstra, N. Ronde, G. P. M. van Klink, D. Vogt, G. van Koten, *Adv. Synth. Catal.* **2003**, *345*, 364-369; H. P. Dijkstra, C. A. Kruithof, N. Ronde, R. van de Coevering, D. J. Ramón, D. Vogt, G. P. M. van Klink, G. van Koten, *J. Org. Chem.* **2003**, *68*, 675-685.
18. G. Rodriguez, M. Lutz, A. L. Spek, G. van Koten, *Chem. Eur. J.* **2002**, *8*, 45-57; C. Schlenk, A. W. Kleij, H. Frey, G. van Koten, *Angew. Chem., Int. Ed.* **2000**, *39*, 3445-3447.
19. M. D. Meijer, B. Mulder, G. P. M. van Klink, G. van Koten, *Inorg. Chim. Acta* **2003**, *352*, 247-252; M. D. Meijer, N. Ronde, D. Vogt, G. P. M. van Klink, G. van Koten, *Organometallics* **2001**, *20*, 3993-4000.
20. G. Guillena, G. Rodriguez, M. Albrecht, G. van Koten, *Chem. Eur. J.* **2002**, *8*, 5368-5376.
21. C. A. Kruithof, M. A. Casado, G. Guillena, M. R. Egmond, A. van der Kerk-van Hoof, A. J. R. Heck, R. J. M. Klein Gebbink, G. van Koten, *Chem. Eur. J.* **2005**, *11*, 6869-6877.
22. M. Gagliardo, D. J. M. Snelders, P. A. Chase, R. J. M. Klein Gebbink, G. P. M. van Klink, G. van Koten, *Angew. Chem., Int. Ed.* accepted for publication.
23. C. R. South, M. N. Higley, K. C. F. Leung, D. Lanari, A. Nelson, R. H. Grubbs, J. F. Stoddart, M. Weck, *Chem. Eur. J.* **2006**, *12*, 3789-3797; J. M. Pollino, M. Weck, *Chem. Soc. Rev.* **2005**, *34*, 193-207; H. Hofmeier, U. S. Schubert, *Chem. Commun.* **2005**, 2423-2432; W. C. Yount, D. M. Loveless, S. L. Craig, *Angew. Chem., Int. Ed.* **2005**, *44*, 2746-2748; J. M. Pollino, L. P. Stubbs, M. Weck, *J. Am. Chem. Soc.* **2004**, *126*, 563-567; W. C. Yount, H. Juwarker, S. L. Craig, *J. Am. Chem. Soc.* **2003**, *125*, 15302-15303.
24. M. Q. Slagt, H. P. Dijkstra, A. McDonald, R. J. M. Klein Gebbink, M. Lutz, D. D. Ellis, A. M. Mills, A. L. Spek, G. van Koten, *Organometallics* **2003**, *22*, 27-29; S. J. Loeb, G. K. H. Shimizu, *J. Chem. Soc., Chem. Commun.* **1993**, 1395-1397.
25. M. Albrecht, M. Lutz, A. M. M. Schreurs, E. T. H. Lutz, A. L. Spek, G. van Koten, *J. Chem. Soc., Dalton Trans.* **2000**, 3797-3804.
26. M. Albrecht, R. A. Gossage, M. Lutz, A. L. Spek, G. van Koten, *Chem. Eur. J.* **2000**, *6*, 1431-1445.
27. S. L. James, G. Verspui, A. L. Spek, G. van Koten, *Chem. Commun.* **1996**, 1309.
28. M. Albrecht, M. Lutz, A. L. Spek, G. van Koten, *Nature* **2000**, *406*, 970-974.
29. K. J. Szabo, *Synlett* **2006**, 811-824; S. Sebelius, V. J. Olsson, K. J. Szabo, *J. Am. Chem. Soc.* **2005**, *127*, 10478-10479; J. Kjellgren, J. Aydin, O. A. Wallner, I. V. Saltanova, K. J. Szabo, *Chem. Eur. J.* **2005**, *11*, 5260-5268; J. Kjellgren, H. Sunden, K. J. Szabo, *J. Am. Chem. Soc.* **2005**, *127*, 1787-1796; O. A. Wallner, K. J. Szabo, *J. Org. Chem.* **2005**, *70*, 9215-9221; J. Zhao, A. S. Goldman, J. F. Hartwig, *Science* **2005**, *307*, 1080-1082; O. A. Wallner, K. J. Szabo, *Org. Lett.* **2004**, *6*, 1829-1831; N. Solin, O. A. Wallner, K. J. Szabo, *Org. Lett.* **2005**, *7*, 689-691; N. Solin, J. Kjellgren, K. J. Szabo, *J. Am. Chem. Soc.* **2004**, *126*, 7026-7033; J. Kjellgren, H. Sunden, K. J. Szabo, *J. Am. Chem. Soc.* **2004**, *126*, 474-475; K. Takenaka, Y. Uozumi, *Org. Lett.* **2004**, *6*, 1833-1835; J. S. Fossey, C. J. Richards, *Organometallics* **2004**, *23*, 367-373; Z. Wang, M. R. Eberhard, C. M. Jensen, S. Matsukawa, Y. Yamamoto, *J. Organomet. Chem.* **2003**, *681*, 189-195; E. Diez-Barra, J. Guerra, V. Hornillos, S. Merino, J. Tejeda, *Organometallics* **2003**, *22*, 4610-4612; J. T. Singleton, *Tetrahedron* **2003**, *59*, 1837-1857; M. E. van der Boom, D. Milstein, *Chem. Rev.* **2003**, *103*, 1759-1792; G. R. Rosa, G. Ebeling, J. Dupont, A. L. Monteiro, *Synthesis* **2003**, 2894-2897; I. G. Jung, S. U. Son, K. H. Park, K.-C. Chung, J. W. Lee, Y. K. Chung, *Organometallics* **2003**, *22*, 4715-4720; J. S. Fossey, C. J. Richards, *Tetrahedron Lett.* **2003**, *44*, 8773-8776; S. Sjoevall, O. F. Wendt, C. Andersson, *J. Chem. Soc., Dalton Trans.* **2002**, 1396-1400; J. M. Seul, S. Park, *J. Chem. Soc., Dalton Trans.* **2002**, 1153-1158; D. Morales-Morales, R. E. Cramer, C. M. Jensen, *J. Organomet. Chem.* **2002**, *654*, 44-50; J. A. Loch, M. Albrecht, E. Peris, J. Mata, J. W. Faller, R. H. Crabtree, *Organometallics* **2002**, *21*, 700-706; B. S. Williams, P. Dani, M. Lutz, A. L. Spek, G. van Koten, *Helv. Chim. Acta* **2001**, *84*, 3519-3530; S. Gruendemann, M. Albrecht, J. A. Loch, J. W. Faller, R. H. Crabtree, *Organometallics* **2001**, *20*, 5485-5488; J. Dupont, M. Pfeffer, J. Spencer, *Eur. J. Inorg. Chem.* **2001**, 1917-1927; D. Morales-Morales, C. Grause, K. Kasaoka, R. Redon, R. E. Cramer, C. M. Jensen, *Inorg. Chim. Acta* **2000**, *300-302*, 958-963; D. Morales-Morales, R. Redon, C. Yung, C. M. Jensen, *Chem. Commun.* **2000**, 1619-1620; M.

A. Stark, G. Jones, C. J. Richards, *Organometallics* **2000**, *19*, 1282-1291; R. A. Gossage, J. T. B. H. Jastrzebski, J. van Ameijde, S. J. E. Mulders, A. J. Brouwer, R. M. J. Liskamp, G. van Koten, *Tetrahedron Lett.* **1999**, *40*, 1413-1416; X. Zhang, J. M. Longmire, M. Shang, *Organometallics* **1998**, *17*, 4374-4379; M. Ohff, A. Ohff, M. E. van der Boom, D. Milstein, *J. Am. Chem. Soc.* **1997**, *119*, 11687-11688; S. E. Denmark, R. A. Stavenger, A.-M. Faucher, J. P. Edwards, *J. Org. Chem.* **1997**, *62*, 3375-3389; F. Gorla, A. Togni, L. M. Venanzi, A. Albinati, F. Lianza, *Organometallics* **1994**, *13*, 1607-1616.

30. R. Chauvin, *Eur. J. Inorg. Chem.* **2000**, 577-591.
31. P. J. Davies, D. M. Grove, G. van Koten, *Organometallics* **1997**, *16*, 800-802.
32. J.-M. Valk, R. van Belzen, J. Boersma, A. L. Spek, G. van Koten, *J. Chem. Soc., Dalton Trans.* **1994**, 2293-2302; J.-M. Valk, J. Boersma, G. van Koten, *J. Organomet. Chem.* **1994**, *483*, 213-216; P. L. Alsters, P. F. Engel, M. P. Hogerheide, M. Copijn, A. L. Spek, G. van Koten, *Organometallics* **1993**, *12*, 1831-1844.
33. P. Steenwinkel, S. L. James, D. M. Grove, H. Kooijman, A. L. Spek, G. van Koten, *Organometallics* **1997**, *16*, 513-515; P. Steenwinkel, J. T. B. H. Jastrzebski, B.-J. Deelman, D. M. Grove, H. Kooijman, N. Veldman, W. J. J. Smeets, A. L. Spek, G. van Koten, *Organometallics* **1997**, *16*, 5486-5498.
34. P. L. Alsters, P. J. Baesjou, M. D. Janssen, H. Kooijman, A. Sicherer-Roetman, A. L. Spek, G. van Koten, *Organometallics* **1992**, *11*, 4124-4135.
35. G. M. Kapteijn, M. D. Meijer, D. M. Grove, N. Veldman, A. L. Spek, G. van Koten, *Inorg. Chim. Acta* **1997**, *264*, 211-217.
36. G. M. Kapteijn, D. M. Grove, H. Kooijman, W. J. J. Smeets, A. L. Spek, G. van Koten, *Inorg. Chem.* **1996**, *35*, 526-533.
37. Excellent solubility properties are important to achieve uniform distribution of the catalyst on the support.
38. D. Braga, F. Grepioni, G. R. Desiraju, *Chem. Rev.* **1998**, *98*, 1375-1405.
39. W. T. S. Huck, F. C. J. M. van Veggel, D. N. Reinhoudt, *J. Mater. Chem.* **1997**, *7*, 1213-1219.
40. P. T. Beurskens, G. Admiraal, G. Beurskens, W. P. Bosman, S. Garcia-Granda, R. O. Gould, J. M. M. Smits, C. Smykalla, *The DIRDIF99 program system, Technical Report of the Crystallography Laboratory*, **1999**, University of Nijmegen, The Netherlands.
41. G. M. Sheldrick, *SHELXL-97 Program for crystal structure refinement*, **1997**, Universität Göttingen, Germany.
42. A. L. Spek, *J. Appl. Cryst.* **2003**, *36*, 7-13.

Chapter 3

Novel Silica Immobilized NCN-Pincer Palladium(II) and Platinum(II) Complexes: Application as Lewis Acid Catalysts*

Abstract

2,6-Bis[(dimethylamino)methyl]phenyl (NCN-pincer) palladium(II) and platinum(II) complexes tethered to a trialkoxysilane coupling agent through a carbamate linkage were immobilized on various types of silica using a grafting or a sol-gel process. The resulting hybrid materials were characterized by IR spectroscopy (DRIFT) and solid state CP/MAS NMR (^{13}C and ^{29}Si). Based on these analyses, a strong H-bond interaction between the carbamate carbonyl group of the complex and free silanol groups on the silica surface was established. The palladium-based materials were tested for their activity as Lewis acid catalysts in the aldol reaction between methyl isocyanoacetate and benzaldehyde. It was found that these materials can indeed be applied as catalysts in this reaction. Their repetitive reuse showed an inferior catalytic efficacy, which presumably was caused by a reconstitution of the silica support. These studies also revealed that simple silver-based salts are active catalysts in this aldol reaction.

*N. C. Mehendale, C. Bezemer, C. A. van Walree, R. J. M. Klein Gebbink and G. van Koten, *J. Mol. Catal. A*, **2006**, *257*, 167-175.

3.1. Introduction

According to the principles of Green Chemistry catalytic systems are superior to the stoichiometric use of reagents.[1] In general, catalysts reduce the amount of reagents required and restrict waste generated in a reaction. They reduce energy requirements and decrease the number of separation steps due to increased selectivity.[2] Complex catalyst systems consisting of (precious) metals and laboriously synthesized (chiral) ligands are developed in homogeneous catalysis to meet these criteria. At the current state of art, recycling and reuse of these expensive catalyst systems become important aspects and the separation of catalysts from product streams poses an economical and environmental challenge.[3]

In this respect, homogeneous and heterogeneous catalysts each fulfill some of the Green Chemistry criteria. Selectivity and activity are better in the case of homogeneous catalysts[4] whereas product separation, catalyst recovery,[5,6] and resistance to drastic operational conditions[7] are advantageous features of heterogeneous catalysts. Combination of these features would be desirable to arrive at an ideal catalyst system. This may be achieved by the immobilization of homogeneous catalysts on a solid support.[8] One approach to achieve this is to use homogeneous catalysts chemically bound to inorganic support materials like silica.[9] The properties of silica include thermal and chemical stability under reaction conditions, easily accessible and well-dispersed surface active sites (a high surface area >100 m^2g^{-1} is required), and a mesoporous structure which is a prerequisite for liquid phase processes (pore size >20 Å to avoid diffusion limitation).[10] A wide range of homogeneous catalysts has been immobilized on silica and successfully recycled.[11-15]

The actual immobilization of a homogeneous catalyst on a heterogeneous support can be achieved mainly by two different approaches. A transition metal is either complexed to ligands already chemically bonded (immobilized) to a support, or a metal complex containing an appropriate coupling agent is tethered to a support.[6] In the first approach, the coordination sphere around the metal center changes during immobilization *via* various ligand exchange processes and the average structural properties of this immobilized complex could be quite different from those of the homogeneous complex. In the second approach, such changes may be minimal provided that the metal ion is strongly complexed to the ligand and that this configuration remains intact during grafting.[11]

In order to investigate the second approach, we decided to first obtain a fully characterized siloxane-functionalized metal complex which can be subsequently immobilized onto a silica support, and to study whether the heterogenized system formed has retained its initial metal-ligand configuration. For this study, we have used platinum and palladium complexes of so-called 'pincer' ligands of the ECE type (where ECE = $[C_6H_3(CH_2E)_2\text{-}2,6]^-$, and E = NR_2, PR_2 or SR)[16] which can act as Lewis acid catalysts in aldol condensation reactions[17-19] and double Michael addition reactions.[20-22] The metal ion in these ECE-metal complexes is strongly bound through a covalent M–C bond which is

complemented by *ortho*-chelation of the two hetero atom containing substituents. This *mer*-ECE terdentate coordination provides considerable stability against metal leaching during catalysis.[23,24] In earlier efforts from our group, complexes of this type have been anchored to a variety of soluble supports like dendritic systems,[17,21,25] hyperbranched polysilanes,[19] methanofullerenes,[22] *etc.*, and were demonstrated to give stable, recyclable catalyst that show no leaching of metal, enabling the use of these systems in a membrane reactor for continuous operation.[26] Therefore, the metallo-pincer catalysts seem ideally suited for the grafting protocol to an insoluble support like silica as envisaged above. SCS- and PCP- type pincer palladium complexes have earlier been immobilized on silica and their use in aldol and Heck reactions was reported.[13,15,27]

We have recently synthesized the siloxy-functionalized NCN-pincer palladium and platinum complexes **1** and **2** (Chart 1) from multipurpose, versatile *para*-OH functionalized NCN-pincer metal complexes, denoted as [MX(NCN-OH)].[28] Here, we present our results on grafting these complexes on different types of amorphous silica surfaces. These immobilized complexes were characterized by various techniques such as IR spectroscopy (DRIFT) and solid-state CP/MAS NMR spectroscopy (^{13}C and ^{29}Si). The immobilized palladium complexes were, furthermore, used in catalysis and the recyclability of these catalysts in the aldol condensation reaction between benzaldehyde and methyl isocyanoacetate (MI) was investigated.

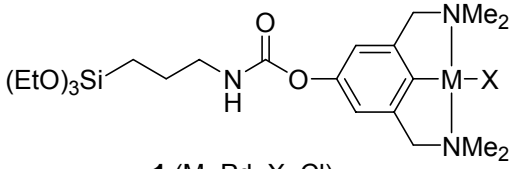

1 (M=Pd, X=Cl)
2 (M=Pt, X=I)

Chart 1 Siloxane-functionalized NCN-pincer complexes **1** and **2**.

3.2. Results and discussion

3.2.1. Siloxy-functionalized pincer complexes

The synthesis of **1** and **2** (Chart 1) was achieved by making use of [MX(NCN-OH)] pincer complexes as reported.[28] These complexes comprise both a trialkoxysilane and an organometallic fragment covalently connected through a carbamate linker. The *n*-propyl-functionalized complex **4** was prepared as a test compound in 90% yield in a similar fashion by refluxing [PdI(NCN-OH)] pincer complex **3** with *n*-propyl isocyanate in the presence of a base combination comprising 0.05 equivalent of 4-(dimethylamino)pyridine (DMAP) and 1.1 equivalent of NEt_3 (Scheme 1). The employed base combination increases the rate of the reaction and drives it to completion. At the same time, product purification was much easier than when larger amounts of DMAP were used.

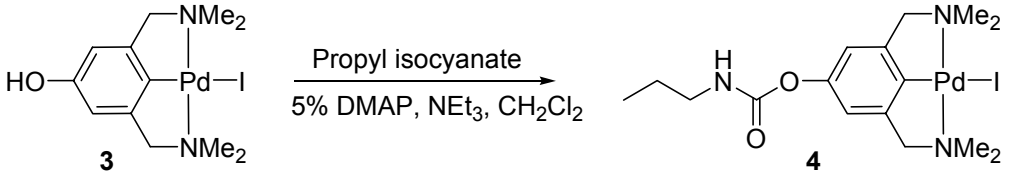

Scheme 1 Synthesis of model complex **4**.

Detailed information on the structural aspects of the organometallic siloxanes **1** and **2** was earlier obtained through the single crystal X-ray structure of **2**.[28] The molecular units in this structure comprise a NCN-Pt complex with normal pincer-metal structural parameters connected to a triethoxysilane through a propyl carbamate linker that adopts an extended conformation. Interestingly, the molecular units are intermolecularly connected through a hydrogen bonding network involving the NH and carbonyl groups of neighboring units (Figure 1). As a result, all the NCN-platinum units are arranged at one site and the $Si(OEt)_3$ groups on the opposite site, creating a kind of model showing the possible arrangement of the NCN-platinum groupings on a silica surface.

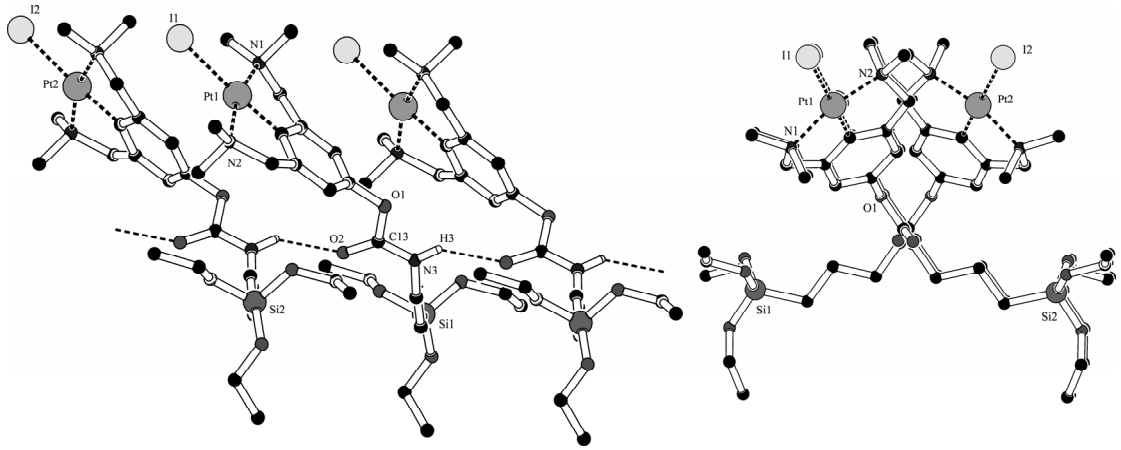

Figure 1 Intermolecular H-bonding in **2**; lateral view (left) and axial view (right) (Hydrogen atoms except those involved in H-bonding have been omitted for clarity).[28]

3.2.2. Grafting on silica

Silica with a particle size of 0.5-1.5 mm and pore diameter of 150 Å was used for the immobilization of **1** and **2**. In a typical process, silica was pre-treated by heating at 100 °C under vacuum for 2 hours. It was then reacted with complex **1** or **2** in refluxing toluene for 24 hours (Scheme 2). Continuous extraction (Soxhlet) of the resulting material with dichloromethane was performed for 24 hours in order to remove any non-covalently attached organic material. After drying *in vacuo*, the functionalized silicas **5** and **6** were obtained as off-white particles.

The results of DRIFT analysis of **5** indicated (*vide infra*) that some of the silanol groups on the silica had remained unreacted during the grafting procedure. To investigate the effect of such groups on catalysis, modified silica **5** was further treated with HMDS in hexane for 24 hours at room temperature to obtain **7**, in which the remaining silanol groups were capped by trimethylsilyl groups (Scheme 2).

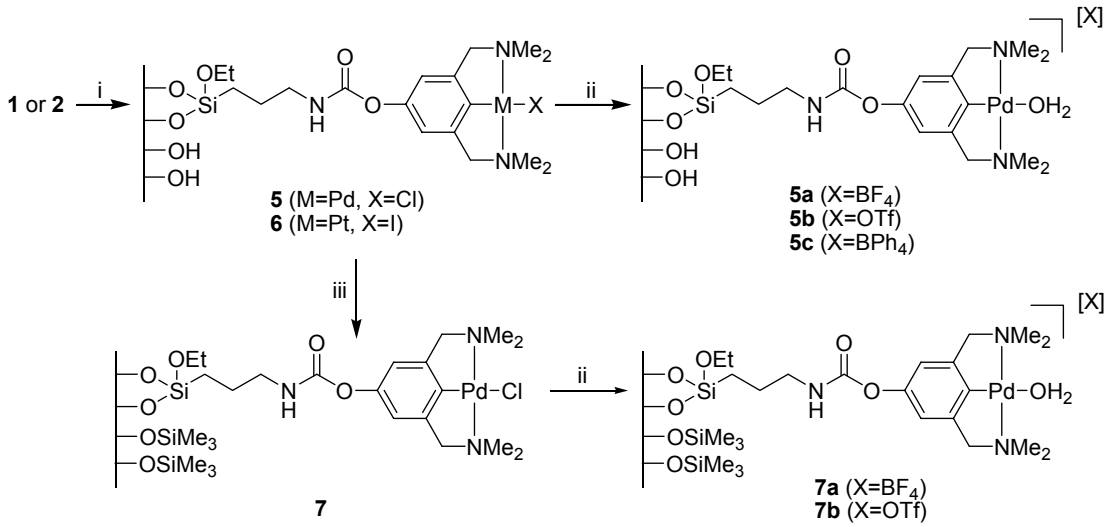

Scheme 2 Immobilization and activation of **1** and **2** on silica; i) silica, toluene, reflux, 24 h; ii) $AgBF_4$ or TMSOTf in CH_2Cl_2, or $NaBPh_4$ in acetone; iii) HMDS, hexane, 24 h.

3.2.3. Characterization of hybrid materials

For the characterization of the modified silicas, various techniques such as IR spectroscopy (DRIFT), solid-state CP/MAS NMR spectroscopy (^{13}C and ^{29}Si), and elemental analysis were used. Comparison of the IR spectrum of plain silica with that of modified silica **5** showed a strong decrease in intensity of the signal for isolated silanol groups at 3742 cm^{-1} (Figure 2).

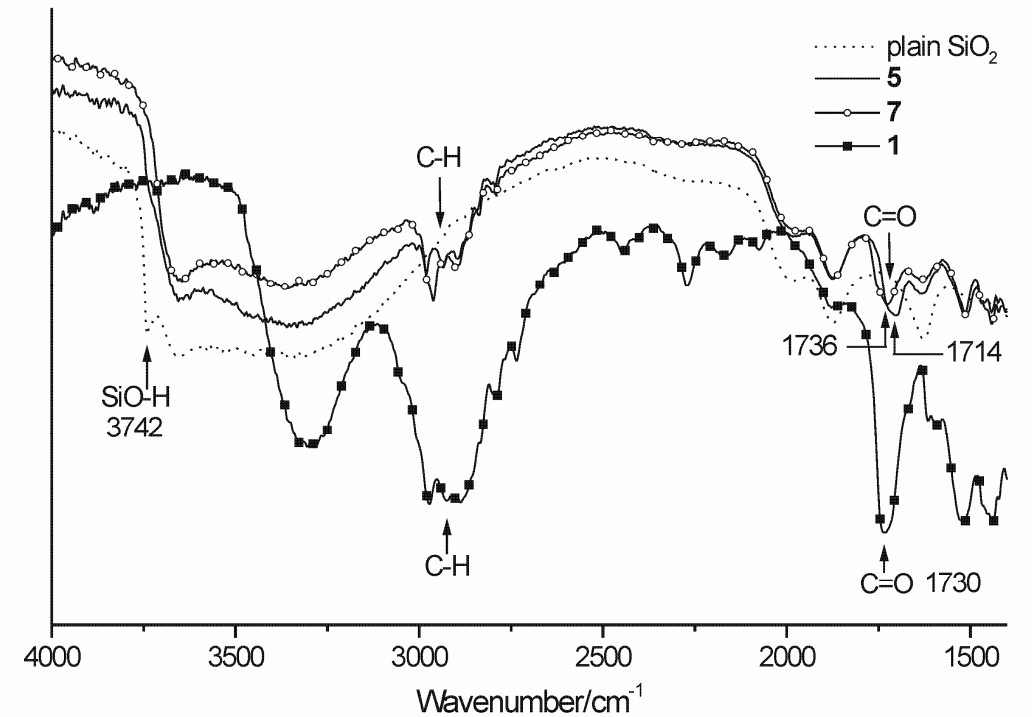

Figure 2 IR spectra (DRIFT) of plain silica, silicas **5** and **7**, and homogeneous complex **1**.

IR spectra of the homogeneous complex **1** and the hybrid material **5** were also compared (Figure 2, Table 1). The signals corresponding to the C–H stretching, C=O stretching, CNH group, and N–H bending vibrations of **1** were observed in the spectrum of **5**. A further decrease in the isolated silanol

signal at 3742 cm^{-1} was observed after treatment of **5** with HMDS to obtain **7**. Additional signals corresponding to C–H stretching (2960 cm^{-1}), symmetric deformation of Si–CH_3 (1265 cm^{-1}), and Si–CH_3 rocking (860, 765 cm^{-1}) vibrations were also observed for this material and appeared comparable to vibrations in the IR spectrum of plain silica after treatment with HMDS (Figure 2, Table 1).

Table 1 IR stretching frequencies in cm^{-1} with assignments.

Compound	N-H	C-H	C=O	CHN	N-H bend.	Other
Pd-complex **1** Solid	3313 (associated)	2975, 2926, 2887	1730 (associated)	1520	1440	1228, 1100, 1074, 956, 731
Solution	3445 (isolated)		1737 (isolated)			
Pt-complex **2**	3340, 3284	2973, 2924, 2888	1712	1522	1441	1232, 1136, 1099, 1073, 943, 796, 764
Grafted Pd-complex **5**		2986, 2935, 2901	1728, 1714	1525	1450	
Grafted Pt-complex **6**		2986, 2930, 2891	1722, 1707	1525	1454	
Grafted Pd-complex **7**		2960, 2901	1736	1521	1450	854, 765
Silica + HMDS[a]		2970, 2908				854, 763

a. plain silica treated with excess HMDS to cap isolated –OH groups with trimethylsilyl groups.

^{13}C and ^{29}Si solid-state NMR spectroscopy on **5** provided further information on the structure of both the organic (spacer and metal-complex) and inorganic part of this hybrid material and is representative for all silica materials presented here. All peaks corresponding to the ^{13}C NMR spectrum of homogeneous complex **1** were present in the ^{13}C spectrum of **5** (Figure 3). Signals corresponding to ethoxy groups on the silicon atom of **1** were present even after grafting (15.3 and 58.3 ppm). This suggests that not all ethoxy groups have reacted and that the covalent immobilization of this complex to the surface takes place *via* either one, two or three silyl ether linkages, *i.e.* the type of silicon atom of the grafted complex is best described as an average of T^1, T^2, and T^3 types (T^n = $RSi(OSi)_n(OEt)_{3-n}$).[29] This observation is supported by ^{29}Si NMR spectroscopy where a broad signal is observed at –52.6 ppm for T^n Si of the complex, corroborating the average of the three types of linkages to the support (Figure 4). Furthermore, two strong signals were observed at –103.1 and at –112.6 ppm corresponding to Q^3 Si and to Q^4 Si from the support, respectively (Q^m = $Si(OSi)_m(OH)_{4-m}$).

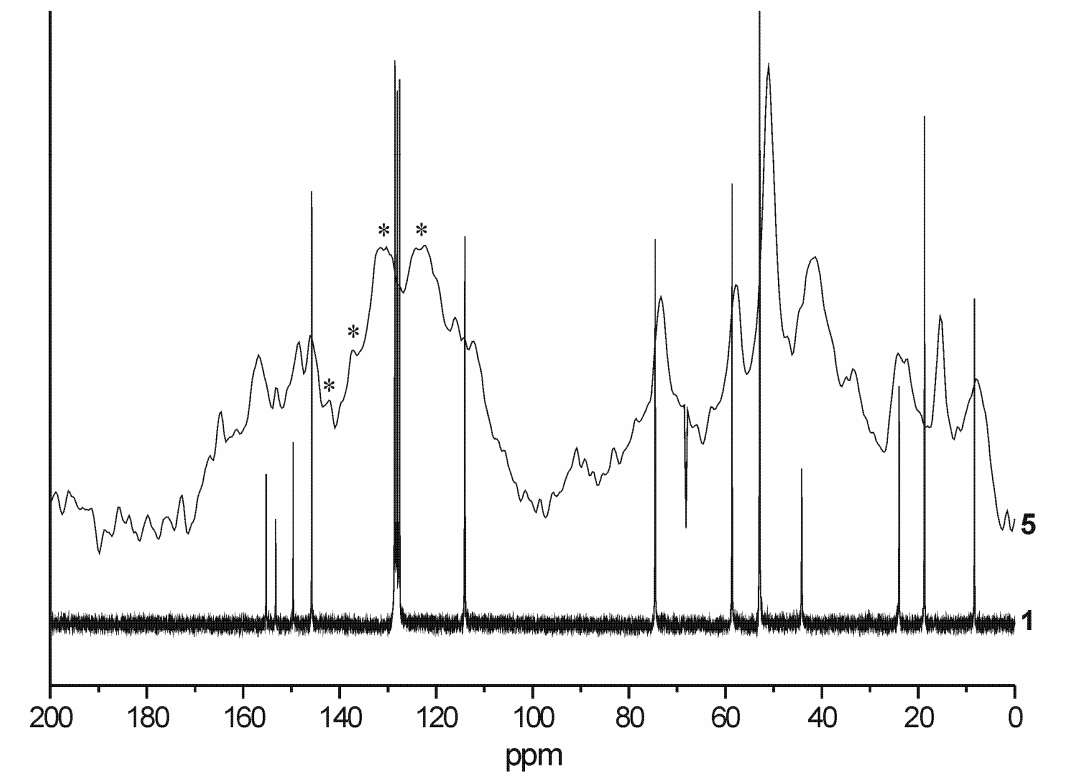

Figure 3 CP/MAS ^{13}C NMR spectrum of silica **5** and ^{13}C NMR spectrum of homogeneous complex **1** (* indicates spinning side-bands).

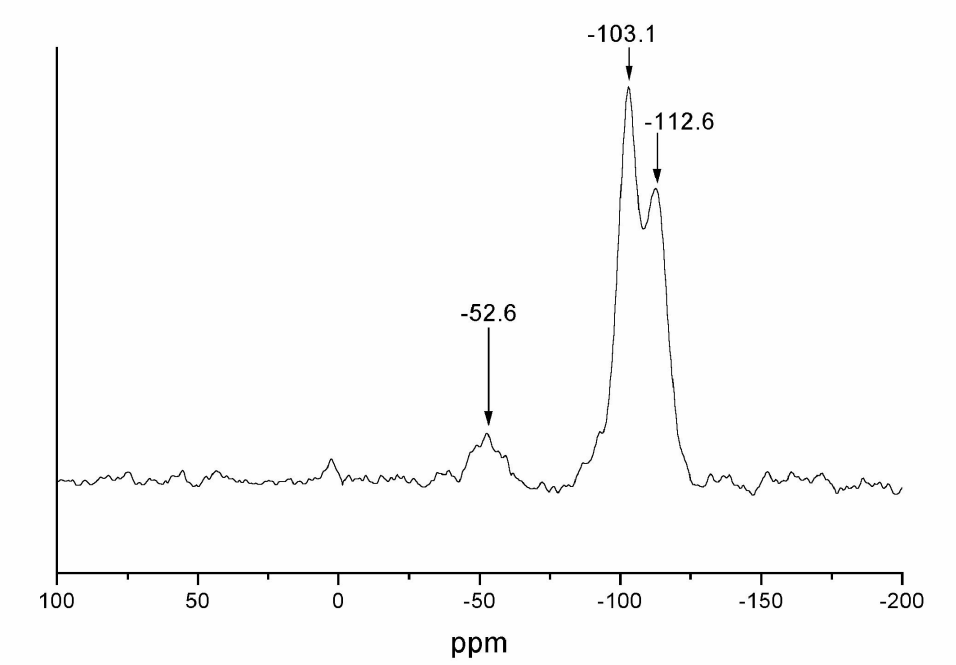

Figure 4 CP/MAS ^{29}Si NMR spectrum of silica **5**.

According to elemental analysis, a loading of 1.63 weight % of Pd and 1.18 weight % of Pt is achieved for **5** and **6**, respectively. Comparison of the relative N and metal content showed their presence in the expected ratio of three according to the formulation of both **1** and **2**.

3.2.4. SO_2 binding test

Square planar NCN-pincer platinum halide complexes are known to reversibly bind SO_2 gas.[30] The adduct thus formed has a bright orange color whereas the SO_2-free complexes are colorless. Coloration tests with SO_2 can thus be used to detect and prove the presence of such complexes to a very low level of concentration and vice versa.[31] Conditions for SO_2 binding and colorization are that the Pt(II) ion is both cyclometalated by an NCN type pincer ligand and that it has a halide ion as its fourth ligand.[32] After immobilizing complex **2** on silica, the colorless, modified silica **6** was exposed to an SO_2 atmosphere upon which it turned orange. By applying vacuum, the silica turned back to colorless, displaying reversible binding of SO_2. These observations provide evidence for the successful grafting of the siloxane as well as for the presence and integrity of the NCN-pincer platinum halide complex on silica.

3.2.5. H-bonding

The crystal structure of the platinum-based complex **2** reveals the presence of intermolecular hydrogen bonds with the carbamate nitrogen as donor and the carbamate carbonyl of a neighboring molecule as acceptor (Figure 1).[28] In the IR spectrum of palladium-based complex **1** in the solid-state, the carbonyl stretching signal is found at 1730 cm^{-1} and the N–H vibration at 3313 cm^{-1} (broad), whereas a diluted solution of **1** in dichloromethane has these vibrations at 1737 cm^{-1} and 3445 cm^{-1} (sharp), respectively, clearly indicating a decrease in H-bonding in solution. Upon immobilization of this complex on silica (**5**), the signal for the carbonyl group is shifted to 1714 cm^{-1} (Figure 2), indicating a stronger H-bonding for the immobilized complex with either a carbonyl moiety of a neighboring complex or, alternatively, with (isolated) silanol groups on the silica surface. Interestingly, when the isolated silanol groups were protected by trimethylsilyl groups (modified silica **7**), the signal for the carbonyl group shifted to the value observed for **1** in solution (1736 cm^{-1}), suggesting a decrease in the H-bonding (Figure 2).

These observations are supported by the considerable shift observed in ^{13}C solid-state NMR for the carbonyl carbon signal (from 155.6 for homogeneous complex **1** to 164.9 for grafted complex **5**), which points to stronger H-bonding in the grafted complex. The combined data suggest that isolated silanol groups from **5** may be involved in H-bonding as a H-bond donor with the carbamate moiety acting as a H-bond acceptor *via* its carbonyl group.

3.2.6. Catalysis

NCN-pincer palladium complexes are known to be excellent pre-catalysts for the formation of Lewis acid catalysts for the aldol condensation reaction between MI and benzaldehyde to form oxazolines (Reaction 1).[33]

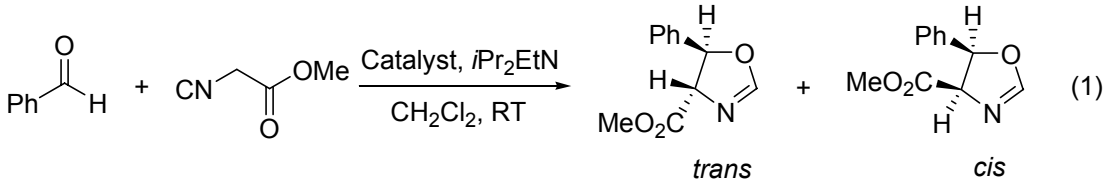

In all previous works, pre-catalyst NCN-pincer palladium halide complexes are activated by removal of the halide ligand in order to generate cationic Pd-aqua complexes, which are believed to be the active catalytic species.[17-19] In this study, we prepared various types of combinations of possible immobilized catalyst systems, each time starting from hybrid material **5** (Scheme 2). The materials thus obtained were tested in a parallel manner in the aldol condensation. The following protocols were considered for creating the catalyst systems: i. use of an activating reagent to form the cationic palladium-center, either $AgBF_4$ or trimethylsilyl triflate (TMSOTf) and, ii. use of either TMS protection or non-protection of free silanol groups after immobilization of complex **1**.

The catalytic results are summarized in Table 2. After treatment with $AgBF_4$ and prior to use in catalysis, silicas **5a** and **7a** were rinsed with fresh dichloromethane several times with the aim to remove all silver salts. Interestingly, the reactivity of the obtained materials was found to be unusually high (Table 2, entry 1 & 2). Upon checking the activity of simple silver salts like AgCl and $AgBF_4$ for this aldol reaction, it was found that both silver salts are active catalysts, too.[34] This unexpected aspect had initially escaped our attention as well as that of previous researchers who used silver-based activating agents for the generation of both homogeneous[17,18,35] and heterogeneous[14,15] cationic palladium catalysts for this reaction. Our observation clearly points out that by the protocols followed, not all silver salts are completely removed from samples such as silicas **5a** and **7a**. In case of the homogeneous complexes, it is possible to separate insoluble silver salts by filtration, although, also in this case care must be taken that soluble $AgBF_4$ has been completely removed. However, in case of the heterogenized complexes, it is difficult to remove silver salts and consequently catalysis will be affected by their presence. Therefore, use of silver-based reagents should be avoided. Hence, silicas **5b** and **7b** were obtained *via* treatment of **5** and **7** with TMSOTf. In this case, the side product is TMSCl which can be easily removed by applying vacuum. These cationic complexes show palladium-based catalysis in the aldol condensation (Table 2, entries 3 and 4). It appeared that recycling of **5b** and **7b** was severely hampered, probably due to the generation of triflic acid, which induces the decomposition of the palladium complex to Pd(0) (silica turned grayish after treatment by TMSOTf). The above described findings prompted us to search for an alternative activating reagent. In this respect, NaOPh, $NaBF_4$, and $NaBPh_4$ were tested. With NaOPh, a Pd–OPh complex is formed[36] which is an active catalyst, but NaOPh at the same time reacts with silica to form basic sites, which themselves promote aldol reactions (plain silica treated with NaOPh was found to be active in the aldol reaction). $NaBF_4$ was ineffective as an

Table 2 Aldol reaction with cationic Pd materials obtained from **5**.[a]

Entry	Activation	Protection	Catalyst	Time/h	% of product	% *trans*
1	$AgBF_4$	No	**5a**	2	70	63
2	$AgBF_4$	Yes	**7a**	2	>80	66
3	TMSOTf	No	**5b**	6	38	68
4	TMSOTf	Yes	**7b**	6	38	67
5	$NaBPh_4$	No	**5c**	6	18	70

a. 1 mol% Pd loading.

activating agent for solubility reasons, whereas $NaBPh_4$ in acetone was found to be useful indeed to form cationic palladium centers (silica **5c**, Table 2, entry 5).

As a blank for the catalytic experiments, we also tested the palladium chloride silicas **5** and **7** without any further treatment. Surprisingly, these materials were also found to be effective catalysts (Table 3).[33] A considerable improvement of the activity of silica **5** was obtained by protecting silanol groups present in this material by capping them with trimethylsilyl groups (**7**). Silicas **5**, **5c**, and **7** were used in subsequent recycling experiments.

Table 3 Aldol reaction with silica immobilized NCN-pincer palladium halide complexes.[a]

Entry	Catalyst	Time/h	% of product	% *trans*
1	**5**	6	18	68%
2	**7**	6	42	70%
3[b]	**7**	3	84	70%

a. 1 mol% Pd loading; b. 2.5 mol% Pd loading.

3.2.7. Recycling

Recycling studies with catalysts **5**, **5c**, and **7** were carried out using overhead stirring and overall 2.5 mol% Pd per catalytic run, following a strict protocol for the work-up of the reaction mixture and recycling. After each run, the reaction vessel was centrifuged to settle the silica. Subsequently, the supernatant reaction mixture containing the reaction product was carefully decanted. The remaining silica was washed twice with dichloromethane and dried *in vacuo*. It was then used for the next run. From these experiments (Table 4, entries 1-3), it was obvious that while these catalysts do show activity during the first few runs, their activity drops gradually after each run.

Table 4 Recycling of catalysts.[a]

Entry	Catalyst	Run 1	Run 2	Run 3	Run 4
1	**5**	60 (6, 71%)	42 (6, 74%)	26 (6, 77%)	
2	**7**	84 (3, 70%)	42 (4, 73%)	22 (4, 76%)	15 (4, 77%)
3	**5c**	60 (23, 70%)	43 (23, 71%)	25 (23, 71%)	23 (23, 76%)
4[b]	**5′**	45 (5)	17 (5)		
5[c]	**10**	50 (20, 79%)	30 (20, 78%)	30 (20, 81%)	
6[d]	**5″**	44 (70, 81%)	38 (70, 80%)		

a. % conversion, (time in hours and % *trans*), amount of Pd 2.5 mol%; b. silica obtained by grafting of **1** in ethanol; c. amount of Pd= 0.75 mol%; d. silica obtained by using **1** in a sol-gel process.

To understand this deactivation, we considered several aspects. First of all it is possible that some sort of catalyst decomposition occurs during catalysis, even though pincer palladium complexes are known for their stability. To test this possibility, a second run was carried out without removing catalyst **5** from the reaction mixture after the first run, simply by adding more substrate to the product mixture. No decrease in activity was observed over the complete reaction time (Figure 5), which suggested that the overall activity of the palladium sites present at the start of the catalytic runs did not change over time.

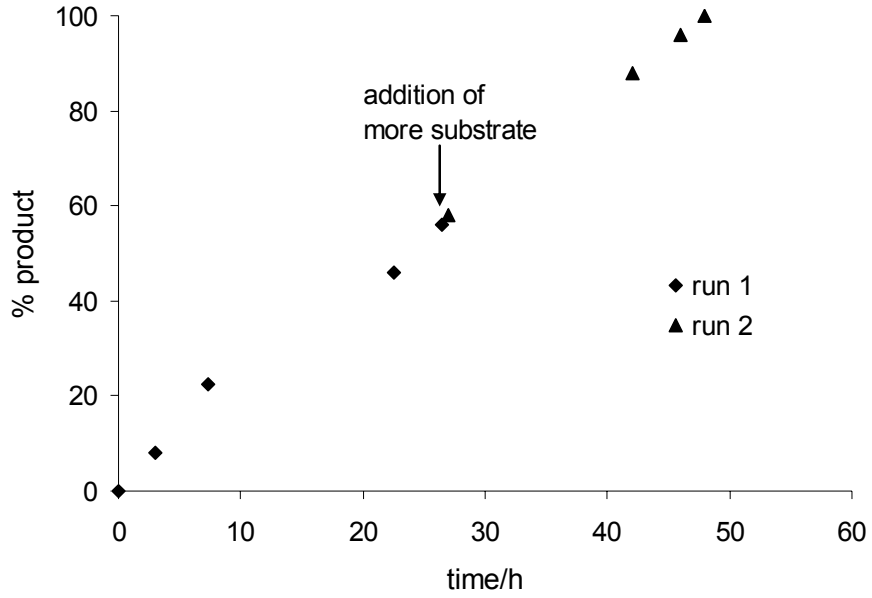

Figure 5 Run 1 and run 2 with silica **5** (amount of Pd 1 mol%) without removal of the catalyst.

Another possible reason for the reduced activity upon recycling may be that part of the palladium sites were removed from the reaction mixture as a result of the chosen work-up procedure. This would either suggest that not all silicious material had settled during the centrifugation protocol or that soluble palladium containing species/particles were formed. In general, immobilized catalysts can leach from the surface mainly by two processes, (a) cleavage of the linker, and (b) cleavage of Si–O–Si bonds from the surface and the catalyst (apart from metal leaching). To check the stability of the carbamate linker, we designed a model compound **4** with an *n*-propyl carbamate linker instead of the siloxy carbamate one in **5** (Scheme 1). No degradation of the carbamate linker was observed (from NMR studies) when this compound was tested under catalytic conditions. Instead, ICP analysis on the supernatants combined with work-up washings of three consecutive runs using **5** as the catalyst provided compelling evidence for substantial loss of catalytic material (Table 5). Furthermore, the observed molar ratio of Si to Pd in the washings amounted to 8.5-11.8, indicating that cleavage of Si–O–Si bonds between silica and the organometallic fragment could not alone account for this ratio (note that the Si/Pd molar ratio would be expected to be close to one for the leached but intact catalyst). On the other hand, surface reconstitution of silica under the reaction conditions could have taken place forming small, inseparable particles. Clearly, the discrepancy

Table 5 Loss of catalyst **5** determined by ICP elemental analysis of supernatants (without silica) after each run.[a]

Run	Catalyst mol%[b]	Si ppm	Pd ppm	Si/Pd molar ratio in the washings[c]	Catalyst wt. decrease (%)[d]	Activity decrease (%)
1	2.4	2700	1200	8.5	10.4	-
2	2.15	2500	800	11.8	7.6	30
3	1.99	1500	500	11.3	5.3	40

a. silica was centrifuged and supernatant filtered over a cotton plug before analysis; b. at the beginning of the run; c. theoretical value in **1** is one; d. at the end of the run.

between the total loss in material weight after work-up and the loss in catalyst activity seems to point to surface reconstitution as the main catalyst deactivation process.

Four types of silicas differing in pore size and particle diameter (Table 6) were then used for the immobilization of NCN-pincer palladium complex **1**. Unreacted silanol groups were capped with trimethylsilyl groups. Aldol reactions using these modified silicas as catalysts were carried out in the same manner as before. Results showed that although all of these materials were active, the activity of each silica decreased considerably after the first run. From the series of silicas tested, no indication could be derived for a relation between the structural properties of the support material and its stability under the catalytic conditions.

Table 6 Catalytic conversion for reaction (1) using various silicas differing in particle size and pore diameter.[a]

Entry	Silica		Run 1	Run 2	Run 3
	Particle size	Pore diameter (Å)			
S1	0.5-1.5 mm	150	50 (68)	25 (73)	18 (74)
S2	50-200 μm	300	70 (69)	25 (74)	18 (77)
S3	50-200 μm	500	55 (70)	20 (75)	14 (79)
S4	60 μm	500	45 (71)	12 (77)	11 (82)

a. amount of silica 100 mg in each case; amount of Pd may vary for each silica due to difference in surface area and hence the ability to immobilize the catalyst; reaction time 5h, % conversion (% *trans* product).

3.2.8. Alternative grafting procedures

Finally, we have tested a number of alternative grafting methods for the synthesis of amorphous silica hybrids containing a grafted NCN-pincer palladium complex. The first protocol involved stirring of silica with a solution of **1** in ethanol at room temperature in the presence of a catalytic amount of NEt_3 for 20 hours. The resulting solid was washed thoroughly with ethanol and dried *in vacuo* to yield a colorless material (**5′**). The catalytic activity of this material is comparable to that of **5**, but again upon reuse, substantial decrease in activity was observed (Table 4, entry 4).

A second protocol involved the change of the nature of the linker to the complex (Scheme 3). Modified silica **10**, with the NCN-pincer Pd moiety attached to silica *via* an amide type of linkage, was prepared from commercially available propylamine functionalized silica **8** and an activated ester

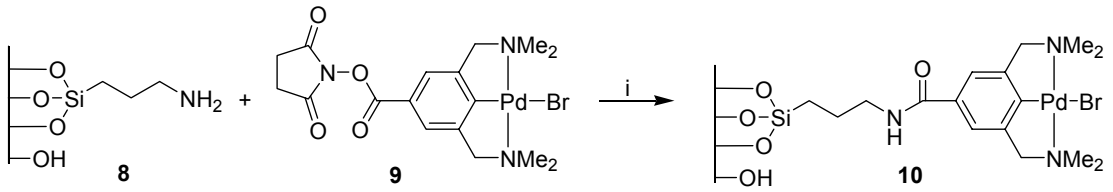

8 9 10

Scheme 3 Silica immobilization of an NCN-Pd halide complex *via* an amide linkage; i) CH_2Cl_2, 16 h.

functionalized NCN-pincer palladium complex **11**.[37] The results of three subsequent runs (Table 4, entry 5) revealed that the activity decreased gradually per cycle.

In a third protocol, a mixture of **1**, TEOS, and NH_3 (29.3% NH_4OH solution) in ethanol was stirred at ambient temperature.[38] Fine gel particles precipitated out of the solution slowly, which were centrifuged to obtain a modified Stöber silica (**5″**). From elemental analysis a palladium content of 0.78% w/w was found for this material. Surface area analysis by N_2 adsorption indicated **5″** to have a smaller surface area than that of commercial silica (23.6 m^2/g against 215.5 m^2/g). Consequently, the catalytic activity of material **5″** was observed to be lower (Table 4, entry 6); interestingly, it presented only a small decrease in activity during the second run suggesting better recycling properties.

3.3. Conclusion

This study shows that new organometallic silica hybrids are accessible *via* the grafting of discrete organometallic siloxane precursors onto commercially available silicas. Analysis of the resulting hybrid materials confirmed the full integrity of both the tether linkage and the organometallic NCN-pincer palladium fragment. The physico-chemical properties of the pincer metal complexes allow for a 'hands-on' structural analysis *via* reversible colorization of pincer platinum materials by SO_2 binding and, in addition, offer various opportunities in catalysis as exemplified by the corresponding pincer palladium materials described in this study. Moreover, the NCN-pincer manifold can be replaced by PCP, SCS, or a variety of other pincer-type combinations and together with specific choices of the metal site this gives access to a variety of catalysts for notable conversions in organic synthesis.[13,15,23,39]

Catalytic testing of the pincer palladium hybrid materials in an aldol condensation reaction initially suffered from drawbacks in terms of insufficient pre-catalyst activation due to the heterogeneous reaction conditions. Serendipitously, the studies revealed that simple silver halide salts are very active catalysts themselves in this aldol condensation reaction. A more detailed analysis of the catalytic activity of silver halide salts can be found in ref. 34. Furthermore, it was established that the neutral NCN-palladium halide complexes, do not need activation by Ag-based reagents in order to apply them as catalysts in the aldol reaction.[33] Recycling studies on the hybrid materials therefore concentrated on these NCN-palladium halide materials. Although poor recyclability was observed,

sufficient evidence was obtained to conclude that detrimental side-reactions involving either the organometallic fragment or its linkage to the silica support are not playing a prominent role in catalyst deactivation. Finally, leaching experiments led us to conclude that reconstitution of the silica surface forming soluble, inseparable species is the main cause of the decrease of catalytic activity of these hybrid materials.

Current efforts focus on the use of organometallic pincer-siloxane reagents for surface modification and on the use of pincer-metal silica hybrid materials for other catalytic conversions (e.g., C–C and C–X bond formation).[23,39,40] The integrity and stability of the silica support will be another important aspect of these studies. A preliminary sol-gel type of grafting method described here already hints at the formation of hybrid materials with increased stability as compared with the (pre-formed) amorphous silicas used in the present study.

3.4. Experimental Section

3.4.1. General Comments

Solvents were dried over appropriate materials and distilled prior to use in a dry N_2-atmosphere. All reagents were obtained from commercial sources and were used without further purification. All siloxane materials were stored under nitrogen atmosphere. Benzaldehyde and Hunig's base were distilled prior to use. Silica was received from Engelhard De Meern B.V., The Netherlands, in a generous amount. Triethoxysilyl-functionalized NCN-pincer metal complexes **1** and **2** and [PdI(NCN-OH)] (**3**) were prepared as described previously.[28] ^{1}H (200 and 300 MHz) and ^{13}C{^{1}H} (50.3 and 75.5 MHz) NMR spectra were recorded at room temperature on either Varian Mercury 200 or Varian Inova 300 spectrometers. ^{13}C (75.5 MHz) and ^{29}Si (59.6 MHz) CP/MAS (cross-polarization/magic angle spinning) NMR spectra were recorded on a Varian Inova 300 spectrometer (Spinning rate 6000 Hz, contact time for ^{13}C 1.50 ms and for ^{29}Si 3.0 ms, number of transients for ^{13}C 6068 and for ^{29}Si 11336). FT-IR and DRIFT (Diffuse reflectance IR Fourier transformation) spectra were recorded using a Mattson Instruments Galaxy Series FTIR 5000 spectrometer with SPECAC diffuse-reflectance assembly. Gas chromatographic analyses were performed with a Perkin Elmer Autosystem XL GC using a 30 m, PE-17 capillary column with an FID detector. Microanalyses were obtained from H. Kolbe Mikroanalytisches Laboratorium, Mülheim an der Ruhr, Germany.

3.4.2. Procedures

*3.4.2.1. Synthesis of [PdI(C_6H_2{CH_2NMe_2}$_2$-2,6-{$Me(CH_2)_2NHC(O)O$}-4)] (**4**)*

n-Propyl isocyanate (25 μL, 0.25 mmol) was added to a solution of **3** (0.1 g, 0.23 mmol), triethylamine (35 μL, 0.25 mmol), and 4-(dimethylamino)pyridine (2 mg, 0.013 mmol) in dry CH_2Cl_2 (10 mL). This reaction mixture was then refluxed for 10 h after which a clear yellowish solution had formed. After allowing the reaction mixture to attain room temperature, all volatiles were removed *in vacuo*. The residue was washed with pentane (2 × 15 mL) and the product extracted from the residue by treating it with C_6H_6 (3 × 15 mL). The combined extracts were filtered over a small silica column to remove

insoluble impurities and the solvent was evaporated *in vacuo* to obtain **4** as a yellowish solid (0.11 g, 90% yield). ^{1}H NMR (300 MHz, C_6D_6, 25 °C): δ = 0.70 (t, $^{3}J_{H,H}$ = 7.5 Hz, 3H, C*H*$_3$); 1.30 (mult., $^{3}J_{H,H}$ = 6.9, 7.5 Hz, 2H, C*H*$_2$); 2.65 (s, 12H, NC*H*$_3$); 3.00 (q, $^{3}J_{H,H}$ = 6.6, 6.9 Hz, 2H, NHC*H*$_2$); 3.22 (s, 4H, ArC*H*$_2$N); 4.85 (t, $^{3}J_{H,H}$ = 6.6 Hz, 1H, N*H*); 6.59 (s, 2H, Ar*H*). ^{13}C NMR (50 MHz, C_6D_6, 25 °C): δ = 11.25 (*C*H$_3$); 23.40 (*C*H$_2$); 43.10 (NH*C*H$_2$); 54.74 (N*C*H$_3$); 73.72 (Ar*C*H$_2$N); 113.91, 146.25, 149.54, 154.93 (Ar*C*); 155.81 (carbonyl). Anal. Calcd. for $C_{16}H_{26}IN_3O_2Pd$ (525.72): C, 36.55; H, 4.98; N, 7.99. Found: C, 36.43; H, 5.06; N, 7.85.

3.4.2.2. Grafting procedure

In a typical procedure, silica (1 g) was pretreated by heating it at 100 °C under vacuum for 2 h. After allowing it to cool to room temperature, a solution of **1** or **2** (0.2 mmol) in dry toluene (100 mL) was introduced. The resulting mixture was stirred to form a suspension and refluxed for 24 h, after which the silica was allowed to settle and the supernatant liquid was decanted. The silica was washed twice with dry CH_2Cl_2 (50 mL) and then it was subjected to Soxhlet extraction using CH_2Cl_2 for 16 h. Finally, it was dried under vacuum yielding about 1 g of material in each case.

Material **5**: IR (KBr, DRIFT): $\tilde{\nu}$ (cm^{-1}) 2960, 2858 (C–H stretching), 1718 (C=O stretching), 1603, 1539 (CNH group), 1472, 1450 (N–H bending). ^{13}C CP/MAS NMR (75.5 MHz, 25 °C): δ = 8.4 (Si*C*H$_2$); 15.3 (OCH$_2$*C*H$_3$); 24.6 (*C*H$_2$); 42.6 (NH*C*H$_2$); 51.1 (N*C*H$_3$); 58.3 (O*C*H$_2$); 73.4 (Ar*C*H$_2$N); 114.36, 145.8, 148.4, 156.8 (Ar*C*); 164.9 (carbonyl). ^{29}Si CP/MAS NMR (59.6 MHz, 25 °C): δ = –112.6, –103.1, –52.6. Anal. Found: C, 3.46; H, 0.75; N, 0.61; Pd, 1.63 (molar ratio of N/Pd 3; found 2.8).

Material **6**: IR (KBr, DRIFT): $\tilde{\nu}$ (cm^{-1}) 2986, 2930, 2891 (C–H, stretching); 1718 (C=O, stretching); 1525 (CHN group); 1454 (N–H, bending). Anal. Found: C, 1.13; H, 0.25; N, 0.27; Pt, 1.18 (molar ratio of N/Pt 3; found 3.2).

3.4.2.3. Protection of free silanol groups with trimethylsilyl groups

In a typical procedure, silica **5** (0.5 g) was treated with 1,1,1,3,3,3-hexamethyldisilazane (HMDS) (5 g, 31 mmol) in hexane (25 mL). The mixture was stirred for 24 h, after which the silica was washed with hexane (3 × 50 mL) and dried under vacuum yielding about 0.5 g silica **7**. IR (KBr, DRIFT): $\tilde{\nu}$ (cm^{-1}) 2960, 2901, 1736, 1521, 1450, 854, 765.

*3.4.2.4. Synthesis of silica **10**; grafting by using amide linkage*

Commercially available 3-aminopropyl functionalized silica **8** (2.4 g, loading ~1 mmol/g NH_2) was treated with a solution of organometallic activated ester **9** [37] (60 mg, 0.12 mmol) in CH_2Cl_2. The mixture was stirred at room temperature for 16 h. After centrifugation and decantation, the silica was washed successively with CH_2Cl_2, acetone, water, and then again with acetone and was finally dried *in vacuo* yielding about 2 g of material **10**. IR (KBr, DRIFT): $\tilde{\nu}$ (cm^{-1}) 2943, 2858 (C–H, stretching); 1658 (C=O, stretching); 1543 (CNH group);1444 (N–H, bending). Anal. Found: C, 8.17; N, 2.27; Pd, 0.55.

*3.4.2.5. Synthesis of **5′**; grafting using ethanol*

A mixture of silica (0.5 g), complex **1** (50 mg, 0.084 mmol) and triethylamine (1 mL, 7.2 mmol) in ethanol (20 mL) was stirred at ambient temperature for 16 h. Silica was filtered, washed with ethanol (3 × 20 mL) and dried *in vacuo* which gave 0.52 g of solid.

*3.4.2.6. Synthesis of **5″**; grafting by Sol-Gel method*

To a solution of NH_3 (29.3% aqueous NH_4OH solution, 7.25 mL) in ethanol (75 mL), complex **1** (95 mg, 0.16 mmol) and tetraethylorthosilicate (TEOS) (3.34 mL, 15 mmol) were added. This clear solution was stirred at ambient temperature. In about 10 minutes, fine gel particles precipitated out of the solution slowly. After stirring the mixture for 1 h, these particles were centrifuged off. Silica was washed with excess of ethanol and dried *in vacuo*. 1.13 g of silica was obtained. IR (KBr, DRIFT): $\tilde{\nu}$ (cm^{-1}) 3230, 1638, 1464, 1059, 955, 796. Anal. Found for **5″**: Pd, 0.78.

3.4.2.7. Catalysis

The catalytic experiments were carried out using *i*Pr_2EtN (Hunig's base, 10 mol%) as a base, functionalized silica materials (approx. Pd content 1 or 2.5 mol%) as catalyst, and MI (1.6 mmol) and benzaldehyde (1.6 mmol) as reagents in CH_2Cl_2 (5 mL) at room temperature. Except for parallel screening, stirring was carried out using an overhead stirrer in order to avoid grinding of silica particles. The reaction progress was monitored by means of GC analysis using pentadecane as internal standard. After each run, the complete reaction mixture was centrifuged and the supernatant was separated. The remainders were washed with CH_2Cl_2 (2 × 20 mL) and dried *in vacuo*. The obtained solid was used for the next run.

3.5. References

1. P. T. Anastas, J. C. Warner, *Green Chemistry: Theory and Practice*, Oxford University Press, New York, **1998**.
2. P. T. Anastas, M. M. Kirchhoff, *Acc. Chem. Res.*, **2002**, *35*, 686-694.
3. R. T. Baker, W. Tumas, *Science*, **1999**, *284*, 1477-1479.
4. G. W. Parshall, S. D. Ittel, *Homogeneous Catalysis*, 2nd ed., Wiley-Interscience, New York, **1992**.
5. D. Brunel, N. Bellocq, P. Sutra, A. Cauvel, M. Laspéras, P. Moreau, F. Di Renzo, G. Anne, F. François, *Coord. Chem. Rev.*, **1998**, *178-180*, 1085-1108.
6. A. Choplin, F. Quignard, *Coord. Chem. Rev.*, **1998**, *178-180*, 1679-1702.
7. B. C. Gates, *Catalytic Chemistry*, Vol. Chapter 6, Wiley, **1992**; D. F. Shriver, P. W. Atkins, *Inorganic Chemistry*, 3rd ed., Oxford University Press, Oxford, **1999**.
8. J. M. Thomas, R. Raja, D. W. Lewis, *Angew. Chem., Int. Ed.*, **2005**, *44*, 6456-6482; F. Quignard, A. Choplin, *Comprehensive Coordination Chemistry II*, **2004**, *9*, 445-470; P. McMorn, G. J. Hutchings, *Chem. Soc. Rev.*, **2004**, *33*, 108-122; L.-X. Dai, *Angew. Chem., Int. Ed.*, **2004**, *43*, 5726-5729; C. E. Song, S. Lee, *Chem. Rev.*, **2002**, *102*, 3495-3524; Y. R. de Miguel, E. Brulé, R. G. Margue, *J. Chem. Soc., Perkin Trans. 1*, **2001**, *23*, 3085-3094; Y. R. de Miguel, *J. Chem. Soc., Perkin Trans. 1*, **2000**, *24*, 4213-4221.
9. J. H. Clark, D. J. Macquarrie, *Chem. Commun.*, **1998**, 853-860.
10. P. M. Price, J. H. Clark, D. J. Macquarrie, *J. Chem. Soc., Dalton Trans.*, **2000**, *2*, 101-110.
11. A. Sakthivel, J. Zhao, M. Hanzlik, A. S. T. Chiang, W. A. Herrmann, F. E. Kuehn, *Adv. Synth. Catal.*, **2005**, *347*, 473-483; E. Lindner, T. Salesch, S. Brugger, F. Hoehn, P. Wegner, H. A. Mayer, *J. Organomet. Chem.*, **2002**, *641*, 165-172; F. A. R. Kaul, G. T. Puchta, H. Schneider, F. Bielert, D. Mihalios, W. A. Herrmann, *Organometallics*, **2002**, *21*, 74-82.
12. R. Chen, R. P. J. Bronger, P. C. J. Kamer, P. W. N. M. Van Leeuwen, J. N. H. Reek, *J. Am. Chem. Soc.*, **2004**, *126*, 14557-14566; E. Dulière, M. Devillers, J. Marchand-Brynaert, *Organometallics*, **2003**, *22*, 804-811; C. Baleizao, A. Corma, H. Garcia, A. Leyva, *Chem. Commun.*, **2003**, 606-607; S. Xiang, Y. Zhang, Q. Xin, C. Li, *Angew. Chem., Int. Ed.*, **2002**, *41*, 821-824; A. Heckel, D. Seebach, *Chem. Eur. J.*, **2002**, *8*,

559-572; A. J. Sandee, J. N. H. Reek, P. C. J. Kamer, P. W. N. M. van Leeuwen, *J. Am. Chem. Soc.*, **2001**, *123*, 8468-8476; M. K. Richmond, S. L. Scott, H. Alper, *J. Am. Chem. Soc.*, **2001**, *123*, 10521-10525; D. Rechavi, M. Lemaire, *Org. Lett.*, **2001**, *3*, 2493-2496; M. Chabanas, A. Baudouin, C. Copéret, J.-M. Basset, *J. Am. Chem. Soc.*, **2001**, *123*, 2062-2063.

13. R. Chanthateyanonth, H. Alper, *Adv. Synth. Catal.*, **2004**, *346*, 1375-1384; R. Chanthateyanonth, H. Alper, *J. Mol. Catal. A*, **2003**, *201*, 23-31.
14. K. Mori, T. Hara, T. Mizugaki, K. Ebitani, K. Kaneda, *J. Am. Chem. Soc.*, **2003**, *125*, 11460-11461.
15. R. Gimenez, T. M. Swager, *J. Mol. Catal. A*, **2001**, *166*, 265-273.
16. M. Albrecht, G. van Koten, *Angew. Chem., Int. Ed.*, **2001**, *40*, 3750-3781.
17. G. Rodriguez, M. Lutz, A. L. Spek, G. van Koten, *Chem. Eur. J.*, **2002**, *8*, 45-57.
18. G. Guillena, G. Rodriguez, G. van Koten, *Tetrahedron Lett.*, **2002**, *43*, 3895-3898; M. Albrecht, B. M. Kocks, A. L. Spek, G. van Koten, *J. Organomet. Chem.*, **2001**, *624*, 271-286; X. Zhang, J. M. Longmire, M. Shang, *Organometallics*, **1998**, *17*, 4374-4379; F. Gorla, A. Togni, L. M. Venanzi, A. Albinati, F. Lianza, *Organometallics*, **1994**, *13*, 1607-1616.
19. C. Schlenk, A. W. Kleij, H. Frey, G. van Koten, *Angew. Chem., Int. Ed.*, **2000**, *39*, 3445-3447.
20. J. S. Fossey, C. J. Richards, *Organometallics*, **2002**, *21*, 5259-5264; M. A. Stark, G. Jones, C. J. Richards, *Organometallics*, **2000**, *19*, 1282-1291.
21. H. P. Dijkstra, M. D. Meijer, J. Patel, R. Kreiter, G. P. M. van Klink, M. Lutz, A. L. Spek, A. J. Canty, G. van Koten, *Organometallics*, **2001**, *20*, 3159-3168.
22. M. D. Meijer, N. Ronde, D. Vogt, G. P. M. van Klink, G. van Koten, *Organometallics*, **2001**, *20*, 3993-4000.
23. J. T. Singleton, *Tetrahedron*, **2003**, *59*, 1837-1857.
24. J. Dupont, M. Pfeffer, J. Spencer, *Eur. J. Inorg. Chem.*, **2001**, 1917-1927.
25. H. P. Dijkstra, C. A. Kruithof, N. Ronde, R. van de Coevering, D. J. Ramón, D. Vogt, G. P. M. van Klink, G. van Koten, *J. Org. Chem.*, **2003**, *68*, 675-685.
26. H. P. Dijkstra, N. Ronde, G. P. M. van Klink, D. Vogt, G. van Koten, *Adv. Synth. Catal.*, **2003**, *345*, 364-369.
27. K. Yu, W. Sommer, J. M. Richardson, M. Weck, C. W. Jones, *Adv. Synth. Catal.*, **2005**, *347*, 161-171; W. Sommer, K. Yu, J. S. Sears, Y. Ji, X. Zheng, R. J. Davis, C. D. Sherrill, C. W. Jones, M. Weck, *Organometallics*, **2005**, *24*, 4351-4361; K. Yu, W. Sommer, M. Weck, C. W. Jones, *J. Catal.*, **2004**, *226*, 101-110.
28. N. C. Mehendale, M. Lutz, A. L. Spek, R. J. M. Klein Gebbink, G. van Koten, *manuscript in prep. (Ch. 2 of this thesis).*
29. E. Lippmaa, M. Mägi, A. Samoson, G. Engelhardt, A.-R. Grimmer, *J. Am. Chem. Soc.*, **1980**, *102*, 4889-4893.
30. J. Terheijden, P. W. Mul, G. van Koten, F. Muller, H. C. Stam, *Organometallics*, **1986**, *5*, 519-525.
31. M. Albrecht, R. A. Gossage, A. L. Spek, G. van Koten, *Chem. Commun.*, **1998**, 1003-1004; M. Albrecht, M. Lutz, A. L. Spek, G. van Koten, *Nature*, **2000**, *406*, 970-974.
32. M. Albrecht, R. A. Gossage, M. Lutz, A. L. Spek, G. van Koten, *Chem. Eur. J.*, **2000**, *6*, 1431-1445.
33. N. C. Mehendale, R. J. M. Klein Gebbink, G. van Koten, *manuscript in prep. (Ch. 6 of this thesis).*
34. N. C. Mehendale, M. Lutz, A. L. Spek, R. J. M. Klein Gebbink, G. van Koten, *manuscript in prep. (Ch. 8 of this thesis).*
35. R. van de Coevering, M. Kuil, R. J. M. K. Gebbink, G. van Koten, *Chem. Commun.*, **2002**, 1636-1637.
36. P. L. Alsters, P. J. Baesjou, M. D. Janssen, H. Kooijman, A. Sicherer-Roetman, A. L. Spek, G. van Koten, *Organometallics*, **1992**, *11*, 4124-4135.
37. B. M. J. M. Suijkerbuijk, M. Q. Slagt, R. J. M. Klein Gebbink, M. Lutz, A. L. Spek, G. van Koten, *Tetrahedron Lett.*, **2002**, *43*, 6565-6568.
38. A. van Blaaderen, A. Vrij, *Langmuir*, **1992**, *8*, 2921-2931.
39. D. E. Bergbreiter, P. L. Osburn, Y.-S. Liu, *J. Am. Chem. Soc.*, **1999**, *121*, 9531-9538.
40. M. Ohff, A. Ohff, M. E. van der Boom, D. Milstein, *J. Am. Chem. Soc.*, **1997**, *119*, 11687-11688; N. Solin, J. Kjellgren, K. J. Szabo, *Angew. Chem., Int. Ed.*, **2003**, *42*, 3656-3658; J. Kjellgren, H. Sunden, K. J. Szabo, *J. Am. Chem. Soc.*, **2004**, *126*, 474-475; N. Solin, J. Kjellgren, K. J. Szabo, *J. Am. Chem. Soc.*, **2004**, *126*, 7026-7033; O. A. Wallner, K. J. Szabo, *Org. Lett.*, **2004**, *6*, 1829-1831.

Chapter 4

PCP- and SCS-Pincer Palladium Complexes Immobilized on Mesoporous Silica: Application in C–C Bond Formation Reactions

Abstract

ECE-pincer palladium(II) complexes (ECE = $[C_6H_3(CH_2E)_2\text{-}2,6]^-$, E = PPh_2 and SPh) tethered to a trialkoxysilane moiety through a carbamate linkage were immobilized on ordered mesoporous silicas SBA-15 and MCM-41 using a grafting process. The resulting hybrid materials were characterized by IR spectroscopy (DRIFT), solid-state CP/MAS NMR (^{13}C, ^{31}P, and ^{29}Si), and elemental analyses. These analyses showed the integrity of the pincer-metal complexes on the supports, which highlights their stability under the applied immobilization conditions. A H-bonding interaction between the carbamate carbonyl group of the complex and free silanol groups on the silica surface was also established. The hybrid materials were found to act as Lewis acid catalysts in the aldol reaction between methyl isocyanoacetate and benzaldehyde. SBA-15 modified with the PCP-pincer Pd-complex was used in up to five runs without loss of activity. Control experiments showed the true heterogeneous nature of the catalyst in this reaction. N_2 adsorption data, XRD, and TEM/EDX analyses of the hybrid materials revealed that the mesoporous structure of these materials was retained during the immobilization process as well as during catalysis.

4.1. Introduction

Catalyst separation from the product solution is an important aspect of homogeneous catalytic processes both from an economical and ecological point of view. Amongst current methods to separate homogeneous catalysts from product streams are distillation and selective extraction of products and catalysts.[1] In many cases these methods may turn out as unsustainable, however, due to the excessive use of energy and solvents, and could, therefore, also be economically less attractive. In this respect, heterogeneous catalytic processes have obvious advantages due to the ease of separation of the (insoluble) heterogeneous catalysts from reaction products. Current research is directed to merge the advantages of both catalytic approaches, for example, by immobilizing homogeneous catalysts on an insoluble support.[2,3] In this way, properties such as catalyst selectivity and activity could be combined with ease of catalyst separation and catalyst reuse. A variety of insoluble supports have been used for the immobilization of homogeneous catalysts.[4,5]

ECE-pincer metal complexes (ECE = $[C_6H_3(CH_2E)_2\text{-}2,6]^-$, E = NR_2, SR, PR_2 *etc.*) are often highly stable and resistant to metal leaching due to a strong M–C σ-bond that is stabilized through metal coordination by two hetero-atoms (*cis* to the M–C bond) forming two five-membered chelate rings.[6] ECE-pincer Pd-complexes are known to catalyze a large variety of C–C and C–X bond formation reactions.[6-10] The robustness of the ECE-pincer metal complexes make them attractive candidates for processes for which recycling and reuse is a prerequisite. Various soluble supports have already been used for the immobilization and recycling of pincer-based metal catalysts, among which are hyperbranched polymers,[9,11] oligo(ethylene glycol),[12] dendronized polymers,[13] carbosilane dendrimers,[14] cartwheel-molecules,[8,15] polycationic dendrimers,[16] and soluble polymers.[10,17] Recently, we as well as others have reported on the grafting of ECE-pincer metal complexes on silica and on their use in aldol-type[18,19] and Heck reactions.[20]

In a recent effort by our group to immobilize NCN-pincer complexes on insoluble supports, we have used *para*-triethoxysilane-functionalized pincer-metal (platinum and palladium) complexes and immobilized these on amorphous silica via surface grafting.[18] Although the heterogenized pincer Pd-complexes were found to be active in the aldol reaction of methyl isocyanoacetate (MI) with benzaldehyde (reaction 1), they showed a poor performance in terms of recycling. Silica reconstitution under the reaction conditions and during work-up presumably led to loss of catalyst due to the formation of small, difficult to separate by filtration and thus non-recyclable silica particles.

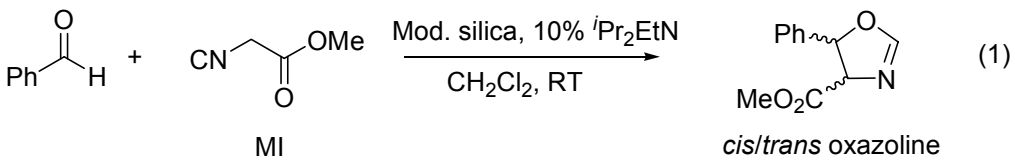

MI *cis*/*trans* oxazoline (1)

Recent investigations on the mechanism of operation of ECE-pincer palladium(II) complexes as homogeneous catalyst have shown that the NCN- and SCS-pincer Pd-complexes undergo isocyanide insertion in the Pd–C bond and that the resulting cyclometalated species are the actual catalytically active species.[21] Remarkably, this insertion takes place for both the neutral halide and the cationic aquo complexes. For the PCP-pincer Pd-complexes, no insertion was observed, but replacement of the halide by a η^1-coordinated isocyanide generated the cationic, catalytically active species. Finally, this study showed that there is no need to generate a cationic palladium(II) species by prior treatment of the neutral species with *e.g.* Ag-reagents (note that Ag-halide salts are catalysts themselves)[22] for the ECE-pincer palladium species to catalyze reaction 1.

In the present study, we have used our experience to immobilize NCN-pincer palladium complexes for the immobilization of the corresponding PCP- and SCS-pincer palladium complexes on silica.[18] To this end, complexes **1** and **2** (Chart 1) were synthesized[23] and subsequently immobilized on silica-based support materials. The choice of support depended on the reaction conditions, ease of functionalization of the surface groups required for attaching the catalyst, as well as on the chemical, mechanical and thermal stability of the support.[5] In the present study, we have used the mesoporous molecular sieves MCM-41 and SBA-15, which fulfill most of the above mentioned requirements and have been used extensively by others.[3,24] Because of their uniform mesopores that are arranged in a hexagonal, honeycomb-like lattice these materials have a high surface area which allows high catalyst loadings. The synthesis and characterization of the pincer palladium-functionalized MCM-41 and SBA-15 materials as well as their performance in reaction 1 are discussed.

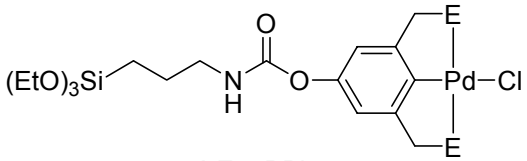

1 E = PPh_2
2 E = SPh

Chart 1 Siloxane-functionalized ECE-pincer palladium(II) chloride complexes.

4.2. Results

4.2.1. Immobilization of PCP- and SCS-pincer palladium complexes on silica

The triethoxysilane-functionalized complexes **1** and **2** (Chart 1) were prepared from the corresponding *para*-hydroxy ECE-pincer complexes as reported previously.[23] These complexes comprise both a trialkoxysilane and an organometallic fragment covalently connected through a carbamate linker. The presence of a long, non-polar tail increases the solubility of these complexes considerably. They are soluble in non-polar solvents such as benzene or toluene, which allows the use of common grafting protocols of homogeneous catalysts on silica in these solvents. This is of importance to arrive at a uniform distribution of the catalyst on the support.

Silica surface grafting of **1** and **2** was carried out using SBA-15 or MCM-41. In a typical process, the silica support was pre-treated by heating it at 100 °C under vacuum for two hours. The support was then reacted with complexes **1** or **2** in toluene at 90 °C for 20 hours (Scheme 1). A continuous extraction (Soxhlet) of the resulting material with boiling dichloromethane was subsequently performed for 16 hours in order to remove any non-covalently attached material. After drying *in vacuo*, the hybrid silicas **3** and **4**, respectively, were obtained as white solids. Subsequently, silica **3** was treated with 1,1,1,3,3,3-hexamethyldisilazane (HMDS) to cap remaining unreacted surface silanol groups with a trimethylsilyl functionality (silica **5**).

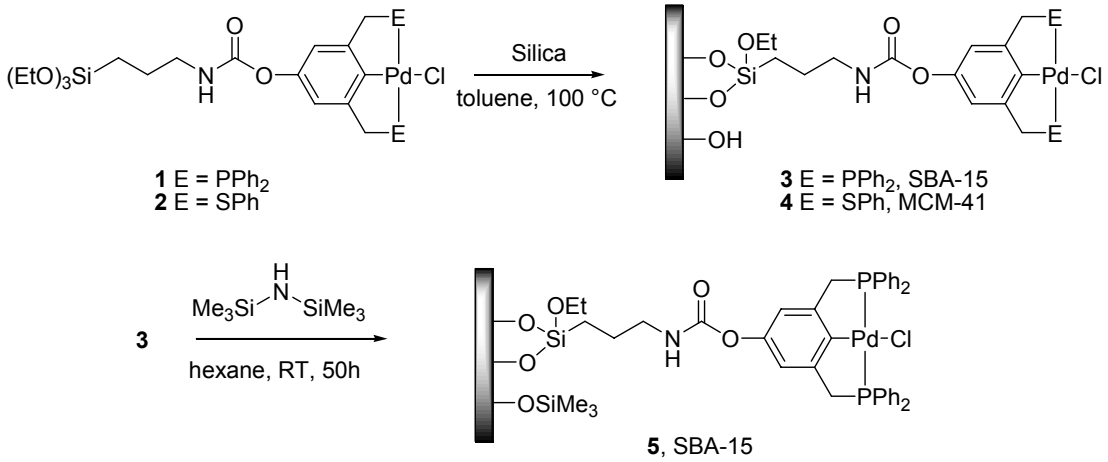

Scheme 1 Synthesis of hybrid materials **3**, **4**, and **5**.

These materials were characterized by using IR spectroscopy (DRIFT), CP/MAS NMR spectroscopy (^{13}C, ^{29}Si, and ^{31}P), and elemental analysis. The impact of the immobilization of **1** and **2** on the structure of MCM-41 and SBA-15 was studied by XRD, TEM, and N_2 adsorption.

4.2.2. Characterization

4.2.2.1. IR studies

Comparison of the IR (DRIFT) spectra of plain silicas (SBA-15 in Figure 1) with those of hybrid materials **3** (see Figure 1) and **4** pointed to a strong decrease in the number of isolated free silanol groups in the latter silicas. Comparison of the IR spectra of **1** and **2** with those of the hybrid materials **3** and **4** revealed that signals corresponding to the C–H stretching, C=O stretching, CNH group, and the N–H bending vibrations of **1** and **2** are present in the spectra of **3** and **4**. The intensity of the signal for isolated free silanol groups in **3** is further decreased in the spectrum of **5** (see Figure 1), showing that at least part of the remaining silanol groups in **3** became capped with a TMS group in **5**. By subtracting the spectrum of plain SBA-15 from that of **5**, a difference spectrum was obtained (top, Figure 2). In this difference spectrum, a sharp decrease in the intensity of the signal at 3745 cm^{-1} was observed indicating that a large number of silanol groups had reacted. Other significant changes were observed for the carbamate C=O stretching vibration. In **1** the $\tilde{\nu}$ C=O

amounted to 1734 cm^{-1} (see Figure 2), which changed to 1725 cm^{-1} in hybrid material **3**, and to 1756 cm^{-1} in TMS-capped **5** (see Figure 1).

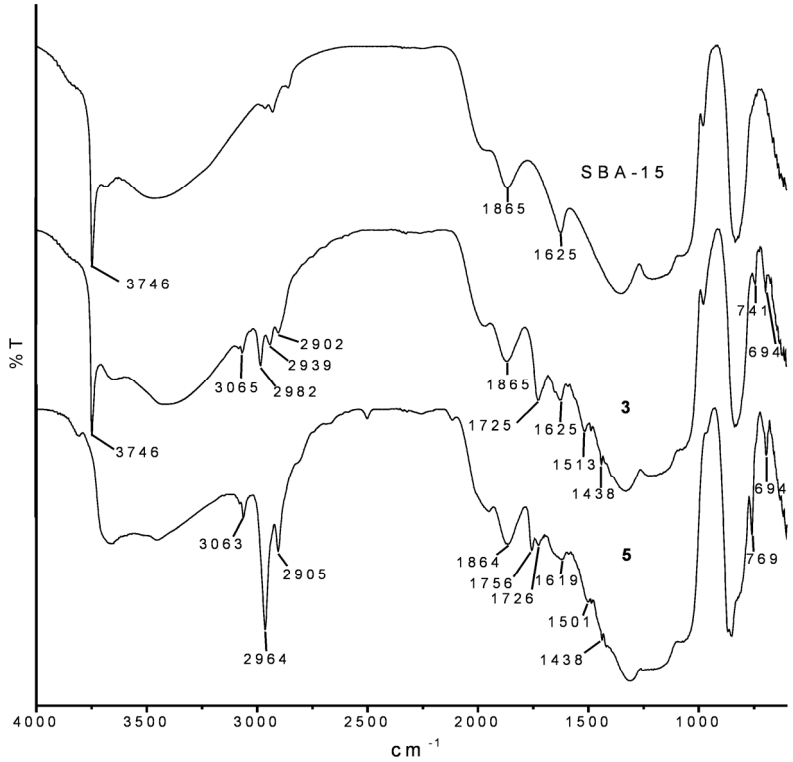

Figure 1 IR (DRIFT) of plain silica (SBA-15) and hybrid materials **3** and **5**.

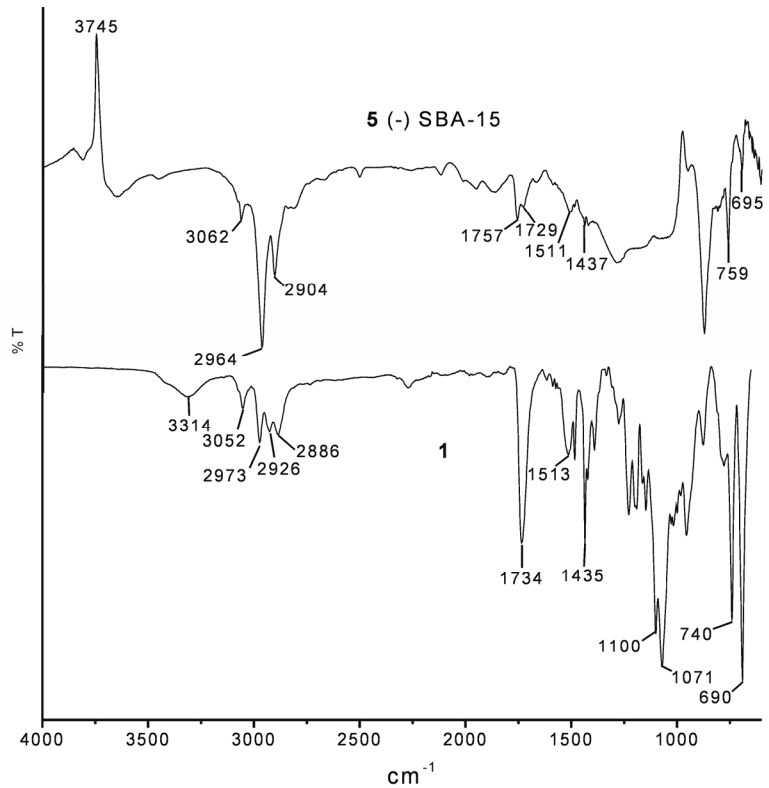

Figure 2 Difference spectrum between the DRIFT spectra of **5** and SBA-15 (top) compared with IR spectrum of non-supported **1** (bottom).

We believe that these shifts are indicative for the presence of H-bonding interactions of the carbamate-carbonyl group with surface silanol groups in **3**, which consequently are much less present in **5**. This observation is consistent with previous observations made on immobilizing related NCN-pincer complexes on silica.[18]

4.2.2.2. CP/MAS Solid State NMR studies

^{13}C and ^{29}Si solid-state NMR spectroscopy on **3**, **4**, and **5** provided further information on the nature of both the organic (spacer and metal-complex) and inorganic part of these hybrid materials. All peaks corresponding to the ^{13}C NMR spectra of the parent complexes **1** and **2** were present in the ^{13}C NMR spectra of the hybrid materials **3** and **4**, respectively. The ^{31}P NMR spectrum of solid **3** (on SBA-15) showed a single peak at 36.01 ppm, while for **1** a resonance at 33.4 ppm (solution NMR in C_6D_6) was found which corresponds to a phosphine grouping coordinated to palladium. Signals at 16 and 58 ppm in the ^{13}C NMR spectra of all hybrid materials pointed to the presence of EtO–Si groups.[23] This supports the notion that not all tethered palladium complexes became immobilized *via* three Si(surface)–O–Si bonds, but rather that grafting occurred through an average of less than or equal to three bonds. The ^{29}Si NMR spectrum of **5** indeed showed all three T^n type signals at –59, –52, and –45 ppm, corresponding to T^3, T^2, and T^1 types of organosilica species, respectively (Figure 3, inset; $T^n = RSi(OSi)_n(OEt)_{3-n}$).

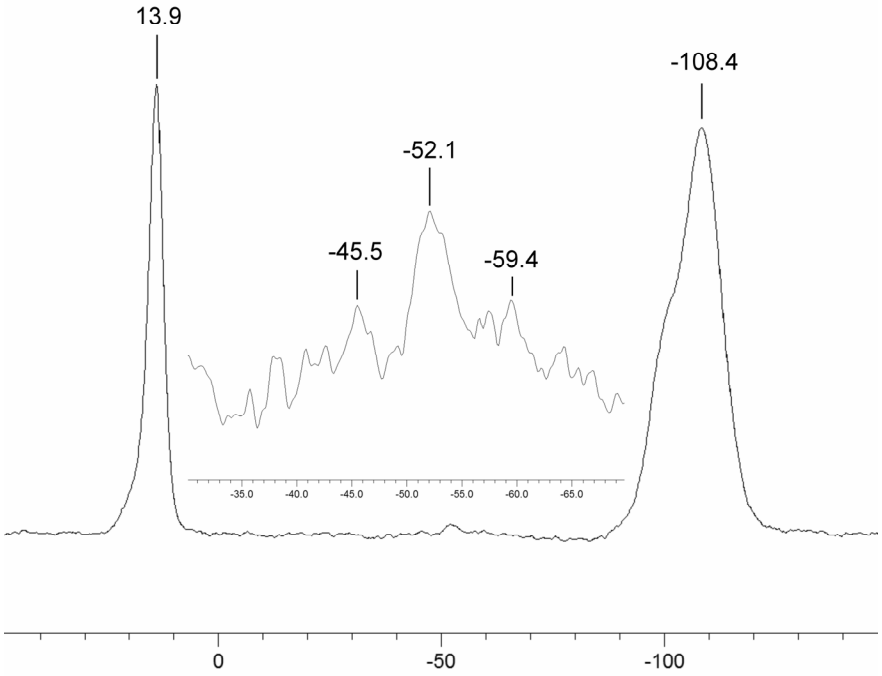

Figure 3 CP/MAS Solid-State ^{29}Si NMR of **5** (inset: expansion of –30 to –70 ppm region).

In addition, the latter spectrum also showed a signal at 13.9 ppm, which can be assigned to Si(surface)–O–SiMe$_3$ groups derived from surface silanols capped with a Me_3Si grouping arising from HMDS treatment of the hybrid material **3**.[25] Two signals were observed for the SiO_2 framework of **3** at –108 and –101 ppm, respectively, corresponding to Q^4 and Q^3 species (Q^m =

Si$(OSi)_m(OH)_{4-m}$), whereas for **5** a signal at –108 ppm (Q^4 species) along with a shoulder at about –100 ppm (decreased number of Q^3 species) was observed, which is in accordance with the partial $SiMe_3$-capping of silanol groups (Q^3 species) in **5** (*vide supra*).

4.2.2.3. Elemental analysis

The palladium, sulfur, phosphorus, and carbon contents of the grafted silicas were determined by ICP analysis (Table 1). The E/Pd ratio (E = S or P) was close to two for **4** as expected from its formula. In the case of **3** and **5**, this ratio was found to be higher than two, which could point to loss of Pd from the PCP-pincer ligand during the grafting process. ^{31}P NMR analysis of these materials did, however, not show the presence of free phosphine or of phosphine oxide moieties. In addition, no Pd(0) formation was observed during the immobilization reaction, which justifies the conclusion that the complex remained intact. In the case of **5**, an increase of the carbon content was found, which most likely is due to the capping of some of the free silanol groups of SBA-15 with $SiMe_3$ groups.

Table 1 Elemental analyses of the hybrid materials **3**-**5**.

Sample	Wt. %C[a] (mmol/g)[b]	Wt. %Pd (mmol/g)	Wt. %E[c] (mmol/g)	E/Pd[d]		C/E[d]	
				Calc.	Found	Calc.	Found
3	4.96 (4.13)	0.82 (0.077)	0.85 (0.275)	2.0	3.6	18	15
4	1.71 (1.43)	0.43 (0.040)	0.28 (0.087)	2.0	2.2	15	16
5	7.66 (6.38)	0.57 (0.054)	0.58 (0.187)	2.0	3.4	-	-

a. % by weight; b. in brackets, mmol per gram silica; c. E=S for SCS and P for PCP; d. atom ratio.

4.2.2.4. N_2 adsorption

In order to gather further information on possible changes of the surface properties at various stages of the grafting process leading to the hybrid materials **3**-**5**, these solids were studied using nitrogen adsorption. The results are summarized in Table 2.

Table 2 N_2 adsorption data of hybrid silica materials.

	Material	S_{tot}[a] ($m^2.g^{-1}$)	D_{pore}[b] (nm)	V_{micro}[c] ($cm^3.g^{-1}$)	V_{meso}[d] ($cm^3.g^{-1}$)	V_{tot}[e] ($cm^3.g^{-1}$)
1	SBA-15	518	5.2	0.07	0.69	0.78
2	SBA-15(HMDS)	460	4.5	0.00	0.45	0.54
3	**3**	442	5.0	0.04	0.57	0.66
4	**5**	433	4.4	0.00	0.43	0.51
5	**5** after run 1	416	4.4	0.00	0.41	0.49
6	**5** after run 5	423	4.4	0.00	0.42	0.50
7	MCM-41	975	3.1	0.00	0.85	1.03
8	**4**	966	2.7	0.00	0.76	0.95

a. S_{tot} = total surface area; b. D_{pore} = pore diameter; c. V_{micro} = micropore volume; d. V_{meso}= mesopore volume; e. V_{tot} = total pore volume.

To study whether the immobilization process affected the nature of the silica support, we refluxed plain SBA-15 in toluene for 20 hours. Results of nitrogen adsorption experiments demonstrated that the structure of this SBA-15 sample remained unchanged. The surface area and mesopore volume

decreased both by only 3%. The steep capillary condensation mesopores-filling step remained unchanged showing that the small pore size distribution (5.2 nm) had not been altered.

Comparison of the nitrogen adsorption data of SBA-15 and hybrid material **3** showed that the surface area and mesopore volume had decreased both by approximately 15 and 17%, respectively, as a result of the immobilization of PCP-pincer palladium complex **1** onto SBA-15. Despite this rather large decrease, the typical steep capillary condensation step with a hysteresis loop indicative of open cylindrical shaped pores and with an average pore size of approximately 5.0 nm remained present in the isotherm. This can be considered as a clear indication that the dinitrogen accessible pores of the material still consist of uniform cylindrically shaped pores and are not damaged during the grafting process. However, the observed decline in surface area and meso-porosity cannot be explained by a decrease of the pore diameter from 5.2 to 5.0 nm as this would only result in a lowering of 4 and 8%, respectively.

Nitrogen adsorption on a SBA-15 sample after HMDS treatment demonstrated that $SiMe_3$-capping of surface silanol groups led to a decrease in pore diameter from 5.2 to 4.5 nm (13% decrease). Obviously this capping made the micropores no longer accessible for dinitrogen as the micropore volume had been reduced to zero. The extent of decrease of the surface area (11%) and mesopore volume (35%) corresponds to the expected decline based on the observed pore diameter shrinkage of 5.2 to 4.5 nm.

Nitrogen adsorption results of hybrid material **5** showed that treatment of **3** with HMDS resulted in a decrease of the pore diameter from 5.0 to 4.4 nm (12% decrease), and of the mesopore volume with 25%, while the surface area decreased by only 2%. The decrease of mesopore volume corresponds to the expected decline based on the observed reduction of the pore diameter by 0.6 nm. The micropore volume declined from 0.04 $cm^3 \cdot g^{-1}$ to zero. Comparison of nitrogen adsorption results of SBA-15 and hybrid material **5** demonstrated that the pore diameter was reduced by 0.8 nm from 5.2 nm to 4.4 nm (15% decrease) after the immobilization and HMDS treatments. The observed decrease of surface area (16%) and meso-porosity (38%) agrees fairly with the expected decrease (15% and 29%, respectively). The nitrogen adsorption results of hybrid material **5** after catalysis demonstrated that the textural properties of the catalyst remained unchanged up to five catalytic runs.

The immobilization of the SCS-pincer palladium complex **2** onto MCM-41, yielding hybrid material **4**, had little effect on the surface area and total pore volume of the support. Also, the steep capillary condensation mesopore-filling step characteristic for cylindrically shaped mesopores was retained. Although the narrow pore size distribution had been preserved, the pore diameter had slightly decreased (from 3.1 to 2.7 nm) upon immobilization of SCS-pincer palladium complex **2**.

4.2.2.5. XRD analysis

The X-ray diffractogram patterns for SBA-15 and corresponding hybrid materials are shown in Figure 4. The pattern of SBA-15 revealed three well-resolved peaks located at 1.15, 2.0, and 2.3

degrees 2θ, which were assigned to the (100), (110) and (200) reflections, respectively, associated with a *p6mm* hexagonal symmetry. Furthermore, these XRD results clearly demonstrated that the mesoscopic hexagonal symmetry is retained for all the hybrid materials; not only after immobilization of the complex, but also after five runs of catalysis.

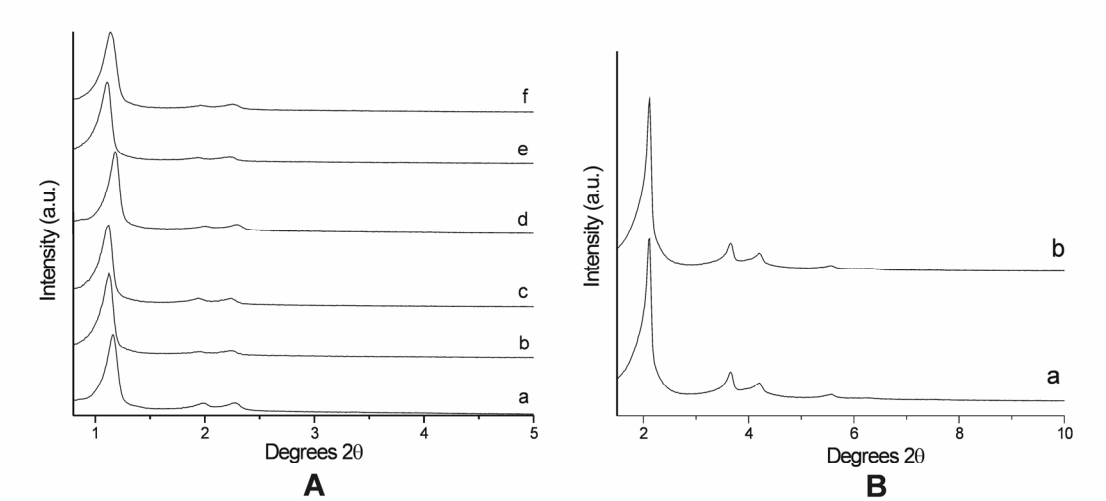

Figure 4 A: XRD patterns of (a) SBA-15, (b) SBA-15(HMDS), (c) **3**, (d) **5**, (e) **5** after run 1 and (f) **5** after run 5; **B**: XRD patterns of (a) MCM-41 and (b) hybrid material **4**.

The XRD patterns for MCM-41 showed four reflections located at 2.1, 3.7, 4.2, and 5.6 degrees 2θ, which can be assigned to the (100), (110), (200) and (210) reflections of the hexagonal lattice of MCM-41, respectively (Figure 4). The XRD pattern of hybrid material **4** clearly demonstrated that the long range order of MCM-41 was not affected by the immobilization process.

4.2.2.6. TEM/EDX analysis

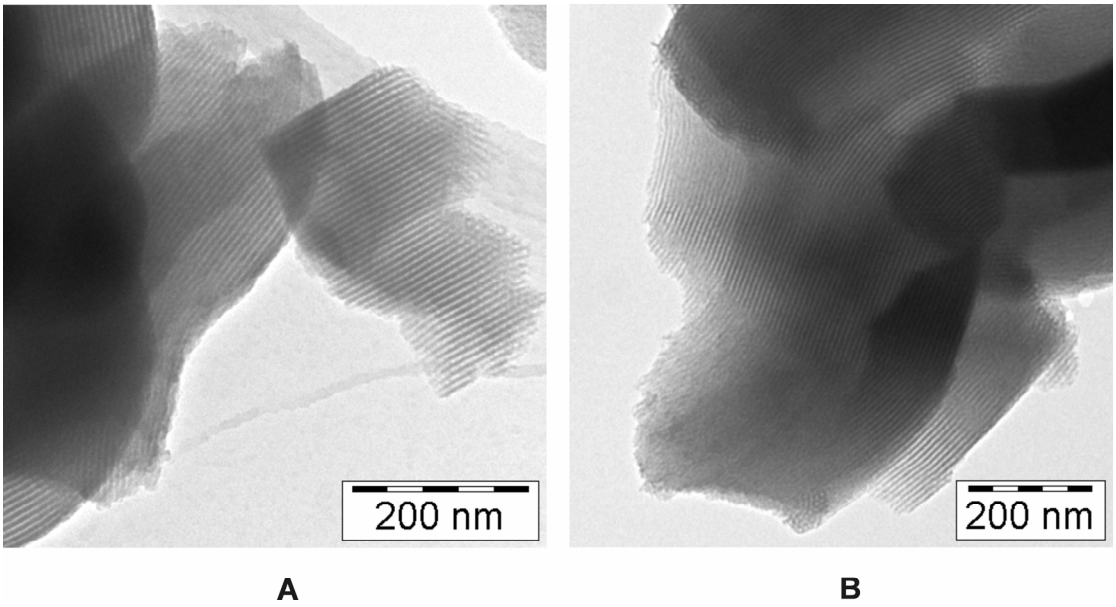

Figure 5 TEM of functionalized SBA-15 **5** (**A**) and **5** after catalysis run 5 (**B**).

Transmission electron microscopy (TEM) analysis of samples of **3** and **5** (SBA-15 materials, Figure 5) as well as of **4** (MCM-41 material; not shown) revealed that the hexagonal mesoporous structures

of both SBA-15 and MCM-41 had been retained during immobilization and that no palladium clusters are formed. EDX analysis confirmed that palladium as well as either phosphorous (for **3** and **5**) or sulfur (for **4**) are present in the structures. This indicated that no Pd(0) was formed during the immobilization and protection processes and that the organometallic groupings **1** and **2** have been molecularly immobilized.

4.2.3. Catalysis

As a test reaction for the catalytic properties of the hybrid materials **3**-**5**, the earlier studied aldol condensation reaction between benzaldehyde and MI (reaction 1) was chosen. For this reaction the ECE-pincer palladium(II) halide complexes can be used as such (see introduction).[21]

As a proof of principle, 250 mg of silica **5** which corresponds to 0.84 mol% of palladium loading was tested. Catalysis using 1.6 mmols of both benzaldehyde and MI was run to 30% conversion (Figure 6).

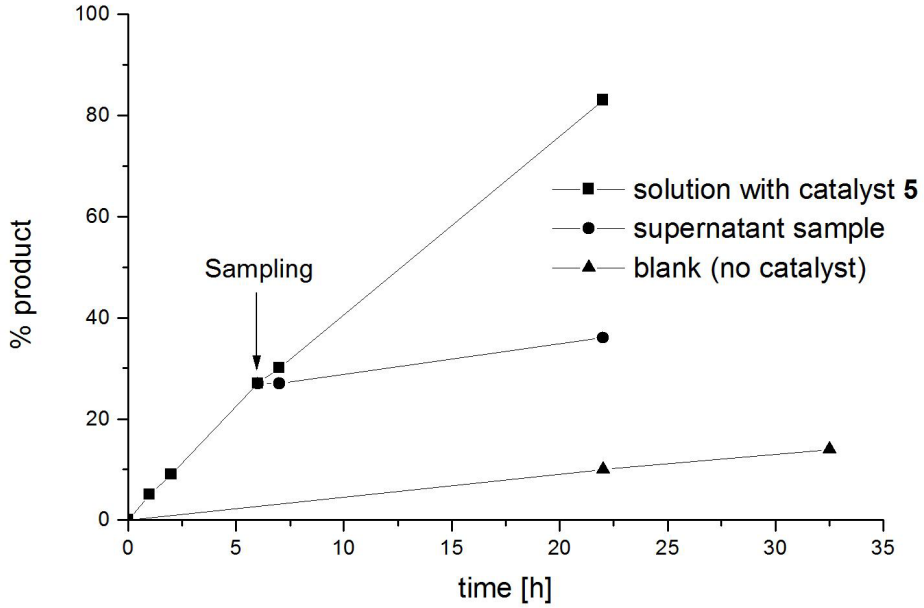

Figure 6 Kinetic traces of aldol reaction 1, showing catalysis only in presence of silica **5**; the supernatant sample (see text) shows the same kinetic trace as the blank.

At this stage stirring was stopped and a small part of the clear supernatant solution was removed and stirred separately. At the same time stirring of the remaining reaction mixture was continued. It was found that in the latter reaction mixture, catalysis in the presence of the hybrid material went further to completion, whereas the rate of the reaction in the sample of the supernatant had considerably slowed down and had become comparable to that of the blank reaction (Figure 6); *i.e.* that of a homogeneous reaction without added ECE-pincer Pd-complex. These observations indicate that the activity in the parent reaction and in the reaction mixture after sampling is associated with the catalytic activity of the (insoluble) hybrid material, *i.e.* with Pd-catalysis of the grafted PCP-catalyst, thereby demonstrating the true heterogeneous nature of the catalyst.

Table 3 Consecutive use of silica **5** in reaction 1.

Run	% conversion after				*trans* product
	2h	4h	6h	24h	
1	20	36	50	-	83%
2	20	34	45	-	84%
3	20	36	41	96	84%
4	-	-	-	96	84%
5	21	36	52	92	83%

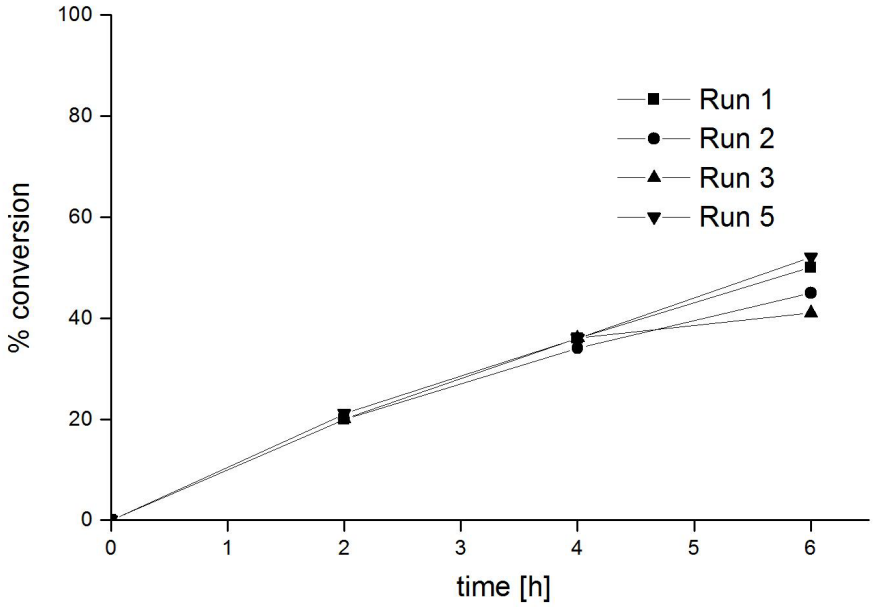

Figure 7 Consecutive use of silica **5** in reaction 1.

Next, the recyclability of hybrid material **5** as catalyst for reaction 1 was investigated. In this series of experiments, 500 mg of **5**, which corresponds to 1.67 mol% of palladium loading, was used. Again 1.6 mmols of both benzaldehyde and MI were utilized. Work-up in between cycles involved centrifugation of the reaction mixture to separate the suspended silica and removal of the clear supernatant solution. The silica was washed twice with dichloromethane and then reused in the subsequent run. In total 5 consecutive runs were carried out. It was found that the activity of the catalyst was fully retained over these runs (Table 3, Figure 7). Comparison of the rate of the aldol reaction catalyzed by homogeneous PCP-pincer palladium complex [PdCl(PCP)] with that of the hybrid material **5** showed that the homogeneous reaction (initial TOF 15 h^{-1}) was faster than the heterogeneous one (initial TOF 6 h^{-1}).

The supernatant reaction mixture for each of these runs was tested for palladium and silicon contents (Table 4). Some leaching of Pd on the ppm level was found but also the presence of Si was observed in the supernatant solutions. The amount of Si was larger as compared to that of Pd. This indicates that the origin of Pd is probably not the complex (which has a Pd/Si ratio of 1) but rather some small particles of silica itself that escaped separation from the solution. Moreover, the fact that the activity

remained constant after each run indicated that leaching of the catalytic species during these experiments was negligible.

Table 4 Elemental analyses of supernatant aldol reaction mixtures catalyzed by **5**.

Sample	ppm Pd	ppm Si	Molar ratio Si/Pd
Run 1	348	856	9.3
Run 2	126	969	29.1
Run 3	144	728	19.1
Run 4	96	113	4.5
Run 5	115	447	14.7

TEM analyses carried out on a sample of **5** after run 1 and after run 5 indicated that the structure of the SBA-15 support was not damaged during catalysis. Furthermore, zerovalent palladium clusters were not observed in any of the investigated samples, *i.e.* no decomposition had occurred. EDX measurements confirmed that palladium and phosphor were present in the samples supporting the presence of the PCP-pincer Pd-complex. Further evidence for the integrity and stability of the hybrid material **5** after using it in aldol reaction 1 over 5 runs comes from solid-state ^{31}P NMR, which showed a single peak at 42.3 ppm. This chemical shift corresponds to that of the P-centre in a cationic PCP-pincer Pd-complex with a coordinated isocyanide ligand instead of a chloride as the fourth ligand. This is consistent with our findings in case of the corresponding homogeneous complex, *i.e.* in a reaction of neutral [PdCl(PCP)] with MI, the ^{31}P NMR resonance shifts from 31 ppm (neutral complex) to 42 ppm (cationic complex [Pd(PCP)(MI)]Cl).[21]

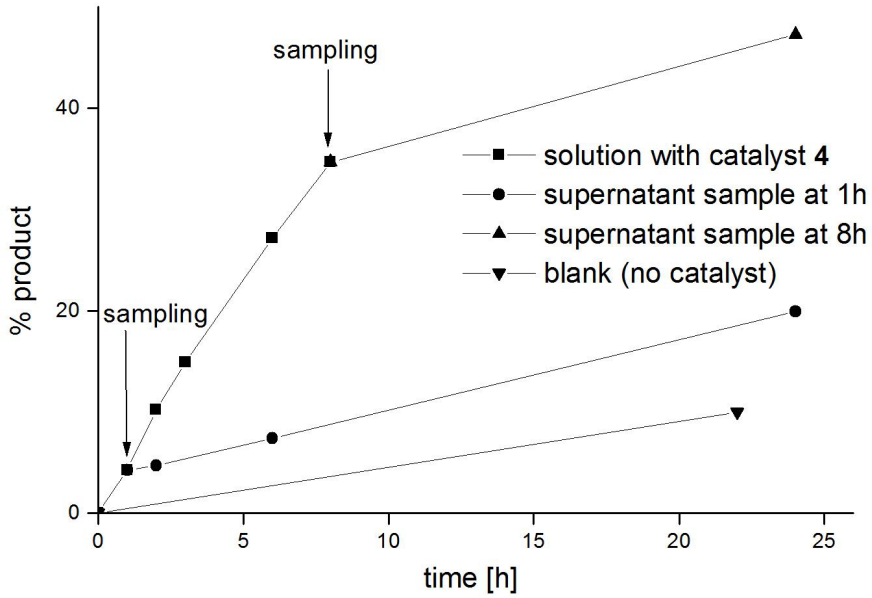

Figure 8 Aldol reaction 1 catalyzed by silica **4**.

Hybrid material **4** (with the SCS-pincer palladium grouping) was found to behave in a similar manner as **5**. Similar experiments involving about 200 mg of silica **4** (0.48 mol% of palladium loading) confirmed that catalysis in the first run took place only because of the presence of **4** (Figure

8). However, upon recycling of **4**, a decreased activity was found. This is most likely due to catalyst deactivation and can be attributed to a low stability of the insertion complex that is formed upon reaction of SCS-pincer Pd-complex with an isocyanide (see reaction 2). Such insertion complexes are not formed in the case of PCP-pincer Pd-complexes[21] and, consequently, no deactivation is observed for hybrid materials derived from these complexes, *i.e.* for **3** and **5**. In the case of hybrid material **4**, a lower initial TOF of 11 h^{-1} was observed whereas with its homogeneous counterpart SCS-pincer palladium complex [PdCl(SCS)] an initial TOF of 45 h^{-1} was found.

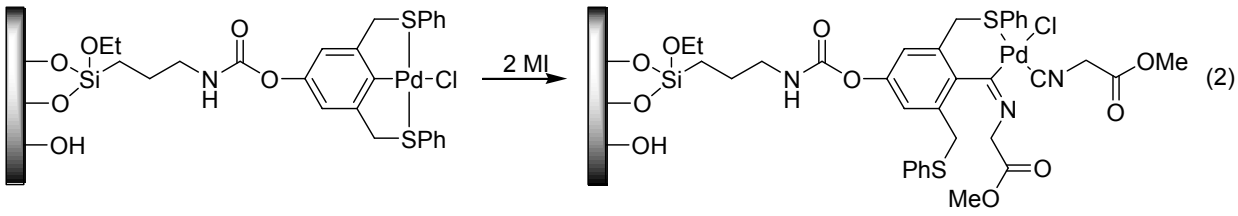

(2)

4.3. Conclusion

In conclusion, we have shown that ECE-pincer Pd-complexes were successfully immobilized on mesoporous silicas. During immobilization the integrity of both the organometallic moiety and the inorganic support remained unchanged. It was found that hybrid mesoporous material **5** derived from PCP-pincer palladium complex showed a good activity and recycling ability, whereas the corresponding hybrid mesoporous material **4** with the SCS-pincer palladium complex, in spite of showing a similar initial activity in the first run, had a poor recycling ability. Likewise, a good initial activity together with a poor recycling ability was observed in the experiments with immobilized NCN-pincer palladium compounds.[18] It must be noted that both NCN- and SCS-pincer palladium complexes undergo a selective insertion reaction with MI, *cf.* reaction 2. As the corresponding PCP-pincer Pd-complex is not suffering from such an insertion reaction, the anchoring of this stable catalyst on a stable silica support like SBA-15 results in an excellent hybrid material **5**, which performs as a true heterogeneous catalyst and can be recycled and reused up to at least five times without loss of activity. Its decreased activity (TOF 6 h^{-1}) as compared to that of its homogeneous counterpart (TOF 15 h^{-1}) is quite acceptable for an immobilized catalyst. The fact that in consecutive catalysis runs the structure and integrity of both organometallic moiety and the inorganic support persisted, nicely meets the objective set to merge properties of a homogeneous and a heterogeneous catalytic system into one sustainable hybrid catalyst.

4.4. Experimental Section

4.4.1. General Comments

Solvents were dried over appropriate materials and distilled prior to use. All reagents were obtained from commercial sources and were used without further purification. All siloxane materials were stored under a nitrogen atmosphere. Compounds **1** and **2** were synthesized using a previously reported procedure.[23]

^{13}C (75.5 MHz), ^{29}Si (59.6 MHz), and ^{31}P (121.5 MHz) CP/MAS (cross-polarization/magic angle spinning) NMR spectra of **3** and **4** were recorded on a Varian Inova 300 spectrometer (Spinning rate 6000 Hz, contact time for ^{13}C 1.50 ms, for ^{29}Si 3.0 ms, and for ^{31}P 2.5 ms; number of transients for ^{13}C 6068, for ^{29}Si 11336, and for ^{31}P 3840). ^{13}C (188.6 MHz), ^{29}Si (149.0 MHz), and ^{31}P (303.7 MHz) CP/MAS NMR spectra of **5** were recorded on a Bruker AV-750 spectrometer (Spinning rate 12 kHz, contact time for ^{13}C 2.048 ms, for ^{29}Si 10.24 ms, and for ^{31}P 2.048 ms; number of transients for ^{13}C 30916, for ^{29}Si 23484, and for ^{31}P 3920). FT-IR and DRIFT spectra were recorded using a Mattson Instruments Galaxy Series FTIR 5000 spectrometer with SPECAC diffuse-reflectance assembly or Perkin Elmer Spectrum One FT-IR spectrometer with Universal ATR sampling accessory. Gas chromatographic analyses were performed with a Perkin Elmer Autosystem XL GC using a 30 m, PE-17 capillary column with an FID detector. Microanalyses were obtained from H. Kolbe Mikroanalytisches Laboratorium, Mülheim an der Ruhr, Germany. Nitrogen adsorption was carried out at 77 K using a Micromeritics Tristar 3000 apparatus. The samples were dried in helium flow for 14 h at 393 K prior to analysis. Surface areas, micropore and mesopore volumes were determined using the t-method with the Harkins and Jura thickness equation.[26] Pore size distributions were calculated from the desorption isotherm using standard BJH theory.[27] Powder X-ray diffraction (XRD) patterns of MCM-41 and hybrid material derived from it (**4**) were obtained from 1.5 to 10° 2θ with a Philips PW1710 setup using Cu-Kα radiation. XRD patterns of SBA-15 and hybrid materials derived from it (**3** and **5**) have been recorded using a Bruker-Nonius D8 Advance X-ray Diffractometer using Co-$K\alpha_1$ radiation. Electron microscopy analysis was performed using a Tecnai 20 microscope operating at 200 kV and equipped with an EDX detector.

4.4.2. Procedures

4.4.2.1. Synthesis of MCM-41

MCM-41 was prepared according to a reported procedure.[28] Degussa Aerosil380 was used as silica source and the molar composition of the synthesis mixture was 1 : 0.27 : 0.19 : 40 (SiO_2 : CTABr : TEAOH : H_2O).

4.4.2.2. Synthesis of SBA-15

SBA-15 was synthesized following a literature procedure.[29] An 8 g portion of $EO_{20}PO_{70}EO_{20}$ (P123) was dissolved in 250 mL demineralized water at 40 °C. After the solution became clear, 48 g of concentrated HCl was added followed by addition of 21.5 mL of TEOS. Subsequently the mixture was stirred for 20 h at 40 °C after which it was transferred to an oven for further reaction at 80 °C for 48 h. The product was collected by filtration, dried in air for 12 h at 80 °C, and calcined for 6 h at 540 °C.

*4.4.2.3. Grafting procedure for silica **3***

In a typical procedure, 3 g of mesoporous silica (SBA-15) was pretreated by heating it at 100 °C under vacuum for 2 h. After allowing it to cool to room temperature, a solution of **1** (0.28 mmol) in dry toluene (100 mL) was introduced. The resulting mixture was stirred to form a suspension and heated at 90 °C for 20 h, after which the silica was allowed to settle and the supernatant liquid was decanted. The silica was

washed twice with dry CH_2Cl_2 (50 mL) and was subjected to Soxhlet extraction using CH_2Cl_2 for 16 h. Finally, it was dried under vacuum yielding 3.2 g of solid **3**.

IR (KBr, DRIFT): $\tilde{\nu}$ (cm^{-1}) 3065, 2982, 2939, 2902 (C–H, stretching); 1725 (C=O, stretching); 1514 (CHN group); 1438 (N–H, bending). CP/MAS ^{13}C NMR (75.5 MHz, 25 °C): δ 8.62 (Si*C*H_2); 16.68 (OCH$_2$*C*H$_3$); 29.4 (*C*H$_2$); 40.27 (Ar*C*H$_2$P and NH*C*H$_2$); 58.61 (O*C*H$_2$); 121.69, 129.15, 131.57, 132.8, 141.65, 153.94, 157.57 (Ar*C*); 160.59 (*C*=O). CP/MAS ^{31}P NMR (121.5 MHz, 25 °C): δ 36.01. CP/MAS ^{29}Si NMR (59.6 MHz, 25 °C): δ –108.66, –101.34. Anal. Found: C, 4.96; P, 0.85; Pd, 0.82 (molar ratio of P/Pd = 2; found 3.6).

*4.4.2.4. Grafting procedure for silica **4***

Using **2** (15.2 mg, 0.021 mmol) and 0.5 g of MCM-41 gave 0.5 g of silica **4** in a similar procedure as for silica **3**.

IR (KBr, DRIFT): $\tilde{\nu}$ (cm^{-1}) 2995, 2959, 2858 (C–H, stretching); 1726 (C=O, stretching); 1465 (N–H, bending); 1395. CP/MAS ^{13}C NMR (75.5 MHz, 25 °C): δ 8.01 (Si*C*H_2); 17.18 (OCH$_2$*C*H$_3$); 23.44 (*C*H$_2$); 42.0 (NH*C*H$_2$); 49.3 (Ar*C*H$_2$S); 59.73 (O*C*H$_2$); 118.74, 127.29, 130.21, 132.63, 148.77, 152.11, 155.23, 162.95 (Ar*C*); 165.45 (*C*=O). CP/MAS ^{29}Si NMR (59.6 MHz, 25 °C): δ –107.91, –99.64, –90.96. Anal. Found: C, 1.71; S, 0.28; Pd, 0.43; (molar ratio of S/Pd = 2; found 2.17).

*4.4.2.5. Synthesis of silica **5***

2.37 g of silica **3** was suspended in a mixture of hexane (20 mL) and 1,1,1,3,3,3-hexamethyldisilazane (10 mL) and stirred at ambient temperature for 20 h, after which the silica was allowed to settle and the supernatant liquid was decanted. The silica was washed twice with dry CH_2Cl_2 (50 mL) and dried under vacuum yielding 2.2 g of solid **5**.

IR (KBr, DRIFT): $\tilde{\nu}$ (cm^{-1}) 3063, 2963, 2905 (C–H, stretching); 1756 (C=O, stretching); 1501 (CHN group); 1485, 1438 (N–H, bending). CP/MAS ^{13}C NMR (188.64 MHz, 25 °C): δ –0.5 (Si*C*H$_3$); 7.9 (Si*C*H_2); 17.1 (OCH$_2$*C*H$_3$); 22.6 (*C*H$_2$); 43.2 (Ar*C*H$_2$P and NH*C*H$_2$); 58.8 (O*C*H$_2$); 117.5, 128.8, 132.6, 145.1 (Ar*C*); 150.4 (C=O). CP/MAS ^{31}P NMR (303.7 MHz, 25 °C): δ 30.2. CP/MAS ^{29}Si NMR (149.0 MHz, 25 °C): δ –108.2, –59.4, –52.1, –45.5, 13.9. Anal. Found: C, 7.66; P, 0.58; Pd, 0.57 (molar ratio of P/Pd = 2; found 3.4).

4.4.2.6. Catalysis

The catalytic experiments were carried out using $^{i}Pr_2EtN$ (Hunig's base, 10 mol%) as a base, hybrid silica materials as catalyst, and methyl isocyanoacetate (1.6 mmol) and benzaldehyde (1.6 mmol) as reagents in CH_2Cl_2 (5 mL) at room temperature. The reaction progress was monitored by means of GC analysis using pentadecane as internal standard. After each run, the complete reaction mixture was centrifuged and the supernatant was separated. The remainders were washed with CH_2Cl_2 (2 × 20 mL) and dried in vacuo. The obtained solid was used for the next run.

4.5. References

1. B. Cornils, W. A. Herrmann, *J. Catal.* **2003**, *216*, 23-31; H.-U. Blaser, A. Indolese, A. Schnyder, *Curr. Sci.* **2000**, *78*, 1336-1344.
2. P. McMorn, G. J. Hutchings, *Chem. Soc. Rev.* **2004**, *33*, 108-122; L.-X. Dai, *Angew. Chem., Int. Ed.* **2004**, *43*, 5726-5729; F. Quignard, A. Choplin, *Comprehensive Coordination Chemistry II* **2004**, *9*, 445-470; D. J. Cole-Hamilton, *Science* **2003**, *299*, 1702-1706; F. R. Hartley, *Supported Metal Complexes*, Kluwer Academic, Dordrecht, **1985**.
3. J. M. Thomas, R. Raja, *J. Organomet. Chem.* **2004**, *689*, 4110-4124.
4. C. E. Song, S.-g. Lee, *Chem. Rev.* **2002**, *102*, 3495-3524; N. E. Leadbeater, M. Marco, *Chem. Rev.* **2002**, *102*, 3217-3274; Y. R. de Miguel, E. Brulé, R. G. Margue, *J. Chem. Soc., Perkin Trans. 1* **2001**, *23*, 3085-3094; Y. R. de Miguel, *J. Chem. Soc., Perkin Trans. 1* **2000**, *24*, 4213-4221; J. H. Clark, D. J. Macquarrie, *Chem. Commun.* **1998**, 853-860; A. Choplin, F. Quignard, *Coord. Chem. Rev.* **1998**, *178-180*, 1679-1702; D. Brunel, N. Bellocq, P. Sutra, A. Cauvel, M. Laspéras, P. Moreau, F. Di Renzo, G. Anne, F. François, *Coord. Chem. Rev.* **1998**, *178-180*, 1085-1108.
5. P. M. Price, J. H. Clark, D. J. Macquarrie, *J. Chem. Soc., Dalton Trans.* **2000**, *2*, 101-110.
6. M. E. van der Boom, D. Milstein, *Chem. Rev.* **2003**, *103*, 1759-1792; M. Albrecht, G. van Koten, *Angew. Chem., Int. Ed.* **2001**, *40*, 3750-3781.
7. K. J. Szabo, *Synlett* **2006**, 811-824; S. Sebelius, V. J. Olsson, K. J. Szabo, *J. Am. Chem. Soc.* **2005**, *127*, 10478-10479; J. Kjellgren, J. Aydin, O. A. Wallner, I. V. Saltanova, K. J. Szabo, *Chem. Eur. J.* **2005**, *11*, 5260-5268; J. Kjellgren, H. Sunden, K. J. Szabo, *J. Am. Chem. Soc.* **2005**, *127*, 1787-1796; O. A. Wallner, K. J. Szabo, *J. Org. Chem.* **2005**, *70*, 9215-9221; J. Zhao, A. S. Goldman, J. F. Hartwig, *Science* **2005**, *307*, 1080-1082; O. A. Wallner, K. J. Szabo, *Org. Lett.* **2004**, *6*, 1829-1831; N. Solin, J. Kjellgren, K. J. Szabo, *J. Am. Chem. Soc.* **2004**, *126*, 7026-7033; N. Solin, O. A. Wallner, K. J. Szabo, *Org. Lett.* **2005**, *7*, 689-691; J. Kjellgren, H. Sunden, K. J. Szabo, *J. Am. Chem. Soc.* **2004**, *126*, 474-475; K. Takenaka, Y. Uozumi, *Org. Lett.* **2004**, *6*, 1833-1835; J. S. Fossey, C. J. Richards, *Organometallics* **2004**, *23*, 367-373; Z. Wang, M. R. Eberhard, C. M. Jensen, S. Matsukawa, Y. Yamamoto, *J. Organomet. Chem.* **2003**, *681*, 189-195; E. Diez-Barra, J. Guerra, V. Hornillos, S. Merino, J. Tejeda, *Organometallics* **2003**, *22*, 4610-4612; J. T. Singleton, *Tetrahedron* **2003**, *59*, 1837-1857; G. R. Rosa, G. Ebeling, J. Dupont, A. L. Monteiro, *Synthesis* **2003**, 2894-2897; I. G. Jung, S. U. Son, K. H. Park, K.-C. Chung, J. W. Lee, Y. K. Chung, *Organometallics* **2003**, *22*, 4715-4720; J. S. Fossey, C. J. Richards, *Tetrahedron Lett.* **2003**, *44*, 8773-8776; S. Sjoevall, O. F. Wendt, C. Andersson, *J. Chem. Soc., Dalton Trans.* **2002**, 1396-1400; G. Guillena, G. Rodriguez, G. van Koten, *Tetrahedron Lett.* **2002**, *43*, 3895-3898; J. M. Seul, S. Park, *J. Chem. Soc., Dalton Trans.* **2002**, 1153-1158; D. Morales-Morales, R. E. Cramer, C. M. Jensen, *J. Organomet. Chem.* **2002**, *654*, 44-50; J. A. Loch, M. Albrecht, E. Peris, J. Mata, J. W. Faller, R. H. Crabtree, *Organometallics* **2002**, *21*, 700-706; B. S. Williams, P. Dani, M. Lutz, A. L. Spek, G. van Koten, *Helv. Chim. Acta* **2001**, *84*, 3519-3530; S. Gruendemann, M. Albrecht, J. A. Loch, J. W. Faller, R. H. Crabtree, *Organometallics* **2001**, *20*, 5485-5488; J. Dupont, M. Pfeffer, J. Spencer, *Eur. J. Inorg. Chem.* **2001**, 1917-1927; D. Morales-Morales, C. Grause, K. Kasaoka, R. Redon, R. E. Cramer, C. M. Jensen, *Inorg. Chim. Acta* **2000**, *300-302*, 958-963; D. Morales-Morales, R. Redon, C. Yung, C. M. Jensen, *Chem. Commun.* **2000**, 1619-1620; M. A. Stark, G. Jones, C. J. Richards, *Organometallics* **2000**, *19*, 1282-1291; R. A. Gossage, J. T. B. H. Jastrzebski, J. van Ameijde, S. J. E. Mulders, A. J. Brouwer, R. M. J. Liskamp, G. van Koten, *Tetrahedron Lett.* **1999**, *40*, 1413-1416; R. A. Gossage, L. A. van de Kuil, G. van Koten, *Acc. Chem. Res.* **1998**, *31*, 423-431; X. Zhang, J. M. Longmire, M. Shang, *Organometallics* **1998**, *17*, 4374-4379; M. Ohff, A. Ohff, M. E. van der Boom, D. Milstein, *J. Am. Chem. Soc.* **1997**, *119*, 11687-11688; S. E. Denmark, R. A. Stavenger, A.-M. Faucher, J. P. Edwards, *J. Org. Chem.* **1997**, *62*, 3375-3389; F. Gorla, A. Togni, L. M. Venanzi, A. Albinati, F. Lianza, *Organometallics* **1994**, *13*, 1607-1616.
8. G. Rodriguez, M. Lutz, A. L. Spek, G. van Koten, *Chem. Eur. J.* **2002**, *8*, 45-57.
9. C. Schlenk, A. W. Kleij, H. Frey, G. van Koten, *Angew. Chem., Int. Ed.* **2000**, *39*, 3445-3447.
10. D. E. Bergbreiter, P. L. Osburn, Y.-S. Liu, *J. Am. Chem. Soc.* **1999**, *121*, 9531-9538.
11. M. Q. Slagt, S.-E. Stiriba, H. Kautz, R. J. M. Klein Gebbink, H. Frey, G. van Koten, *Organometallics* **2004**, *23*, 1525-1532; M. Q. Slagt, S.-E. Stiriba, R. J. M. Klein Gebbink, H. Kautz, H. Frey, G. van Koten, *Macromolecules* **2002**, *35*, 5734-5737; A. W. Kleij, R. A. Gossage, J. T. B. H. Jastrzebski, J. Boersma, G. van Koten, *Angew. Chem. Int. Ed.* **2000**, *39*, 176-178.
12. D. E. Bergbreiter, S. Furyk, *Green Chem.* **2004**, *6*, 280-285.
13. B. M. J. M. Suijkerbuijk, L. Shu, R. J. M. Klein Gebbink, A. D. Schlueter, G. van Koten, *Organometallics* **2003**, *22*, 4175-4177.
14. M. Q. Slagt, J. T. B. H. Jastrzebski, R. J. M. Klein Gebbink, H. J. van Ramesdonk, J. W. Verhoeven, D. D. Ellis, A. L. Spek, G. van Koten, *Eur. J. Org. Chem.* **2003**, 1692-1703; A. W. Kleij, R. J. M. Klein Gebbink, P. A. J. van den Nieuwenhuijzen, H. Kooijman, M. Lutz, A. L. Spek, G. van Koten, *Organometallics* **2001**, *20*, 634-647; A. W. Kleij, R. A. Gossage, R. J. M. Klein Gebbink, N. Brinkmann, E. J. Reijerse, U. Kragl, M. Lutz, A. L. Spek, G. van Koten, *J. Am. Chem. Soc.* **2000**, *122*, 12112-12124.

15. H. P. Dijkstra, C. A. Kruithof, N. Ronde, R. van de Coevering, D. J. Ramon, D. Vogt, G. P. M. van Klink, G. van Koten, *J. Org. Chem.* **2003**, *68*, 675-685; H. P. Dijkstra, N. Ronde, G. P. M. van Klink, D. Vogt, G. van Koten, *Adv. Synth. Catal.* **2003**, *345*, 364-369; H. P. Dijkstra, G. P. M. van Klink, G. van Koten, *Acc. Chem. Res.* **2002**, *35*, 798-810.
16. R. van de Coevering, A. P. Alfers, J. D. Meeldijk, E. Martinez-Viviente, P. S. Pregosin, R. J. M. Klein Gebbink, G. van Koten, *J. Am. Chem. Soc.* **2006**, *128*, 12700-12713; R. van de Coevering, M. Kuil, R. J. M. Klein Gebbink, G. van Koten, *Chem. Commun.* **2002**, 1636-1637.
17. D. E. Bergbreiter, *Chem. Rev.* **2002**, *102*, 3345-3384; D. E. Bergbreiter, P. L. Osburn, J. D. Frels, *J. Am. Chem. Soc.* **2001**, *123*, 11105-11106.
18. N. C. Mehendale, C. Bezemer, C. A. van Walree, R. J. M. Klein Gebbink, G. van Koten, *J. Mol. Catal. A* **2006**, *257*, 167-175.
19. R. Gimenez, T. M. Swager, *J. Mol. Catal. A* **2001**, *166*, 265-273.
20. K. Yu, W. Sommer, J. M. Richardson, M. Weck, C. W. Jones, *Adv. Synth. Catal.* **2005**, *347*, 161-171; W. Sommer, K. Yu, J. S. Sears, Y. Ji, X. Zheng, R. J. Davis, C. D. Sherrill, C. W. Jones, M. Weck, *Organometallics* **2005**, *24*, 4351-4361; K. Yu, W. Sommer, M. Weck, C. W. Jones, *J. Catal.* **2004**, *226*, 101-110; R. Chanthateyanonth, H. Alper, *Adv. Synth. Catal.* **2004**, *346*, 1375-1384; R. Chanthateyanonth, H. Alper, *J. Mol. Catal. A* **2003**, *201*, 23-31.
21. N. C. Mehendale, R. W. A. Havenith, M. Lutz, A. L. Spek, R. J. M. Klein Gebbink, G. van Koten, *manuscript in prep. (Ch. 5 and 6 of this thesis).*
22. N. C. Mehendale, M. Lutz, A. L. Spek, R. J. M. Klein Gebbink, G. van Koten, *manuscript in prep. (Ch. 8 of this thesis).*
23. N. C. Mehendale, M. Lutz, A. L. Spek, R. J. M. Klein Gebbink, G. van Koten, *manuscript in prep. (Ch. 2 of this thesis).*
24. A. Sakthivel, J. Zhao, M. Hanzlik, A. S. T. Chiang, W. A. Herrmann, F. E. Kuehn, *Adv. Synth. Catal.* **2005**, *347*, 473-483; N. K. K. Raj, S. S. Deshpande, R. H. Ingle, T. Raja, P. Manikandan, *Catal. Lett.* **2004**, *98*, 217-224; V. Ayala, A. Corma, M. Iglesias, F. Sanchez, *J. Mol. Catal. A* **2004**, *221*, 201-208; J. V. Nguyen, C. W. Jones, *Macromolecules* **2004**, *37*, 1190-1203; H. Ma, J. He, D. G. Evans, X. Duan, *J. Mol. Catal. B* **2004**, *30*, 209-217; C. González-Arellano, A. Corma, M. Iglesias, F. Sánchez, *Adv. Synth. Catal.* **2004**, *346*, 1316-1328; P. N. Liu, P. M. Gu, F. Wang, Y. Q. Tu, *Org. Lett.* **2004**, *6*, 169-172; P. Stepnicka, J. Demel, J. Cejka, *J. Mol. Catal. A* **2004**, *224*, 161-169; J.-H. Kim, G.-J. Kim, *Catal. Lett.* **2004**, *92*, 123-130.
25. M. W. McKittrick, C. W. Jones, *J. Catal.* **2004**, *227*, 186-201.
26. W. D. Harkins, G. Jura, *J. Chem. Phys.* **1943**, *11*, 431-432.
27. E. P. Barret, L. S. Joyner, P. P. Halenda, *J. Am. Chem. Soc.* **1951**, *73*, 373-380.
28. C.-F. Cheng, D. H. Park, J. Klinowski, *J. Chem. Soc., Faraday Trans.* **1997**, *93*, 193-197.
29. D. Zhao, J. Feng, Q. Huo, N. Melosh, G. H. Fredrickson, B. F. Chmelka, G. D. Stucky, *Science* **1998**, *279*, 548.

Chapter 5

Insertion of Methyl Isocyanoacetate in the M–C Bond of ECE-Pincer Metal-d^8 Complexes

Abstract

A series of NCN-, SCS-, and PCP-pincer metal complexes have been reacted with methyl isocyanoacetate (MI). It appears that 2,6-bis[(dimethylamino)methyl]phenyl (NCN-pincer) palladium(II) and platinum(II) chloride ([MCl(NCN)] where M = Pd and Pt), and 2,6-bis[(thiophenyl)methyl]phenyl (SCS-pincer) palladium(II) chloride ([PdCl(SCS)]) undergo a 1:1 insertion reaction in the C_{ipso}–M (Pd or Pt) bond. In the resulting imidoyl-metal complex a second MI becomes coordinated to the metal center. In contrast, the reaction of 2,6-bis[(diphenylphosphino)methyl]phenyl (PCP-pincer) palladium(II) chloride ([PdCl(PCP)]) with MI stops at the stage of the formation of the [Pd(PCP)(MI)]Cl coordination complex, *i.e.*, in this case an isocyanide insertion reaction does not occur. A mechanism for the insertion reaction is proposed involving prior coordination of two isocyanides to the metal, not by halide displacement (*cf.* formation of [Pd(PCP)(MI)]Cl), but by ligand exchange with the coordinating amino or thioether substituents of the NCN- or SCS-pincer ligand, respectively, followed by insertion of one isocyanide molecule into the M–C bond. A similar reactivity pattern has been found when NCN-, SCS-, and PCP-pincer complexes are treated with tert-butylisocyanide. The X-ray crystal structure of a dimeric insertion product derived from [PdCl(SCS)] with MI is reported.

5.1. Introduction

Insertion of organic isocyanides into the Pd–C bond of cyclopalladated complexes has been extensively studied.[1-5] Depalladation of the resulting insertion product gives rise to the formation of interesting heterocyclic compounds.[4,6] Both [PdCl(NCN)][7] (NCN = $[C_6H_3(CH_2NMe_2)_2\text{-}2,6]^-$) and [PdCl(MeSCS)][8] (MeSCS = $[C_6H_3(CH_2SMe)_2\text{-}2,6]^-$) complexes have been reported to undergo insertion into the Pd–C bond upon treatment with two equivalents of tert-butylisocyanide (^{t}BuNC) at room temperature, forming imidoyl complexes with the general structure shown in Chart 1. Recently, we observed that also cationic NCN- and SCS-pincer (SCS = $[C_6H_3(CH_2SPh)_2\text{-}2,6]^-$) palladium complexes undergo insertion upon treatment with methyl isocyanoacetate (MI). In parallel, we found that these new imidoyl-palladium complexes, containing a 6-membered, cyclometalated ring are active Lewis acid catalysts for the aldol reaction between MI and benzaldehyde forming oxazolines (reaction 1).[9] These studies prompted a more detailed study on the reactivity of ECE-pincer palladium and platinum complexes as also [MX(PCP)] (M = Pd or Pt, PCP = $[C_6H_3(CH_2PPh_2)_2\text{-}2,6]^-$) catalysts have been used for this aldol reaction.[10] The present paper reports on the preparation and mechanism of formation of various new insertion products formed by reacting different isocyanides with a series of pincer-type Pd-halide complexes (Scheme 1). It has been found that whereas [PdCl(NCN)], [PdCl(SCS)], and the cationic derivatives $[Pd(NCN)(H_2O)](BF_4)$ and $[Pd(SCS)(MeCN)](BF_4)$ undergo rapid insertion with MI and with ^{t}BuNC, the corresponding [PdCl(PCP)] complex and its cationic derivative $[Pd(PCP)(MeCN)](BF_4)$ react with MI to give the cationic 1:1 coordination complex [Pd(PCP)(MI)]X.

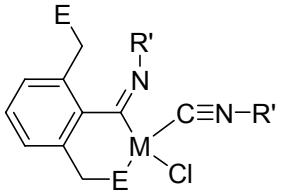

M = Pd, Pt
E = SR, NR_2

Chart 1 General structure of the imidoyl-insertion complex.

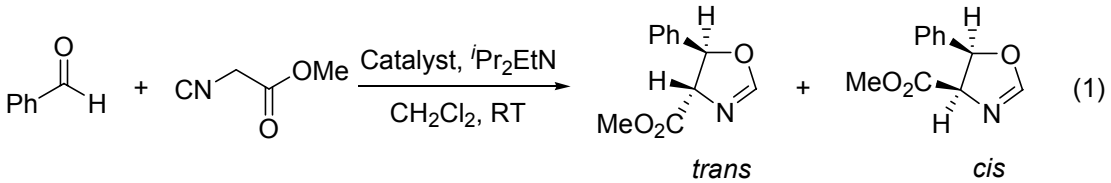

5.2. Results

5.2.1. Synthesis

Various NCN- and SCS-pincer derived palladium and platinum insertion complexes were synthesized (Scheme 1). The reaction of two equivalents of MI with [PdCl(NCN)] (**1**) in

dichloromethane afforded the imidoyl insertion product **4** within several minutes. This complex comprises two molecules of MI, one inserted in the (aryl)C–Pd bond, which is thereby being converted into an imidoyl-palladium moiety, and the second C-coordinated to Pd, leaving one of the amino ligands of the former NCN-pincer ligand non-coordinated. The insertion product was precipitated from solution as a yellow solid by addition of diethyl ether and was isolated in 80% yield. According to this procedure, insertion complexes **4**-**8** were prepared starting from the respective NCN- and SCS-pincer palladium and platinum complexes. Their composition and identity were established by (variable temperature) NMR and IR spectroscopic measurements (Table 1) and elemental analysis.

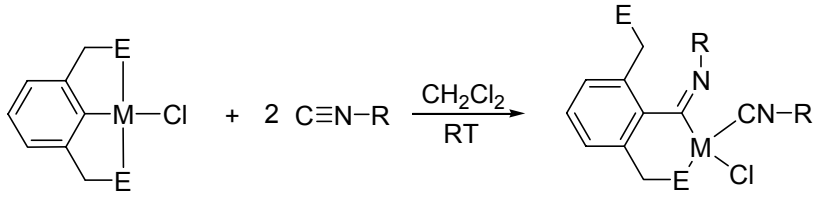

M = Pd, E = NMe_2 (**1**)
E = SPh (**2**)
M = Pt, E = NMe_2 (**3**)

	M	E	R
4	Pd	NMe_2	CH_2CO_2Me
5			^tBu
6		SPh	CH_2CO_2Me
7			^tBu
8	Pt	NMe_2	^tBu

Scheme 1 The imidoyl-palladium and platinum insertion products formed by reaction of two equivalents of isocyanide with the respective NCN- or SCS-pincer metal complexes.

*5.2.2. Imidoyl complexes derived from NCN-pincer palladium complex **1***

Insertion product **4** shows a ^1H NMR spectrum that is characteristic of the proposed structure in Scheme 1. Two different sets of signals, one for the inserted and one for the C-coordinated MI fragment are observed in both the ^1H and ^{13}C NMR spectrum. Diagnostic is also the presence of two singlets for diastereotopic NMe_2 methyl groups pointing to a coordinated NMe_2 grouping and one singlet for homotopic NMe_2 methyl groups as expected for a non-coordinating NMe_2 ligand because of fast pyramidal inversion occurring at the free N-atom. At ambient temperature, the 3- and 5-aryl protons (*i.e.* the protons *ortho* to the -CH_2NMe_2 substituents) are non-equivalent, which is consistent with a structure in which only one of the two -CH_2NMe_2 groupings is coordinated to palladium. The four CH_2 groupings, *i.e.* the two benzylic ones of the former NCN ligand, the CH_2 group of the imidoyl-metal unit and of the coordinated MI ligand appear as four different signals. At –40 °C these signals decoalesce into four AB patterns, indicating that each of CH_2 groupings have diastereotopic protons as a result of lack of an (apparent) molecular symmetry plane containing the respective C-centers. The fact that both resonance patterns, which correspond to coordinated and non-coordinated dimethylamino groups of the former NCN-pincer ligand do not coalesce at these temperatures indicate that exchange between these groups does not take place on the NMR time scale.

The FT-IR spectrum of **4** shows vibrations at 2233 cm^{-1} assigned to the C-coordinated isocyanide molecule $\tilde{\nu}$(C≡N), and at 1637 cm^{-1} corresponding to the imidoyl moiety $\tilde{\nu}$(C=N) (Table 1). The latter value is close to the value for known imidoyl groupings.[5] Both vibrations were used to monitor the formation of **4** by *in situ* IR spectroscopy.

Table 1 Characteristic IR vibrations of various insertion complexes.

	$\tilde{\nu}$ (C≡N)	$\tilde{\nu}$ (C=O)	$\tilde{\nu}$ (C=N)
4 : [PdCl(NCN)]+2MI	2231	1767	1642
11 : [Pd(NCN)(H_2O)](BF_4)+2MI	2223	1760	1681
6 : [PdCl(SCS)]+2MI	2234	1742	1644
14 : [PdCl(PCP)]+2MI	2225	1765	-
8 : [PtCl(NCN)]+2^{t}BuNC	2233	1738	1637
5 : [PdCl(NCN)]+2^{t}BuNC	2196	-	1643
7 : [PdCl(SCS)]+2^{t}BuNC	2199	-	1646
dimer **16**	-	1742	1573
MI[a]	2166	1761	-
^{t}BuNC[b]	2134	-	-

a. IR of MI (cm^{-1}), 2969, 2166, 1761, 1440, 1424; b. IR of ^{t}BuNC (cm^{-1}), 2986, 2134, 1477, 1466.

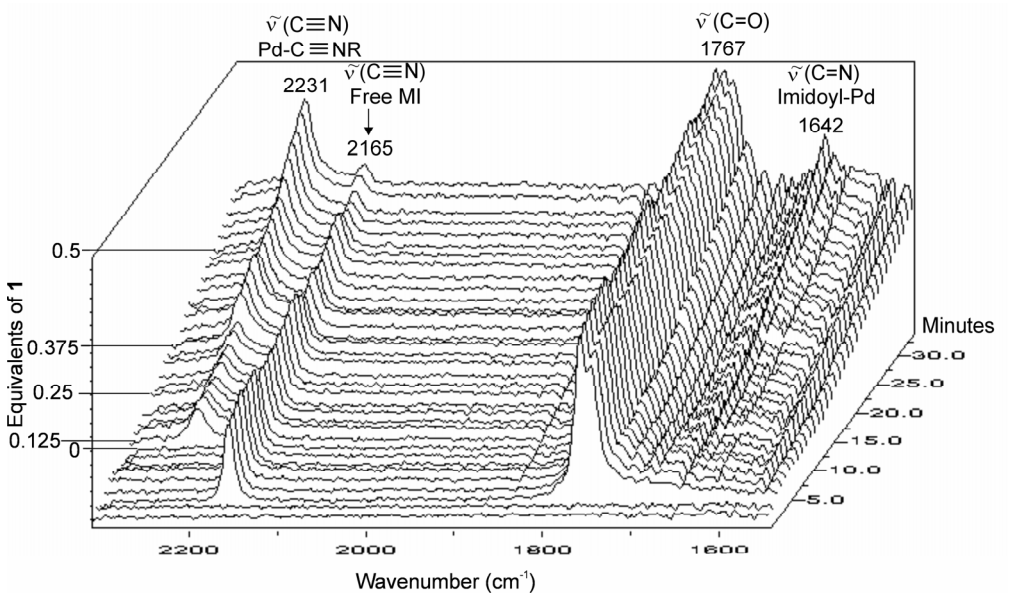

Figure 1 *In situ* IR study of the portionwise (0.125 equivalent portion) addition of a dichloromethane solution of [PdCl(NCN)] (**1**) to MI.

In a first titration experiment, a dichloromethane solution of one equivalent of **1** was added in aliquots of 0.125 equivalents to a dichloromethane solution of two equivalents of MI; *i.e.* **1** was reacted in the presence of excess of MI (Figure 1). After each addition, changes in the IR pattern were observed. When the pattern was stable again, the next aliquot was added. Here, the vibration at 2165 cm^{-1} (free MI) was diagnostic as this vibration gradually disappeared along with the concomitant appearance of vibrations at 2231 and 1642 cm^{-1} which were assigned to the presence of the imidoyl-Pd complex **4**.

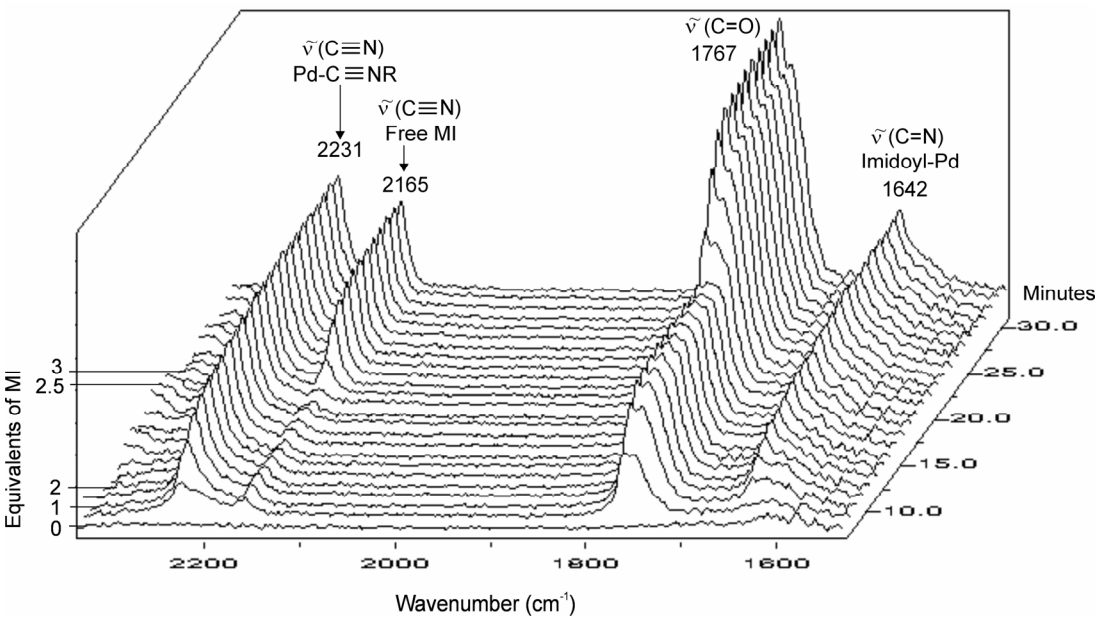

Figure 2 *In situ* IR study of the portionwise (0.5 equivalent portion) addition of MI to a dichloromethane solution of [PdCl(NCN)] (**1**).

In a second titration experiment MI was added in aliquots of 0.5 equivalents to a dichloromethane solution of **1** (one equivalent). After the first addition, an immediate increase of the intensity of vibrations at 2231 and 1642 cm^{-1} was observed, which went along with a color change of the solution from colorless to orange-red (Figure 2). At the point when two equivalents of MI were added, all [PdCl(NCN)] **1** had reacted to form the imidoyl-Pd complex **4**. Further addition of MI only affected the vibration of free MI (2165 and 1767 cm^{-1}). These observations show that even at early stages of this experiment where neutral [PdCl(NCN)] (**1**) was present in excess the insertion complex **4** is formed and no intermediates (*e.g.* [Pd(NCN)(MI)]Cl or [Pd(imidoyl)]Cl) were detected (see Scheme 2). In other words, as long as compound **1** is available, there is immediate complexation of MI to the metal-center. Also it is clear that the isocyanide complexation and insertion processes can not be discriminated by IR at room temperature.

An *in situ* IR experiment in which an equimolar amount of MI was added slowly to a solution of **9**, vibrations at 2223 (Pd–C≡N) and 1764 cm^{-1} (C=O) were observed to increase (Figure 3). In a reverse addition experiment in which the ionic complex [Pd(NCN)(H_2O)](BF_4) (**9**) was added to MI, *i.e.* MI was present in excess, showed that the vibration at 2165 cm^{-1} (free MI) gradually decreased as the solution of **9** (one equivalent total) was added (Figure 4). Concomitantly the vibration at 2223 cm^{-1} (Pd–C≡N) gradually appeared. The results of these experiments clearly demonstrate that coordination of MI to **9** takes place by replacing the aqua ligand forming a 1:1 complex [Pd(NCN)(MI)](BF_4) (**10**, Scheme 2). It is interesting to note the different $\tilde{\nu}$(C≡N) values of coordinated MI in **4** (2231 cm^{-1}, *trans* to NMe_2) and in **10** (2223 cm^{-1}, *trans* to C_{ipso}). These experiments furthermore show that starting from cationic complex **9**, insertion of MI only takes place beyond the presence of one equivalent of MI.

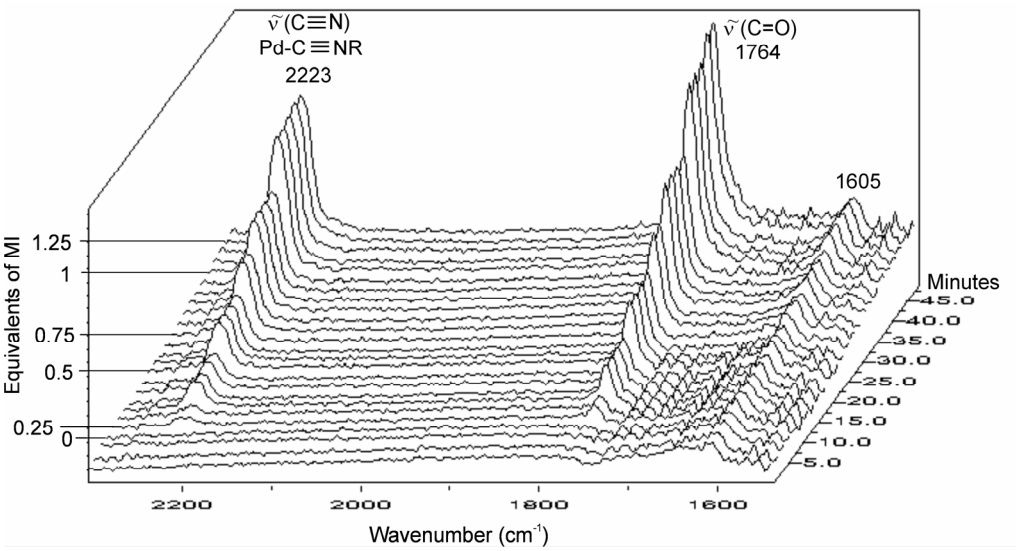

Figure 3 *In situ* IR of the portionwise (0.25 equivalent portion) addition of MI to a dichloromethane solution of [Pd(NCN)(H_2O)](BF_4) (**9**).

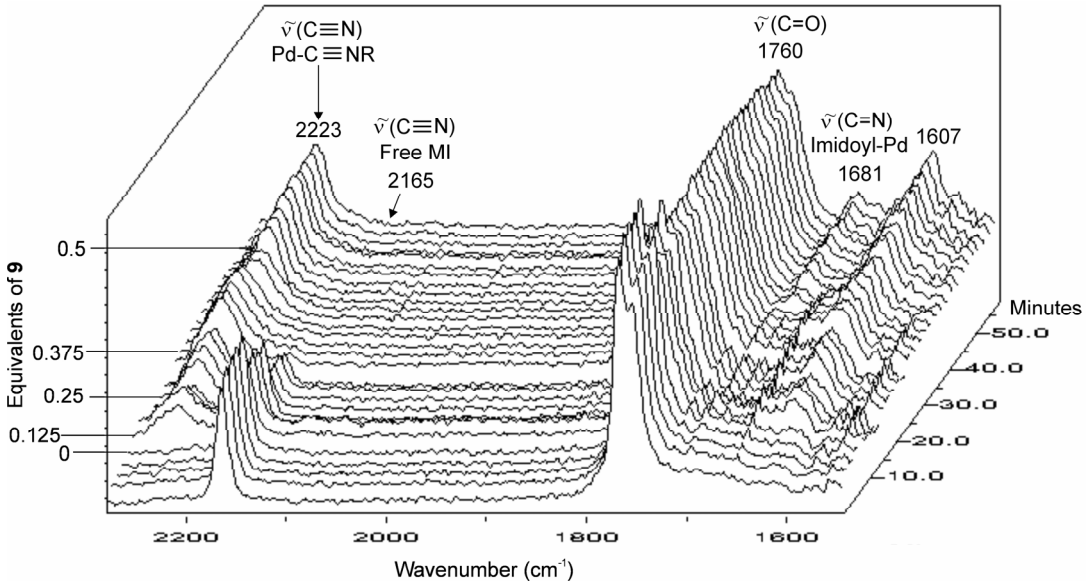

Figure 4 *In situ* IR of the portionwise (0.125 equivalent portion) addition of a dichloromethane solution of [Pd(NCN)(H_2O)](BF_4) (**9**) to MI.

These observations were confirmed by the results of a ^{1}H NMR titration experiment. Aliquots (0.5 equivalents) of MI in CD_2Cl_2 were added to a colorless solution of **9** in CD_2Cl_2. Distinctly different resonance patterns assigned to **9** and **10** were observed for the yellow to red-brown reaction mixture indicating a clean exchange of H_2O by MI. At an MI:**9** molar ratio of one, a rather simple spectrum was obtained similar to that of **9** but with additional signals for complexed MI, according to the (pseudo) C_2-symmetric nature of **10**.[11] On further addition of (excess of) MI, a complex NMR spectrum was observed which was rather comparable to the spectrum of **4** and, therefore, suggests formation of **11**, comprising insertion of MI into the Pd–C bond, *i.e.* the formation of an imidoyl-Pd species with coordination of two MI ligands (Scheme 2).

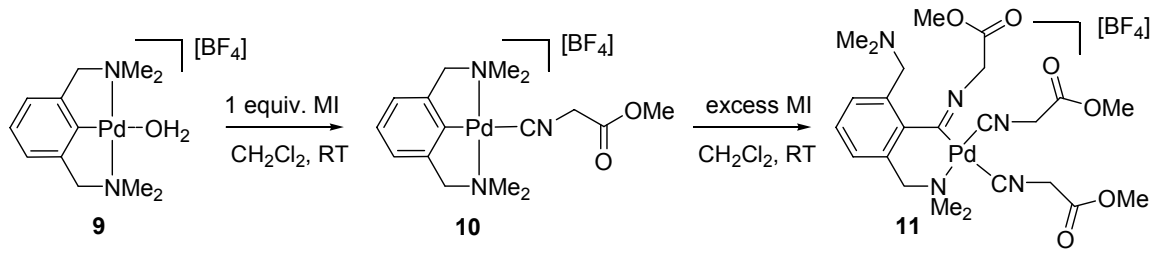

9 **10** **11**

Scheme 2 Stepwise reaction of **9** with MI to form **10** and subsequently **11**.

*5.2.3. Imidoyl complexes derived from SCS-pincer palladium complex **2***

Pfeffer *et al.* reported on the formation of imidoyl complexes from the reaction of [PdCl(MeSCS)] with ^{t}BuNC.[8] Using a similar protocol as discussed above for [PdCl(NCN)] (**1**), we prepared the imidoyl complex **6** starting from [PdCl(PhSCS)] (**2**) and two equivalents of MI. The isolated compound was analyzed by ^{1}H and ^{13}C NMR spectroscopy as well as by elemental analysis. Broad peaks were observed for the C*H*$_2$ hydrogens at 4.0 (benzylic) and 4.9 ppm (MI), as well as for the aromatic hydrogen nuclei in the ^{1}H NMR spectrum of **6** at 25 °C. As the temperature was lowered, these peaks resolved into multiplets. At –55 °C, an AB pattern was observed for each C*H*$_2$ moiety. Separate signals were observed for coordinated (4.2 ppm) and non-coordinated (3.2 ppm) benzylic C*H*$_2$ moieties as well as for coordinated (4.9 ppm) and inserted (4.0 ppm) MI C*H*$_2$ moieties. The aromatic protons of the pincer ligand backbone showed two doublets and a triplet, indicating non-equivalence of all three aromatic hydrogens; a pattern very similar to that found for insertion complex **4**. Upon increasing the temperature from –55 °C, both benzylic CH_2 signals started to coalesce around –35 °C into a broad signal, indicating exchange of S-coordination to palladium between the two *ortho*-CH_2SPh substituents on the NMR time-scale. ^{13}C NMR at –60 °C showed a total of four singlet resonances for the benzylic and MI *C*H$_2$ moieties as well as two singlets for O*C*H$_3$ moieties.

We also studied the formation of **6** from **2** by *in situ* IR spectroscopy and observed similar trends as were found for the reactions of MI with the NCN-pincer complexes. Upon addition of a dichloromethane solution of **2** to a solution containing two equivalents of MI, a decrease of the vibration at 2165 cm^{-1} (free MI) with concomitant increase of vibration at 2234 and 1644 cm^{-1} was observed (Figure 5), which is fully consistent with the formation of insertion product **6**. Similar to the insertion reaction of [PdCl(NCN)], these IR studies did not provide evidence for the nature of any of the reaction intermediates (among which the 1:1 coordination complex).

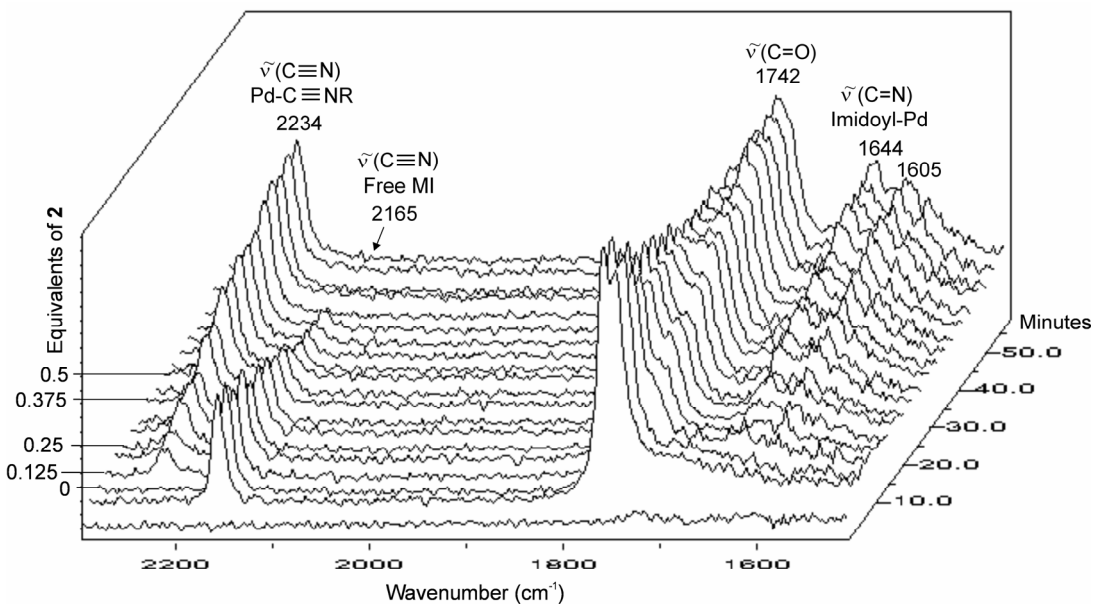

Figure 5 *In situ* IR of the portionwise (0.125 equivalent portion) addition of a dichloromethane solution of [PdCl(SCS)] (**2**) to MI.

5.2.4. In situ reactions of MI with PCP-pincer palladium complexes

In situ IR studies on the reaction of the PCP-pincer palladium complexes **12** and **13** with MI showed that the reaction stops at the stage of the respective 1:1 coordination complexes, *i.e.* no imidoyl insertion product was formed (Scheme 3). MI was found to substitute the fourth ligand, be it a Cl anion as in **12** or a neutral acetonitrile ligand as in the cationic complex **13**. In contrast to the results with the NCN- and SCS-pincer metal halide complexes, in the case of **12** the cationic complex **14** is formed (*cf.* the $\tilde{\nu}$(C≡N) at 2225 cm^{-1}, Figure 6), *i.e.* both PPh_2 substituents remain coordinated to the Pd-center.

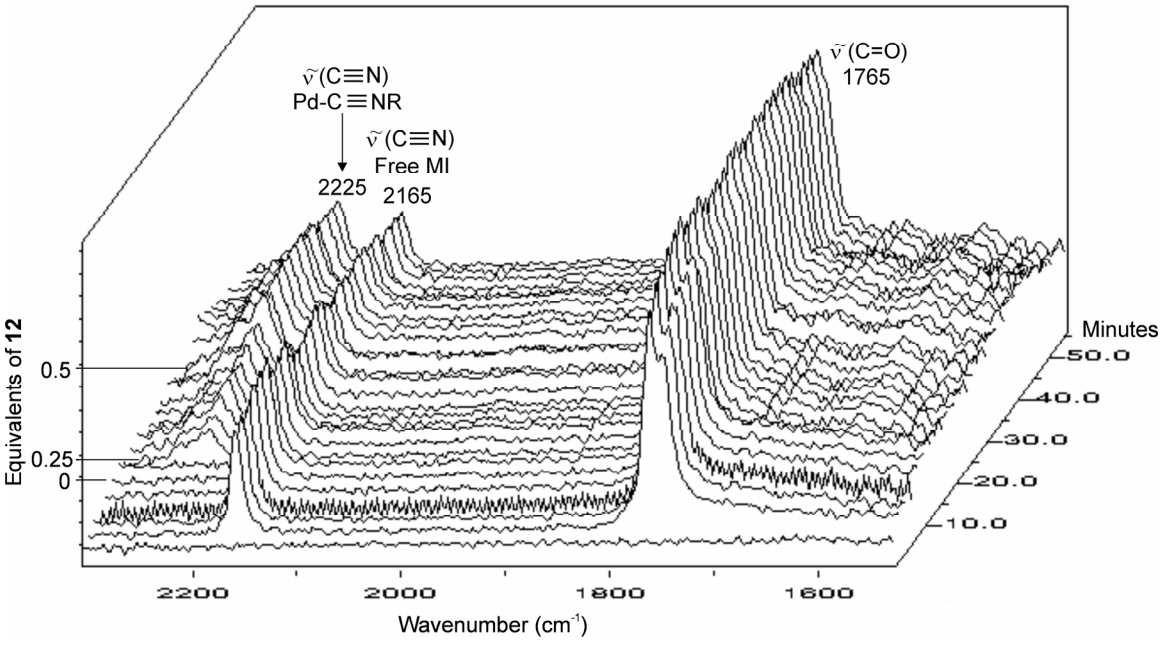

Figure 6 *In situ* IR of the portionwise (0.25 equivalent portion) addition of [PdCl(PCP)] (**12**) solution to MI.

This finding is supported by ^{31}P NMR data. Upon treatment of **12** with MI, the singlet resonance in the ^{31}P NMR spectrum shifts from 34.4 ppm in **12** to 46.1 ppm in the 1:1 coordination complex **14**. Similarly, reaction of **13** with MI resulted in a shift from 41.8 (**13**) to 46.3 ppm (1:1 complex **15**). The presence of a single peak in the ^{31}P NMR spectrum indicates that both phosphorous donors in the 1:1 coordination product are equivalent, which corroborates with the proposed structures of **14** and **15**. These compounds were generated *in situ* and have not been isolated.

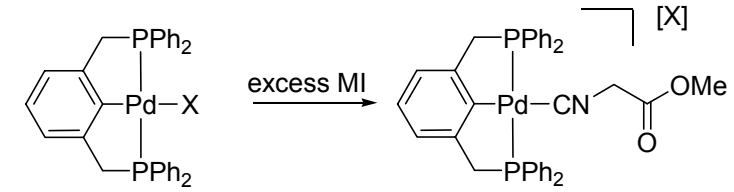

X = Cl (**12**), (MeCN)BF_4 (**13**) X = Cl (**14**), BF_4 (**15**)

Scheme 3 Reaction of PCP-pincer palladium complexes **12** and **13** with excess MI.

*5.2.5. Imidoyl complexes derived from NCN-pincer platinum complex **3***

Insertion of isocyanides into the Pt–C bond of NCN-pincer platinum complex **3** has never been reported. However, we observed that even this complex undergoes an insertion reaction with ^{t}BuNC to form imidoyl complex **8** (Scheme 1). This complex was characterized by NMR, IR (Table 1), and elemental analysis. The reactions of NCN- and SCS-pincer palladium complexes with ^{t}BuNC yielded similar insertion products.

*5.2.6. Structure of dimeric insertion complex (**16**)*

To obtain additional proof for the structure of the insertion products, we attempted to grow single crystals of the various 1:1 coordination and imidoyl insertion products. This remained unsuccessful for the imidoyl-palladium compound **4** derived from [PdCl(NCN)].[12] However, from a concentrated solution of the imidoyl-palladium complex **6** in chloroform, single crystals could be obtained. X-ray crystal structure determination of these crystals revealed that instead of the expected compound **6**, which is a 1:1 complex of an imidoyl-palladium chloride moiety with a further equivalent of MI, the dimeric complex **16** shown in Figure 7 was obtained. The molecular structure of **16** comprises a central six-membered [Pd–C=N–Pd–C=N] metalacycle in a *pseudo*-boat conformation (N(2)–C(221) and C(121)–N(1) run almost parallel), which is formed by the dimerization of two imidoyl-palladium chloride moieties each containing a three-coordinate Pd-center, *i.e.* dimerization of **6** after loss of coordinated MI. The Pd···Pd distance amounts to 3.1092(4) Å, which is comparable to those found in related imidoyl-bridged complexes.[13] Both palladium centers have a distorted square planar geometry with interplanar angles between Cl(1)–Pd(1)–S(11) and N(2)–Pd(1)–C(121) of 2.86(13)° and between Cl(2)–Pd(2)–S(21) and N(1)–Pd(2)–C(221) of 11.00(15)°. The *cis* angles vary from 88.10(4) to 91.84(1)° at Pd(1) and from 89.05(3) to 91.12(8)° at Pd(2). The N–Pd–S angle is 176.95(8)° at Pd(1) and 169.10(9)° at Pd(2).

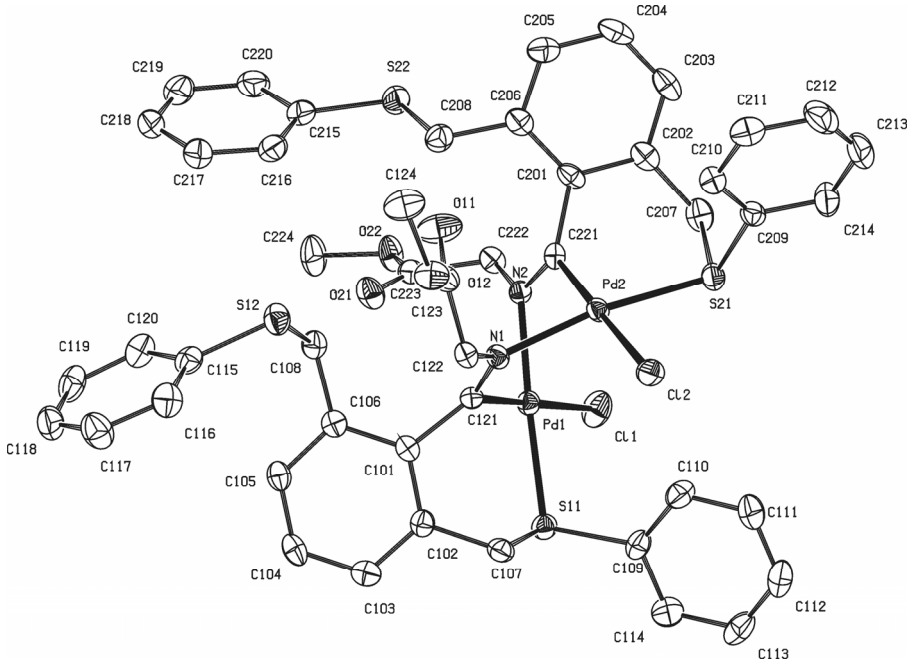

Figure 7 Displacement ellipsoid plot (drawn at 50% probability level) of dimer **16** (hydrogen atoms and $CHCl_3$ are excluded for clarity). Selected bond lengths (Å) and angle (deg): Pd(1)–Cl(1) 2.3855(10), Pd(1)–C(121) 1.992(4), Pd(1)–N(2) 2.055(3), Pd(1)–S(11) 2.2872(9), Pd(1)–Pd(2) 3.1092(4), C(121)–N(1) 1.291(4); C(121)–Pd(1)–N(2) 89.18(12), C(121)–Pd(1)–S(11) 91.84(10), N(1)–Pd(2)–S(21) 169.10(9), N(2)–Pd(1)–S(11) 176.95(8).

In the IR spectrum of **16** in the solid-state, a vibration at 1573 cm^{-1} is observed which can be assigned to the imidoyl entity which subsequently is N-coordinated to the Pd-center of the second unit in the dimeric structure. This value is distinctly different from the 1637 cm^{-1} vibration assigned to the imidoyl moiety in **6**. Furthermore, no vibrations for coordinated or free MI were observed.

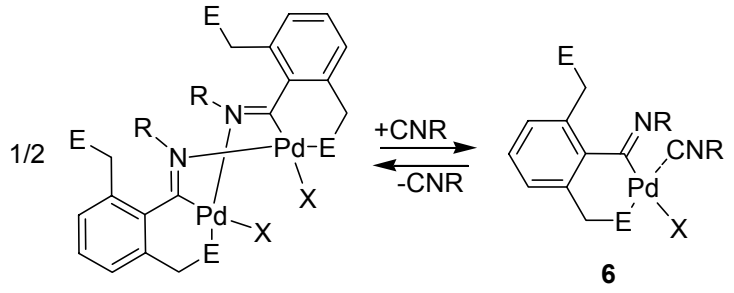

16 E = SPh, R = CH_2CO_2Me

Scheme 4 Interconversion between dimer **16** and monomer **6**.

Treatment of **16** in dichloromethane solution with one equivalent of MI per Pd produced an IR spectrum that was identical to that of **6**, indicating break-down of the dimeric structure of **16** into monomeric units as a result of isocyanide coordination (Scheme 4).

5.3. Discussion

Insertion of isocyanides into the metal-carbon bond of *C,N*-[3,4] and *C,S*-[1] cyclometalated complexes is a well known process. Recently, Kim *et al.* have reported insertion of isocyanides in the case of

cyclopalladated compounds with a *C,N,N*-donor ligand.[14] For ECE-pincer palladium complexes, Pfeffer *et al.* reported ^{t}BuNC insertion products of the type **7**.[8] Our group has earlier reported the insertion product obtained from the reaction of NCN-pincer palladium complex with n-butyl isocyanide.[7] Our current investigations corroborate these findings. In addition they showed that, in the case of a cationic NCN-pincer palladium (**9**) complex, initially a 1:1 product (**10**) is formed after the reaction with one equivalent isocyanide, which after addition of excess isocyanide, is followed by the formation of insertion product (**11**). *In situ* IR studies showed that the insertion is fast, *i.e.* intermediate species were not detected. Furthermore, in the case of neutral and cationic PCP-pincer palladium complexes, similar insertion reactions do not take place. Only a replacement of a fourth ligand by an isocyanide occurs without altering the *mer-P,C,P* coordination of the pincer ligand.

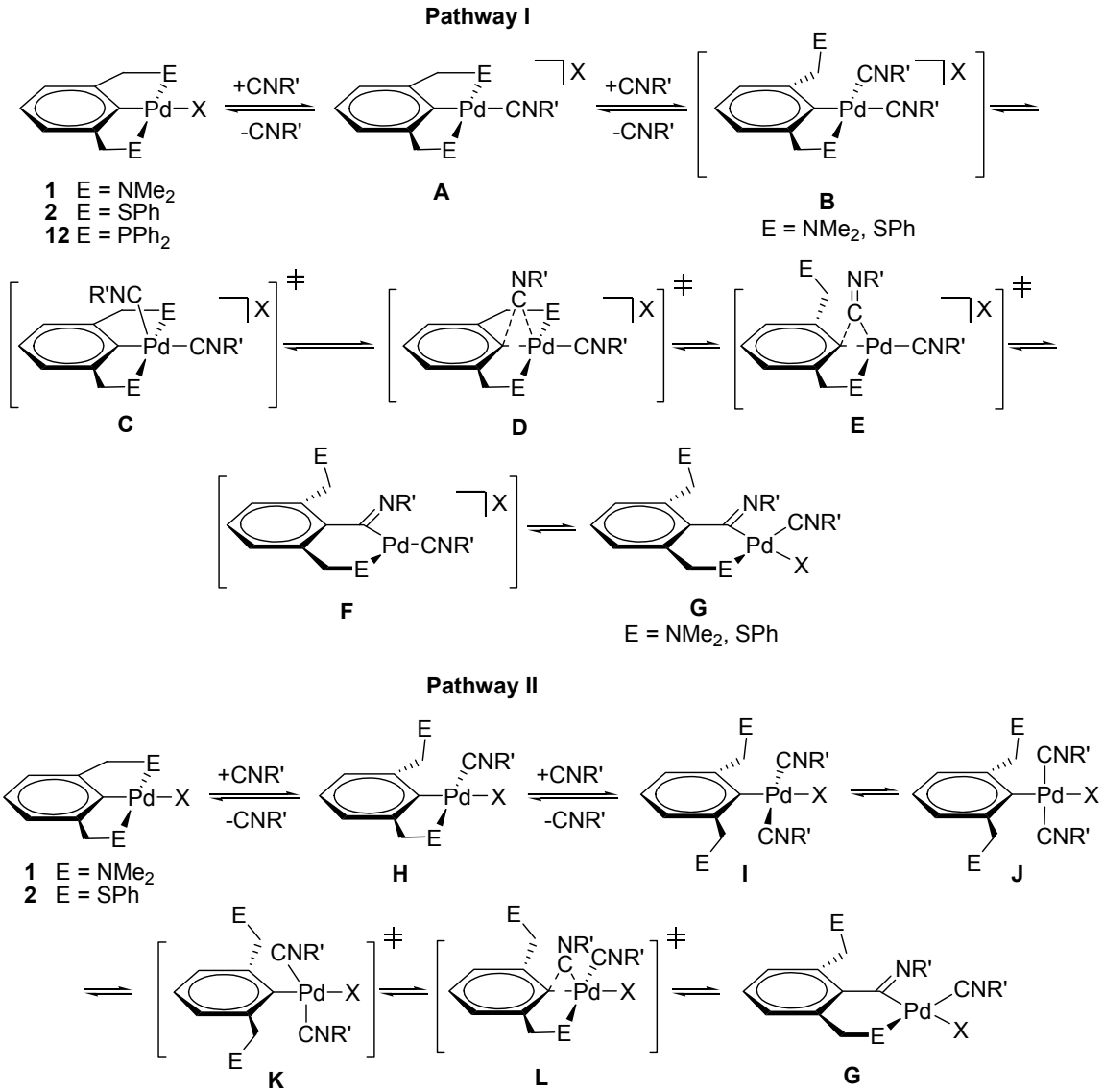

Scheme 5 Proposed mechanism for the insertion reaction.

From these results, we propose a mechanism for the insertion of pincer complexes as shown in Scheme 5. Upon addition of the isocyanide to the complex, there are two possibilities; replacement of the halide (**A**, pathway I) or decomplexation of one of the coordinating arms (**H**, pathway II). In

the former case, a second isocyanide molecule decomplexes the coordinating *ortho*-substituent placing it *cis* with respect to the Pd–C bond (**B**). This molecule of isocyanide is then pushed to the axial position by re-coordination of the *ortho*-substituent so that it is placed *cis* to both Pd–C and Pd–E bonds (**C**).[8,15] This axial isocyanide inserts into the Pd–C bond with subsequent decomplexation of the coordinating arm. The vacant site created is then reoccupied by the halide counter ion to provide insertion product **G**. Alternatively in pathway II, two molecules of MI first decoordinate both pincer arms placing themselves *trans* with respect to each other (**I**). Rotation around the Pd–C bond will place both isocyanide molecules in the axial position for attack on C_{ipso} (**J**), which also will relieve steric strain.

Theoretical calculations (B3LYP) were performed to discriminate between the different proposed routes. The results are reported in Table 2. These calculations were performed on NCN-pincer complex **1** (X = Cl) and two molecules of methyl isocyanide (MeNC) as a model system. The species used for the calculation are depicted in Scheme 6. For comparison, an appropriate number of MeNC molecules were added to the total energy of the individual species, *e.g.* **1** + 2 MeNC, **B'** + 1 MeNC, *etc.*

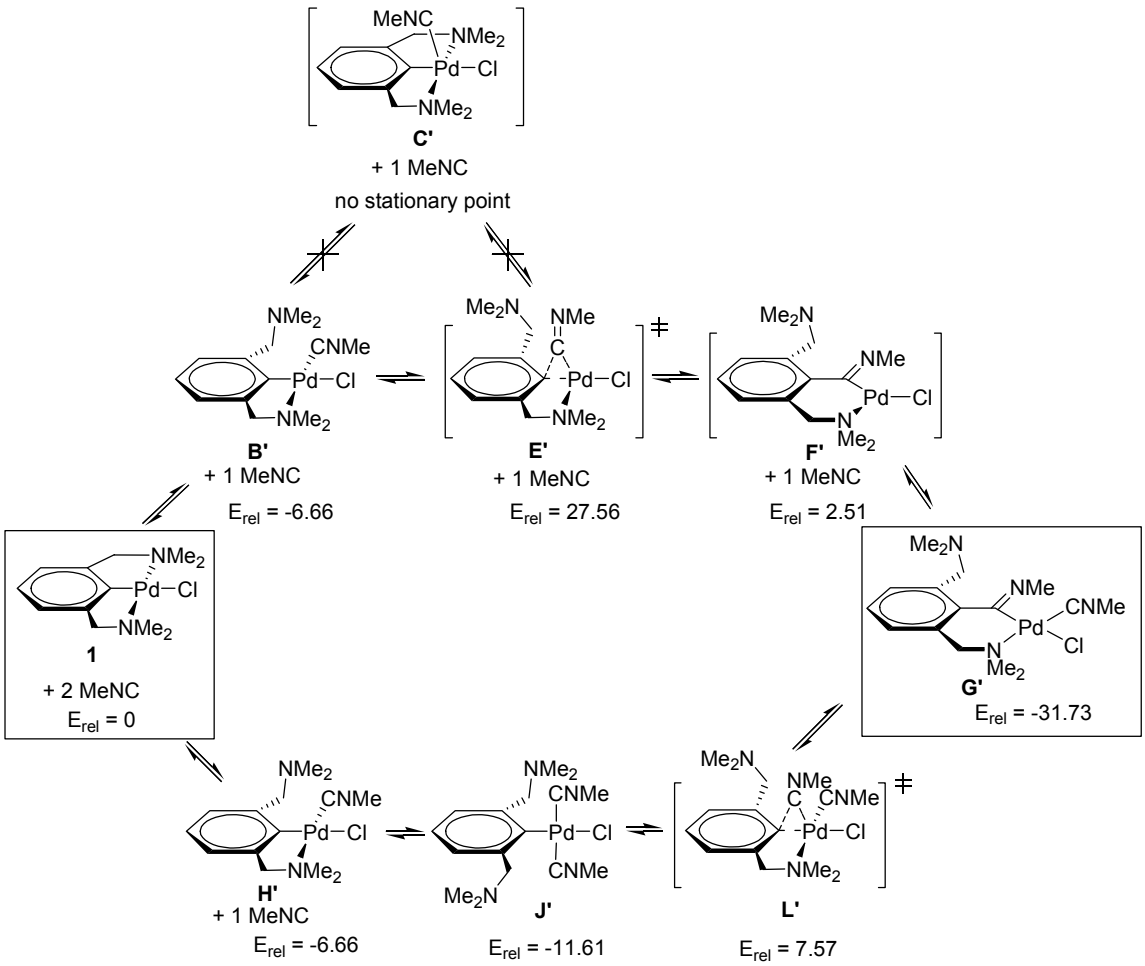

Scheme 6 Selected species from the proposed mechanisms and their relative energies in kcal/mol.

Table 2 B3LYP/LANL2-DZ total energy (E_{B3LYP} (E_h)), zero-point vibrational energy (ZPVE (E_h)), their sum (E_h), the relative energy (E_{rel} (kcal/mol)) and the number of imaginary frequency (n_{img} (cm^{-1})).

Intermediate	E_{B3LYP}	ZPVE	E_{B3LYP} + ZPVE	E_{rel}	n_{img}
1 + 2 MeNC	–985.2785969	0.3901985	–984.8883984	0.00	0
B' + 1 MeNC	–985.2897742	0.3907677	–984.8990065	–6.66	0
E' + 1 MeNC	–985.2322304	0.3877532	–984.8444772	27.56	1 (310.2*i*)
F' + 1 MeNC	–985.2762427	0.3918451	–984.8843976	2.51	0
J'	–985.2972757	0.3903705	–984.9069052	–11.61	0
L'	–985.2656882	0.3893473	–984.8763409	7.57	1 (288.7*i*)
G'	–985.3337935	0.3948392	–984.9389543	–31.73	0

Intermediate **C'** could not be located as a stationary point at the B3LYP/LANL2-DZ level of theory. Coordination of isocyanide to the palladium in axial position does not occur. **E'** was found to be the transition state between **B'** and **F'**, with a relative energy of 27.56 kcal/mol with respect to **1** + 2 MeNC. These findings suggest that species **C'** and **D** do not occur as either transition states or intermediates. The calculations on pathway II revealed that **I** does not occur as an intermediate, and that **L'** was found as a transition state between **J'** and **G'** with a relative energy of only 7.57 kcal/mol with respect to **1** + 2 MeNC. Thus, the preferred pathway for isocyanide insertion is the formation of intermediate **J'** from **1** + 2 MeNC,[16] which then reacts immediately to **G'** *via* transition state **L'**. When one equivalent of isocyanide is added to complex **1**, a mixture of **G'** and unreacted complex **1** is formed, indicating that after the first molecule of isocyanide has become coordinated, the second molecule of MI reacts faster with the species generated. This is possible in the case of **H** (pathway II) which contains severe steric interference between the non-coordinated *ortho*-NMe_2 substituent and the coordinated MeNC molecule. Release of the steric hindrance is then accomplished by rotation around Pd–C bond (**J**).

5.4. Conclusions

NCN- and SCS-pincer palladium complexes undergo insertion of MI in the Pd–C bond to form imidoyl-based, six-membered cyclopalladated ring compounds. No such insertion was observed in case of PCP-pincer palladium complexes suggesting that the stronger binding of the phosphorous substituents as compared to that of the NMe_2 and SPh in the corresponding NCN- and SCS-pincers to the metal center (Pd) prevents the insertion reaction. Only replacement of the chloride anion in case of the neutral PCP-pincer palladium chloride complex or of the MeCN ligand in case of a cationic PCP-pincer complex was observed. Interestingly, the Pt–C bond of NCN-pincer platinum complex likewise undergoes the same insertion reaction when reacted with ^{t}BuNC to give the corresponding imidoyl-platinum(II) insertion product.

From theoretical calculations (B3LYP), a mechanism of the insertion reaction in case of the NCN- and SCS-pincer complexes is proposed. In concert with the experimental observations (IR, NMR), first, decoordination of both *ortho*-CH_2E arms of a pincer complex takes place by two isocyanide

molecules followed by insertion of one of the isocyanides in the M–C bond and simultaneous recoordination of one of the pincer arms to form the final product.

5.5. Experimental Section

5.5.1. General Comments

All synthetic procedures were conducted under a dry nitrogen atmosphere using standard Schlenk techniques. Solvents were dried over appropriate materials and distilled prior to use. All reagents were obtained from commercial sources and were used without further purification. Complexes **1**,[17] **2**,[18] **3**,[19] **9**,[20] **12**,[21] and **13**[21] were prepared as described previously. ^{1}H (200 and 300 MHz) and ^{13}C{^{1}H} (50.3 and 75.5 MHz) NMR spectra were recorded on either Varian Mercury 200, Varian Inova 300 or Bruker 300 spectrometers. FT-IR spectra were recorded using a Mattson Instruments Galaxy Series FTIR 5000 spectrometer. *In situ* IR spectra were recorded using a Mettler Toledo ReactIR™ 1000 spectrometer with a SiComp™ probe. Microanalyses were obtained from H. Kolbe Mikroanalytisches Laboratorium, Mülheim an der Ruhr, Germany.

All geometries were optimized at the B3LYP/LANL2-DZ level of theory using GAMESS-UK.[22] All stationary points were characterized as either minima or transition states by means of Hessian calculations. Reported energy differences are corrected for zero-point vibrational energies.

5.5.2. General procedure for the synthesis of the imidoyl-metal insertion products

NCN- or SCS-pincer palladium complexes (1 equivalent) were dissolved in dry CH_2Cl_2 and isocyanide (2.1 equivalents) was added slowly. The reaction mixture was stirred at room temperature for 2 hours. The solution was then concentrated and Et_2O was added to precipitate the product. Centrifugation followed by drying in vacuum led to the isolation of the insertion products as solids.

5.5.2.1. [PdCl({CNCH$_2$CO$_2$Me}$_2$C$_6$H$_3${CH$_2$NMe$_2$}$_2$-2,6)] ***4***

Starting from **1** (0.2 g, 0.6 mmol) and MI (0.11 mL, 1.26 mmol), **4** was isolated by Et_2O precipitation in 73% (0.23 g) yield.

^{1}H NMR (300 MHz, CD_2Cl_2, 25 °C): δ = 2.24 (s, 6H, NMe_2); 2.56 (s, 3H, NMe_2); 2.86 (s, 3H, NMe_2); 2.96 (d, $^{2}J_{H,H}$ = 11.7 Hz, 2H, ArC*H*$_2$N); 3.43 (d, $^{2}J_{H,H}$ = 13.8 Hz, 1H, ArC*H*$_2$N); 3.64 (d, $^{2}J_{H,H}$ = 13.8 Hz, 1H, ArC*H*$_2$N); 3.78 (s, 3H, OMe); 3.86 (s, 3H, OMe); 4.56 (s, 2H, C(O)C*H*$_2$); 4.78 (s, 2H, C(O)C*H*$_2$); 7.08 (d, $^{3}J_{H,H}$ = 7.2 Hz, 1H, Ar*H*); 7.26 (t, $^{3}J_{H,H}$ = 7.5 Hz, 1H, Ar*H*); 7.54 (d, $^{3}J_{H,H}$ = 7.2 Hz, 1H, Ar*H*). ^{1}H NMR (300 MHz, CD_2Cl_2, –40 °C): δ = 2.22 (s, 6H, NMe_2, non-coordinated); 2.53 (s, 3H, NMe_2, coordinated); 2.83 (s, 3H, NMe_2, coordinated); 2.96 (d, $^{2}J_{H,H}$ = 12 Hz, 2H, ArC*H*$_2$N, non-coordinated); 3.46 (ABq, $^{2}J_{H,H}$ = 20.1, 13.8 Hz, 2H, ArC*H*$_2$N, coordinated); 3.74 (s, 3H, OMe); 3.82 (s, 3H, OMe); 4.58 (ABq, $^{2}J_{H,H}$ = 19.2, 4.2 Hz, 2H, C(O)C*H*$_2$); 4.78 (ABq, $^{2}J_{H,H}$ = 13.2, 4.5 Hz, 2H, C(O)C*H*$_2$); 7.08 (d, $^{3}J_{H,H}$ = 7.2 Hz, 1H, Ar*H*); 7.26 (t, $^{3}J_{H,H}$ = 7.5 Hz, 1H, Ar*H*); 7.52 (d, $^{3}J_{H,H}$ = 7.8 Hz, 1H, Ar*H*). ^{13}C NMR (75.5 MHz, $CDCl_3$, 25 °C): δ = 44.26, 45.88, 48.46, 51.40, 52.19, 53.88, 58.79, 61.49, 65.93, 70.66; 128.06, 128.53 129.34, 131.71, 133.31, 133.78 (Ar*C*); 140.44 (*C*=N); 163.33 (*C*≡N); 171.31 (*C*=O); 186.66

(*C*=O). IR (ATR): $\tilde{\nu}$ = 2952, 2233, 1738, 1637, 1537 cm^{-1}. Anal. Calcd. for $C_{20}H_{29}ClN_4O_4Pd$ (349.16): C, 45.21; H, 5.50; N, 10.54. Found: C, 45.33; H, 5.59; N, 10.38.

5.5.2.2. [PdCl({CN^{t}Bu}$_2$C$_6$H$_3${CH$_2$NMe$_2$}$_2$-2,6)] ***5***

Starting from **1** (0.2 g, 0.6 mmol) and ^{t}BuNC (0.14 mL, 1.26 mmol), **5** was isolated in 60% (0.18 g) yield. This product remained soluble after addition of Et_2O and was isolated by concentrating the resulting solution after filtration.

^{1}H NMR (300 MHz, $CDCl_3$, 25 °C): δ = 1.48 (s, 9H, ^{t}Bu); 1.61 (s, 9H, ^{t}Bu); 2.26 (s, 6H, NMe_2); 2.61 (s, 3H, NMe_2); 2.81 (s, 3H, NMe_2); 2.81 (d, $^2J_{H,H}$ = 11.7 Hz, 1H, ArC*H*$_2$N, coordinated); 3.26 (d, $^2J_{H,H}$ = 14.1 Hz, 1H, ArC*H*$_2$N, non-coordinated); 3.42 (d, $^2J_{H,H}$ = 14.4 Hz, 1H, ArC*H*$_2$N); 3.49 (d, $^2J_{H,H}$ = 11.4 Hz, 1H, ArC*H*$_2$N, coordinated); 6.95 (d, $^3J_{H,H}$ = 7.2 Hz, 1H, Ar*H*); 7.13 (t, $^3J_{H,H}$ = 7.2, 8.1 Hz, 1H, Ar*H*); 7.49 (d, $^3J_{H,H}$ = 7.8 Hz, 1H, Ar*H*). ^{13}C NMR (75.5 MHz, $CDCl_3$, 25 °C): δ = 30.10 (C*C*H$_3$); 31.44 (C*C*H$_3$); 46.08 (N*C*H$_3$); 48.86 (*C*CH$_3$); 50.95 (*C*CH$_3$); 56.92 (*C*H$_2$); 59.87 (PdN*C*H$_3$); 65.71 (PdN*C*H$_3$); 70.63 (*C*H$_2$); 126.45, 128.23, 129.69 (Ar*C*); 130.81 (*C*≡N); 131.77, 132.01, 140.03 (Ar*C*); 172.47 (*C*=N). IR (ATR): $\tilde{\nu}$ = 2966, 2818, 2772, 2196, 1643, 1608, 1456 cm^{-1}.

5.5.2.3. [PdCl({CNCH$_2$CO$_2$Me}$_2$C$_6$H$_3${CH$_2$SPh}$_2$-2,6)] ***6***

Starting from **2** (0.2 g, 0.43 mmol) and MI (0.08 mL, 0.91 mmol), **6** was isolated by Et_2O precipitation in 70% (0.2 g) yield.

^{1}H NMR (300 MHz, $CDCl_3$, 25 °C): δ = 3.75 (s, 3H, OMe); 3.76 (s, 3H, OMe); 3.92 (bs, 4H, SC*H*$_2$); 4.0 (bs, 2H, C(O)C*H*$_2$); 4.91 (s, 2H, C(O)C*H*$_2$); 7.02 (t, $^3J_{H,H}$ = 6.6 Hz, 1H, Ar*H*); 7.27 (m, 6H, Ar*H*); 7.45 (m, 6H, Ar*H*). ^{1}H NMR (300 MHz, $CDCl_3$, –60 °C): δ = 3.06 (d, $^2J_{H,H}$ = 19.2 Hz, 1H, SC*H*$_2$, non-coordinated); 3.56 (d, $^2J_{H,H}$ = 13.2 Hz, 1H, SC*H*$_2$, coordinated); 3.74 (s, 3H, OMe); 3.82 (s, 3H, OMe); 3.98 (d, $^2J_{H,H}$ = 19.2 Hz, 1H, SC*H*$_2$, non-coordinated); 4.01 (d, $^2J_{H,H}$ = 13.2 Hz, 1H, SC*H*$_2$, coordinated); 4.11 (d, $^2J_{H,H}$ = 10.8 Hz, 1H, C(O)C*H*$_2$); 4.39 (d, $^2J_{H,H}$ = 10.5 Hz, 1H, C(O)C*H*$_2$); 4.83 (d, $^2J_{H,H}$ = 16.8 Hz, 1H, C(O)C*H*$_2$); 5.01 (d, $^2J_{H,H}$ = 16.8 Hz, 1H, C(O)C*H*$_2$). ^{13}C NMR (75.5 MHz, $CDCl_3$, –60 °C): δ = 32.4 (S*C*H$_2$, non-coordinated); 41.0 (S*C*H$_2$, coordinated); 44.4 (C(O)*C*H$_2$, inserted); 52.7, 53.9 (O*C*H$_3$); 61.3 (C(O)*C*H$_2$, coordinated); 125.1, 125.4, 127.3, 128.9, 129.2, 129.6, 129, 130.2, 130.5, 131.9, 133.3, 133.9, 134.3, 138.3 (Ar*C*); 139.8 (C=N); 163.2 (C≡N); 171.0 (C=O); 184.2 (C=O). IR (ATR): $\tilde{\nu}$ = 2951, 2906, 2234, 1762, 1726, 1637, 1581 cm^{-1}. Anal. Calcd. for $C_{28}H_{27}ClN_2O_4PdS_2$ (661.53) C, 50.84; H, 4.11; N, 4.23; S, 9.69. Found: C, 50.69; H, 4.06; N, 4.21; S, 9.62.

5.5.2.4. [PdCl({CN^{t}Bu}$_2$C$_6$H$_3${CH$_2$SPh}$_2$-2,6)] ***7***

Starting from **2** (0.2 g, 0.43 mmol) and ^{t}BuNC (0.1 mL, 0.91 mmol), **7** was isolated by Et_2O precipitation in 75% (0.2 g) yield.

^{1}H NMR (300 MHz, $CDCl_3$, 25 °C): δ = 1.39 (s, 9H, ^{t}Bu); 1.60 (s, 9H, ^{t}Bu); 3.68 (bs, 2H, SC*H*$_2$); 4.15 (ABq, $^2J_{H,H}$ = 14.7, 14.4 Hz, 2H, PdSC*H*$_2$); 6.77 (d, $^3J_{H,H}$ = 5.1 Hz, 1H, Ar*H*); 7.03 (t, $^3J_{H,H}$ = 7.5, 8.1 Hz, 1H, Ar*H*); 7.15 (t, $^3J_{H,H}$ = 7.2, 7.5 Hz, 1H, Ar*H*); 7.25-7.37 (m, 7H, Ar*H*); 7.49 (d, $^3J_{H,H}$ = 8.1 Hz, 1H, Ar*H*); 7.63 (d, $^3J_{H,H}$ = 6.6 Hz, 2H, Ar*H*). ^{13}C NMR (50.3 MHz, $CDCl_3$, 25 °C): δ = 29.88 (C*C*H$_3$); 31.30 (C*C*H$_3$); 34.83 (S*C*H$_2$); 39.77 (S*C*H$_2$); 57.84 (CH$_3$*C*); 58.67 (CH$_3$*C*); 125.86, 126.81, 128.35, 129.07,

129.13, 129.51, 129.74, 130.85, 131.69, 132.13 (Ar*C*); 136.91; 140.08. IR (ATR): $\tilde{\nu}$ = 3058, 2968, 2869, 2199, 1646, 1582, 1481, 1440 cm^{-1}.

5.5.2.5. [PtCl({CN^{t}Bu}$_2$C$_6$H$_3${CH$_2$NMe$_2$}$_2$-2,6)] ***8***

Starting from **3** (0.2 g, 0.5 mmol) and ^{t}BuNC (0.11 mL, 1.0 mmol), **8** was isolated in 75% (0.22 g) yield. This product remained soluble after addition of Et_2O and was isolated by concentrating the resulting solution after filtration.

^{1}H NMR (300 MHz, $CDCl_3$, 25 °C): δ = 1.50 (s, 9H, ^{t}Bu); 1.64 (s, 9H, ^{t}Bu); 2.21 (s, 6H, NMe_2); 2.75 (t, $^3J_{H,Pt}$ = 27 Hz, 9H, NMe_2); 3.54 (s, 4H, NCH_2); 3.97 (t, $^3J_{H,Pt}$ = 29.1 Hz 4H, NCH_2); 6.91 (d, $^3J_{H,H}$ = 6.6 Hz, 1H, Ar*H*); 6.99 (t, $^3J_{H,H}$ = 7.5, 8.1 Hz, 1H, Ar*H*); 7.2 (d, $^3J_{H,H}$ = 7.5 Hz, 1H, Ar*H*). ^{13}C NMR (75.5 MHz, $CDCl_3$, 25 °C): δ = 29.99 (C*C*H$_3$); 30.18 (C*C*H$_3$); 45.72 (*C*H$_3$); 51.06 (*C*H$_2$); 53.75 (*C*H$_3$); 59.82 (*C*H$_3$); 68.08 (*C*H$_3$); 74.51 (*C*H$_2$); 121.4, 124.95, 126.92, 129.84, 138.65, 141.63 (Ar*C*); 146.24; 150.26. IR (ATR): $\tilde{\nu}$ = 2952, 2233, 1738, 1637, 1537 cm^{-1}. Anal. Calcd. for $C_{22}H_{37}ClN_4Pt$ (588.09): C, 44.93; H, 6.34; N, 9.53. Found: C, 45.07; H, 6.28; N, 9.42.

5.5.3. General procedure for in situ IR experiments

All experiments were carried out in a 5 mL CH_2Cl_2 solution. Vibrations from the solvent are subtracted from all the spectra. In a typical experiment, compound **1** (0.05 mmol, 1 equivalent) was dissolved in the solution and vibrations were scanned until there were no more changes. To this solution, aliquots of MI (0.025 mmol, 0.5 equivalents) were added (in total two equivalents). After each addition, changes in the IR vibrations were observed. When a stable spectrum was obtained, the next aliquot was added. Finally, excess of MI was added in aliquots to observe any further changes.

5.5.4. X-ray crystal structure determination of ***16***

$C_{48}H_{44}Cl_2N_2O_4Pd_2S_4 \cdot CHCl_3$, Fw = 1244.16, yellow needle, 0.30 x 0.06 x 0.06 mm^3, triclinic, $P\bar{1}$ (no. 2), a = 13.4510(2), b = 14.0689(2), c =14.5129(2) Å, α = 96.9286(7), β = 92.7639(7), γ = 110.7319(5)°, V = 2537.58(6) $Å^3$, Z = 2, D_x = 1.628 g/cm^3, μ = 1.182 mm^{-1}. 38552 Reflections were measured on a Nonius Kappa CCD diffractometer with rotating anode (graphite monochromator, λ = 0.71073 Å) at a temperature of 150(2) K up to a resolution of $(\sin\theta/\lambda)_{max}$ = 0.65 $Å^{-1}$. Intensities were integrated with HKL2000.[23] The reflections were corrected for absorption and scaled on the basis of multiple measured reflections with the program SORTAV[24] (0.78-0.93 correction range). 11531 Reflections were unique (R_{int} = 0.0819). The structure was solved with the program DIRDIF-99[25] using automated Patterson Methods and refined with SHELXL-97[26] against F^2 of all reflections. Non hydrogen atoms were refined with anisotropic displacement parameters. All hydrogen atoms were located in the difference Fourier map and refined with a riding model. 597 Parameters were refined with no restraints. R1/wR2 [$I > 2\sigma(I)$]: 0.0410/0.0832. R1/wR2 [all refl.]: 0.0769/0.0972. S = 1.019. Residual electron density between –0.82 and 0.99 e/$Å^3$. Geometry calculations and checking for higher symmetry was performed with the PLATON program.[27]

5.6. References

1. J. Dupont, M. Pfeffer, J. C. Daran, Y. Jeannin, *Organometallics* **1987**, *6*, 899-901.
2. A. D. Ryabov, *Synthesis* **1985**, 233-252.
3. R. D. O'Sullivan, A. W. Parkins, *J. Chem. Soc., Chem. Commun.* **1984**, 1165-1166; Y. Yamamoto, H. Yamazaki, *Inorg. Chim. Acta* **1980**, *41*, 229-232; J. F. van Baar, J. M. Klerks, O. P., D. J. Stufkens, K. Vrieze, *J. Organomet. Chem.* **1976**, *112*, 95-103.
4. Y. Yamamoto, H. Yamazaki, *Synthesis* **1976**, 750-751.
5. Y. Yamamoto, H. Yamazaki, *Inorg. Chem.* **1974**, *13*, 438-443; Y. Yamamoto, H. Yamazaki, *Coord. Chem. Rev.* **1972**, *8*, 225-239.
6. J. Vincente, I. Saura-Llamas, C. Grünwald, C. Alcaraz, P. G. Jones, D. Bautista, *Organometallics* **2002**, *21*, 3587-3595; J. Vincente, I. Saura-Llamas, J. Turpín, M. C. R. de Arellano, P. G. Jones, *Organometallics* **1999**, *18*, 2683-2693.
7. A. Zografidis, K. Polborn, W. Beck, B. A. Markies, G. van Koten, *Z. Naturforsch., B* **1994**, *49*, 1494-1498.
8. J. Dupont, M. Pfeffer, *J. Chem. Soc., Dalton Trans.* **1990**, 3193-3198.
9. N. C. Mehendale, R. J. M. Klein Gebbink, G. van Koten, *manuscript in prep. (Ch. 6 of this thesis).*
10. G. Rodriguez, M. Lutz, A. L. Spek, G. van Koten, *Chem. Eur. J.* **2002**, *8*, 45-57; G. Guillena, G. Rodriguez, G. van Koten, *Tetrahedron Lett.* **2002**, *43*, 3895-3898; Y. Motoyama, H. Kawakami, K. Shimozono, K. Aoki, H. Nishiyama, *Organometallics* **2002**, *21*, 3408-3416; J. S. Fossey, C. J. Richards, *Organometallics* **2002**, *21*, 5259-5264; M. D. Meijer, N. Ronde, D. Vogt, G. P. M. van Klink, G. van Koten, *Organometallics* **2001**, *20*, 3993-4000; M. Albrecht, B. M. Kocks, A. L. Spek, G. van Koten, *J. Organomet. Chem.* **2001**, *624*, 271-286; C. Schlenk, A. W. Kleij, H. Frey, G. van Koten, *Angew. Chem., Int. Ed.* **2000**, *39*, 3445-3447; J. M. Longmire, X. Zhang, M. Shang, *Organometallics* **1998**, *17*, 4374-4379; M. A. Stark, C. J. Richards, *Tetrahedron Lett.* **1997**, *38*, 5881-5884; F. Gorla, A. Togni, L. M. Venanzi, A. Albinati, F. Lianza, *Organometallics* **1994**, *13*, 1607-1616.
11. ^{1}H NMR (300 MHz, CD_2Cl_2, 25 °C) data for **9**: 2.45 (H_2O), 2.86 (NCH_3), 4.0 (ArCH_2), 6.80 (d, $^2J_{H,H}$ = 7.8 Hz, 2H, Ar*H*), 7.03 (t, $^2J_{H,H}$ = 7.5 Hz, 1H, Ar*H*); for **10**, 3.01 (s, 12H, NCH_3); 3.87 (s, 3H, OCH_3); 4.12 (s, 4H, ArCH_2); 4.71 (s, 2H, C(O)CH_2); 6.90 (d, $^2J_{H,H}$ = 7.5 Hz, 2H, Ar*H*); 7.09 (t, $^2J_{H,H}$ = 7.5 Hz, 1H, Ar*H*).
12. Earlier, we have reported the X-ray structure of the insertion product obtained by treatment of **1** with n-butyl isocyanide; see ref. 7
13. R. Usón, J. Forniés, P. Espinet, E. Lalinde, A. García, P. G. Jones, K. Meyer-Bäse, G. M. Sheldrick, *J. Chem. Soc., Dalton Trans.* **1986**, 259-264; R. Usón, J. Forniés, P. Espinet, A. García, M. Tomas, C. Foces-Foces, F. H. Cano, *J. Organomet. Chem.* **1985**, *282*, C35-C38; R. Usón, J. Forniés, P. Espinet, E. Lalinde, P. G. Jones, G. M. Sheldrick, *J. Organomet. Chem.* **1983**, *253*, C47-C49; R. Usón, J. Forniés, P. Espinet, E. Lalinde, P. G. Jones, G. M. Sheldrick, *J. Chem. Soc., Dalton Trans.* **1982**, 2389-2395.
14. Y.-J. Kim, X. Chang, J.-T. Han, M. S. Lim, S. W. Lee, *Dalton Trans.* **2004**, 3699-3708.
15. M. Albrecht, R. A. Gossage, A. L. Spek, G. van Koten, *J. Am. Chem. Soc.* **1999**, *121*, 11898-11899; M. Albrecht, A. L. Spek, G. van Koten, *J. Am. Chem. Soc.* **2001**, *123*, 7233-7246.
16. G. Rodriguez, M. Albrecht, J. Schoenmaker, A. Ford, M. Lutz, A. L. Spek, G. van Koten, *J. Am. Chem. Soc.* **2002**, *124*, 5127-5138; M. Albrecht, P. Dani, M. Lutz, A. L. Spek, G. van Koten, *J. Am. Chem. Soc.* **2000**, *122*, 11822-11833.
17. J. Terheijden, G. van Koten, F. Muller, D. M. Grove, K. Vrieze, E. Nielsen, C. H. Stam, *J. Organomet. Chem.* **1986**, *315*, 401-417.
18. N. Lucena, J. Casabo, L. Escriche, G. Sanchez-Castello, F. Teixidor, R. Kivekäs, R. Sillanpää, *Polyhedron* **1996**, *15*, 3009-3018.
19. D. M. Grove, G. van Koten, J. N. Louwen, J. G. Noltes, A. L. Spek, H. J. C. Ubbels, *J. Am. Chem. Soc.* **1982**, *104*, 6609-6616.
20. P. Steenwinkel, R. A. Gossage, T. Maunula, D. M. Grove, G. van Koten, *Chem. Eur. J.* **1998**, *4*, 763-768.
21. H. Rimml, L. M. Venanzi, *J. Organomet. Chem.* **1983**, *259*, C6-C7.
22. M. F. Guest, I. J. Bush, H. J. J. van Dam, P. Sherwood, J. M. H. Thomas, J. H. van Lenthe, R. W. A. Havenith, J. Kendrick, *Mol. Phys.* **2005**, *103*, 719-747.
23. Z. Otwinowski, W. Minor, *Methods in Enzymology* **1997**, *276*, 307-326.
24. R. H. Blessing, *Acta Cryst.* **1995**, *A51*, 33-38.
25. P. T. Beurskens, G. Admiraal, G. Beurskens, W. P. Bosman, S. Garcia-Granda, R. O. Gould, J. M. M. Smits, C. Smykalla, *The DIRDIF99 program system, Technical Report of the Crystallography Laboratory*, **1999**, University of Nijmegen, The Netherlands.
26. G. M. Sheldrick, *SHELXL-97 Program for crystal structure refinement*, **1997**, University of Göttingen, Germany.
27. A. L. Spek, *J. Appl. Cryst.* **2003**, *36*, 7-13.

Chapter 6

NCN-, SCS-, and PCP-Pincer Palladium Halide Complexes as Lewis Acid Catalysts in Aldol Reactions with Methyl Isocyanoacetate: the Nature of the Palladium Catalyst Revisited

Abstract

The reactivity of various ECE-pincer palladium halide complexes as Lewis acid catalysts in the aldol reaction of benzaldehyde with methyl isocyanoacetate (MI) was studied. In contrast to previous assumptions that these complexes require activation, *i.e.* the formation of cationic complexes by removal of the halide ligand, these neutral palladium halide complexes can be used directly. Upon reaction of MI with 2,6-bis[(dimethylamino)methyl]phenyl-, and 2,6-bis[(phenylthio)methyl]phenyl palladium(II) (NCN- and SCS-pincer Pd, respectively) halide complexes an insertion reaction takes place to form Pd-imidoyl complexes. These imidoyl complexes are the actual catalysts in the aldol reaction. In contrast, 2,6-bis[(diphenylphosphino)methyl]phenyl palladium(II) (PCP-pincer Pd) halide complexes are stable towards this insertion reaction and react as such with MI by replacement of the halide ligand to form the corresponding cationic PCP-pincer-MI complexes. In this case, these cationic complexes are the catalysts in the aldol reaction. They do not have to be preformed but are instead formed spontaneously at the onset of the catalytic reaction.

6.1. Introduction

Cationic ECE-pincer palladium and platinum aquo complexes (E = N, S or P; see **B** in Scheme 1) have extensively been used as Lewis acid catalysts in the aldol reaction between benzaldehyde and methyl isocyanoacetate (MI). In general, these reactions afford a mixture of diastereomeric oxazolines (reaction 1).[1-5]

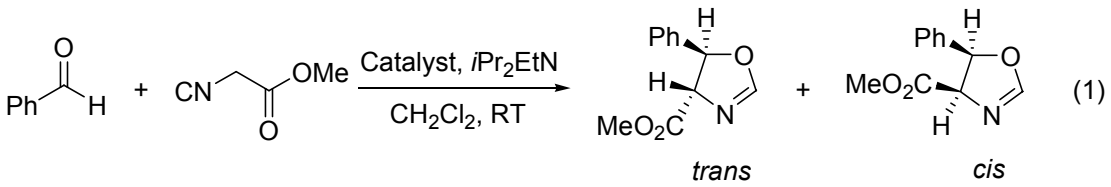

The cationic ECE-pincer metal complexes (**B**) are formed by halide abstraction from the corresponding metal halide complexes (**A**) using reagents like $AgBF_4$ or AgOTf (Scheme 1). The resulting cationic aquo complexes $[M(ECE)(H_2O)]X$ (**B**)[1-5] can be easily converted into related [M(ECE)L]X complexes by reaction of **B** with more nucleophilic ligands L, like cyanides or isocyanides (see **C**).

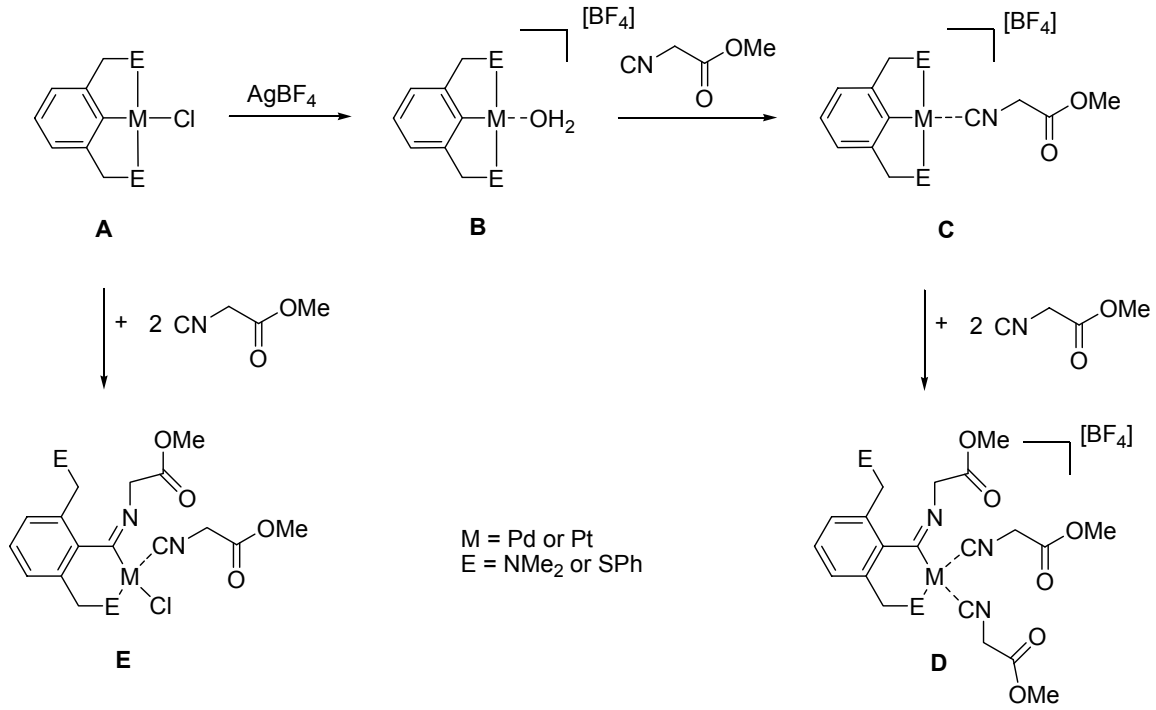

Scheme 1 Insertion products formed by reaction between NCN- or SCS-pincer metal complexes and MI.

In a mechanistic proposal of the reaction of benzaldehyde with MI, it is assumed that species **C** is the key intermediate in which the MI α-hydrogen atoms are activated and can be abstracted by a mild base (*e.g.* iPr_2EtN) present in the reaction mixture. So far, the corresponding ECE-metal halide complexes (**A**) have not been reported to show activity in this reaction. Presumably because these complexes lack a vacant site to bind a nucleophilic ligand, they have not been considered as possible catalysts.

During our study on the immobilization of NCN-pincer palladium and platinum complexes on silica surfaces,[6] several observations prompted us to reinvestigate some of this chemistry. Firstly, we faced the problem of removing insoluble silver(I) halide salts from the functionalized silica after reaction (activation) of immobilized NCN-pincer metal halide moieties with a silver reagent. This removal became a prerequisite because, surprisingly, separate experiments revealed that these silver salts are active catalysts themselves in aldol condensation reaction (1).[7] As a consequence, the selected activation method of the catalyst can severely affect the observed overall catalytic activity of the functionalized silica materials. Secondly, by performing catalytic 'blank' reactions, we observed that NCN-pincer Pd-halide complexes themselves are active catalysts in the aldol condensation reaction. It has been particularly this latter finding which led us to reinvestigate in more detail the reactivity of these neutral halide complexes towards various isocyanides.

Insertion of isocyanides into the Pd–C bond of cyclopalladated complexes has been extensively studied.[8] In fact, NCN-[9] and SCS-pincer[10] palladium chloride complexes have been reported to undergo an insertion reaction upon treatment with two equivalents of an alkyl isocyanide at room temperature, forming an insertion product as shown in Scheme 1 (**E**). To the best of our knowledge, these inserted complexes have not been tested as potential catalysts. Here, we report on a study of a series of *para*-substituted NCN-pincer complexes **1**, henceforth denoted as [PdX(NCN-Z)], as well as the non-substituted SCS- and PCP-pincer palladium complexes **2** and **3**, see Chart 1. It appeared that whereas **1** and **2** undergo a ready insertion reaction with MI, [PdCl(PCP)] (**3)** does not. Instead, the halide ligand is displaced by MI to form a cationic complex. The insertion products were previously characterized[11] and are now tested as catalysts in the reaction of benzaldehyde with MI. The influence of the presence of a *para*-substituent in **1** on the insertion reaction as well as the resulting catalytic activity of the insertion product has been studied.

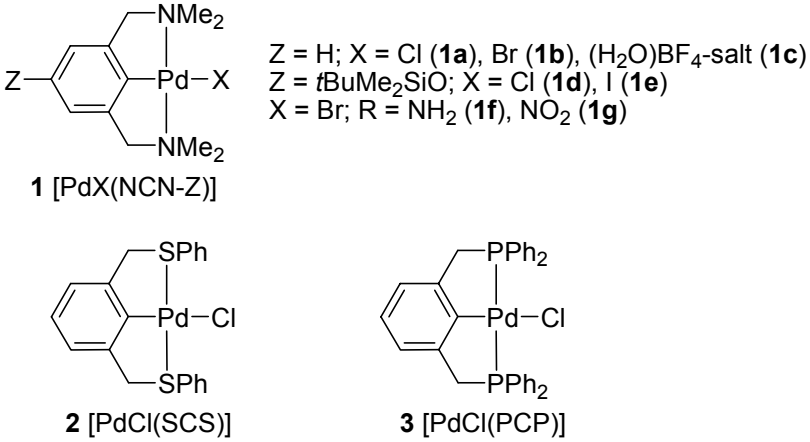

Chart 1 Pincer metal complexes used in this study.

6.2. Results

The catalytic activity of the insertion complexes was initially studied by means of *in situ* IR techniques. For NCN-pincer complex **1a**, the insertion complex was formed *in situ* by treating it

with two equivalents of MI, after which excess of benzaldehyde and MI were added in an equimolar ratio (Figure 1).

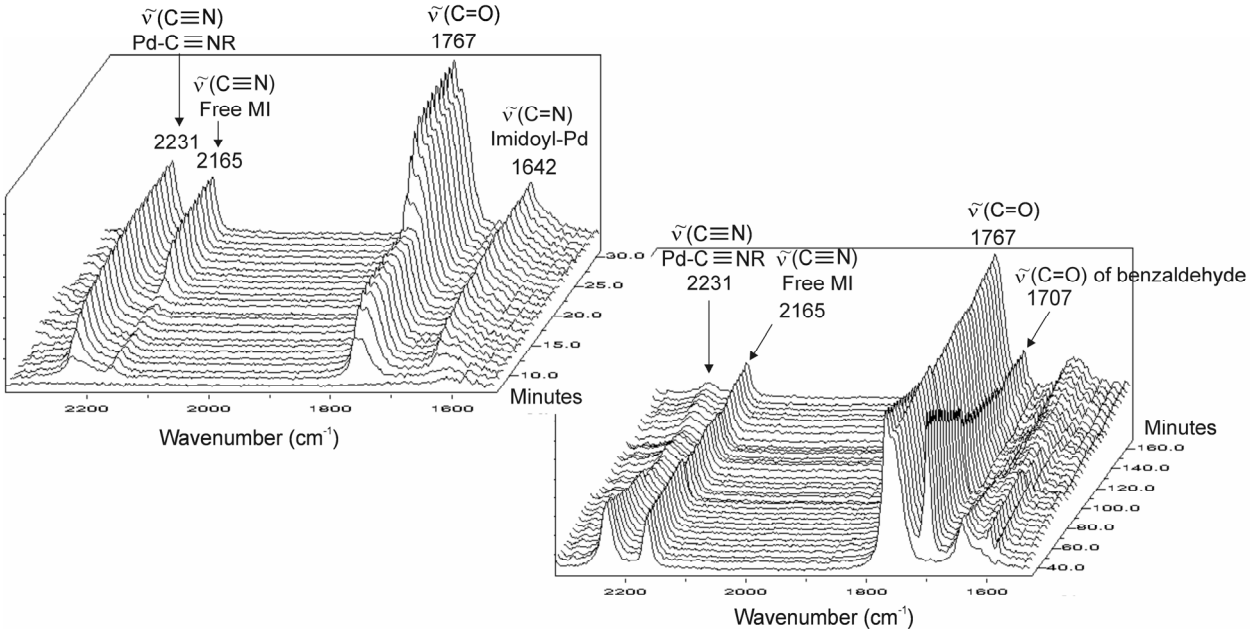

Figure 1 First spectrum: *In situ* IR study of the portionwise (0.5 equivalent portion) addition of in total 2.0 equivalents MI to a CH_2Cl_2 solution of 1.0 equivalent of [PdCl(NCN)] (**1a**); absorptions at 2231 (ν(C≡N)) and 1642 cm^{-1} (ν(C=N)) increase till all the complex has reacted (22 min.); addition of excess MI affects the absorption of free MI (2165 and 1767 cm^{-1}) only. Second spectrum: progression of aldol reaction after addition of benzaldehyde (without base); absorptions at 1707 cm^{-1} (ν(C=O) of benzaldehyde) decreases gradually; amount of **1a** is comparable to reagents (not catalytic) for sufficient intensities of the peaks.

It was found that the intensities of the peaks at 2231 and 1707 cm^{-1}, corresponding to coordinated MI and to benzaldehyde, respectively, were decreasing slowly (second spectrum, Figure 1). A peak at 1600 cm^{-1}, corresponding to oxazoline products, appeared simultaneously. It is interesting to note that the reaction takes place without the use of an external base. Most likely, the free *ortho*-(dimethylamino)methyl group of the insertion complex (**E**, scheme 1) acts as an internal base. Indeed, *in situ* IR studies of the reaction catalyzed by the insertion product **E** derived from [PdCl(SCS)] (**2**) and MI showed that subsequent aldol reaction of benzaldehyde with MI does not proceed in the absence of external base after the SCS-pincer insertion complex had been generated. Addition of an external base (iPr_2EtN) to the latter reaction mixture caused the immediate formation of aldol reaction product. In case of the cationic complex $[Pd(NCN)(H_2O)]BF_4$ (**1c**), *in situ* IR as well as NMR studies showed that upon addition of one equivalent MI, a 1:1 coordination product **C** (Scheme 1) is formed by displacing the water molecule. Upon addition of excess of MI, this complex undergoes an insertion reaction as well, presumably forming **D**.

These studies showed that insertion products **D** (obtained from cationic complexes, Scheme 1) and **E** (obtained from neutral complexes) are formed almost instantaneously after addition of MI to the various pincer palladium complexes, and that these catalyze aldol reaction (1). For catalytic

purposes, it is, therefore, not necessary to first synthesize either the pure insertion complexes or the cationic pincer complexes as pre-catalysts. Actually, the neutral pincer Pd-halide complexes can be used directly, which has the advantage that activation of the pincer catalysts with silver salts can be avoided. In fact, MI is not only the reactant in the aldol reaction but also the 'activating agent' for the generation of the insertion palladium compounds **E**, which are the actual aldol condensation catalysts.

The various NCN-, SCS-, and PCP-pincer palladium halide complexes (Chart 1) were then used as Lewis acid pre-catalysts for the aldol condensation reaction (Table 1). Kinetic traces of some of the catalytic reactions are shown in Figure 2 and Figure 3. The catalytic experiments were carried out using *i*Pr_2EtN (Hunig's base, 10 mol%) as a base, 1 mol% of ECE-pincer Pd-complex, and MI and benzaldehyde (1:1) in dichloromethane at room temperature. The reaction was monitored by means of GC analysis using pentadecane as the internal standard.

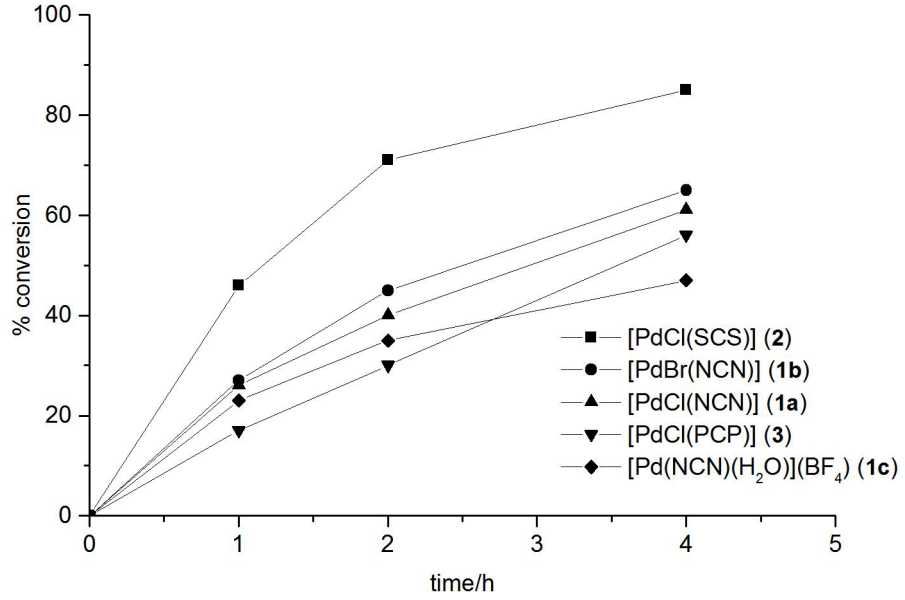

Figure 2 Kinetic profiles of the aldol reaction catalyzed by various ECE-pincer palladium complexes.

The insertion product derived from [PdCl(SCS)] (**2**) showed the highest activity in comparison to the catalysts derived from [PdCl(NCN)] **1a** and [PdCl(PCP)] (**3**), respectively. The reaction reached 85% completion within 4 h and showed a decreased *trans*-selectivity (Table 1, entry 2), while **1a** and **3** gave 61 and 56% conversion, respectively, in 4 h (entries 1 and 3). The [PdCl(PCP)] derived catalyst showed the highest *trans*-selectivity (82%). The blank reaction in the absence of a Pd-complex was likewise tested. After 24 h, no aldol product was detected in the absence of Hunig's base; with 10 mol% added base, 32% of product was formed in 24 h (entry 13).

The reaction of **1a** (entry 1) reached 61% conversion in 4 h as compared to 47% for the cationic aquo complex **1c** (entry 4). Surprisingly, reaction of **1a** without the use of an external base (entry 5) was as fast as the one in which an external base was used (entry 1), the only difference being that

58% *trans*-product is produced in the former case as compared to 74% in the latter. For cationic complex **1c**, the reaction without base was slower (entry 6). The lower activity of the cationic complexes as compared to the neutral halide complexes is probably due to the lower stability of the insertion complex. Changing the counter ion from BF_4 to triflate did not have any influence on the reactivity as well as selectivity (entry 7). When chloride in the neutral complex **1a** was replaced by bromide (**1b**), a slight increase in the rate was observed (entry 8), indicating a small influence of the halide ligand.

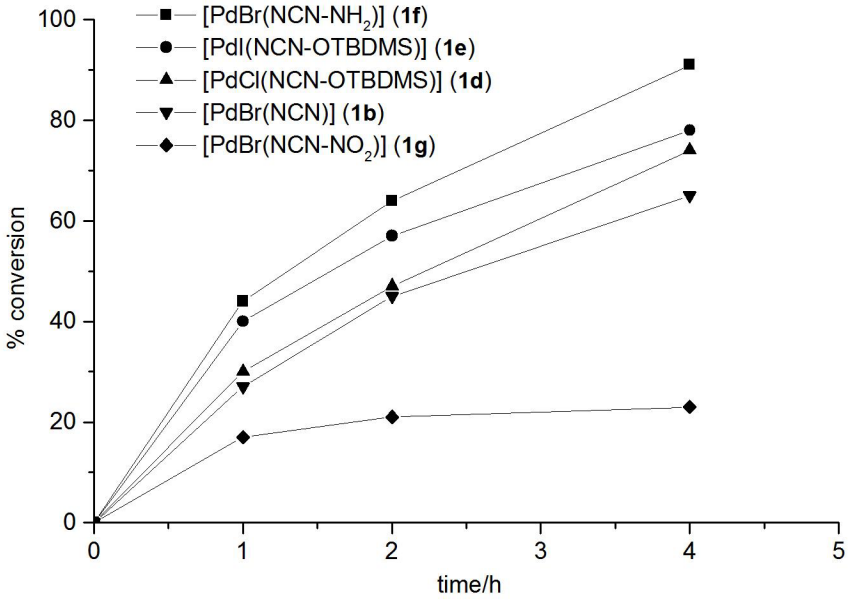

Figure 3 Kinetic profiles of the aldol reaction catalyzed by NCN-pincer palladium halide complexes.

Table 1: Aldol reaction with various catalysts.[a]

Entry	Catalyst	% Conversion (h)	% *Trans*
1	[PdCl(NCN)] (**1a**)	61 (4)	74
2	[PdCl(SCS)] (**2**)	85 (4)	59
3	[PdCl(PCP)] (**3**)	56 (4)	82
4	[Pd(NCN)(H_2O)](BF_4) (**1c**)	47 (4)	62
5	[PdCl(NCN)] (**1a**, without base)	60 (4)	58
6	[Pd(NCN)(H_2O)](BF_4) (**1c**, without base)	31 (4)	56
7	[Pd(NCN)(H_2O)](OTf)	46 (4)	64
8	[PdBr(NCN)] (**1b**)	65 (4)	71
9	[PdBr(NCN-NH_2)] (**1f**)	91 (4)	62
10	[PdBr(NCN-NO_2)] (**1g**)	23 (4), 48 (20)	81
11	[PdCl(NCN-OTBDMS)] (**1d**)	74 (4)	67
12	[PdI(NCN-OTBDMS)] (**1e**)	78 (4)	62
13	Blank (with 10% HB)	0 (6); 32 (24)	85
14	Blank (without base)	0 (24)	-

a. Catalyst (0.016 mmol, 1 mol%), MI (1.6 mmol), benzaldehyde (1.6 mmol), pentadecane (0.4 mmol, internal standard), and *i*Pr_2EtN (0.16 mmol, 10 mol%) in 5 mL distilled CH_2Cl_2 stirred at room temperature.

Variation of the *para*-substituent on the pincer aryl ring (complexes [PdX(NCN-Z)] **1d-1g**) was found to have a distinct influence on the rate of the reaction of MI with benzaldehyde with respect to

the parent compound [PdBr(NCN)]. The presence of electron donating amino or siloxy groups as Z-substituents increased the reaction rate, whereas an electron withdrawing nitro group decreased this rate (Table 1, entries 9, 10, 11 and 12 as compared to 8; Figure 3). From the Hammett plot using three *para*-substituted [PdBr(NCN-Z)] complexes (Z = NH_2, H and NO_2), a ρ value of –0.5 was obtained, which indicates a small effect of the *para*-substituent on the rate of the reaction (Figure 4).

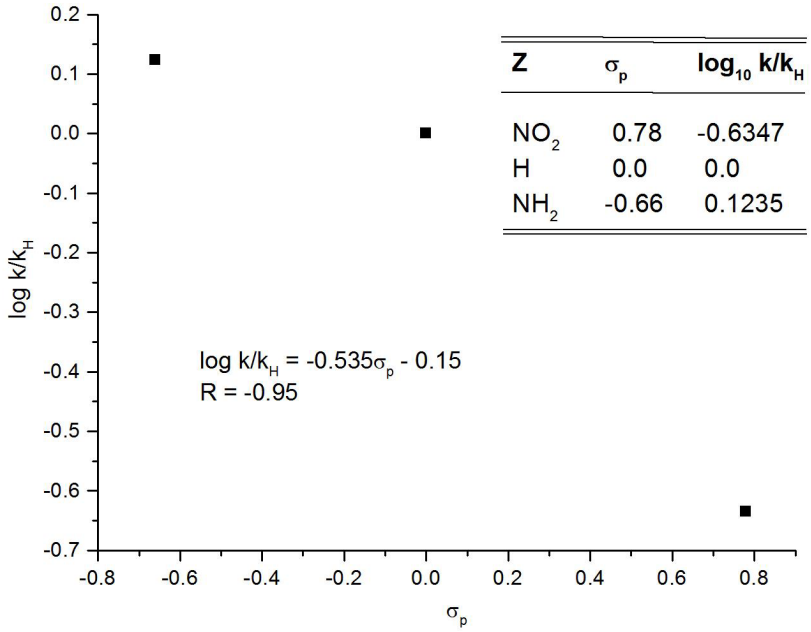

Figure 4 Hammett substituent analysis of Z in [PdBr(NCN-Z)] in aldol reaction 1. σ_p values are taken from reference 12.

6.3. Discussion

These results show that the insertion complexes **E** and **D** (see Scheme 1) formed from the neutral and cationic NCN- and SCS-pincer palladium complexes with MI are the actual catalysts for the aldol condensation (reaction 1). In the case of the neutral PCP-pincer complex **3**, displacement of the halide ligand and subsequent coordination of one MI ligand provides **C** as the active catalyst. Whereas for the PCP-pincer palladium catalysts a catalytic cycle involving **C** as the key intermediate has been proposed, the present results show that for the NCN- and SCS-pincer palladium catalysts a different cycle has to be considered. A proposed cycle is shown in Scheme 2. First, neutral [PdX(NCN)] (**1**), [PdX(SCS)] (**2**) or cationic [Pd(NCN)(H_2O)](BF_4) (**1c**) complexes undergo insertion of MI to form the active catalytic species **E** or **D**, respectively. In the inserted species, the vacant sites are occupied either by a halide or a further molecule of MI. The α-hydrogens of the coordinated MI molecule are activated and can be abstracted by either an external (Hunig's base) or an internal base (a free Me_2NCH_2 substituent) to form a Pd-coordinated α-isocyano enolate (C- (**F'**) or O- (**F''**) enolate). Nucleophilic attack of this carbanion on the aldehyde moiety of benzaldehyde then creates the new C–C bond (either *threo*- or *erythro*-product). Subsequently, the resulting alcoholate (**G**) collapses to form a Pd-coordinated oxazolinate (**H**). The oxazoline product (either *cis*

or *trans*) is liberated upon protonation, making the reaction catalytic in Pd as well as in base. At this stage, the catalyst can either enter in an equilibrium with a dimeric "resting state" or start another cycle upon coordination of a new isocyanide substrate (The X-ray structure of a compound that models the resting state has been published, see ref. 11). In case an external base is absent, the free amino arm of the NCN insertion complex can also function as an internal base.[13] Conversely, the free thioether arm is not basic enough to drive the aldol reaction catalyzed by the insertion product derived from **2**. As a result, this reaction requires the presence of an external base.

For the NCN complexes, the rate of reaction is influenced by the *para*-substituent of the ligand; electron donating groups increase the rate whereas electron withdrawing groups decrease it. Intuitively, one would expect that electron donating groups would diminish the Lewis acid character of Pd and would, therefore, decrease the reaction rate. On the other hand, the activating effect of electron donating groups, *i.e.* the increase of negative charge on the imidoyl carbon atom increases the charge on the *C*-enolate in intermediate **F'** (Scheme 2). In fact the electron donating effect of the *Z*-substituent in the pincer ligand is transmitted through the Pd^{2+} centre. The observation that the nature of the *Z*-substituent has an effect on the overall reaction rate, therefore, suggests that attack of the aldehyde on a coordinated isocyano enolate is overall rate determining step as was earlier proposed by Venanzi *et al.*[5] (for reactions catalyzed by [PtCl(PCP)] complexes).

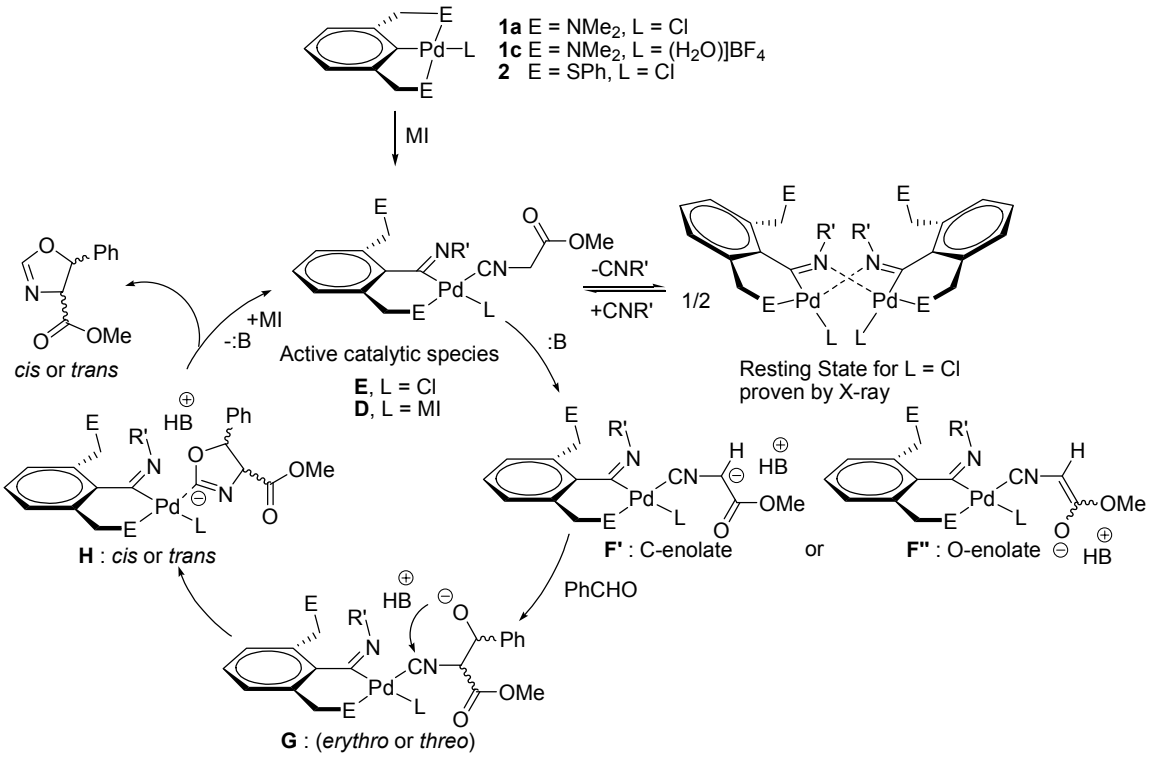

Scheme 2 Proposed mechanism of aldol reaction catalyzed by NCN- or SCS-pincer complexes.

Selectivity towards formation of the *trans*-product is presumably kinetically controlled.[2,14] In terms of product selectivity, it generally seems that the faster the reaction, the less selective it is to form the *trans*-product. Presumably, the *cis*-product is the kinetic product while the *trans*-product is the

thermodynamic product. This selectivity is determined at the stage when *C*-enolate in intermediate **F'** attacks the aldehyde to form C–C bond generating *erythro* or *threo* product. The fact that it is the rate determining step fits with the observations that selectivity leading to *cis* or *trans* product is determined at this stage. [PdCl(PCP)] (**3**) is an exception to this observation. In this case, the *trans*-product was formed in 82% at a reaction rate comparable to **1a** (56% in 4h). The reaction is driven by displacement of the halide ligand and subsequent coordination of an isocyanide without insertion in the Pd–C bond and is, therefore, mechanistically different from the NCN- and SCS-pincer catalyzed reactions.

Several groups have reported on the use of chiral NCN- and SCS-pincer complexes as catalysts for the aldol condensation (reaction 1) and low ee's were generally observed.[2,3,15] The notion that isocyanide insertion complexes form in these reactions and that these complexes are the actual catalysts therein may help to explain these observations. Upon formation of an insertion complex the C_2 symmetry of the initial pincer complex is lost and only one of the pincer donor arms remains coordinated to the central metal, resulting in an overall C_1 symmetry. The fact that the highest ee's are observed with PCP-pincer complexes corroborate this explanation, as in this case no insertion reaction takes place and the C_2 symmetry of the catalyst is not violated.[4,5]

6.4. Conclusion

In summary, we have shown that NCN- and SCS-pincer palladium complexes can be activated by isocyanides to form 6-membered cyclometalated complexes. These complexes can be employed as catalysts for aldol reactions, while the same isocyanides in the subsequent aldol condensation reaction are converted as one of the two substrates. This reaction profile is found for both the neutral halide and the cationic aquo complexes. Therefore, the use of activating agents like $AgBF_4$ or AgOTF to create the respective cationic NCN- or SCS-pincer palladium complexes can be avoided and the neutral pincer palladium halide complexes can be used directly for catalytic purposes. The stronger donor ability of the phosphorous donors (as compared to both the NMe_2 and SPh donors and to that of the halide anion and coordinated MI) in the corresponding PCP-pincer palladium complexes prevents the insertion of isocyanides and ensures the tridentate nature of the pincer ligand throughout the catalytic reaction. In fact, in this case the excess of isocyanide is able to displace the halide ligand resulting in the formation of the actual catalyst. This allows the direct use of PCP-pincer metal halide complexes in this kind of catalysis.

6.5. Experimental Section

CH_2Cl_2 was dried over calcium hydride and distilled prior to use. Benzaldehyde and Hunig's base were distilled prior to use. Methyl isocyanoacetate was used without further purification. NCN-,[16] SCS-[17] and PCP-pincer[18] complexes were prepared as described previously. *In situ* IR spectra were recorded using a

Mettler Toledo ReactIR™ 1000 spectrometer with a SiComp™ probe. Gas chromatographic analyses were performed with a Perkin Elmer Autosystem XL GC using a 30 m, PE-17 capillary column with an FID detector.

Catalytic experiments were performed using a standard protocol. In a typical experiment, 1 mol% (0.016 mmol) of pincer metal complex was dissolved in 5 mL distilled CH_2Cl_2. MI (1.6 mmol), benzaldehyde (1.6 mmol), pentadecane (0.4 mmol, internal standard), and *i*Pr_2EtN (Hunig's base, 0.16 mmol, 10 mol%) were added and the reaction mixture was stirred at room temperature. The reaction was monitored by means of GC analysis.

6.6. References

1. G. Rodriguez, M. Lutz, A. L. Spek, G. van Koten, *Chem. Eur. J.* **2002**, *8*, 45-57; G. Guillena, G. Rodriguez, G. van Koten, *Tetrahedron Lett.* **2002**, *43*, 3895-3898; M. D. Meijer, N. Ronde, D. Vogt, G. P. M. van Klink, G. van Koten, *Organometallics* **2001**, *20*, 3993-4000; M. Albrecht, B. M. Kocks, A. L. Spek, G. van Koten, *J. Organomet. Chem.* **2001**, *624*, 271-286; C. Schlenk, A. W. Kleij, H. Frey, G. van Koten, *Angew. Chem., Int. Ed.* **2000**, *39*, 3445-3447.
2. Y. Motoyama, H. Kawakami, K. Shimozono, K. Aoki, H. Nishiyama, *Organometallics* **2002**, *21*, 3408-3416.
3. J. S. Fossey, C. J. Richards, *Organometallics* **2002**, *21*, 5259-5264; M. A. Stark, C. J. Richards, *Tetrahedron Lett.* **1997**, *38*, 5881-5884.
4. J. M. Longmire, X. Zhang, M. Shang, *Organometallics* **1998**, *17*, 4374-4379.
5. F. Gorla, A. Togni, L. M. Venanzi, A. Albinati, F. Lianza, *Organometallics* **1994**, *13*, 1607-1616.
6. N. C. Mehendale, C. Bezemer, C. A. van Walree, R. J. M. Klein Gebbink, G. van Koten, *J. Mol. Catal. A* **2006**, *257*, 167-175.
7. N. C. Mehendale, M. Lutz, A. L. Spek, R. J. M. Klein Gebbink, G. van Koten, *manuscript in prep. (Ch. 8 of this thesis).*
8. J. Vincente, I. Saura-Llamas, C. Grünwald, C. Alcaraz, P. G. Jones, D. Bautista, *Organometallics* **2002**, *21*, 3587-3595; J. Dupont, M. Pfeffer, J. C. Daran, Y. Jeannin, *Organometallics* **1987**, *6*, 899-901; A. D. Ryabov, *Synthesis* **1985**, 233-252; R. D. O'Sullivan, A. W. Parkins, *J. Chem. Soc., Chem. Commun.* **1984**, 1165-1166; Y. Yamamoto, H. Yamazaki, *Inorg. Chim. Acta* **1980**, *41*, 229-232; Y. Yamamoto, H. Yamazaki, *Synthesis* **1976**, 750-751; J. F. van Baar, J. M. Klerks, O. P., D. J. Stufkens, K. Vrieze, *J. Organomet. Chem.* **1976**, *112*, 95-103; Y. Yamamoto, H. Yamazaki, *Coord. Chem. Rev.* **1972**, *8*, 225-239.
9. A. Zografidis, K. Polborn, W. Beck, B. A. Markies, G. van Koten, *Z. Naturforsch., B* **1994**, *49*, 1494-1498.
10. J. Dupont, M. Pfeffer, *J. Chem. Soc., Dalton Trans.* **1990**, 3193-3198.
11. N. C. Mehendale, R. W. A. Havenith, M. Lutz, A. L. Spek, R. J. M. Klein Gebbink, G. van Koten, *manuscript in prep. (Ch. 5 of this thesis).*
12. C. Hansch, A. Leo, R. W. Taft, *Chem. Rev.* **1991**, *91*, 165-195.
13. Y. Ito, M. Sawamura, E. Shirakawa, K. Hayashizaki, T. Hayashi, *Tetrahedron Lett.* **1988**, *29*, 235-238; Y. Ito, M. Sawamura, E. Shirakawa, K. Hayashizaki, T. Hayashi, *Tetrahedron* **1988**, *44*, 5253-5262; Y. Ito, M. Sawamura, T. Hayashi, *J. Am. Chem. Soc.* **1986**, *108*, 6405-6406.
14. Y. Motoyama, K. Shimozono, K. Aoki, H. Nishiyama, *Organometallics* **2002**, *21*, 1684-1696; A. Togni, S. D. Pastor, *J. Org. Chem.* **1990**, *55*, 1649-1664.
15. J. S. Fossey, C. J. Richards, *Organometallics* **2004**, *23*, 367-373; R. Gimenez, T. M. Swager, *J. Mol. Catal., A* **2001**, *166*, 265-273; R. Nesper, P. Pregosin, K. Püntener, M. Wörle, A. Albinati, *J. Organomet. Chem.* **1996**, *507*, 85-101.
16. M. Q. Slagt, R. J. M. Klein Gebbink, M. Lutz, A. L. Spek, G. van Koten, *J. Chem. Soc., Dalton Trans.* **2002**, 2591-2592; P. Steenwinkel, R. A. Gossage, T. Maunula, D. M. Grove, G. van Koten, *Chem. Eur. J.* **1998**, *4*, 763-768; J. Terheijden, G. van Koten, F. Muller, D. M. Grove, K. Vrieze, E. Nielsen, C. H. Stam, *J. Organomet. Chem.* **1986**, *315*, 401-417; D. M. Grove, G. van Koten, J. N. Louwen, J. G. Noltes, A. L. Spek, H. J. C. Ubbels, *J. Am. Chem. Soc.* **1982**, *104*, 6609-6616.
17. N. Lucena, J. Casabo, L. Escriche, G. Sanchez-Castello, F. Teixidor, R. Kivekäs, R. Sillanpää, *Polyhedron* **1996**, *15*, 3009-3018.
18. H. Rimml, L. M. Venanzi, *J. Organomet. Chem.* **1983**, *259*, C6-C7.

Chapter 7

PCS-Pincer Palladium Complex: Insertion of Methyl Isocyanoacetate and Catalytic Aldol Reactivity

Abstract

The unsymmetric PC(H)S-pincer-arene ligand 1-[(diphenylphosphino)methyl]-3-[(phenylthio)methyl]benzene was synthesized. Reaction of PC(H)S-pincer arene with $[Pd(MeCN)_4](BF_4)_2$ selectively formed the bis(*ortho*)palladated pincer-complex $[PdCl(C_6H_3(CH_2PPh_2)$-2-(CH_2SPh)-6)] ([PdCl(PCS)]). This complex undergoes a rapid insertion reaction with methyl isocyanoacetate (MI) leading to an imidoyl palladium compound. NMR spectra show that the P-donor is bonded to Pd, whereas the S-donor is non-coordinated. [PdCl(PCS)] catalyzes the aldol reaction of MI with benzaldehyde at a faster rate than [PdCl(SCS)] and [PdCl(PCP)], respectively, the later one being the slowest catalyst. For [PdCl(PCS)] and [PdCl(SCS)], the respective insertion complexes are the actual catalysts, whereas for [PdCl(PCP)], it is this compound itself.

7.1. Introduction

Monoanionic ECE-pincer ligands ($[C_6H_3(CH_2E)_2$-2,6$]^-$, where E = NR_2, PR_2, AsR_2, OR, or SR) are a versatile class of monoanionic, potentially terdentate ligands due to their unique properties to bind the metal through a strong M–C σ-bond and forming two metalacycles having this bond in common and comprising M–E coordination.[1] The properties of the metal center can be controlled by both the nature of the E-donor and the various substituents R on the E-group, as well as by the nature of the *para*-substituent on the aryl ring of the pincer ligand itself.[2] A variety of ECE-pincer metal complexes display interesting catalytic activities in various synthetically important organic reactions including C–C and C–X bond formation reactions.[3] The fact that the ECE-pincer metal complexes can be *para*-functionalized allowed to explore their use as immobilized catalysts on various soluble and insoluble supports which include silica,[4] polymers,[5] functionalized dendrimers,[6] and other materials.[7] The primary motivation for this research is the quest for sustainable catalysts in organic synthesis to meet new challenges of reactivity, selectivity, feedstock and energy use.

Insertion of an isocyanide into the M–C bond of metalacyclic compounds has been extensively studied[8] and includes insertion reactions in the Pd–C bond of NCN-[9,10] and SCS-pincer[11] palladium d^8 complexes. Interestingly, PCP-pincer palladium(II) halide complexes appear to be stable towards insertion reactions with isocyanides.[10] This behavior is explained by the stronger Pd–P coordination of both *ortho*-(diphenylphosphino)methyl substituents to the palladium(II) centre as compared to the Pd–N and Pd–S bonding in the corresponding NCN- and SCS-pincer palladium(II) complexes. Recently we showed that a likely reaction mechanism for the insertion reaction involves coordination of an isocyanide *cis* to the aryl C–Pd bond of the respective ECE-pincer palladium (E = NMe_2 or SPh) complexes. This can only occur through prior decoordination of one or both of the *ortho* ligands. This result prompted us to study the synthesis as well as the reactivity of the corresponding PCS-pincer palladium chloride complex (**6** in Scheme 1), *i.e.* a complex having one *ortho*-(diphenylphosphino)methyl and one *ortho*-(phenylsulfide)methyl substituent. The present novel PC(H)S-pincer arene ligand has a precedent in reports concerning PC(H)N-pincer arene ligands.[12]

7.2. Results

7.2.1. Synthesis of the PCS-pincer palladium complex

The unsymmetric PC(H)S-pincer arene ligand can be synthesized *via* two routes. Starting from easily accessible 1,3-*bis*(bromomethyl)benzene (**1**), either the S- or the P-functional group can be introduced first. We have attempted both routes, but found that prior introduction of the diphenylphosphino group was the most straightforward approach.

The dibromide **1** was treated with one equivalent of the BH_3-protected lithium diphenylphosphide salt. This salt was added slowly to **1** in order to get a maximum yield of the BH_3-protected mono-

phosphine **2** (Scheme 1). The reaction mixture contained some 1,3-*bis*-phosphine (PC(H)P-pincer) along with unreacted **1**. According to the ^{1}H NMR analysis of the reaction mixture, the molar ratio of PC(H)P-pincer : **2** : **1** amounted to 1:2.9:1.7 (18, 52, and 30%, respectively). Actually, the $^{31}P\{^{1}H\}$ NMR spectrum (in $CDCl_3$) of the reaction mixture showed one broad peak at 18.4 ppm, indicating the presence of a mixture of two BH_3-protected phosphines. At this point, we did not attempt to separate the three compounds. In fact this mixture was further treated with excess thiophenol and K_2CO_3 to make sure that all remaining benzylic bromides were converted to thioethers.

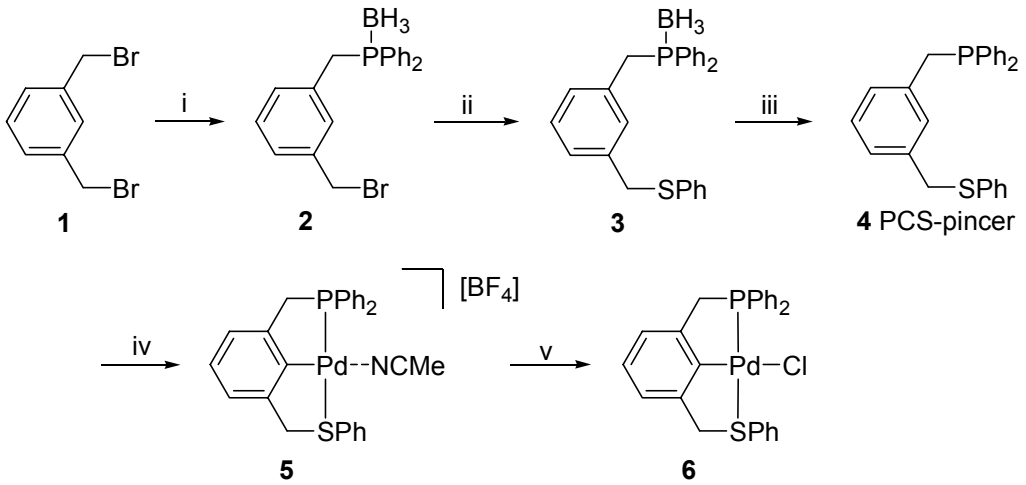

Scheme 1 i. $(BH_3)LiPPh_2$, dry THF; ii. PhSH, K_2CO_3, 18-crown-6, THF, pure after column chromatography; iii. HBF_4, degassed Et_2O; iv. $[Pd(MeCN)_4](BF_4)_2$, MeCN; v. excess NaCl, CH_2Cl_2/H_2O.

In this way, a mixture of again three compounds was obtained, namely, PC(H)P-, PC(H)S-, and SC(H)S-pincer (each P donor atom is protected with BH_3) in the same molar ratio (1:2.9:1.7, respectively). Obviously, the thiophenol had reacted only with benzylic bromides, even after having used an excess. Column chromatography of the mixture afforded pure **3** in 37% yield with respect to **1**. In the next step, the BH_3 protection was removed using $HBF_4{\cdot}OEt_2$, followed by a basic work-up, to yield the PC(H)S-pincer arene ligand **4**. This reaction was carried out under N_2 atmosphere using degassed solvents. $^{31}P\{^{1}H\}$ NMR analysis of a solution of the BH_3-protected PC(H)S-pincer arene ligand **3** in $CDCl_3$ showed a broad peak at 19.3 ppm. ^{1}H NMR analysis of **3** in $CDCl_3$ showed a doublet at 3.6 ppm (PCH_2, $^{2}J_{H,P}$ = 12.0 Hz) and a singlet at 3.98 ppm (SCH_2). ^{13}C NMR analysis in $CDCl_3$ showed a doublet at 33.95 ppm (PCH_2, $^{1}J_{C,P}$ = 31.8 Hz) and a singlet at 38.64 (SCH_2). PC(H)S-pincer arene **4** showed a singlet at 3.39 ppm (PCH_2) in ^{1}H NMR, while $^{31}P\{^{1}H\}$ NMR of the same sample showed a singlet at –7.23 ppm (PPh_2). ^{13}C NMR of **4** revealed a doublet at 35.99 ppm (PCH_2, $^{1}J_{C,P}$ = 15.9 Hz). (For comparison of NMR data of related pincer arene ligands, see Table 1).

Palladation of **4** was carried out by using carefully purified $[Pd(MeCN)_4]BF_4$ as a source of palladium. A commonly used route for the preparation of $[Pd(MeCN)_4]BF_4$ involves the reaction of $[PdCl_2(MeCN)_2]$ with two equivalents of $AgBF_4$. During this reaction, the formed AgCl precipitates

from the solution. However, as AgCl is slightly soluble in acetonitrile, it is very important to carefully remove all AgCl from $[Pd(MeCN)_4]BF_4$ solution. This was achieved by dissolution and subsequent filtration of the solution of $[Pd(MeCN)_4]BF_4$ in acetonitrile, and repeating this process three times. It appeared that the presence of even small amounts of AgCl substantially slowed down the palladation of **4**. The palladation of **4** with pure $[Pd(MeCN)_4]BF_4$ was carried out in degassed acetonitrile. After mixing of the reactants, an immediate color change to orange was observed. $^{31}P\{^1H\}$ NMR of the reaction mixture indicated that the palladation reaction was completed within one hour directly affording the ionic complex [Pd(PCS)(MeCN)](BF_4) (**5**). This complex was isolated in almost 90% yield. Treatment of **5** with NaCl yielded the neutral complex [PdCl(PCS)] (**6**) in quantitative yield.

Table 1 NMR data of selected ECE-pincer arene ligands and corresponding palladium complexes.[a]

Compound	^{31}P	^1H (PCH_2)	^1H (SCH_2)	^{13}C (PCH_2)	^{13}C (SCH_2)
PC(H)P-pincer arene[13]	–10.1	3.88 (s)	-	36.5 (d, $^1J_{C,P}$ 15.9)	-
SC(H)S-pincer arene [14]	-	-	4.05	-	39.0
BH_3-PC(H)S-pincer arene (**3**)	19.4 (bs)	3.61 (d, $^2J_{H,P}$ 12)	3.98 (s)	34.0 (d, $^1J_{C,P}$ 31.8)	38.6 (s)
PC(H)S-pincer arene (**4**)	–7.2	3.39 (s)	4.02 (s)	36.0 (d, $^1J_{C,P}$ 15.9)	39.0 (s)
[PdCl(PCP)][13]	33.4	3.98 (vt, $J_{H,P}$ 4.7)	-	42.0 (vt, $J_{C,P}$ 15)	-
[PdCl(SCS)][15]	-	-	4.55 (bs)	-	51.7
[Pd(PCS)(MeCN)](BF_4) (**5**)	49.7	4.15 (d, $^2J_{H,P}$ 12.3)	4.65 (s)	42.4 (d, $^1J_{C,P}$ 36.6)	48.7 (s)
[PdCl(PCS)] (**6**)	45.0	3.99 (d, $^2J_{H,P}$ 12.2)	4.48 (s)	43.9 (d, $^1J_{C,P}$ 36.1)	49.0 (s)

a. P = PPh_2, S = SPh; pincer arene = $C_6H_4(CH_2E)_2$-1,3 (E = P or S). All values are in *ppm*, *J* in *Hz*; s = singlet, d = doublet, bs = broad singlet, vt = virtual triplet.

^1H NMR analysis of a solution of **5** in CD_3CN showed a doublet at 4.15 ppm ($^2J_{H,P}$ = 12.3 Hz) for PCH_2 and a singlet at 4.65 ppm for SCH_2. $^{31}P\{^1H\}$ NMR spectra of **5** showed a singlet at 49.7 ppm. ^{13}C NMR spectra of **5** showed a doublet at 42.4 ppm (PCH_2, $^1J_{C,P}$ = 36.6 Hz) whereas, a singlet at 48.7 ppm was observed for the SCH_2 carbon. The neutral complex **6** showed a similar trend in its ^1H and ^{13}C NMR spectra. Its $^{31}P\{^1H\}$ NMR spectrum showed one singlet at 45.0 ppm.

7.2.2. Insertion of isocyanide

[PdCl(PCS)] complex **6** readily undergoes insertion of methyl isocyanoacetate (MI) into the Pd–C bond. Reaction of **6** with two equivalents of MI in dichloromethane afforded product **7** as shown in Scheme 2. The 2:1 MI/**6** stoichiometry in **7** was established by elemental analysis and NMR spectroscopic data. In the ^1H NMR spectrum of **7** in CD_2Cl_2, two patterns were observed; one for an inserted and one for the coordinated MI. The methylene hydrogen signal at 3.52 ppm was assigned to the non-coordinated CH_2SPh group. The doublet signal of the methylene hydrogen at 4.25 ppm of the CH_2PPh_2 group is characteristic for a coordinated CH_2PPh_2 grouping. This conclusion was supported by $^{31}P\{^1H\}$ NMR which revealed a ^{31}P resonance at 47.8 ppm (*vs.* –7.2 ppm for the

PC(H)S-pincer arene). Further evidence for the formation of an insertion complex came from IR spectroscopy, in which absorptions for a *C*-coordinated C≡N $\tilde{\nu}$ (C≡N) at 2230 cm^{-1} (*vs.* 2166 cm^{-1} for free MI) and for the imidoyl moiety $\tilde{\nu}$ (C=N) at 1627 cm^{-1} were observed.

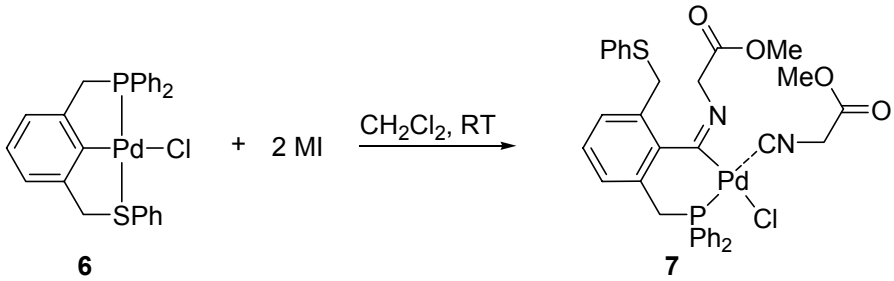

6 **7**

Scheme 2 Insertion of MI into the Pd–C bond of the neutral [PdCl(PCS)] complex **6**.

7.2.3. Catalysis

Complex **6** was tested as a Lewis acid pre-catalyst for aldol condensation reaction 1. The catalytic experiments were carried out using $^{i}Pr_2EtN$ (Hunig's base, 10 mol%) as a base, catalyst (1 mol%), MI and benzaldehyde (1:1) in dichloromethane at room temperature. The reaction was monitored by means of GC analysis using pentadecane as internal standard. In Table 2, the results of the reaction catalyzed by **6**, [PdCl(SCS)] (**8**) and [PdCl(PCP)] (**9**) respectively, have been included. The TOF's for the various reactions show that the [PdCl(PCS)] catalyzed reaction is by far the fastest with a TOF of 75 h^{-1}. The *trans*/*cis* ratio of the product was comparable with that of the reaction catalyzed by [PdCl(SCS)] (**8**).

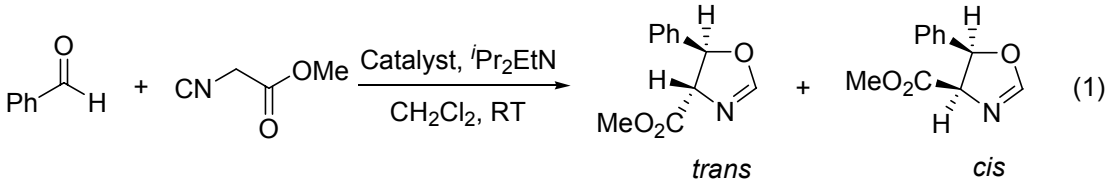

Table 2 Comparison between pincer complexes for the activity in the aldol reaction.

Catalyst	TOF[a]	% trans
[PdCl(PCS)] (**6**)	75	57
[PdCl(SCS)] (**8**)	46	59
[PdCl(PCP)] (**9**)	17	82

a. mol of product per mol of catalyst in the first hour.

7.3. Discussion

According to the present procedure, the PC(H)S-pincer arene ligand can be obtained pure in a reasonable yield. The [PdCl(PCS)] complex (**6**) was obtained *via* regioselective C–H activation reaction with $[Pd(MeCN)_4](BF_4)_2$. In principle, both complexes **5** and **6** have a molecular structure comprising two chiral elements, *i.e.* a coordinative Pd–S interaction renders the S-center stereogenic and the five membered chelate rings (Pd–C_{ipso}–C_{ortho}–C–E) exist in two conformers δ and λ.

Moreover, the Pd-coordination plane contains four different ligands, which removes the C_2 axis commonly present in homo-donor ECE-pincer metal complexes. The interconversion process of the two chelate ring conformers has a low barrier of activation, which does not affect the stereogenity at the S-center. In fact, this should render the benzylic protons diastereotopic, *i.e.* one AB-pattern for SCH_2 (two δ's, $J_{H,H}$) and another for PCH_2 (two δ's, $J_{H,H}$) should be observed (of which the later also shows a $J_{H,P}$ coupling). Instead, only one singlet is observed for SCH_2- and a doublet for PCH_2-grouping. This could be due to the fact that also the PCH_2 protons become homotopic (same δ), not because of reversible Pd–P coordination but because of reversible Pd–S coordination and concomitant conversion of configuration at the S-donor atom which creates an apparent molecular symmetry plane (the palladium coordination plane) causing the PCH_2 as well as the SCH_2 hydrogens to become homotopic. Further studies are required to study the influence of the substituents R on both the S- and P-donor atoms on the Pd–S coordination.

The successful and rapid insertion of MI in the case of [PdCl(PCS)] is in concert with the assumption that an initial step in the insertion process involves prior decoordination of one of the *ortho*-E ligands as shown in Scheme 2. From this conclusion, it can be anticipated that also in the aldol reaction, prior MI insertion in the Pd–C bond occurs by decoordination of the S-ligand, which eventually leads to the formation of complex **7** *in situ*. The η^1-coordinated second isocyanide then undergoes the aldol reaction. Both PCS- and SCS-pincer complexes undergo isocyanide insertion and the resulting imidoyl palladium complexes each have a higher TOF than the PCP-pincer palladium complex, which does not undergo this insertion reaction.

7.4. Experimental Section

7.4.1. General Comments

All synthetic procedures were conducted under a dry nitrogen atmosphere using standard Schlenk techniques. Solvents were dried over appropriate materials and distilled and degassed using freeze-thaw cycles prior to use. 1,3-Bis(bromomethyl)benzene, diphenylphosphine and thiophenol were obtained from commercial sources and were used without further purification. *N.B. Careful handling of 1,3-bis(bromomethyl)benzene (**1**) and materials containing this substance is required.* Complexes 8[15] and 9[13] were synthesized according to the literature procedure. ^{1}H (200.1 and 300.1 MHz), ^{13}C{^{1}H} (50.3 and 75.5 MHz), and ^{31}P{^{1}H} NMR (81.02 MHz) NMR spectra were recorded at room temperature on either Varian Mercury 200, Varian Inova 300 or Bruker 300 spectrometers. FT-IR spectra were recorded using a Mattson Instruments Galaxy Series FTIR 5000 spectrometer. Gas chromatographic analyses were performed with a Perkin Elmer Autosystem XL GC using a 30 m, PE-17 capillary column with an FID detector. Microanalyses were obtained from H. Kolbe Mikroanalytisches Laboratorium, Mülheim an der Ruhr, Germany.

7.4.2. Procedures

*7.4.2.1. Synthesis of BH_3-protected 1-[(diphenylphosphino)methyl]-3-[bromomethyl]benzene (**2**)*

Diphenylphosphine (1.3 mL, 7.5 mmol) was dissolved in 10 mL of dry degassed Et_2O. To this solution, $BH_3{\cdot}(SMe_2)$ (1.2 mL, 12.5 mmol) was added and the reaction mixture was stirred for 16 h. The resulting solution was concentrated to dryness and dry THF (25 mL) was added. The solution was cooled to –78 °C and ^{n}BuLi (4.7 mL, 7.5 mmol, 1.6 M solution in hexane) was added slowly. After the addition was complete, the reaction mixture was allowed to warm to room temperature. The solution of the *in situ* prepared BH_3-protected diphenylphosphidolithium salt was transferred to a dropping funnel (under N_2 atmosphere) and was added drop wise to the solution of 1,3-bis(bromomethyl)benzene (**1**, 2 g, 7.5 mmol) in dry THF (125 mL). The resulting solution was stirred for 16 h. Again the reaction solution was concentrated to dryness and the residue was dissolved in a biphasic mixture of Et_2O and water. The organic layers were separated, washed with water, combined and dried over $MgSO_4$. Filtration and concentration of the filtrate *in vacuo* yielded a white solid of which ^{1}H NMR analysis (in $CDCl_3$) showed that a mixture of PC(H)P-pincer, **2**, and **1** in 1:2.9:1.7 (18, 52 and 30%) molar ratio, respectively. This mixture was used without further purification.

*7.4.2.2. Synthesis of BH_3-protected 1-[(diphenylphosphino)methyl]-3-[(phenylthio)methyl]benzene (PC(H)S-pincer arene **3**)*

The mixture obtained in the previous step was dissolved in dry THF (50 mL), along with K_2CO_3 (2 g, 15 mmol) and 18-Crown-6 (0.4 g, 1.5 mmol). To this mixture, thiophenol (2 mL, 20 mmol) was added and subsequently stirred at ambient temperature for 20 h. ^{1}H NMR analysis confirmed complete conversion of all benzylic bromide groupings. The solution was filtered and the filtrate concentrated to dryness affording a colorless solid. This was dissolved in a minimal amount of Et_2O which was then subjected to column chromatography using silica and 1:9 v/v Et_2O/hexane mixture as eluent. The three compounds were eluted in the sequence SC(H)S-pincer, **3**, and finally (BH_3-protected) PC(H)P-pincer in a molar ratio of 1.7:2.9:1 (30, 52 and 18%), respectively. The overall yield for **3** from **1** in two steps was 37%.

^{1}H NMR (300.1 MHz, $CDCl_3$, 25 °C): δ = 1.2 (bs, 3H, BH_3); 3.61 (d, $^2J_{H,P}$ = 12.0 Hz, 2H, ArCH_2P); 3.98 (s, 2H, ArCH_2S); 6.8-7.7 (m, 19H, ArH). ^{31}P NMR (81.02 MHz, $CDCl_3$, 25 °C): δ = 19.35 (bs). ^{13}C NMR (75.47 MHz, $CDCl_3$, 25 °C): δ = 33.95 (d, $^1J_{C,P}$ = 31.8 Hz, ArCH$_2$PBH$_3$); 38.64 (s, ArCH$_2$S); 126.23, 127.42 (d, $J_{C,P}$ = 3 Hz), 128.16 (d, $J_{C,P}$ = 2.4 Hz), 128.64, 128.77, 128.84, 129.16 (d, $J_{C,P}$ = 4.9 Hz), 129.57, 130.87 (d, $J_{C,P}$ = 4.3 Hz), 131.32 (d, $J_{C,P}$ = 2.5 Hz), 132.21 (d, $J_{C,P}$ = 4.3 Hz), 132.64 (d, $J_{C,P}$ = 9 Hz), 136.39, 137.25 (d, $J_{C,P}$ = 2.5 Hz) (ArC). Anal. Calcd. for $C_{26}H_{26}BPS$ (412.33): C, 75.73; H, 6.36; P, 7.51; S, 7.78. Found: C, 75.66; H, 6.35; P, 7.64; S, 7.73.

*7.4.2.3. Synthesis of 1-[(diphenylphosphino)methyl]-3-[(phenylthio)methyl]benzene (PC(H)S-pincer arene **4**)*

Compound **3** (1.15g, 2.78 mmol) was dissolved in dry degassed CH_2Cl_2 (10 mL). To this solution, HBF_4 (2 mL of a 54% solution in Et_2O, 14 mmol) was added slowly. The resulting solution was stirred for 20 h at room temperature. A saturated aqueous $NaHCO_3$ solution was added drop wise until the gas evolution

stopped. The resulting mixture was stirred at room temperature for 1 h. The organic layer was separated and dried using $MgSO_4$. Upon removal of all volatiles *in vacuo*, the colorless solid of PC(H)S-pincer arene **4** was obtained in 74% yield.

^{1}H NMR (300.1 MHz, $CDCl_3$, 25 °C): δ = 3.39 (s, 2H, ArC*H*$_2$P); 4.02 (s, 2H, ArC*H*$_2$S); 6.8-7.8 (m, 19H, Ar*H*). ^{31}P NMR (81.02 MHz, $CDCl_3$, 25 °C): δ = –7.23. ^{13}C NMR (75.47 MHz, $CDCl_3$, 25 °C): δ = 35.99 (d, $^1J_{C,P}$ = 15.9 Hz, Ar*C*H$_2$P); 39.0 (s, Ar*C*H$_2$S); 126.23, 127.42 (d, $J_{C,P}$ = 3 Hz), 128.16 (d, $J_{C,P}$ = 2.4 Hz), 128.64, 128.77, 128.84, 129.16 (d, $J_{C,P}$ = 4.9 Hz), 129.57, 130.87 (d, $J_{C,P}$ = 4.3 Hz), 131.32 (d, $J_{C,P}$ = 2.5 Hz), 132.21 (d, $J_{C,P}$ = 4.3 Hz), 132.64 (d, $J_{C,P}$ = 9 Hz), 136.39, 137.25 (d, $J_{C,P}$ = 2.5 Hz) (Ar*C*). Anal. Calcd. for $C_{26}H_{23}PS$ (398.5): C, 78.36; H, 5.82. Found: C, 78.26; H, 5.71.

7.4.2.4. Synthesis of [Pd(MeCN)$_4$](BF$_4$)$_2$

[Pd(MeCN)$_2$]Cl$_2$ (0.33 g, 1.26 mmol) was dissolved in refluxing MeCN (30 mL). $AgBF_4$ (0.49 g, 2.52 mmol) dissolved in MeCN (10 mL) was added to this solution, upon which immediate precipitation of AgCl was observed. The resulting reaction mixture was stirred for 1 h, after which the precipitate was allowed to settle. The supernatant was decanted and filtered over celite. The organics were evaporated from the filtrate and the resulting residue redissolved in acetonitrile. Again the solution was filtered which removed the remaining AgCl. This procedure was repeated twice until all AgCl was removed. [Pd(MeCN)$_4$](BF$_4$)$_2$ was obtained in a near quantitative yield (0.55 g) as a light yellow solid.

*7.4.2.5. Synthesis of [Pd(PCS)(MeCN)](BF$_4$) (**5**)*

A solution of [Pd(MeCN)$_4$](BF$_4$)$_2$ (0.85 g, 1.9 mmol) in degassed MeCN (10 mL) was mixed with a solution of PC(H)S-pincer **4** (0.73 g, 1.9 mmol) in degassed MeCN (40 mL). An orange colored solution was obtained which was stirred at ambient temperature for 1 h. The solvent was evaporated under reduced pressure and the residue was redissolved in CH_2Cl_2 and then filtered. After concentration of the resulting filtrate to a minimum amount, the product was precipitated by addition of Et_2O. This process was repeated which resulted in a product that was dried *in vacuo* leaving a light yellow colored powder (1.05 g, 1.66 mmol, 87% yield).

^{1}H NMR (300.1 MHz, CD_3CN, 25 °C): δ = 4.15 (d, $^2J_{H,P}$ = 12.3 Hz, 2H, ArC*H*$_2$P); 4.65 (s, 2H, ArC*H*$_2$S); 7.06 (d, $^3J_{H,H}$ = 3.9 Hz, 2H, Ar*H*); 7.13 (t, $^3J_{H,H}$ = 4.7 Hz, 1H, Ar*H*); 7.46-7.64 (m, 9H, Ar*H*); 7.72-7.84 (m, 6H, Ar*H*). ^{31}P NMR (81.02 MHz, CD_3CN, 25 °C): δ = 49.7 (s). ^{13}C NMR (75.47 MHz, CD_3CN, 25 °C): δ = 42.37 (d, $^1J_{C,P}$ = 36.6 Hz, Ar*C*H$_2$P); 48.70 (s, Ar*C*H$_2$S); 124.39, 125.32 (d, $^2J_{C,P}$ = 25 Hz), 127.89, 130.31, 130.46, 131.01, 131.10, 132.34 (d, $J_{C,P}$ = 1.8 Hz), 133.14 (d, $J_{C,P}$ = 3.02 Hz), 133.73, 133.88, 148.02 (d, $^3J_{C,P}$ = 17.06 Hz), 151.81, 156.75 (d, $J_{C,P}$ = 2.49 Hz) (Ar*C*). IR (ATR): $\tilde{\nu}$ (cm^{-1}) 3058, 2976, 2935, 2317, 2287, 1579, 1484, 1437, 1049, 1023, 743, 689. Anal. Calcd. for $C_{28}H_{25}BF_4NPPdS$ (631.77): C, 53.23; H, 3.99; N, 2.22. Found: C, 53.09; H, 4.06; N, 2.14. ESI-MS: *m/z* 544.19 ([M–BF$_4$]$^+$), 503.16 ([M–MeCN–BF$_4$]$^+$).

*7.4.2.6. Synthesis of [PdCl(PCS)] (**6**)*

To a yellow solution of **5** (0.2 g, 0.276 mmol) in CH_2Cl_2 (3 mL), a solution of NaCl (0.24 g, 4.1 mmol) in dist. H_2O (5 mL) was added. A turbid orange mixture was obtained which was stirred for 2 h at ambient

temperature. The mixture was diluted with CH_2Cl_2 (10 mL) and the organic layer was separated and washed with water. The organic layer was dried over $MgSO_4$ and filtered and evaporated to dryness leaving a yellow solid. This was washed with Et_2O and dried *in vacuo* to obtain a light yellow powder in 95% yield (0.14 g, 0.26 mmol).

^{1}H NMR (300 MHz, $CDCl_3$, 25 °C): δ = 3.99 (d, $^2J_{H,P}$ = 12.2 Hz, 2H, ArC*H*$_2$P); 4.48 (s, 2H, ArC*H*$_2$S); 6.99 (d, $^3J_{H,H}$ = 4.2 Hz, 2H, Ar*H*); 7.09 (t, $^3J_{H,H}$ = 4.8, 3.6 Hz, 1H, Ar*H*); 7.24-7.46 (m, 9H, Ar*H*); 7.74-7.92 (m, 6H, Ar*H*). ^{31}P NMR (81.02 MHz, $CDCl_3$, 25 °C): δ = 45.02 (s). ^{13}C NMR (75.47 MHz, $CDCl_3$, 25 °C): δ = 43.94 (d, $^1J_{C,P}$ = 36.07 Hz, Ar*C*H$_2$P); 49.01 (s, Ar*C*H$_2$S); 122.52, 123.30 (d, $J_{C,P}$ = 24.38 Hz), 125.56, 128.80, 128.94, 129.01, 129.48, 131.04, 131.07, 132.85, 133.0, 147.02 (d, $J_{C,P}$ = 18.34 Hz), 150.32, 160.67 (Ar*C*). IR (ATR): $\tilde{\nu}$ (cm^{-1}) 3051, 2972, 2864, 1579, 1482, 1435, 1103, 1055, 1025, 740, 688. Anal. Calcd. for $C_{26}H_{22}ClPPdS$ (539.36): C, 57.90; H, 4.11; P, 5.74; S, 5.94. Found: C, 57.83; H, 4.19; P, 5.84; S, 5.86. ESI-MS: *m/z* 503.2 ([M–Cl]$^+$).

7.4.2.7. Synthesis of the methyl isocyanoacetate insertion complex 7

To a solution of [PdCl(PCS)] (**6**, 100 mg, 0.185 mmol) in CH_2Cl_2 (5 mL), MI (36 µL, 0.4 mmol) was added. The resulting solution was stirred at ambient temperature for 20 minutes. The solvent was evaporated to a minimum level followed by the addition of pentane (10 mL) to induce precipitation of the product. It was allowed to settle down and the supernatant solution was decanted. The precipitate was dried under reduced pressure to give a yellow solid **7** (70 mg, 0.093 mmol, 50% yield). ^{1}H NMR (300 MHz, CD_2Cl_2, 25 °C): δ = 3.52 (s, 2H, SC*H*$_2$); 3.78 (s, br, 6H, OMe); 4.1 (s, br, 2H, C(O)C*H*$_2$); 4.25 (d, $^2J_{H,P}$ = 10.8 Hz, 2H, PC*H*$_2$); 4.85 (s, 2H, C(O)C*H*$_2$); 6.89 (1H, Ar*H*); 7.05-7.24 (m, 3H, Ar*H*); 7.3-7.6 (m, 10H, Ar*H*); 7.7-7.94 (m, 3H, Ar*H*); 8.0-8.1 (m, 1H, Ar*H*). ^{31}P NMR (81.02 MHz, CD_2Cl_2, 25 °C): δ = 47.76. ^{13}C NMR (75.47 MHz, CD_2Cl_2, 25 °C): δ = 30.8 (s, Ar*C*H$_2$S) 44.0 (d, $^1J_{C,P}$ = 36 Hz, Ar*C*H$_2$P); 46.0 (s, C(O)*C*H$_2$); 49.5 (s, O*C*H$_3$); 51.0 (s, O*C*H$_3$); 62.0 (s, C(O)*C*H$_2$); 122.8, 123.0, 125.0, 125.8, 126.5, 127.5, 127.8, 129.2, 129.7, 131.1, 131.5, 131.9, 133.1, 138.2, 150.5, 163.0, 171.0, 186.0. IR (ATR): $\tilde{\nu}$ (cm^{-1}) 3053, 2953, 2230, 1750, 1627, 1582, 1482, 1436, 1219, 1179, 1102, 1055, 1025, 999, 742, 690. Anal. Calcd. for $C_{34}H_{32}ClN_2O_4PPdS$ (737.54): C, 55.37; H, 4.37; N, 3.80. Found: C, 55.26; H, 4.44; N, 3.69.

7.4.2.8. General procedure for catalysis

Catalytic experiments were performed using a standard protocol. In a typical experiment, 1 mol% (0.016 mmol) of complex was dissolved in 5 mL distilled CH_2Cl_2. MI (1.6 mmol), benzaldehyde (1.6 mmol), pentadecane (internal standard, 0.4 mmol), and *i*Pr$_2$EtN (Hunig's base, 0.16 mmol, 10 mol%) were added and the reaction mixture was stirred at room temperature. The reaction was monitored by means of GC analysis.

7.5. References

1. G. van Koten, *Pure Appl. Chem.* **1989**, *61*, 1681-1694.
2. M. Albrecht, G. van Koten, *Angew. Chem., Int. Ed.* **2001**, *40*, 3750-3781.
3. K. J. Szabo, *Synlett* **2006**, 811-824; O. A. Wallner, K. J. Szabo, *J. Org. Chem.* **2005**, *70*, 9215-9221; N. Solin, O. A. Wallner, K. J. Szabo, *Org. Lett.* **2005**, *7*, 689-691; S. Sebelius, V. J. Olsson, K. J. Szabo, *J. Am. Chem. Soc.* **2005**, *127*, 10478-10479; J. Kjellgren, H. Sunden, K. J. Szabo, *J. Am. Chem. Soc.* **2005**, *127*, 1787-1796; J. Kjellgren, J. Aydin, O. A. Wallner, I. V. Saltanova, K. J. Szabo, *Chem. Eur. J.* **2005**, *11*, 5260-5268; K. Yu, W. Sommer, J. M. Richardson, M. Weck, C. W. Jones, *Adv. Synth. Catal.* **2005**, *347*, 161-171; W. Sommer, K. Yu, J. S. Sears, Y. Ji, X. Zheng, R. J. Davis, C. D. Sherrill, C. W. Jones, M. Weck, *Organometallics* **2005**, *24*, 4351-4361; J. Zhao, A. S. Goldman, J. F. Hartwig, *Science* **2005**, *307*, 1080-1082; K. Takenaka, Y. Uozumi, *Org. Lett.* **2004**, *6*, 1833-1835; N. Solin, J. Kjellgren, K. J. Szabo, *J. Am. Chem. Soc.* **2004**, *126*, 7026-7033; Z. Wang, M. R. Eberhard, C. M. Jensen, S. Matsukawa, Y. Yamamoto, *J. Organomet. Chem.* **2003**, *681*, 189-195; E. Diez-Barra, J. Guerra, V. Hornillos, S. Merino, J. Tejeda, *Organometallics* **2003**, *22*, 4610-4612; J. T. Singleton, *Tetrahedron* **2003**, *59*, 1837-1857; M. E. van der Boom, D. Milstein, *Chem. Rev.* **2003**, *103*, 1759-1792; G. R. Rosa, G. Ebeling, J. Dupont, A. L. Monteiro, *Synthesis* **2003**, 2894-2897; I. G. Jung, S. U. Son, K. H. Park, K.-C. Chung, J. W. Lee, Y. K. Chung, *Organometallics* **2003**, *22*, 4715-4720; S. Sjoevall, O. F. Wendt, C. Andersson, *J. Chem. Soc., Dalton Trans.* **2002**, 1396-1400; G. Rodriguez, M. Lutz, A. L. Spek, G. van Koten, *Chem. Eur. J.* **2002**, *8*, 45-57; G. Guillena, G. Rodriguez, G. van Koten, *Tetrahedron Lett.* **2002**, *43*, 3895-3898; J. M. Seul, S. Park, *J. Chem. Soc., Dalton Trans.* **2002**, 1153-1158; D. Morales-Morales, R. E. Cramer, C. M. Jensen, *J. Organomet. Chem.* **2002**, *654*, 44-50; J. A. Loch, M. Albrecht, E. Peris, J. Mata, J. W. Faller, R. H. Crabtree, *Organometallics* **2002**, *21*, 700-706; J. S. Fossey, C. J. Richards, *Organometallics* **2002**, *21*, 5259-5264; M. Albrecht, B. M. Kocks, A. L. Spek, G. van Koten, *J. Organomet. Chem.* **2001**, *624*, 271-286; J. Dupont, M. Pfeffer, J. Spencer, *Eur. J. Inorg. Chem.* **2001**, 1917-1927; S. Gruendemann, M. Albrecht, J. A. Loch, J. W. Faller, R. H. Crabtree, *Organometallics* **2001**, *20*, 5485-5488; C. Schlenk, A. W. Kleij, H. Frey, G. van Koten, *Angew. Chem., Int. Ed.* **2000**, *39*, 3445-3447; D. Morales-Morales, R. Redon, C. Yung, C. M. Jensen, *Chem. Commun.* **2000**, 1619-1620; X. Zhang, J. M. Longmire, M. Shang, *Organometallics* **1998**, *17*, 4374-4379; M. Ohff, A. Ohff, M. E. van der Boom, D. Milstein, *J. Am. Chem. Soc.* **1997**, *119*, 11687-11688; S. E. Denmark, R. A. Stavenger, A.-M. Faucher, J. P. Edwards, *J. Org. Chem.* **1997**, *62*, 3375-3389; F. Gorla, A. Togni, L. M. Venanzi, A. Albinati, F. Lianza, *Organometallics* **1994**, *13*, 1607-1616.
4. R. Chanthateyanonth, H. Alper, *Adv. Synth. Catal.* **2004**, *346*, 1375-1384; R. Chanthateyanonth, H. Alper, *J. Mol. Catal. A* **2003**, *201*, 23-31; R. Gimenez, T. M. Swager, *J. Mol. Catal. A* **2001**, *166*, 265-273; N. C. Mehendale, C. Bezemer, C. A. van Walree, R. J. M. Klein Gebbink, G. van Koten, *J. Mol. Catal. A* **2006**, *257*, 167-175.
5. D. E. Bergbreiter, P. L. Osburn, A. Wilson, E. M. Sink, *J. Am. Chem. Soc.* **2000**, *122*, 9058-9064; D. E. Bergbreiter, P. L. Osburn, Y.-S. Liu, *J. Am. Chem. Soc.* **1999**, *121*, 9531-9538; D. E. Bergbreiter, P. L. Osburn, J. D. Frels, *J. Am. Chem. Soc.* **2001**, *123*, 11105-11106; D. E. Bergbreiter, S. Furyk, *Green Chem.* **2004**, *6*, 280-285; D. E. Bergbreiter, J. D. Frels, P. L. Osburn, *Polym. Prep.* **2000**, *41*, 1360; D. E. Bergbreiter, *Chem. Rev.* **2002**, *102*, 3345-3383; M. Q. Slagt, J. T. B. H. Jastrzebski, R. J. M. Klein Gebbink, H. J. van Ramesdonk, J. W. Verhoeven, D. D. Ellis, A. L. Spek, G. van Koten, *Eur. J. Org. Chem.* **2003**, 1692-1703; M. Q. Slagt, S.-E. Stiriba, H. Kautz, R. J. M. Klein Gebbink, H. Frey, G. van Koten, *Organometallics* **2004**, *23*, 1525-1532; M. Q. Slagt, S.-E. Stiriba, R. J. M. Klein Gebbink, H. Kautz, H. Frey, G. van Koten, *Macromolecules* **2002**, *35*, 5734-5737.
6. R. van de Coevering, A. P. Alfers, J. D. Meeldijk, E. Martinez-Viviente, P. S. Pregosin, R. J. M. Klein Gebbink, G. van Koten, *J. Am. Chem. Soc.* **2006**, *128*, 12700-12713; B. M. J. M. Suijkerbuijk, L. Shu, R. J. M. Klein Gebbink, A. D. Schlueter, G. van Koten, *Organometallics* **2003**, *22*, 4175-4177; H. P. Dijkstra, C. A. Kruithof, N. Ronde, R. van de Coevering, D. J. Ramon, D. Vogt, G. P. M. van Klink, G. van Koten, *J. Org. Chem.* **2003**, *68*, 675-685; H. P. Dijkstra, N. Ronde, G. P. M. van Klink, D. Vogt, G. van Koten, *Adv. Synth. Catal.* **2003**, *345*, 364-369; H. P. Dijkstra, M. Albrecht, S. Medici, G. P. M. van Klink, G. van Koten, *Adv. Synth. Catal.* **2002**, *344*, 1135-1141; R. van de Coevering, M. Kuil, R. J. M. Klein Gebbink, G. van Koten, *Chem. Commun.* **2002**, 1636-1637; H. P. Dijkstra, M. D. Meijer, J. Patel, R. Kreiter, G. P. M. van Klink, M. Lutz, A. L. Spek, A. J. Canty, G. van Koten, *Organometallics* **2001**, *20*, 3159-3168.
7. C. A. Kruithof, M. A. Casado, G. Guillena, M. R. Egmond, A. van der Kerk-van Hoof, A. J. R. Heck, R. J. M. Klein Gebbink, G. van Koten, *Chem. Eur. J.* **2005**, *11*, 6869-6877; S. Kocher, G. P. M. van Klink, G. van Koten, H. Lang, *J. Organomet. Chem.* **2003**, *684*, 230-234; M. D. Meijer, N. Ronde, D. Vogt, G. P. M. van Klink, G. van Koten, *Organometallics* **2001**, *20*, 3993-4000.
8. Y. Yamamoto, H. Yamazaki, *Coord. Chem. Rev.* **1972**, *8*, 225-239; Y. Yamamoto, H. Yamazaki, *Inorg. Chem.* **1974**, *13*, 438-443; J. F. van Baar, J. M. Klerks, O. P., D. J. Stufkens, K. Vrieze, *J. Organomet. Chem.* **1976**, *112*, 95-103; Y. Yamamoto, H. Yamazaki, *Synthesis* **1976**, 750-751; Y. Yamamoto, H. Yamazaki, *Inorg. Chim. Acta* **1980**, *41*, 229-232; A. D. Ryabov, *Synthesis* **1985**, 233-252; J. Vincente, I.

Saura-Llamas, J. Turpín, M. C. R. de Arellano, P. G. Jones, *Organometallics* **1999**, *18*, 2683-2693; J. Vincente, I. Saura-Llamas, C. Grünwald, C. Alcaraz, P. G. Jones, D. Bautista, *Organometallics* **2002**, *21*, 3587-3595; Y.-J. Kim, X. Chang, J.-T. Han, M. S. Lim, S. W. Lee, *Dalton Trans.* **2004**, 3699-3708.

9. A. Zografidis, K. Polborn, W. Beck, B. A. Markies, G. van Koten, *Z. Naturforsch., B* **1994**, *49*, 1494-1498.
10. N. C. Mehendale, R. W. A. Havenith, M. Lutz, A. L. Spek, R. J. M. Klein Gebbink, G. van Koten, *manuscript in prep. (Ch. 5 and 6 of this thesis)*.
11. J. Dupont, M. Pfeffer, J. C. Daran, Y. Jeannin, *Organometallics* **1987**, *6*, 899-901; J. Dupont, M. Pfeffer, *J. Chem. Soc., Dalton Trans.* **1990**, 3193-3198.
12. M. Gandelman, A. Vigalok, L. J. W. Shimon, D. Milstein, *Organometallics* **1997**, *16*, 3981-3986; A. Sundermann, O. Uzan, J. M. L. Martin, *Organometallics* **2001**, *20*, 1783-1791; M. Gandelman, L. Konstantinovski, H. Rozenberg, D. Milstein, *Chem. Eur. J.* **2003**, *9*, 2595-2602.
13. H. Rimml, L. M. Venanzi, *J. Organomet. Chem.* **1983**, *259*, C6-C7.
14. I. Romero, G. Sanchez-Castello, F. Teixidor, C. R. Whitaker, J. Rius, C. Miravitlles, T. Flor, L. Escriche, J. Casabo, *Polyhedron* **1996**, *15*, 2057-2065.
15. N. Lucena, J. Casabo, L. Escriche, G. Sanchez-Castello, F. Teixidor, R. Kivekäs, R. Sillanpää, *Polyhedron* **1996**, *15*, 3009-3018.

Chapter 8

Reactivity of Simple (In)soluble Silver(I) Salts in an Isocyanide Aldol Reaction

Abstract

AgCl dissolves readily in dichloromethane upon addition of methyl isocyanoacetate (MI). The latter compound exists as a dimeric structure in the solid-state which crystallizes in the presence of excess MI as a 1:2 (Ag/MI) complex ($[Ag_2Cl_2(MI)_4]$) having two silver ions bridged by two chloride ions forming a four-membered ring. Each silver centre binds two MI molecules resulting in a distorted tetrahedral geometry around each Ag. Silver-based salts catalyze the aldol reaction of MI with benzaldehyde (TOF of more than 70 h^{-1}). This highlights that both soluble as well as insoluble Ag-salts are active catalysts for this reaction and puts a question mark on the use of silver-based reagents for the activation of metal halide compounds as catalysts (*e.g.* ECE-pincer metal halide complexes) for this reaction.

8.1. Introduction

Various silver(I) complexes have been used in aldol-type reactions. Examples include soluble chiral BINAP·Ag(I) complexes reported by Yamamoto and soluble Ag(I) complexes with a chiral bis(diphenylphosphino)ferrocene ligand communicated by Ito.[1] Although such soluble complexes have frequently been used, reports about the application of insoluble silver halide salts as catalysts in aldol type reactions are lacking.

In our study on Pd-based pincer-type complexes as catalysts in aldol reaction (1) between benzaldehyde and methyl isocyanoacetate (MI), we found a strong evidence for a surprising activity of Ag-halide salts (*e.g.* AgCl) in this reaction.[2]

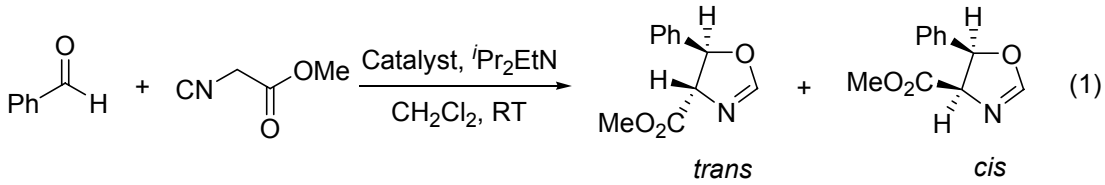

$AgBF_4$ and AgOTf are used as reagents to activate the metal centre of ECE-pincer metal complexes, whereby the halide is abstracted to form the corresponding cationic species [M(ECE)L]X. This species can act as a Lewis acid catalyst in aldol reaction (1). Insoluble Ag-halide salts are generated in stoichiometric amount as by-product in the activation step and have to be removed by filtration. We now report evidence for the necessity to follow a strict protocol to completely remove any silver-based species as any traces of insoluble silver salts left behind can act as a catalyst, thereby causing a background reaction to that of the actual [M(ECE)L]X pincer-based catalysts. These aldol reactions are typically carried out in dichloromethane, a solvent in which AgCl is insoluble. Nevertheless, we observed that AgCl itself catalyzes aldol reaction (1). Therefore, we decided to investigate how insoluble AgCl can act as an effective catalyst in this reaction. Here we report these results and make a proposal for the actual catalytic species that is involved.

8.2. Results

Addition of an excess of MI to a suspension of AgCl in dichloromethane resulted in the formation of a clear dark brown colored solution. From this solution, a sticky solid was isolated after evaporation of all volatiles. Based on elemental analysis, a compound with a 1:1 Ag:MI, *i.e.*, AgCl(MI) stoichiometry was obtained (Scheme 1). Its IR spectrum showed a vibration at 2207 cm^{-1} which points to metal-isocyanide coordination ($\tilde{\nu}$(C≡N) of free MI appears at 2163 cm^{-1}). ^{1}H NMR analysis of a solution of this solid in $CDCl_3$ revealed a downfield shift of the CH_2-signal of MI (from 4.24 to 4.40 ppm).[3] ^{13}C NMR analysis showed a shift of the isonitrile C≡N signal from 161 to 159 and the methylene CH_2 signal from 43.6 to 44.09, whereas the carbonyl signal remained unchanged at 164 ppm. These observations point to coordination of the isocyanide to Ag through the isonitrile C-atom.

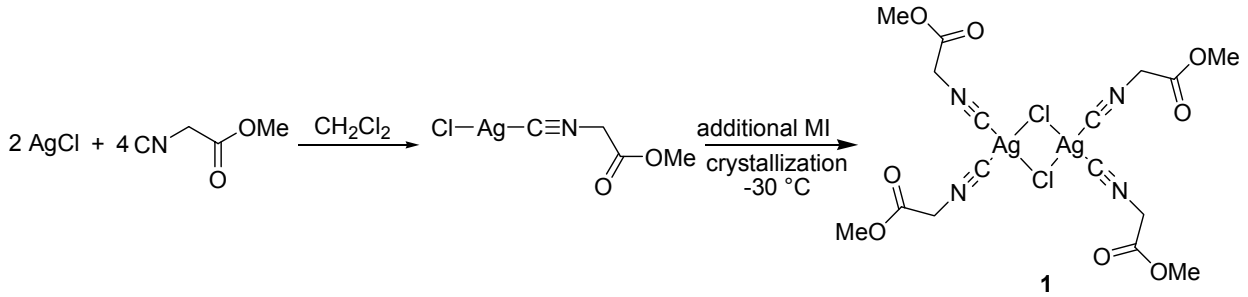

Scheme 1 Reaction between AgCl and MI, formation of a dimeric species **1**.

To gain more insight into the structure of this complex, we attempted to obtain its structure in solid state. A sufficiently diluted solution in dichloromethane containing additional MI was kept at a temperature of –30 °C until colorless crystals had formed. Single crystal X-ray structure determination revealed its molecular structure involving centrosymmetric dimer $[Ag_2Cl_2(MI)_4]$ in which the two silver ions are bridged by two chloride ions (Figure 1). Consequently, crystallization of the initially formed 1:1 AgCl : MI complex occurred with coordination of an additional MI ligand.

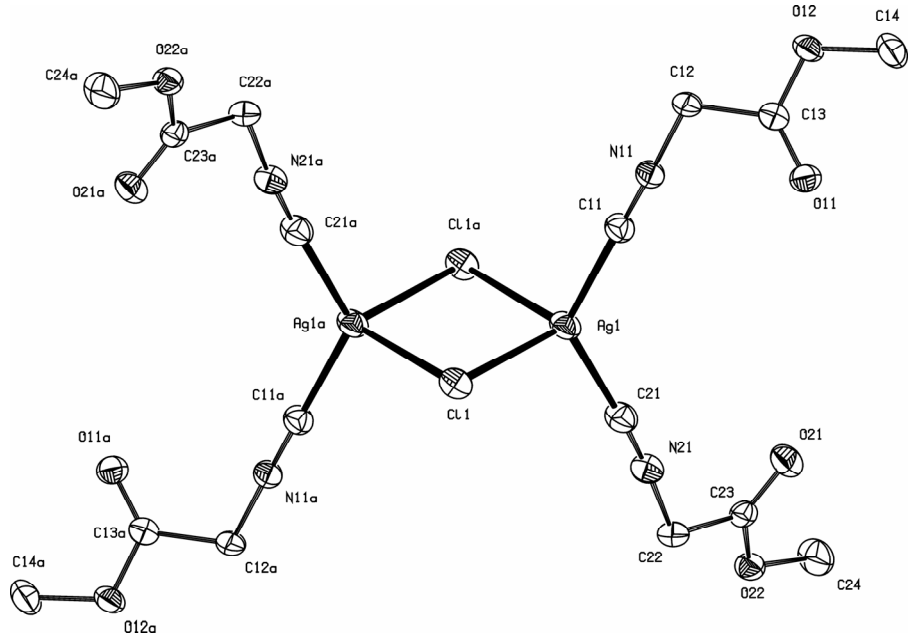

Figure 1 Displacement ellipsoid plot (drawn at 50% probability level) of dimer **1** (hydrogen atoms and CH_2Cl_2 are excluded for clarity). Selected bond lengths (Å) and angle (deg): Ag(1)···Ag(1)a 3.6586(3), Cl(1)···Cl(1)a 3.8985(7), Ag(1)–Cl(1) 2.6213(5), Ag(1)–Cl(1)a 2.7240(5), Ag(1)–C(11) 2.1405(18), Ag(1)–C(21) 2.145(2), C(11)–N(11) 1.138(2), C(21)–N(21) 1.145(2), N(11)–C(12) 1.425(2), N(21)–C(22) 1.425(2), Cl(1)–Ag(1)–Cl(1)a 93.639(14), C(11)–Ag(1)–C(21) 127.38(7). Symmetry operation a: –x, –y, 1–z.

Each silver ion binds to two MI molecules forming a tetrahedral geometry.[4] Distances found for the Ag_2Cl_2 square are Ag(1)···Ag(1)a, 3.6586(3); Cl(1)···Cl(1)a, 3.8985(7); Ag(1)–Cl(1), 2.6213(5) and Ag(1)–Cl(1)a, 2.7240(5) Å. These are close to the average distances found in such four-membered ring complexes (an average of 19 structures from CSD reported by Molina *et al.*).[5] The ionic radii

(r_{ion}) for Ag^+ and Cl^- are 1.08 and 1.67, respectively, while the covalent radii (r_{cov}) are 1.44 and 0.99 Å, respectively.[6] The Ag–Cl ionic bond is thus about 2.75 and the covalent bond is about 2.43 Å. The bond length of 2.62 Å in this structure indicates that it is not a purely ionic bond but tends to acquire a covalent character. The angle between Cl–Ag–Cl is, however, 93.639(14)°, which is close to the maximum reported value. The C–Ag–C angle is 127.38(7)°, pointing to an overall distorted tetrahedral geometry around Ag.

When AgOTf and $AgBF_4$ are treated with MI, coordination of MI *via* the isocyanide C-atom to silver takes place as expected. ^{1}H NMR analysis of the reaction product showed a downfield shift of the methylene signal of MI (from 4.24 to 4.55 ppm). ^{13}C NMR analysis showed a shift of the isonitrile C≡N signal from 161 to 146, and of the methylene CH_2 signal from 43.6 to 44.98 ppm. The carbonyl signal again remained unchanged. Elemental analysis of the product isolated in almost quantitative yield from this reaction pointed to a ratio of 1:4 between Ag and MI. This indicates that a reaction as shown in Scheme 2 had taken place, in which a tetrakis(MI) product is formed. Attempts to grow crystals for X-ray analysis however were not successful.

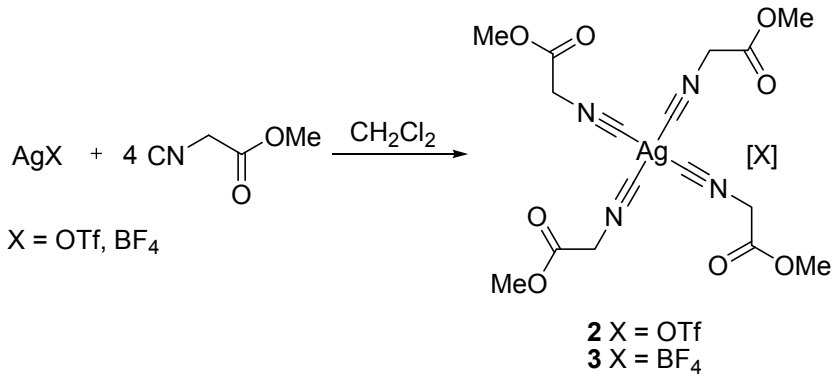

Scheme 2 Reaction between ionic Ag-salts and MI, formation of a monomeric species.

Aldol reaction (1) was carried out by using simple Ag-salts such as AgCl and $AgBF_4$ as catalysts (Table 1). It was found that both of them catalyze this reaction with a similar TOF and give similar *trans/cis* ratio of products. This may indicate that the same type and number of catalytic sites are operative in both systems.

Table 1 Aldol reaction using silver salts.[a]

Catalyst	% product[b]	TOF (h^{-1})[c]	% *trans*
AgCl	86	74	75%
$AgBF_4$	84	72	73%

a. Catalysis carried out using 1.6 mmol of reagents in 5 mL dichloromethane solution, 10 mol% Hunig's base and 2.5 mol% catalyst. Values are obtained from GC readings using pentadecane as an internal standard; b. after 1 hour; c. TOF calculated after 20 minutes, at about 50% conversion.

8.3. Discussion

In aldol reactions between MI and benzaldehyde (reaction 1), palladium and platinum(II) based pincer halide complexes were used as precatalysts. Initially we activated these halide complexes by

treatment with silver reagents like $AgBF_4$ or AgOTf and separated the resulting Ag-halide from the activated (cationic) catalysts.[7] Our current study shows, however that it is very important to remove all insoluble Ag-salts from these complexes before using them as catalysts in aldol reaction of benzaldehyde with MI. For example, during our study of silica immobilized palladium pincer complexes, complete removal of insoluble AgCl after activation step appeared to be impossible.[2] In an experiment to illustrate the effect of residual silver salts at silica support on catalysis, we mixed silica suspended in dichloromethane with a Ag-salt (either AgCl, $AgNO_3$ or $AgBF_4$). The resulting silicas were washed several times with dichloromethane to remove any silver salt not attached to the silica. When these materials were used in aldol reaction (1), a high activity was observed in each case. These observations illustrate the risks involved in using Ag-salts to activate (immobilized) metal complexes.[8] Traces of silver left behind in solution or on the solid support can mask the actual catalytic activity of ECE-pincer palladium halide complexes. Also in the case of homogeneous catalysis, care must be taken to find ways to remove all silver salts, both the soluble starting reagent ($AgBF_4$ or AgOTf) and the insoluble side-product (AgCl) formed. In recent studies, we showed that this activation is not required for catalytic activity to occur. In many cases, the neutral ECE-pincer palladium chloride complexes nicely catalyze aldol reaction without prior activation.[9]

8.4. Experimental Section

8.4.1. General Comments

CH_2Cl_2 was dried over calcium hydride and distilled prior to use. Benzaldehyde and Hunig's base were distilled prior to use. MI was used without further purification. Gas chromatographic analyses were performed with a Perkin Elmer Autosystem XL GC using a 30 m, PE-17 capillary column with an FID detector.

Catalytic experiments were performed using a standard protocol. In a typical experiment, 2.5 mol% (0.04 mmol) of complex was dissolved in 5 mL of distilled CH_2Cl_2. MI (1.6 mmol), benzaldehyde (1.6 mmol), pentadecane (0.4 mmol, internal standard), and $^{i}Pr_2EtN$ (Hunig's base, 0.16 mmol, 10 mol%) were added and the reaction mixture was stirred at room temperature. The reaction was monitored by means of GC analysis.

8.4.2. Procedures

*8.4.2.1. Synthesis of $[AgCl(CNCH_2CO_2Me)_2]_2$ (**1**)*

AgCl (50 mg, 0.35 mmol) was suspended in CH_2Cl_2 followed by the addition of MI (0.16 mL, 1.75 mmol) upon which AgCl dissolved. The dark brown colored reaction solution was stirred for another 2 h. Subsequently all volatiles were removed *in vacuo* which left a sticky brown solid in a near quantitative yield. When this product was treated with CH_2Cl_2, it formed a turbid solution, which became clear by addition of an extra amount of MI. From this solution crystals were obtained at –30 °C.

^{1}H NMR (300.1 MHz, $CDCl_3$, 25 °C): δ = 3.80 (s, 3H, OCH_3); 4.40 (s, 2H, CH_2). ^{13}C NMR (75.5 MHz, $CDCl_3$, 25 °C): δ = 44.09 (OCH_3); 53.54 (CH_2); 158.79 (CN); 163.98 (CO). IR (ATR): $\tilde{\nu}$ (cm^{-1}) = 2958, 2903, 2207, 1748, 1439, 1419, 1362, 1280, 1215, 1186, 1020, 944, 706. Anal. Calcd. for $C_4H_5AgClNO_2$ (242.41, [AgCl(MI)]): C, 19.82; H, 2.08; N, 5.78. Found: C, 19.85; H, 1.87, N, 5.50.

*8.4.2.2. Synthesis of [Ag(CNCH$_2$CO$_2$Me)$_4$]OTf (**2**)*

To a suspension of AgOTf (0.3 g, 1.2 mmol) in CH_2Cl_2 (5 mL), MI (0.45 mL, 5 mmol) was added. Subsequently, the solution was stirred at room temperature for 2 h in the dark. The clear brown solution was passed over Celite to remove any Ag(0) particles. The filtrate was concentrated to almost dryness and Et_2O was added affording a brown oil to separate out. This oil was isolated and dried. The product **2** was obtained in a near quantitative yield.

^{1}H NMR (300.1 MHz, $CDCl_3$, 25 °C): δ = 3.84 (s, 3H, OCH_3); 4.55 (s, 2H, CH_2). ^{13}C NMR (75.5 MHz, $CDCl_3$, 25 °C): δ = 44.98 (CH_2); 53.80 (OCH_3); 145.99 (CN); 163.55 (C=O). IR (ATR): $\tilde{\nu}$ (cm^{-1}) = 2987, 2960, 2213, 1752, 1441, 1421, 1363, 1262, 1217, 1187, 1152, 1029, 946, 850, 707. Anal. Calcd. for $C_{17}H_{20}AgF_3N_4O_{11}S$ (653.29): C, 31.25; H, 3.09; N, 8.58. Found: C, 31.07; H, 3.15, N, 8.46.

*8.4.2.3. Synthesis of [Ag(CNCH$_2$CO$_2$Me)$_4$]BF$_4$ (**3**)*

A similar procedure was followed as described above for compound **2**. Starting from $AgBF_4$ (0.3 g, 1.5 mmol) and MI (0.6 mL, 6 mmol), the compound **3** was obtained as a light-yellow colored powder in a quantitative yield.

^{1}H NMR (300.1 MHz, $CDCl_3$, 25 °C): δ = 3.73 (s, 3H, OCH_3); 4.55 (s, 2H, CH_2). ^{13}C NMR (75.5 MHz, $CDCl_3$, 25 °C): δ = 44.73 (OCH_3); 53.52 (CH_2); 143.95 (CN); 163.76 (C=O). IR (ATR): $\tilde{\nu}$ (cm^{-1}) = 2987, 2960, 2213, 1752, 1441, 1421, 1363, 1262, 1217, 1187, 1152, 1029, 946, 850, 707. Anal. Calcd. for $C_{16}H_{20}AgBF_4N_4O_8$ (591.02): C, 32.51; H, 3.41; N, 9.48. Found C, 32.60; H, 3.48; N, 9.44

*8.4.3. X-ray crystal structure determination of **1***

$C_{16}H_{20}Ag_2Cl_2N_4O_8 \cdot 2CH_2Cl_2$, Fw = 852.85, colorless plate, 0.36 × 0.24 × 0.09 mm^3, monoclinic, $P2_1/c$ (no. 14), a = 8.0157(5), b = 8.8035(3), c = 23.0556(16) Å, β = 106.941(5)°, V = 1556.34(15) $Å^3$, Z = 2, D_x = 1.820 g/cm^3, μ = 1.82 mm^{-1}. 21386 reflections were measured on a Nonius Kappa CCD diffractometer with rotating anode (graphite monochromator, λ = 0.71073 Å) at a temperature of 150 K up to a resolution of $(\sin\theta/\lambda)_{max}$ = 0.65 $Å^{-1}$. Intensities were integrated with EvalCCD[10] using an accurate description of the experimental setup for the prediction of the reflection contours. The reflections were corrected for absorption and scaled on the basis of multiple measured reflections with the program SADABS[11] (0.67-0.85 correction range). 3570 reflections were unique (R_{int} = 0.0233). The structure was solved with the program DIRDIF-99[12] using automated Patterson Methods and refined with SHELXL-97[13] against F^2 of all reflections. Non hydrogen atoms were refined with anisotropic displacement parameters. All hydrogen atoms were located in the difference Fourier map and refined with a riding model. 174 parameters were refined with no restraints. R1/wR2 [I > 2σ(I)]: 0.0194/0.0455. R1/wR2 [all refl.]: 0.0259/0.0484. S = 1.085. Residual electron density between –0.36 and 0.40 e/$Å^3$. Geometry calculations and checking for higher symmetry was performed with the PLATON program.[14]

8.5. References

1. M. Wadamoto, N. Ozasa, A. Yanagisawa, H. Yamamoto, *J. Org. Chem.* **2003**, *68*, 5593-5601; E. Cesarotti, S. Araneo, I. Rimoldi, S. Tassi, *J. Mol. Catal. A* **2003**, *204-205*, 221-226; A. Yanagisawa, Y. Matsumoto, K. Asakawa, H. Yamamoto, *Tetrahedron* **2002**, *58*, 8331-8339; M. Ohkouchi, D. Masui, M. Yamaguchi, T. Yamagishi, *Nippon Kagaku Kaishi* **2002**, 223-229; A. Yanagisawa, Y. Nakatsuka, K. Asakawa, H. Kageyama, H. Yamamoto, *Synlett* **2001**, 69-72; M. Ohkouchi, D. Masui, M. Yamaguchi, T. Yamagishi, *J. Mol. Catal. A* **2001**, *170*, 1-15; M. Ohkouchi, M. Yamaguchi, T. Yamagishi, *Enantiomer* **2000**, *5*, 71-81; A. Yanagisawa, Y. Matsumoto, K. Asakawa, H. Yamamoto, *J. Am. Chem. Soc.* **1999**, *121*, 892-893; A. Yanagisawa, H. Kageyama, Y. Nakatsuka, K. Asakawa, Y. Matsumoto, H. Yamamoto, *Angew. Chem., Int. Ed.* **1999**, *38*, 3701-3703; A. Yanagisawa, Y. Matsumoto, H. Nakashima, K. Asakawa, H. Yamamoto, *J. Am. Chem. Soc.* **1997**, *119*, 9319-9320; V. A. Soloshonok, T. Hayashi, K. Ishikawa, N. Nagashima, *Tetrahedron Lett.* **1994**, *35*, 1055-1058; T. Hayashi, Y. Uozumi, A. Yamazaki, M. Sawamura, H. Hamashima, Y. Ito, *Tetrahedron Lett.* **1991**, *32*, 2799-2802; M. Sawamura, H. Hamashima, Y. Ito, *J. Org. Chem.* **1990**, *55*, 5935-5936.
2. N. C. Mehendale, C. Bezemer, C. A. van Walree, R. J. M. Klein Gebbink, G. van Koten, *J. Mol. Catal. A* **2006**, *257*, 167-175.
3. NMR data of free MI ^{1}H: 3.84 (O*Me*), 4.24 (CH_2); ^{13}C: 43.6 (*C*H$_2$), 53.6 (O*Me*), 161.1 (*C*N), 164.4 (*C*O).
4. D. Perreault, M. Drouin, A. Michel, P. D. Harvey, *Inorg. Chem.* **1993**, *32*, 1903-1912.
5. J. El-Bahraoui, J. A. Dobado, J. M. Molina, *Theochem* **1999**, *493*, 249-257.
6. F. A. Cotton, G. Wilkinson, P. L. Gauss, *Basic Inorganic Chemistry, Pg. 60*, 2nd ed., Wiley, Toronto, **1987**.
7. R. van de Coevering, A. P. Alfers, J. D. Meeldijk, E. Martinez-Viviente, P. S. Pregosin, R. J. M. Klein Gebbink, G. van Koten, *J. Am. Chem. Soc.* **2006**, *128*, 12700-12713; G. Guillena, G. Rodriguez, G. van Koten, *Tetrahedron Lett.* **2002**, *43*, 3895-3898; G. Rodriguez, M. Lutz, A. L. Spek, G. van Koten, *Chem.-Eur. J.* **2002**, *8*, 45-57; Y. Motoyama, H. Kawakami, K. Shimozono, K. Aoki, H. Nishiyama, *Organometallics* **2002**, *21*, 3408-3416; J. S. Fossey, C. J. Richards, *Organometallics* **2002**, *21*, 5259-5264; A. W. Kleij, R. J. M. Klein Gebbink, P. A. J. van den Nieuwenhuijzen, H. Kooijman, M. Lutz, A. L. Spek, G. van Koten, *Organometallics* **2001**, *20*, 634-647; M. D. Meijer, N. Ronde, D. Vogt, G. P. M. van Klink, G. van Koten, *Organometallics* **2001**, *20*, 3993-4000; M. Albrecht, B. M. Kocks, A. L. Spek, G. van Koten, *J. Organomet. Chem.* **2001**, *624*, 271; C. Schlenk, A. W. Kleij, H. Frey, G. van Koten, *Angew. Chem., Int. Ed.* **2000**, *39*, 3445-3447; X. Zhang, J. M. Longmire, M. Shang, *Organometallics* **1998**, *17*, 4374-4379; M. A. Stark, C. J. Richards, *Tetrahedron Lett.* **1997**, *38*, 5881-5884; F. Gorla, A. Togni, L. M. Venanzi, A. Albinati, F. Lianza, *Organometallics* **1994**, *13*, 1607-1616; R. Nesper, P. S. Pregosin, K. Puntener, M. Worle, *Helv. Chim. Acta* **1993**, *76*, 2239-2249.
8. K. Mori, T. Hara, T. Mizugaki, K. Ebitani, K. Kaneda, *J. Am. Chem. Soc.* **2003**, *125*, 11460-11461; R. Gimenez, T. M. Swager, *J. Mol. Catal. A* **2001**, *166*, 265-273.
9. N. C. Mehendale, R. W. A. Havenith, M. Lutz, A. L. Spek, R. J. M. Klein Gebbink, G. van Koten, *manuscript in prep. (Ch. 5 and 6 of this thesis).*
10. A. J. M. Duisenberg, L. M. J. Kroon-Batenburg, A. M. M. Schreurs, *J. Appl. Cryst.* **2003**, *36*, 220-229.
11. G. M. Sheldrick, *SADABS: Area-Detector Absorption Correction, v2.10*, **1999**, Universität Göttingen, Germany.
12. P. T. Beurskens, G. Admiraal, G. Beurskens, W. P. Bosman, S. Garcia-Granda, R. O. Gould, J. M. M. Smits, C. Smykalla, *The DIRDIF99 program system, Technical Report of the Crystallography Laboratory*, **1999**, University of Nijmegen, The Netherlands.
13. G. M. Sheldrick, *SHELXL-97 Program for crystal structure refinement*, **1997**, Universität Göttingen, Germany.
14. A. L. Spek, *J. Appl. Cryst.* **2003**, *36*, 7-13.

Summary

Science is continuously striving for a sustainable progress of society. This progress must be made on the economical as well as the environmental front concomitantly. Many industrial processes are being reviewed to make them environmentally more sustainable. Catalysis emerges as an important player to achieve this goal. No wonder, about 85% of the present chemical processes are run using a catalyst. Out of these about 75% are run based on heterogeneous catalysts due to their advantage of easy separation from product streams and of their recycling and reuse. On the other hand, homogeneous catalysts are appreciated in terms of their activity and selectivity, particularly in the case of enantioselective processes. These catalysts generally consist of a transition metal surrounded by an ingeniously designed (chiral) ligand system to fine tune the catalytic properties. This often makes homogeneous catalyst systems expensive and consequently, recycling and reuse of these catalysts become pertinent. One solution to achieve this is by immobilizing the homogeneous catalyst on an insoluble support, *i.e.* by heterogenizing the homogeneous catalyst. An inexpensive and abundantly available support is silica. In this thesis, efforts have been made to anchor ECE-pincer metal complexes on silica surfaces (both amorphous and structured silica) and to use the resulting systems in catalysis. *Chapter 1* provides an overview of the various approaches to immobilize homogeneous catalysts on to silica support. *Chapter 2* describes the synthesis of various *para*-OH functionalized ECE-pincer metal complexes and their functionalization with a siloxane tether in order to immobilize them on silica. In *Chapters 3* and *4*, these complexes are immobilized on various silicas, ordinary as well as mesoporous materials such as MCM-41 and SBA-15. The resulting hybrid materials have been used in an aldol condensation reaction and their recovery and reuse was investigated. *Chapters 5* and *6* provide details of the role that the various ECE-pincer metal catalysts play in the aldol condensation reaction and a new catalytic mechanism is proposed. In *Chapter 7*, the synthesis of a novel PCS-pincer palladium complex is described along with its activity in the aldol reaction. Finally, the involvement of silver-based reagents as catalysts in the aldol reaction is discussed in *Chapter 8*.

Self-assembly and polymerization of para-OH functionalized ECE-metalated pincer complexes (Chapter 2)

The synthesis of various *para*-OH functionalized ECE-pincer palladium and platinum complexes [MX(ECE-OH)L_n] (ECE-OH = $[C_6H_2(CH_2E)_2$-2,6-OH-4$]^-$) is described. The X-ray crystal structures of neutral [PdCl(SCS-OH)] and [PdCl(NCN-OH)] halide complexes show how these complexes

self-assemble to form polymeric chains *via* non-covalent H-bonding involving the *para*-OH group and the halide ligand on the metal (Figure 1, structure **A**). Alternatively, the halide ligand can be replaced by a monodentate aryloxy-O ligand, produced as a result of HCl elimination from [PdCl(ECE-OH)], leading to the formation of dimer **B** (Figure 1) as proven by X-ray crystallography.

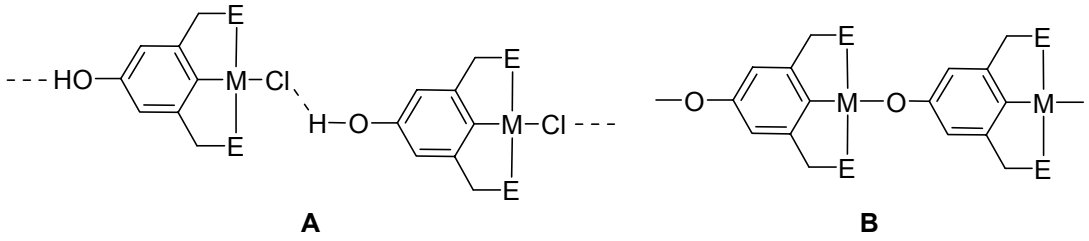

Figure 1

The *para*-OH functionalized pincer-metal complexes have also been tethered at the *para*-position through a carbamate linker to a siloxane functionality with the aim to immobilize the resulting species *via* the siloxane grouping on a silica support.

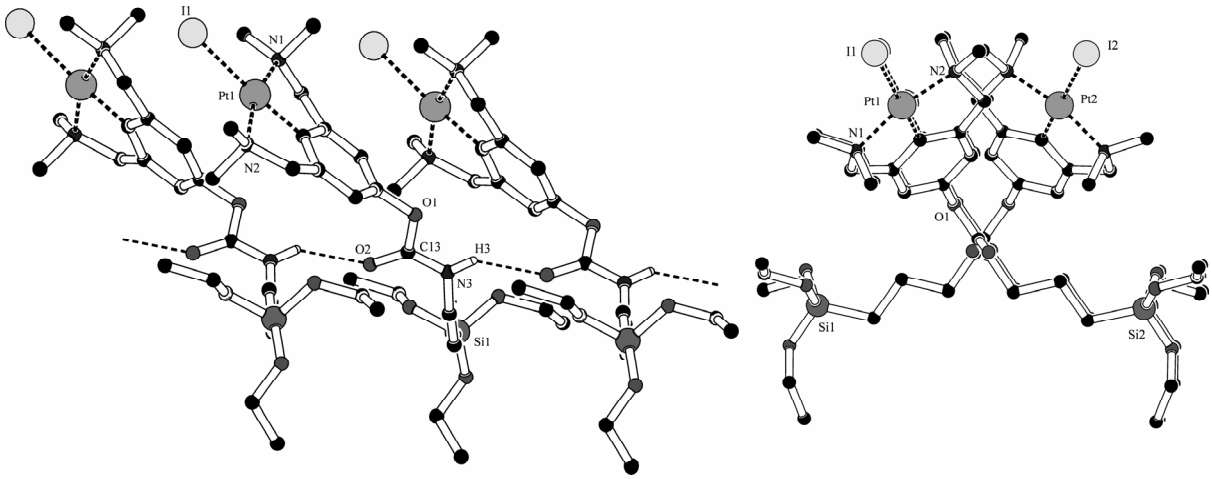

Figure 2

The X-ray structure of a siloxane-functionalized [PtI(NCN-Z)] complex exemplifies how other H-bonding interactions, not involving the metal-halide, but the carbamate groupings, can also lead to polymeric networks (Figure 2).

Silica immobilized ECE-pincer palladium(II) and platinum(II) complexes: application as Lewis acid catalysts (Chapters 3 and 4)

The trialkoxysilane-tethered NCN-pincer Pd(II) and Pt(II) complexes developed in *Chapter 2* have been immobilized on various types of silica using either a grafting or a sol-gel process. In an analogous manner, PCP- and SCS-pincer palladium(II) complexes were also immobilized on the ordered mesoporous silicas SBA-15 and MCM-41 using a grafting process. The resulting hybrid materials were characterized by IR spectroscopy (DRIFT) and solid state CP/MAS NMR (^{13}C and

[29]Si). The palladium-based materials were tested for their activity as Lewis acid catalysts in the aldol condensation reaction between methyl isocyanoacetate (MI) and benzaldehyde (Figure 3).

It was found that NCN- and SCS-pincer based materials have an inferior catalytic efficacy upon repetitive use. This is presumably caused by reconstitution of the amorphous silica support and/or the instability of their MI-insertion complexes, which are formed under the employed reaction conditions (*vide infra*). In contrast, SBA-15 modified with the PCP-pincer Pd-complex can be used up to five runs without any loss of activity (in fact this pincer-metal complex does not undergo insertion of MI). The results of control experiments established the anticipated heterogeneous nature of this hybrid catalyst in this reaction. These findings illustrate the synergic effect of using both a stable catalyst and a robust support. N_2 adsorption data, XRD, and TEM/EDX analyses of the hybrid materials revealed that the mesoporous structure of these materials is retained during the immobilization process as well as during catalysis.

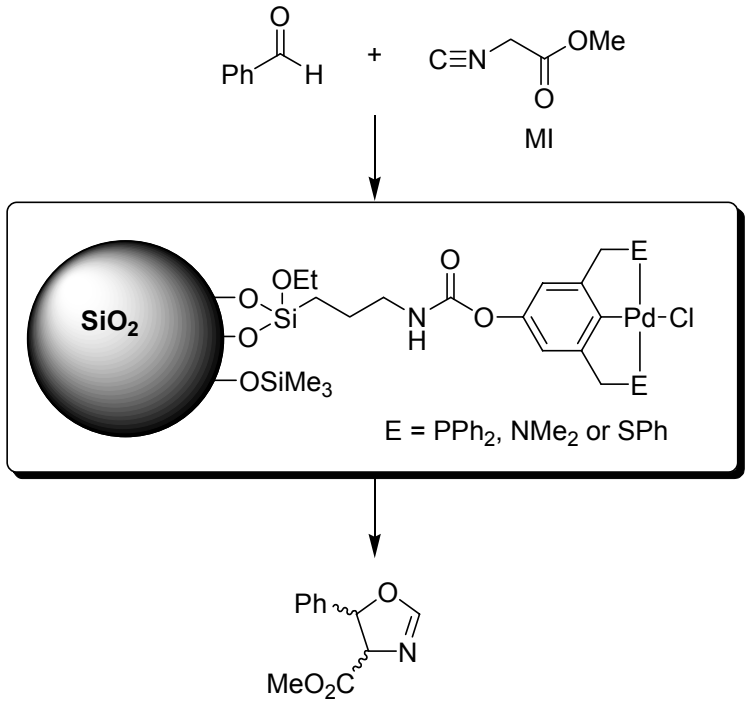

Figure 3

Insertion of methyl isocyanoacetate in the M–C bond of ECE-pincer metal-d^8 complexes: reaction mechanism and importance in aldol condensation reactions involving isocyanides (Chapter 5 and 6)

In order to design a better catalyst for a given reaction, it is important to understand the mechanism by which the catalytic reaction is taking place. To improve the performance of ECE-pincer complexes in the aldol reaction in Figure 3, the reactivity of these complexes towards isocyanides was investigated. It appeared that both NCN- and SCS-pincer palladium halide complexes undergo a 1:1 insertion reaction with isocyanides, where the isocyanide inserts into the C_{ipso}–M bond forming an imidoyl-metal moiety (Figure 4). The metal coordination sphere is complemented by an MI ligand and a halide or a second MI

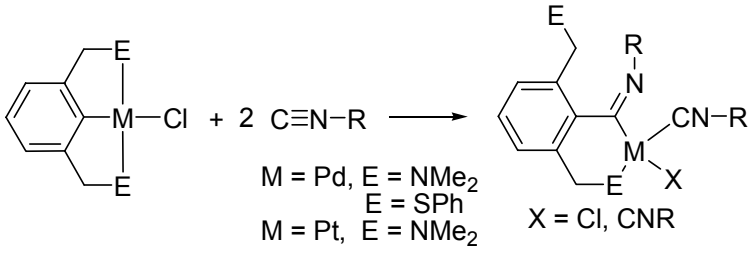

Figure 4

ligand. In contrast, the reaction of PCP-pincer palladium(II) chloride with MI stops at the stage of the formation of a [Pd(PCP)(MI)]Cl coordination complex, *i.e.*, in this case the isocyanide displaces the halide ligand and subsequent isocyanide insertion does not occur.

A mechanism for the insertion reaction is proposed based on theoretical calculations. It involves prior coordination of the isocyanides to the metal by ligand exchange with one or both of the coordinating amino or thioether donor arms of the NCN- or SCS-pincer ligand, respectively, followed by isocyanide insertion into the M–C bond. The X-ray crystal structure of the dimeric insertion product derived from the reaction of [PdCl(SCS)] with MI is reported.

These findings have consequences for the understanding of the different Lewis acidic properties of the various ECE-metal complexes when used as catalysts in the aldol condensation reaction of MI with benzaldehyde to give oxazolines. In the case of the NCN- and SCS-pincer complexes, the 1:1 imidoyl-metal insertion products are the actual catalysts for this reaction, whereas catalysis with the PCP-pincer palladium complex involves a cationic PCP-pincer palladium complex. The reactivity of various ECE-pincer palladium complexes as Lewis acid catalysts and pre-catalysts in the aldol reaction was studied in *Chapter 6*. These studies show the higher catalytic activity of the SCS-pincer complexes as compared to their NCN- and PCP-pincer analogues. A small, but distinct substituent effect of the *para*-substituent Z in [PdCl(NCN-Z)] complexes on the reaction rate points to the release of the oxazoline product as the overall rate determining step. Most importantly, these studies point out that catalyst activation, i.e. halide abstraction, is not required for the ECE-pincer Pd-complexes to act as catalysts in the aldol reaction.

A PCS-pincer palladium complex: insertion of methyl isocyanoacetate and catalytic aldol reactivity (Chapter 7)

A new type of pincer complex [PdCl($C_6H_3(CH_2PPh_2)$-2-(CH_2SPh)-6)] ([PdCl(PCS)]) was synthesized (Figure 5). Structurally and electronically as well as topologically this complex can be seen as a hybrid between PCP- and SCS-pincer complexes as was concluded from NMR analysis. The [PdCl(PCS)] complex acts as a pre-catalyst in the aldol reaction between MI and benzaldehyde. It is proposed that this complex initially undergoes the insertion reaction with MI by selective release of the S-donor arm from palladium. The resulting imidoyl-Pd complex then acts as the catalyst. The catalytic activity of this complex is superior over the symmetric SCS-, PCP- and NCN-pincer palladium complexes.

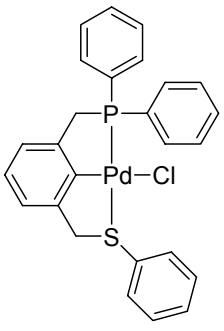

Figure 5

Reactivity of simple (in)soluble silver(I) salts in an isocyanide aldol reaction (Chapter 8)

Silver-based reagents such as $AgBF_4$ and AgOTf are widely used to form cationic metal centers by the abstraction of a halide ligand from, *e.g.*, neutral pincer-metal complex. In the case of soluble

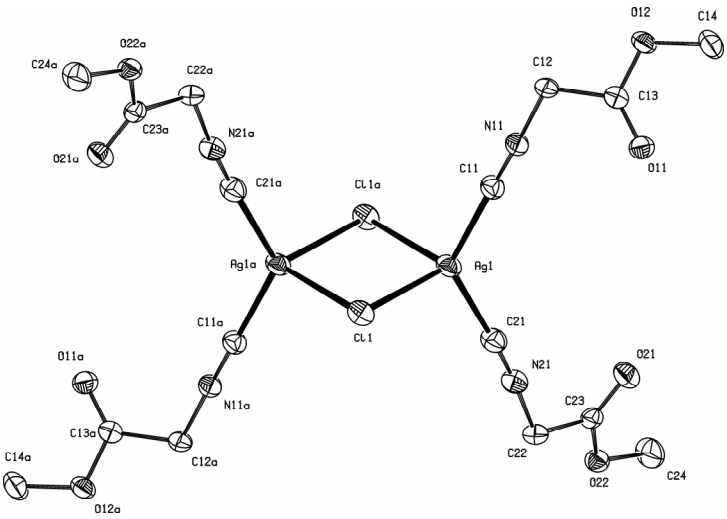

Figure 6

complexes, separation of the insoluble AgCl by-product is possible. In the case of insoluble or immobilized pincer-metal complexes, it is difficult to remove all AgCl. We have now found that in fact insoluble AgCl does act itself as a highly active catalyst in the aldol reaction between MI and benzaldehyde. A dimeric complex of the type $[Ag_2Cl_2(MI)_4]$ was isolated from the reaction of AgCl with MI. X-ray crystallographic analysis revealed a dimeric structure in which two silver ions are bridged by two chloride ions forming a four-membered ring (Figure 6). Each silver ion is further coordinated by two MI molecules in this structure.

Subsequently, various silver salts have been employed as catalysts in the aldol condensation reaction and were found to give an initial TOF above 70 h^{-1}. These findings highlight that Ag-salts are active catalysts for this reaction and puts a question mark on the use of these reagents for the activation of pre-catalysts (*e.g.* of ECE-pincer metal complexes) used for this reaction.

Samenvatting

De wetenschap streeft continu naar een duurzame vooruitgang van de samenleving. Deze vooruitgang moet afgewogen worden op zowel economisch als ecologisch aspecten. Veel industriële processen worden herzien om ze ecologisch duurzamer te maken. Katalysatoren ontpoppen zich als een belangrijke speler om dit doel te bereiken. Geen wonder, ongeveer 85% van de huidige chemische processen maken gebruik van katalysatoren. Hiervan is 75% gebaseerd op heterogene katalyse vanwege het voordeel van een eenvoudige afscheiding van de productstroom en van het recyclen en hergebruiken van de katalysator. Aan de andere kant zijn homogeen katalytische systemen superieur in termen van activiteit en selectiviteit, in het bijzonder in enantioselectieve processen. Deze homogene katalysatoren bestaan over het algemeen uit een overgangsmetaal omringd door ingenieus ontworpen (chirale) ligandsystemen om zodoende de katalysatoreigenschappen te optimaliseren. Dikwijls maakt dit homogene katalysatorsystemen duur en daardoor wordt recycling en hergebruik een vereiste voor hun toepassing. Een oplossing om dit te bereiken is het immobiliseren van de homogene katalysator op een onoplosbare drager, d.w.z. het heterogeniseren van de homogene katalysator. Een goedkoop en ruimschoots beschikbare drager is silica. Dit proefschrift beschrijft studies naar de koppeling van ECE-tang-metaalcomplexen aan een silica-oppervlakte (zowel amorf als gestructureerd silica) en het gebruik van dergelijke hybride systemen in katalyse. *Hoofdstuk 1* geeft een overzicht van diverse benaderingen m.b.t. het immobiliseren van homogene katalysatoren op een silica-oppervlak. *Hoofdstuk 2* beschrijft de synthese van diverse *para*-OH gefunctionaliseerde ECE-tang-metaalcomplexen en hun modificatie met een siloxaaneenheid om ze te kunnen immobiliseren. In de *hoofdstukken 3* en *4* zijn deze complexen geïmmobiliseerd op diverse soorten silica, amorfe alsmede mesoporeuze materialen zoals MCM-41 en SBA-15. De resulterende hybridematerialen zijn gebruikt in een aldol-condensatiereactie. Ook het terugwinnen en hergebruiken van de materialen is onderzocht. *Hoofdstukken 5* en *6* geven details over de rol die diverse ECE-tang-metaalkatalysatoren spelen in aldol-condensatiereacties. Bovendien wordt een nieuw katalytisch mechanisme voorgesteld. In *hoofdstuk 7* wordt de synthese van een nieuw PCS-tang-palladiumcomplex beschreven, tezamen met diens activiteit in de aldolreactie. In *hoofdstuk 8* wordt het gebruik van zilver-gebaseerde reagentia als katalysatoren in de aldolreactie besproken.

Zelf-organisatie en polymerisatie van para-OH-gefunctionaliseerde ECE-tang-metaalcomplexen (Hoofdstuk 2)

De synthese van diverse *para*-OH-gefunctionaliseerde ECE-tang-palladium- en platinacomplexen $[MX(ECE\text{-}OH)L_n]$ (ECE-OH=$[C_6H_2(CH_2E)_2$-2,6-OH-4$]^-$) is beschreven. De Röntgen kristalstructuren van de neutrale [PdCl(SCS-OH)] en [PdCl(NCN-OH)] halide complexen laten zien hoe deze complexen zichzelf organiseren in polymere ketens via niet-covalente H-bindingen tussen de *para*-OH-groep en het halideligand op het metaal (Figuur 1, structuur **A**).

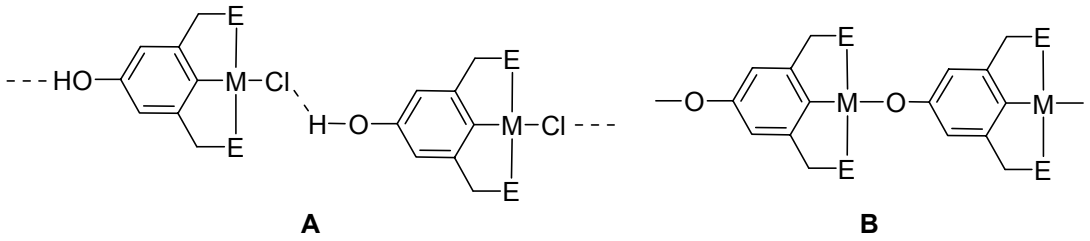

Figuur 1

Daarnaast kan het halideligand worden vervangen door een monodentaat aryloxy-O-ligand, verkregen als gevolg van HCl-eliminatie van [PdCl(ECE-OH)], wat leidt tot de vorming van dimeer **B** (Figuur 1) zoals bewezen door röntgenkristallografie.

De *para*-OH-gefunctionaliseerde tang-metaalcomplexen zijn op de *para*-positie tevens via een carbamaatspacer verbonden met een siloxaanfunctionaliteit om zodoende de verkregen verbindingen te immobiliseren op een silicaat-oppervlak. De Röntgenstructuur van een siloxaan-gefunctionaliseerd [PtI(NCN-Z)]-complex illustreert hoe andere H-bindingen, die niet betrokken zijn bij het metaal-halide maar bij het carbamaat-gedeelte, kunnen leiden tot polymere netwerken (Figuur 2).

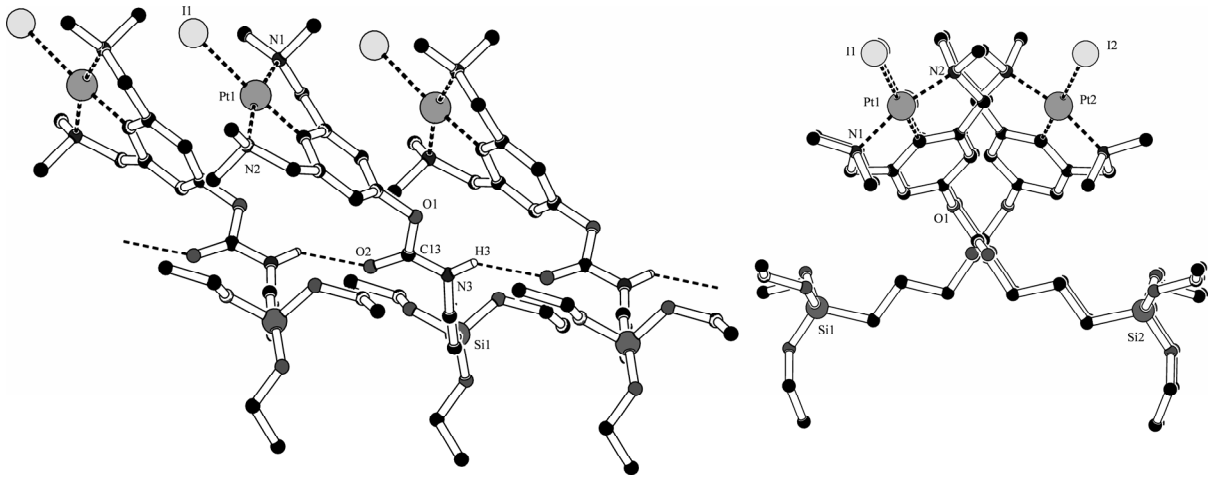

Figuur 2

Silica-geïmmobiliseerde ECE-tang-palladium(II)- en platina(II)complexen: toepassing als Lewis-zure katalysator (Hoofdstuk 3 en 4)

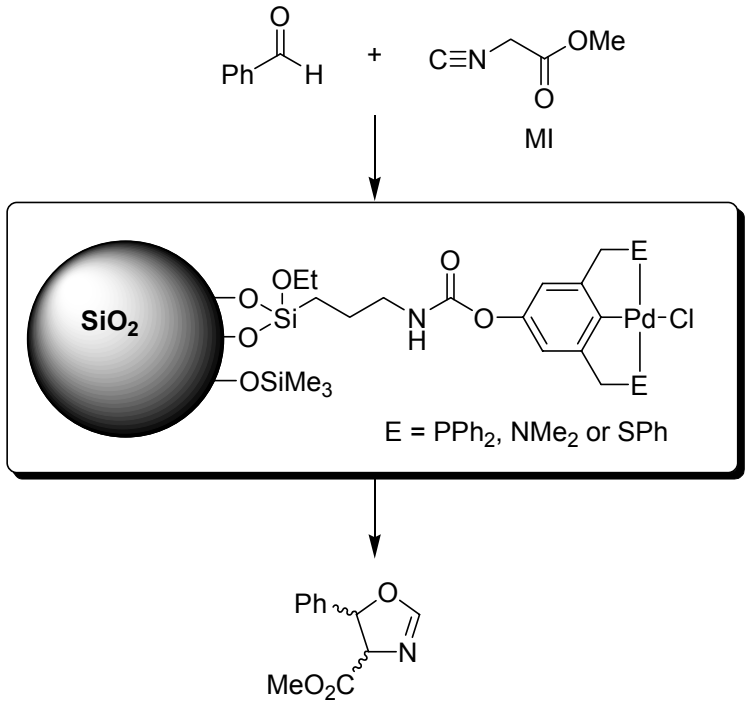

Figuur 3

De trialkoxysilane-gefunctionaliseerde NCN-tang-Pd(II)- en Pt(II)complexen ontwikkeld in *hoofdstuk 2* zijn geïmmobiliseerd op diverse types silica via "grafting" of via de "sol-gel" methode. Op analoge wijze zijn PCP- en SCS-tang-palladium(II)-complexen geïmmobiliseerd op de mesoporeuze silicas SBA-15 en MCM-41. De resulterende hybridematerialen zijn gekarakteriseerd met IR-spectroscopie (DRIFT) en vaste stof CP/MAS NMR (^{13}C and ^{29}Si). De palladium-gebaseerde materialen zijn getest op hun activiteit als Lewis-zure katalysatoren in de aldol-condensatiereactie tussen methyl isocyanoacetaat (MI) en benzaldehyde (Figuur 3). De NCN- en SCS-tang-gebaseerde materialen bleken een verminderde katalytische activiteit te hebben bij herhaaldelijk gebruik. Dit wordt waarschijnlijk veroorzaakt door de reconstitutie van het amorfe silica-oppervlak en/of de instabiliteit van hun MI-insertiecomplexen, die zijn gevormd worden onder de gehanteerde reactiecondities (*vide infra*). In tegenstelling tot deze materialen kan SBA-15 gemodificeerd met het PCP-tang-Pd-complex minstens 5 keer gebruikt worden zonder verlies van de activiteit (feitelijk ondergaat dit tang-metaal complex niet de insertie van MI als een nevenreactie). De resultaten van controle-experimenten bevestigen de verwachte heterogene aard van deze hybridekatalysator in deze reactie. Deze bevindingen illustreren de synergetische effecten van het benutten van zowel een stabiele katalysator als een robuust dragermateriaal. N_2-absorptie gegevens en XRD en TEM/EDX analyse van de hybridematerialen onthullen dat de mesoporeuze structuur van deze materialen behouden blijft tijdens zowel de immobilisatie als de katalyse.

Insertie van methyl isocyanoacetaat in de M–C binding van ECE-tang-d^8-metaalcomplexen: reactiemechanisme en implicaties voor aldol-condensatiereacties met betrekking tot isocyanides (Hoofdstuk 5 en 6)

Om een betere katalysator te ontwerpen voor een bepaalde reactie is het belangrijk het mechanisme van de katalytische reactie te begrijpen. Ter verbetering van de gekatalyseerde aldolreactie in Figuur 3 is de reactiviteit van ECE-tang-palladiumcomplexen met isocyanides onderzocht. Het bleek dat zowel NCN- als SCS-tang-palladium-halidecomplexen een 1:1 insertie met isocyanides ondergaan, waarbij het isocyanide inserteert in de C_{ipso}–M binding om zodoende een imidoyl-metaalcomplex te vormen (Figuur 4). De Pd-coordinatiesfeer in het resulterende complex wordt verder gevuld door een MI-ligand en een halide of tweede MI-ligand. In tegenstelling tot de NCN- en SCS-complexen stopt de reactie van PCP-tang-palladium(II)chloride met MI bij het vormen van een Pd(PCP)(MI)]Cl coördinatie-complex, d.w.z. in dit geval vervangt de isocyanide het halide en vervolgens blijft de isocyanide insertie achterwege. Een mechanisme voor de insertiereactie is voorgesteld op basis van theoretische berekeningen. In dit mechanisme vindt eerst coordinatie van de isocyanide(s) aan het metaal plaats door liganduitwisseling met één of twee van de coördinerende amino- of thioetherarmen van het NCN- of SCS-tangligand, gevolgd door isocyanide-insertie in de M–C binding. De Röntgen kristalstructuur van het dimere insertieproduct verkregen uit de reactie van [PdCl(SCS)] met MI is beschreven.

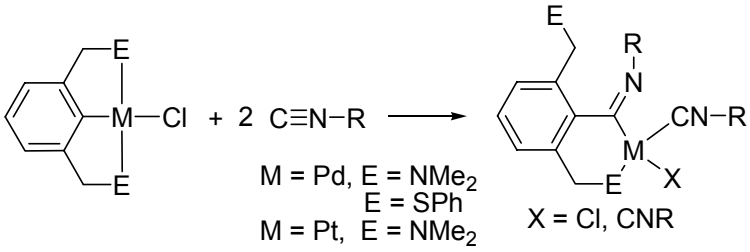

Figuur 4

Deze bevindingen hebben consequenties voor het begrijpen van de verschillende Lewis-zure eigenschappen van de diverse ECE-metaalcomplexen als katalysatoren in de aldol-condensatiereactie van MI met benzaldehyde tot oxazolines. In het geval van de NCN- en SCS-tangcomplexen zijn de 1:1 imidoyl-metaalinsertieproducten de eigenlijke katalysatoren voor deze reactie, terwijl katalyse met het PCP-tang-palladiumcomplex een kationisch PCP-tang-palladiumcomplex betreft. De reactiviteit van diverse ECE-tang-palladiumcomplexen als Lewis-zure katalysatoren en pre-katalysatoren in de aldol reactie is bestudeerd in *hoofdstuk 6*. Deze studies tonen de hogere katalytische activiteit van de SCS-tangcomplexen in vergelijking met de NCN- en PCP-analogen. Een klein, maar duidelijk substituenteffect van de *para*-substituent Z in [PdX(NCN-Z)] op de reactiesnelheid wijst op het vrijmaken van het oxazolineproduct als de overall snelheidsbepalende stap. Wat deze studies vooral aantoonden is dat katalysatoractivering, d.w.z. halide-abstractie, niet vereist is voor ECE-tang-palladiumcomplexen om als katalysator te kunnen fungeren in aldolreacties.

Een PCS-tang-palladiumcomplex: insertie van methyl isocyanoacetaat en reactiviteit in de aldolreactie (Hoofdstuk 7)

Een nieuw type tangcomplex [PdCl(C_6H_3(CH_2PPh_2)-2-(CH_2SPh)-6)] ([PdCl(PCS)]) is gesynthetiseerd (Figuur 5). Zowel structureel als electronisch en topologisch kan dit complex worden gezien als een hybride tussen PCP- en SCS-tang complexen, zoals werd aangetoond met NMR-spectroscopie. Het [PdCl(PCS)]-complex fungeert als een pre-katalysator in de aldolreactie tussen MI en benzaldehyde. Voorgesteld wordt dat dit complex aanvankelijk de insertiereactie met MI ondergaat door selectieve decoördinatie van de S-donorarm van palladium. Het resulterende imidoyl-Pd-complex treedt dan op als de katalysator. De katalytische activiteit van dit complex is beter dan van de symmetrische NCN-, SCS- en PCP-tangcomplexen.

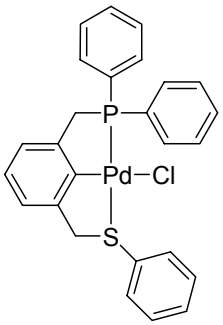

Figuur 5

Reactiviteit van eenvoudige (on)oplosbare zilver(I)zouten in een isocyanide aldol condensatie (Hoofdstuk 8)

Zilver-gebaseerde reagentia zoals $AgBF_4$ en AgOTf worden veelvuldig gebruikt om kationische metaalcentra te vormen door het abstraheren van een halideligand van neutrale tang-metaalcomplexen. In het geval van oplosbare complexen, afscheiding van het onoplosbare AgCl-bijproduct is mogelijk. In het geval van onoplosbare of geïmmobiliseerde tang-metaalcomplexen is het moeilijk alle AgCl van het tang-metaalcomplex te scheiden. Uit controle-experimenten is nu gebleken dat onoplosbaar AgCl zelf optreed als zeer actieve katalysator in de aldolreactie tussen MI en benzaldehyde. Een dimeer complex van het type [$Ag_2Cl_2(MI)_4$] werd geïsoleerd uit de reactie van AgCl met MI. Röntgen-kristallografische analyse onthulde de dimere structuur, waarbij twee zilverionen zijn gebrugd door twee chloorionen waarbij een vier-ring gevormd wordt (Figuur 6). Elk zilver ion is tevens gecoördineerd door twee MI-moleculen. Vervolgens zijn diverse zilverzouten gebruikt als katalysatoren in de aldol-condensatiereactie en bleken een TOF boven 70 h^{-1} te geven. Deze bevindingen benadrukken dat zilverzouten zeer actieve katalysatoren zijn voor deze reactie en roepen vraagtekens op bij het gebruik van deze reagentia voor de activering van pre-katalysatoren (bijv. van ECE-tang-metaalcomplexen) gebruikt voor deze reactie.

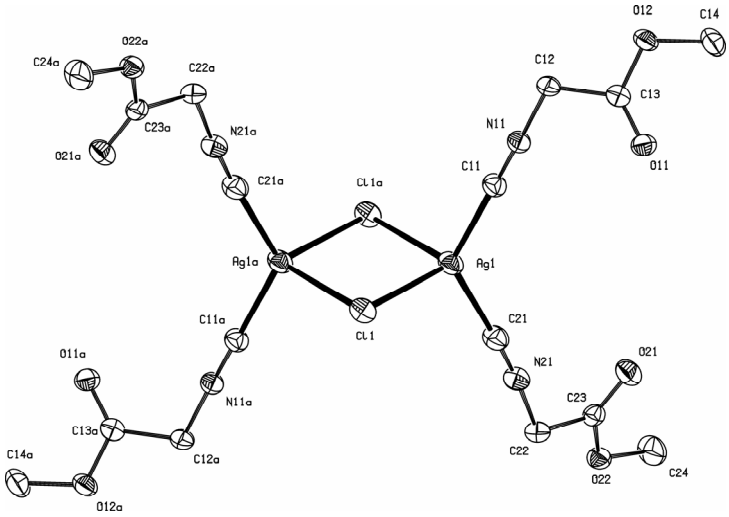

Figuur 6

Graphical Abstract

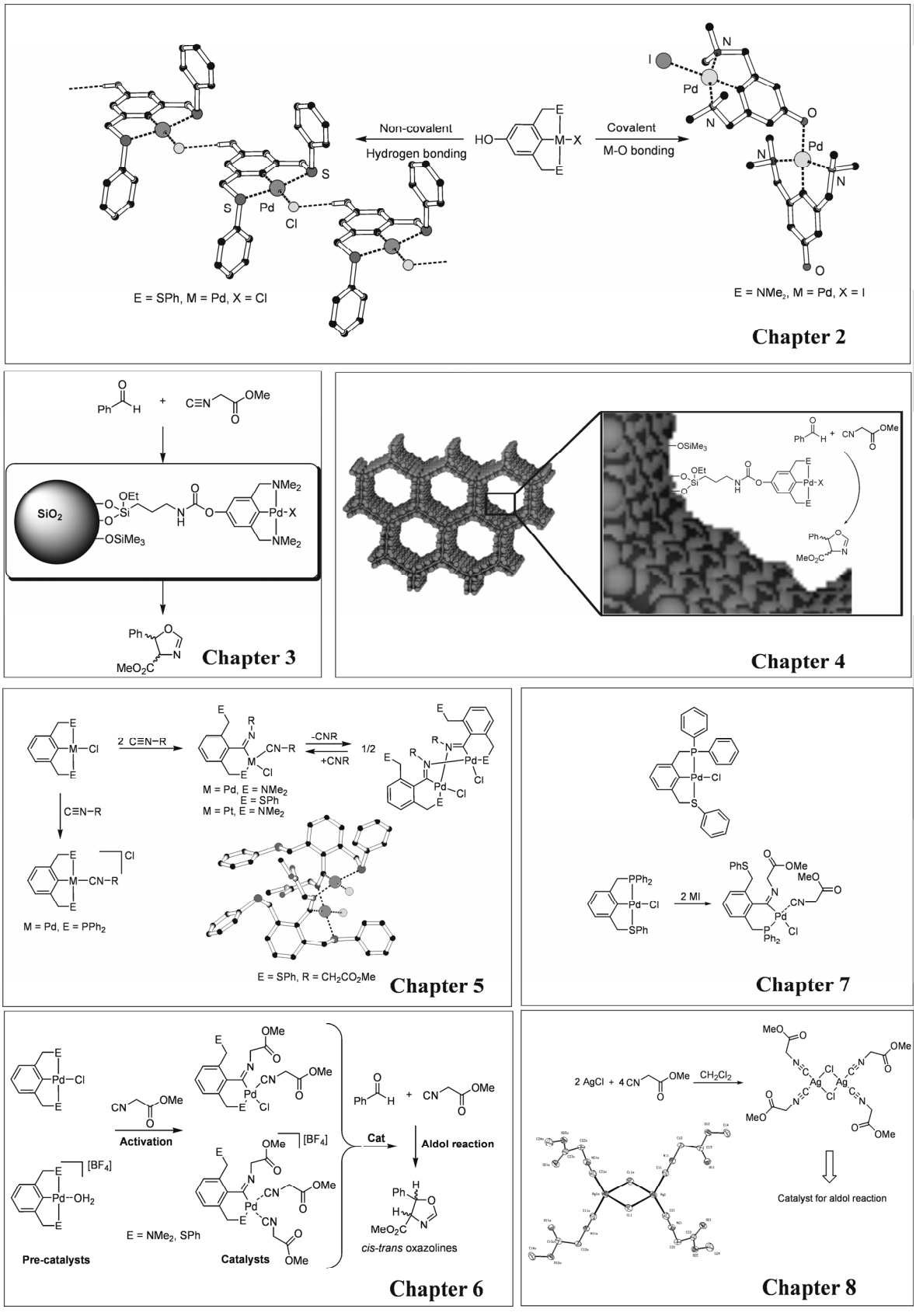

Acknowledgements

It is a great pleasure to write the final pages of acknowledgements. The period of Ph.D. has brought a lot of ups and downs in my life. Without the help of many people, inside as well as outside the lab, it would have been impossible to overcome difficulties and to reach at this stage of writing "dankwoord".

First of all, I would like to express my sincere thanks to prof. dr. Gerard van Koten and prof. dr. Robertus Klein Gebbink, my supervisors. Dear Gerard, it was a wonderful period of learning, not only scientific aspect but also management of my work in Utrecht. You constantly inspired me in my work and gave complete freedom to perform new experiments which resulted in this thesis. I hope to benefit from your knowledge in future as well. Dear Bert, your help in the absence of Gerard was equally valuable. In the day-to-day business, you were always around to guide me. It was most helpful of you to go through my manuscripts many times to attain the current state of my book.

I would also like to thank other members of the "van Koten" group for their advice and guidance, dr. Gerard van Klink, dr. Johann Jastrzebski, dr. Berth-Jan Deelman, and dr. Jaap Boersma. Dear Henk Kleijn and Peter Wijkens, thank you for your assistance in the lab. The secretaries of the group have been very important in managing the activities within the group. Dear Margo, thank you very much for your help in administrative work. Especially, during my first days in the Netherlands, your help was extremely useful in arranging many documents and housing. I would also like to thank Milka Westbeek for her help in communication and exchange of manuscripts during my thesis completion. I also appreciate assistance from Hester and Thea Pozzi on various occasions.

During my tenure in Utrecht, I had an opportunity to collaborate with two groups. I would like to acknowledge prof. dr. Albert Philipse from Physical and Colloid Chemistry group for his guidance in the project on magnetic silica colloids. Dear Karen Butter, it was a lot of fun to work with you on this project. Also, thank you for your help during my early days in Utrecht and for making me familiar with the new city. Dear Maria Claesson, thank you for the contribution in the final stages of the project. I enjoyed very much working with you on the project and also the discussions on chemistry and Sweden and India.

I would like to acknowledge prof. dr. Krijn de Jong from Inorganic Chemistry and Catalysis group for his help on the project which resulted in chapter 4 of this thesis. Also, your talks in various conferences and in the NIOK school were very inspiring and informative. Dear Jelle Sietsma, our collaboration resulted in not only a nice chapter but also a lot of knowledge in the field of

heterogeneous catalysis. Apart from the collaboration, our friendship has continued despite the Groningen-Utrecht distance.

I would like to thank dr. Martin Lutz and prof. dr. Anthony Spek from Crystal and Structural Chemistry group for their help on X-ray crystal structure determination. Dear Martin, thanks a lot for your special efforts on my manuscripts at such a short notice.

I sincerely thank Hans Meeldijk for his help in TEM analysis of some of my silica samples. My sincere thanks to Dr. Kees van Walree from Physical Organic Chemistry group and Dr. Johan Hollander from Leiden University for their help in Solid-State NMR analysis of my silica samples.

I would also like to thank dr. Remco Havenith from Theoretical Chemistry group for his contribution in chapter 5 of this thesis. Dear Remco, it was very informative to discuss my chemistry from organic and theoretical point of view. I learnt a lot from our collaboration.

I wish to thank my students, Rik, Robert-Jan and Alfred who helped me on various projects. The team work offered us a good opportunity to learn from each other about chemistry and other subjects such as gliding and parachute diving.

Special thanks are due to Jan den Boesterd, Ingrid van Rooijen and Aloys Lurvink for their help in preparing various posters and designing the cover of this book. Also very special thanks to Mr. Vijay Gavhankar for the beautiful painting on the cover of this book.

It was very important to have glass-blowing and mechanical workshop close to hand. Their prompt help in providing and repairing various glass-wares and instruments was crucial in daily experimental work.

The day-to-day help extended by my colleagues was the most important in completing the lab-work for this thesis. I would like to thank all of them; from the south wing, Kees, Aidan, Alexey, Monika, Patrick, Harm, Elwin, Sander, Joep, Michel, Scott, Martijn, Gabriella, Marcella, Pieter, Silvia, Judith, Jeroen, Rob C., Rob K., Catelijne, Jie and from the west wing, Anne, Gema, Guido, Bart, Preston, Sipke, Marianne, Alexandro, Serenella, and Elena.

Dear Kees, we started on this mission together and faced many difficulties along the way. And here we are finally at the end of our endeavor. Wish you a great success in your future career. Dear Marianne, you and Ruben have been very helpful in more than one ways. Your company, not only in the lab, but also in kitchen performing interesting experiments is memorable for both me and Meenal. Dear Erwin, we shared the train journey for almost two years. We learnt and enjoyed so much from each other that a strong bond of life-long friendship is developed. I am very happy to have you as my “paranimf”.

Working at Syncom has been full of good experiences and life in Groningen has been a lot of fun, thanks to my colleagues and friends at Syncom. Particularly, I would like to mention my labmates Bart-Jan, Ronald, Oscar, Han, and Maarten. Dear Anja, Jessica, Niels, and Marcel, it has been a lot of fun at jogging, squash and drinks thereafter.

I would like to thank my numerous teachers from New English School and Vartak College in Vasai and Balmohan Vidyamandir in Mumbai whose contribution has been important in building my career. Particular mention must be made of Dr. Chikate, Dr. Kale and Rahul Pungaliya from Garware College, Pune, Dr. Gejji, Dr. Kulkarni and Dr. Dhavale from Pune University and Dr. Sarkar from NCL. My special gratitude is to dear Appa Barve (Vasai) whose teachings about life during the lessons on French language have been most important. Dear Appa, your book "Affidavit" has been a source of inspiration for me. This story of your life as a freedom-fighter, a social worker, a scientist, a farmer and a teacher has lessons on every page.

My family in the Netherlands has helped me in all possible ways during my stay here and made my weekends and holidays enjoyable. Dear Marcel, Pramod and Kanutje, you helped me to settle in the new country and were always available when I needed the family support. Lieve Gerrit en Truus, bedankt voor jullie rol als mijn Nederlandse opa en oma. Jullie liefde en steun was erg belangrijk om zo ver te komen. Dear Sameer, Jolla, Manutje and Sujata, it was fun to visit you in vibrant Amsterdam and spend peaceful time in Lurcy-Lévis, France.

माझ्या आयुष्यातील पीएच्. डी. मिळवण्याच्या यशात, या महत्त्वाच्या क्षणी, मित्र आणि नातेवाइकांचा सर्वात मोठा सहभाग आहे. प्रिय प्रशांत-भावना आणि करिष्मा, तुमची मैत्री आणि आपले पत्त्यांचे डाव हॉलंडमधल्या वास्तव्यातील सुखदायक अनुभव व आठवणी आहेत. इथून पुढील आयुष्यात असेच अनेक सुंदर दिवस तुमच्याबरोबर अनुभवण्याचा योग येत रहावा. प्रिय गौतम, आपली मैत्री एक आयुष्याचे नाते आहे. तुझ्या मैत्रीचा आधार, इथे हॉलंडमधेही मला सतत होता. कामानिमित्त दुरावलेले आपण पुन्हा एकत्र येऊ अशी मी आशा करतो.

भारतातील माझ्या सर्व नातेवाइकांचे मला भरपूर प्रेम लाभले. लहानपणापासून माझी काळजी घेणाऱ्या मावश्या आणि काका-काकू या सर्वांचा माझ्या इथवरच्या प्रवासात प्रेमळ हातभार आहे.

प्रिय आई, बाबा आणि विशाल, तुम्ही माझ्या आयुष्यात आल्यापासून तुमचा सहभाग अत्यंत आनंददायक आहे. दूर असून देखील आपल्या नात्यात एका कुटुंबाची आत्मियता आहे ती तुम्ही मला दिलेल्या प्रेमामुळेच.

प्रिय आजी व अण्णा, लहानपणापासून आई व पप्पांइतकीच तुम्ही माझी काळजी घेतली आहेत. आजपर्यंत, तुमच्याकडून मी अनेक गोष्टी शिकलो, व आयुष्याच्या अनेक महत्त्वाच्या वळणांवर तुमच्या प्रेमाचा आधार मला सतत मिळाला आहे.

प्रिय निखिल, आई व पप्पा, हे पुस्तक माझ्या आयुष्यातील अतिशय महत्त्वाचा टप्पा आहे. हा व इतर अनेक टप्पे तुमच्याशिवाय शक्यच झाले नसते. निखिल व माझ्या संगोपनावर व शिक्षणावर तुम्ही घेतलेल्या अनेक कष्टांची फळे आज आम्ही उपभोगत आहोत.

प्रिय मीनल, सहा वर्षांपूर्वी आपण दोघे आयुष्यातील महत्त्वाच्या वळणावर एकत्र आलो. या प्रवासात अनेक अडचणी व अनेक सुंदर आठवणी आपण एकत्र अनुभवल्या. आज आपल्या दोघांची स्वप्ने पूर्ण होत आहेत. तुझ्याशिवाय हे कसे शक्य झाले असते याचा मी विचारही करु शकत नाही. पुढील आव्हानांना आज आपण दोघेही समर्थपणे नव्या जोमाने सामोरे जाण्यास तयार आहोत.

नीलेश

Nilesh

Curriculum Vitae

The author of this thesis was born on 1st August 1975 in Baramati, India. After the completion of his school education in Mumbai and a three-year experience in the Merchant Navy, he graduated with a distinction in Chemistry from M.E.S. Garware College, Pune in 1998, followed by a Master of Science degree with a distinction from Pune University in 2000. During his M.Sc., he also qualified for the JRF from CSIR and passed the NET examination. He started his Ph.D. study at Utrecht University in 2001 in the group of Prof. Dr. Gerard van Koten under the supervision of Prof. Dr. R. J. M. Klein Gebbink. His research activities focused on the immobilization of pincer-type metal complexes on silica and their use in catalysis and culminated in this thesis. The project was financially supported by the Dutch Technology Foundation STW and by Utrecht University.

During his Ph.D. tenure, the author followed several courses including courses on Advance Catalysis Engineering (Delft, 2003), X-ray crystallography (Utrecht, 2003), Integrated Catalysis (NIOK, Schiermonnikoog, 2001), and various schools organized by the former Debye Institute of Utrecht University. Parts of the work published in this thesis have been presented at national and international meetings and conferences like ISHC (Munich, 2004), COST Meeting (Uppsala, 2004), NCCC (III-VI, Noordwijkerhout, 2002-2005), NRSC-C workshops, Gratama Workshop (Utrecht, 2003), and van der Kerk Symposium (Utrecht, 2002). He supervised three Master's students in their research projects during his tenure in Utrecht University.

From 1st July 2005, the author is working as a research scientist at Syncom B.V. in Groningen.

List of Publications

Novel Silica Immobilized NCN-Pincer Palladium(II) and Platinum(II) Complexes: Application as Lewis Acid Catalysts
Nilesh C. Mehendale, Chris Bezemer, Cornelis A. van Walree, Robertus J. M. Klein Gebbink and Gerard van Koten, *J. Mol. Catal. A* **2006**, 257, 167-175.

Magnetic Silica Colloids for Catalysis
E. Maria Claesson, Nilesh C. Mehendale, Robertus J. M. Klein Gebbink, Gerard van Koten, and Albert P. Philipse, *J. Mag. Mag. Mater.*, **2006**, accepted.

Self-Assembly and Polymerization of Para-OH Functionalized ECE-Metalated Pincer Complexes
Nilesh C. Mehendale, Martin Lutz, Anthony L. Spek, Robertus J. M. Klein Gebbink and Gerard van Koten, manuscript in prep.

PCP- and SCS-Pincer Palladium Complexes Immobilized on Mesoporous Silica: Application in C–C Bond Formation Reactions
Nilesh C. Mehendale, Jelle R. A. Sietsma, Krijn P. de Jong, Robertus J. M. Klein Gebbink and Gerard van Koten, manuscript in prep.

Insertion of Methyl Isocyanoacetate in the M–C Bond of ECE-Pincer Metal d^8 Complexes
Nilesh C. Mehendale, Remco W. A. Havenith, Martin Lutz, Anthony L. Spek, Robertus J. M. Klein Gebbink and Gerard van Koten, manuscript in prep.

NCN-, SCS-, and PCP-Pincer Palladium Halide Complexes as Lewis Acid Catalysts in Aldol Reactions with Methyl Isocyanoacetate: The Nature of the Palladium Catalyst Revisited
Nilesh C. Mehendale, Robertus J. M. Klein Gebbink and Gerard van Koten, manuscript in prep.

PCS-Pincer Palladium complex: Insertion of Methyl Isocyanoacetate and Catalytic Aldol Reactivity
Nilesh C. Mehendale, Robertus J. M. Klein Gebbink and Gerard van Koten, manuscript in prep.

Reactivity of Simple (In)soluble Silver(I) Salts in an Isocyanide Aldol Reaction

Nilesh C. Mehendale, Martin Lutz, Anthony L. Spek, Robertus J. M. Klein Gebbink and Gerard van Koten, manuscript in prep.